Vol. 8, Part A-1, No. 12, December 1970

Journal of Polymer Science

Part A-1: Polymer Chemistry

Contents

(continued inside)

Published by INTERSCIENCE PUBLISHERS a division of John Wiley & Sons, Inc.

Journal of Polymer Science: **Part A-1: Polymer Chemistry**

Contents (*continued*), *Vol. 8*

NOTES

(continued on inside back cover)

The Journal of Polymer Science is published in four sections as follows: Part A-1, Polymer Chemistry, monthly; Part A-2, Polymer Physics, monthly; Part B, Polymer Letters, monthly; Part C, Polymer Symposia, irregular.

Published monthly by Interscience Publishers, a Division of John Wiley & Sons, Inc., covering one volume annually. Publication Office at 20th and Northampton Sts., Easton, Pa. 18042. Executive, Editorial, and Circulation Offices at 605 Third Avenue, New York, N. Y. 10016. Second-class postage paid at Easton, Pa. Subscription price, $325.00 per volume (including Parts A-2, B, and C). Foreign postage $15.00 per volume (including Parts A-2, B, and C).

JOURNAL OF POLYMER SCIENCE: PART A-1 VOL. 8, 3373-3389 (1970)

High-Resolution NMR Spectrum of Deuterated and Undeuterated Poly(propene Sulfone)*

K. J. IVIN and M. NAVRÁTIL, *Department of Chemistry, The Queen's University of Belfast, Belfast, Northern Ireland*

Synopsis

100 MHz spectra have been obtained for DMSO-d_6 solutions of poly(propene sulfone) made from propene (I), propene-1,1,3,3,3-d_5 (II), propene-*cis*-1,2-d_2 (III) and propene-2-d_1 (IV) by copolymerization with sulfur dioxide; also by oxidation of poly(propene-2-d_1 sulfide)s of different tacticities.

The following chemical shifts and coupling constants were determined: $\tau_A = 6.06$, 6.12, 6.19; $\tau_B = 6.43$, 6.51; $\tau_C = 6.05$; $\tau_{CH_3} = 8.44$; $J_{CH_3,H_C} = 6.5$ Hz; $J_{AB} = 14.0$ Hz.

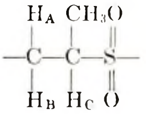

$$\begin{array}{ccccc} & H_A & CH_3 & O & \\ & | & | & \| & \\ — & C & —\,C\,— & S & — \\ & | & | & \| & \\ & H_B & H_C & O & \end{array}$$

Both the A and B protons are sensitive to tacticity, giving rise to five lines in the methylene spectrum of III and ten lines, consisting of four overlapping AB quartets, in the methylene spectrum of IV. From a consideration of the relative intensities of the peaks in the spectra of poly(propene-2-d_1 sulfone)s of different tacticities the following assignment to triad structures has been made: τ_A: 6.06 h_i, 6.12 i and s, 6.19 h_s; τ_B: 6.43 h_i and i, 6.51 s and h_s. The proportions of the four triad structures correspond to a single-parameter model for chain growth in which the probability of an isotactic placement σ is 0.50 for the free-radical copolymerization of propene and sulfur dioxide, 0.55 for the $ZnCO_3$-initiated polymerization of propene sulfide and 0.64 for the $CdCO_3$-initiated polymerization of propene sulfide. The spectrum of III shows that for polymer made at −90°C, one mode of addition is preferred. By analogy with other systems it is assumed that this is *trans* addition. For polymer made at 60°C, both *trans* and *cis* addition occur in nearly equal proportions. Assuming that *cis* addition occurs via the inversion of the intermediate alkyl radical, the activation energy for inversion is found to exceed that for addition of sulfur dioxide by 2.7 kcal/mole (11 kJ/mole). This appears to be the first reported case of a preferred mode of addition to an ethylenic bond in a free radically initiated polymerization.

High resolution NMR spectra of polymers in solution have provided much detailed information on configurational sequences in vinyl polymers[1] and copolymers.[2] However, polymers containing three-atom repeat units have been very little investigated. Ramey and Field[3] showed that the spectrum of poly(propene oxide) was sensitive to the method of prepara-

---

* Presented in part at the International Symposium on Macromolecular Chemistry, Toronto, Canada, 1968, Paper A4.4.

tion of the polymer, but spin-coupling of adjacent protons prevented detailed analysis. Spin-coupling can be reduced by deuteration in appropriate positions and the CH_2 part of the spectrum of $\text{+}CH_2CD(CH_3)O\text{+}$ has recently been shown[4] to consist of two AB quartets ascribed to isotactic and syndiotactic dyads; a weak third quartet was assigned to a small amount of tail-tail structure. White-noise-spin-decoupled, natural abundance ^{13}C NMR spectra also give valuable information on the stereoregularity of poly(propene oxide).[5] Very recently the CH_2 part of the spectrum of $\text{+}CH_2CDC(CH_3)_3O\text{+}$ has been shown[6] to consist of a single AB quartet for isotactic polymer and four AB quartets for amorphous polymer.

In a recent paper[7] we reported that the CH_2 part of the spectrum of $\text{+}CH_2CD(CH_3)S\text{+}$ consisted of two AB quartets whose relative intensity varied with catalyst used to polymerize propene sulfide. The present paper is concerned with an investigation of the NMR spectrum of poly(propene sulfone), $\text{+}CH_2CH(CH_3)SO_2\text{+}$, deuterated in various positions to facilitate interpretation. The polymer has been made both by the free-radical copolymerization of propene and sulfur dioxide and by oxidation of polysulfides prepared by using different catalysts.

EXPERIMENTAL

Propene was kindly supplied by I.C.I., Heavy Organic Chemicals Division. Deuterated propenes were purchased from Merck, Sharp and Dohme of Canada Ltd., with the following specifications: propene-2-d_1, 98 atom-% D; propene-1,1,3,3,3-d_5, 98 atom-% D; propene-*cis*-1,2-d_2, 98 atom-% D, 3.2% d_1, 96.8% d_2, made by hydroboration of methyl acetylene with sodium borodeuteride, followed by reaction with acetic acid-d_1.

Poly(propene sulfone) was prepared by two methods. In the first method measured amounts of gaseous propene and sulfur dioxide were condensed into a tube which was then sealed off and irradiated with ultraviolet light at constant temperature (±0.5°C). The polymer was dissolved in dimethyl sulfoxide (DMSO), reprecipitated in methanol, and dried in vacuum at 20°C. In the second method, poly(propene sulfide), prepared as described previously,[7] was dissolved in trifluoroacetic acid and allowed to react with an excess of hydrogen peroxide for two days.[8] The polysulfone precipitated as it formed and was purified as in the first method.

The NMR spectra were run as 5% solutions in DMSO-d_6, usually at 60°C, on a Varian HA100 spectrometer with TMS as internal standard (10τ). The optimum temperature was 60°C; prolonged exposure to higher temperatures caused decomposition of the polymer, while lower temperatures caused broadening of the absorption peaks.

RESULTS AND DISCUSSION

Undeuterated Polymer, I

Figure 1 shows the spectrum of the main-chain protons in I prepared by the first method, together with the spectra of the corresponding oxide and sulfide polymers.

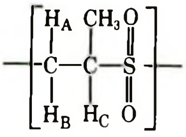

$$\left[\begin{array}{ccc} H_A & CH_3 & O \\ | & | & \| \\ -C- & -C- & -S- \\ | & | & \| \\ H_B & H_C & O \end{array} \right]$$

I

The protons in I are labeled A, B, and C in anticipation of the later interpretation of the spectra. The methyl doublets are centered on 8.44, 8.63, 8.87τ, with $J_{CH_3H_C}$ = 6.5, 6.2, 6.0 Hz for the sulfone, sulfide, and oxide polymers, respectively. The order of chemical shifts for the methyl reso-

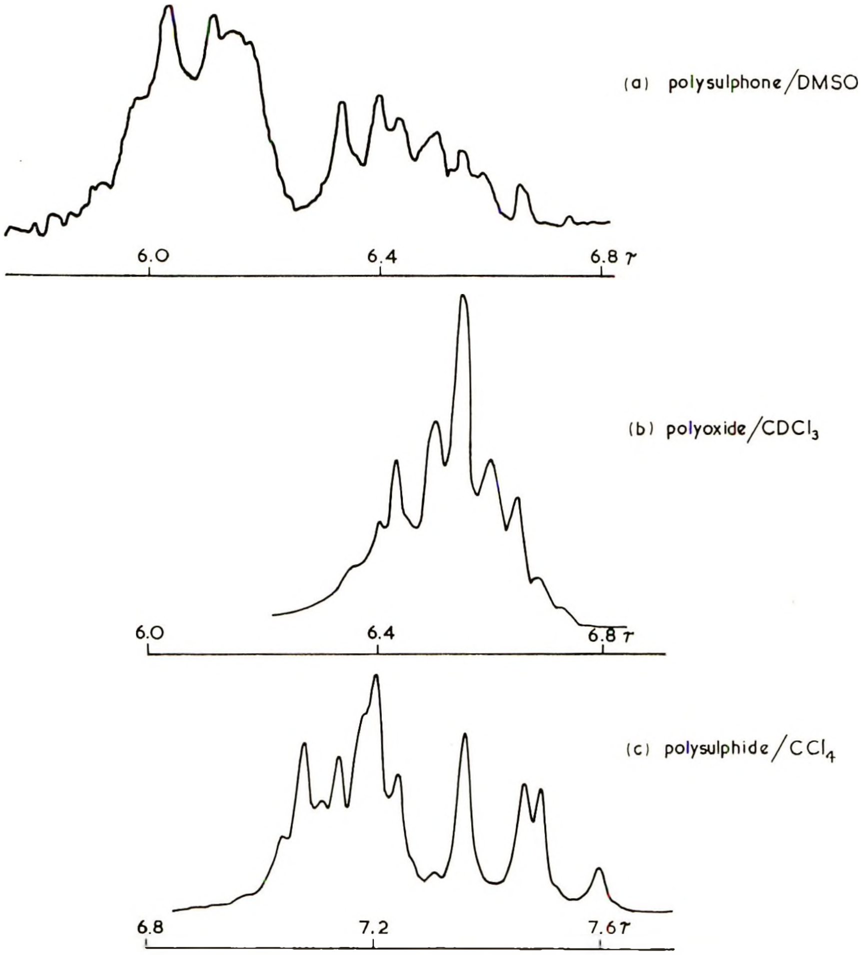

Fig. 1. 100 MHz NMR spectra of amorphous polymers of the type [$CH_2CH(CH_3)X$]: (*a*) X = SO_2, solvent DMSO-d_6 at 100°C, polymer prepared by free radical copolymerization of propene and sulfur dioxide; (*b*) X = O, solvent $CDCl_3$ at 30°C, data of Ramey and Field;[3] (*c*) X = S, solvent CCl_4 at 25°C, polymer prepared by $ZnCO_3$-initiated polymerization of propene sulfide.

nance, sulfone < sulfide < oxide, is as expected from the dipole moments of the corresponding diethyl compounds (4.41, 1.58, 1.14 D, respectively[9]). The order for the main-chain protons, however, is sulfone < oxide < sulfide. It should be noted that in all cases the methyl resonance consists of one doublet only and is thus insensitive to the tacticity of the chain.

In the cases of the polysulfide and polysulfone there is a distinct separation of the spectrum of the main chain protons into a downfield part (two protons) and an upfield part (one proton). The upfield part consists of a single quartet in the case of the polysulfide and of two quartets in the case of the polysulfone. We will return to the analysis of the latter after considering the spectra of the deuterated polymers.

Deuterated Polymers, II and III

The spectrum of II prepared by the first method (Fig. 2*a*) shows a single peak for H_C at 6.05τ. This falls in the downfield part of the spectrum of I; therefore, as in the polysulfide, the methylene protons in I must be nonequivalent, one having a chemical shift in the upfield part of the spectrum and one in the downfield part. The single peak for H_C in II shows that this resonance is insensitive to the tacticity of the chain, as for the methyl resonance.

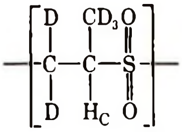

$$\left[\begin{array}{ccccc} \mathrm{D} & & \mathrm{CD_3} & & \mathrm{O}\\ | & & | & & \| \\ -\mathrm{C} & - & \mathrm{C} & - & \mathrm{S}- \\ | & & | & & \| \\ \mathrm{D} & & \mathrm{H_C} & & \mathrm{O}\end{array}\right]$$

II

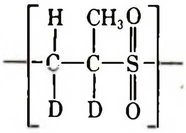

$$\left[\begin{array}{ccccc} \mathrm{H} & & \mathrm{CH_3} & & \mathrm{O}\\ | & & | & & \| \\ -\mathrm{C} & - & \mathrm{C} & - & \mathrm{S}- \\ | & & | & & \| \\ \mathrm{D} & & \mathrm{D} & & \mathrm{O}\end{array}\right]$$

IIIc

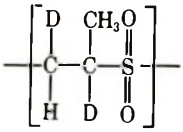

$$\left[\begin{array}{ccccc} \mathrm{D} & & \mathrm{CH_3} & & \mathrm{O}\\ | & & | & & \| \\ -\mathrm{C} & - & \mathrm{C} & - & \mathrm{S}- \\ | & & | & & \| \\ \mathrm{H} & & \mathrm{D} & & \mathrm{O}\end{array}\right]$$

IIIt

The polysulfone III made from *cis*-propene-1,2-d_2 has a spectrum which depends on the temperature of preparation (see Figs. 2*b* and 2*c*). Five peaks are observed, three downfield, centered on 6.12τ (group A) with intensity ratio 1:2:1, and two upfield centered on 6.47τ (group B) with intensity ratio 1:1. The overall intensity ratio (A:B) varies from about 1:4 when the polymer is made at −90°C to about 1:1 when the polymer is made at 60°C. For the higher temperature the five lines are thus in the intensity ratio 1:2:1:2:2.

Mechanism of Formation of III

There is clearly a preferred mode of addition to propene-*cis*-1,2-d_2 at low temperatures. By comparison with analogous systems,[10] such as the free radically induced addition of HBr to *cis*- and *trans*-2-bromobut-2-ene,[11] we may assume that at low temperature the preferred mode of addition is *trans*, leading to structure IIIt. If the intermediate alkyl radical inverts its configuration before the addition of sulfur dioxide, structure IIIc results (apparent *cis* addition). Group B peaks, being predominant for polymer made at low temperature, are thus to be identified with structure IIIt, and group A peaks with structure IIIc. The increasing proportion of *cis* addi-

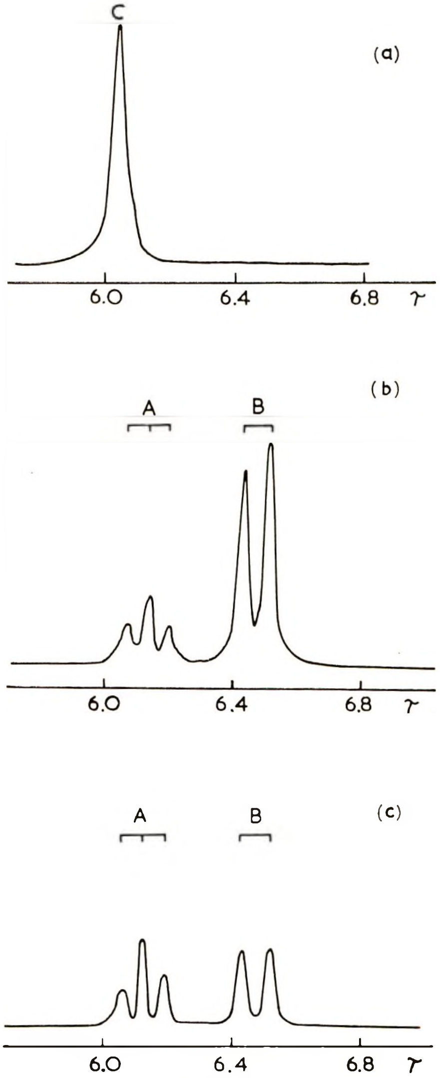

Fig. 2. 100 MHz spectra of (*a*) [$CD_2CH(CD_3)SO_2$]; (*b*) [$CDHCD(CH_3)SO_2$] prepared at −80°C; (*c*) [$CDHCD(CH_3)SO_2$] prepared at 25°C. Solvent DMSO-d_6 at 60°C. Assignment

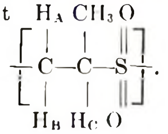

$$\left[-\overset{H_A}{\underset{H_B}{C}}-\overset{CH_3}{\underset{H_C}{C}}-\overset{O}{\underset{O}{\overset{\|}{\underset{\|}{S}}}}-\right].$$

tion at higher temperatures means that the inversion process must have a higher activation energy than addition of sulfur dioxide.

The proposed mechanism is set out below, assuming that the intermediate alkyl radical has a pyramidal structure. An exactly parallel mechanism can be written down assuming a "planar" alkyl radical (i.e. with the three atoms joined to the carbon radical coplanar with the carbon atom); the inversion process then consists of rotation through 180° about the $CHD—\dot{C}D(CH_3)$ bond.

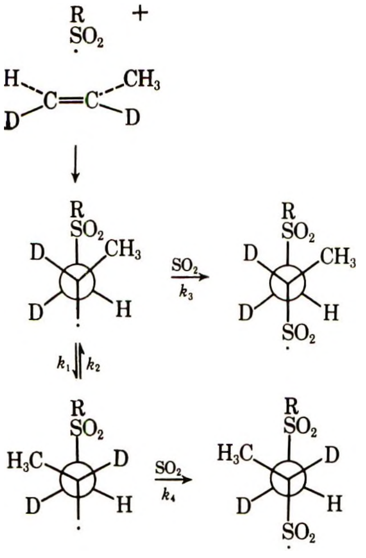

Fischer projection formulae

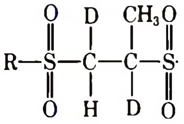

$$\begin{array}{ccccccccc} & & O & & D & & CH_3 & & O \\ & & \| & & | & & | & & \| \\ R & - & S & - & C & - & C & - & S\cdot \\ & & \| & & | & & | & & \| \\ & & O & & H & & D & & O \end{array}$$

trans addition IIIt (B group)

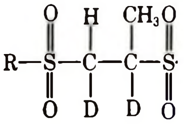

$$\begin{array}{ccccccccc} & & O & & H & & CH_3 & & O \\ & & \| & & | & & | & & \| \\ R & - & S & - & C & - & C & - & S\cdot \\ & & \| & & | & & | & & \| \\ & & O & & D & & D & & O \end{array}$$

cis addition IIIc (A group)

It should be noted that compared with the overhead Natta-Danusso[12] projection of the planar zigzag chain the positions of the substituents on alternate main-chain atoms must be reversed in order to obtain the Fischer projection formulae.

A stationary state treatment of the above mechanism, making the very reasonable assumptions that $k_1 = k_2$ and $k_3 = k_4$, leads to eq. (1), where B/A denotes the total area under group B peaks divided by the total area under group A peaks.

$$(k_3/k_1)[SO_2] = (B/A) - 1 \tag{1}$$

As already noted, B/A tends to 1 at high temperatures, in accordance with the assumption that $k_1 = k_2$. Figure 3 shows a plot of the right-hand side of eq. (1) against reciprocal temperature for a series of experiments in which the reactant composition was held constant at 1:1 propene:sulfur dioxide, corresponding to an approximately constant value of $[SO_2]$ equal to 8.5 mole/l. In each case, B/A was determined from the average of five integral curves of the NMR spectrum. The errors (twice the standard deviation of the mean) are indicated by the vertical lines. These are inevitably largest at the extremes of temperature. From the slope, $E_1 - E_3 = 11.1 \pm 1.5$ kJ/mole (2.7 ± 0.4 kcal/mole) and from the intercept $A_3\,[SO_2]/A_1 = 3 \times 10^{-3}$ whence $A_3/A_1 = 3 \times 10^{-4}$ l./mole. The activation energy of the inversion process is not likely to be much greater than 3 kcal/mole so that E_3 must be close to zero. Also if $A_1 \approx 10^{13}$ sec^{-1}, $A_3 \approx 10^9$ l./mole-sec. Thus it seems likely that the addition of sulfur dioxide to the alkyl radical

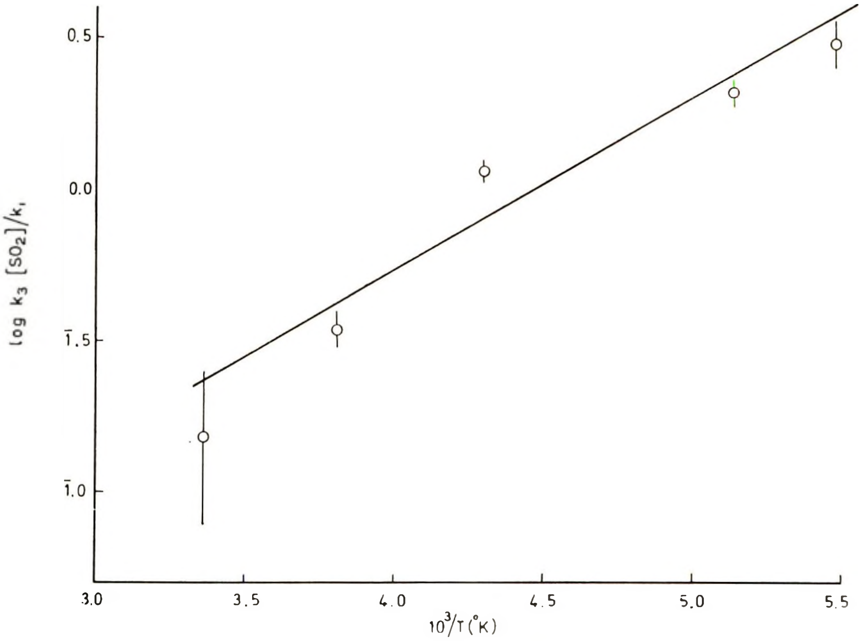

Fig. 3. Arrhenius plot of $k_3[SO_2]/k_1$.

is diffusion-controlled or nearly so. However, on the above evidence it cannot be entirely ruled out that propagation proceeds via addition of 1:1 propene:SO_2 complexes, although it can be said that if such complexes do take part in the reaction they must add to alkyl-type radicals and not to sulfonyl-type radicals since otherwise there would be no possibility for isomerization of the intermediate radicals.

Although a preferred mode of addition (*cis* or *trans*) has been demonstrated in the polymerization of several other β-deuterated monomers, such as propene,[12,13] acrylonitrile,[14] methyl[15] and isopropyl[16] acrylate, methyl and ethyl methacrylate,[16] the present system appears to be the first in which this has been shown to occur in a homogeneous, *free radically* initiated polymerization. It is likely that this would be found in other free-radical polymerizations if they were investigated at low temperature.

Fine Structure of Spectrum of III

We now turn to the question of the fine structure of the group A and group B spectra in polymer III. Changing the preparation conditions over wide limits had no effect on the relative intensities of the component peaks within each group, for example, the following were without effect: (a) temperature (−90° to 60°C); (b) propene:sulfur dioxide ratio (1:10 to 10:1); (c) addition of an excess of *n*-hexane. Also the conditions under which the NMR spectrum was run were without effect on the relative intensities. Thus changing the temperature from −10 to 80°C or changing the medium by the addition of an equal volume of CCl_4 to DMSO-d_6, were without effect. It thus seems unlikely that the fine structure is in any way ascribable to long-lived rotational isomeric states. The single chemical shift for H_C also makes such an explanation unlikely. We conclude that the fine structure results from configurational effects. Whereas in the polysulfide only the A protons are sensitive to configuration,[7] with the polysulfone both the A and the B protons are sensitive. Furthermore, whereas in the polysulfide the A protons showed only two distinct chemical shifts, in the polysulfone the A protons show three distinct chemical shifts. (Actually in the polysulfide there are indications in some cases of further fine structure[7].) It is clear therefore that we must take account of triad as well as dyad structures.

There are eight distinct triad structures which are set out below in skeleton form. The four triad structures with a *trans* central unit are denoted by *ti*, *th*$_i$, *th*$_s$ *and ts*. There is one isotactic triad (i), one syndiotactic triad (s) and two heterotactic triads (h_i and h_s), the subscripts i and s denoting the dyad structure (enclosed by the box) from which the triad is derived; similarly for the four triad structures with a *cis* central unit.

ti
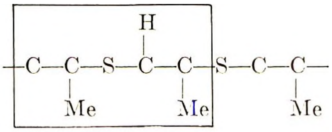
$$-\mathrm{C}-\underset{\mathrm{Me}}{\mathrm{C}}-\mathrm{S}-\overset{\mathrm{H}}{\mathrm{C}}-\underset{\mathrm{Me}}{\mathrm{C}}-\mathrm{S}-\mathrm{C}-\underset{\mathrm{Me}}{\mathrm{C}}-$$

ci
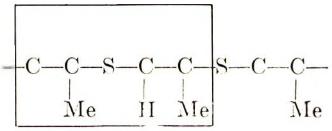
$$-\mathrm{C}-\underset{\mathrm{Me}}{\mathrm{C}}-\mathrm{S}-\underset{\mathrm{H}}{\mathrm{C}}-\underset{\mathrm{Me}}{\mathrm{C}}-\mathrm{S}-\mathrm{C}-\underset{\mathrm{Me}}{\mathrm{C}}-$$

th$_i$
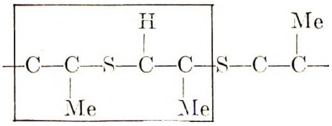
$$-\mathrm{C}-\underset{\mathrm{Me}}{\mathrm{C}}-\mathrm{S}-\overset{\mathrm{H}}{\mathrm{C}}-\underset{\mathrm{Me}}{\mathrm{C}}-\mathrm{S}-\mathrm{C}-\overset{\mathrm{Me}}{\mathrm{C}}-$$

ch$_i$
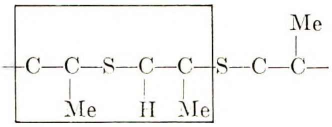
$$-\mathrm{C}-\underset{\mathrm{Me}}{\mathrm{C}}-\mathrm{S}-\underset{\mathrm{H}}{\mathrm{C}}-\underset{\mathrm{Me}}{\mathrm{C}}-\mathrm{S}-\mathrm{C}-\overset{\mathrm{Me}}{\mathrm{C}}-$$

th$_s$
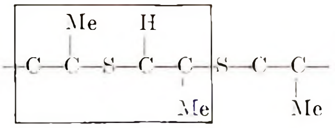
$$-\mathrm{C}-\overset{\mathrm{Me}}{\mathrm{C}}-\mathrm{S}-\overset{\mathrm{H}}{\mathrm{C}}-\underset{\mathrm{Me}}{\mathrm{C}}-\mathrm{S}-\mathrm{C}-\underset{\mathrm{Me}}{\mathrm{C}}-$$

ch$_s$
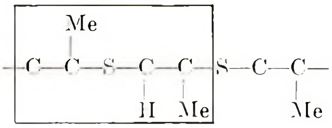
$$-\mathrm{C}-\overset{\mathrm{Me}}{\mathrm{C}}-\mathrm{S}-\underset{\mathrm{H}}{\mathrm{C}}-\underset{\mathrm{Me}}{\mathrm{C}}-\mathrm{S}-\mathrm{C}-\underset{\mathrm{Me}}{\mathrm{C}}-$$

ts
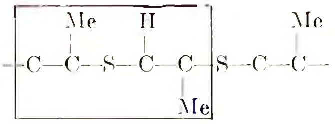
$$-\mathrm{C}-\overset{\mathrm{Me}}{\mathrm{C}}-\mathrm{S}-\overset{\mathrm{H}}{\mathrm{C}}-\underset{\mathrm{Me}}{\mathrm{C}}-\mathrm{S}-\mathrm{C}-\overset{\mathrm{Me}}{\mathrm{C}}-$$

cs
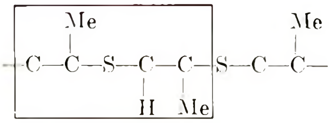
$$-\mathrm{C}-\overset{\mathrm{Me}}{\mathrm{C}}-\mathrm{S}-\underset{\mathrm{H}}{\mathrm{C}}-\underset{\mathrm{Me}}{\mathrm{C}}-\mathrm{S}-\mathrm{C}-\overset{\mathrm{Me}}{\mathrm{C}}-$$

The constant intensity ratios for the *trans* peaks (2:2) and the *cis* peaks (1:2:1) show that all four structures are equally probably for both *cis* and *trans* addition. This means that attack of the RSO_2 radical on the propene molecule must occur with equal facility from either side of the plane of the molecule, i.e., if there is any interaction between the methyl groups in the polymer chain and the methyl group in the approaching propene molecule, isotactic and syndiotactic placements are equally favored.

The problem now is to assign the five peaks to the eight triad structures. The two *trans* peaks (B protons) presumably correspond to isotactic and syndiotactic dyads so that we may bracket ti with th_i, and th_s with ts. We cannot say, *a priori*, which peak corresponds to the isotactic dyads, since the line ordering varies from polymer to polymer.[17] We have seen that in the polysulfide the downfield A proton is likely to correspond to the isotactic dyad structure,[7] but this will not necessarily be the order for the B protons in the polysulfone. Further light can be thrown on the problem by examining the spectrum of IV made by different methods.

Spectrum of Polymer IV; Assignment of group B lines in III

The spectra of the main-chain protons of IV made by three different methods are shown in Figure 4.

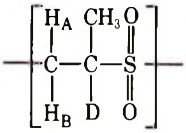

$$\left[\begin{array}{ccccc} H_A & & CH_3 & & O \\ | & & | & & \| \\ -C & - & C & - & S- \\ | & & | & & \| \\ H_B & & D & & O \end{array}\right]$$

IV

There are ten peaks, divided into a downfield group of six arising from the A protons and an upfield group of four arising from the B protons. From the spectrum of III and the interpretation already given we may expect that the spectrum of IV will consist of four overlapping AB quartets corresponding to the triad structures i, h_i, h_s, and s, each quartet being obtained by coupling one of the group A protons with one of the group B protons in the spectrum of III. For the free radically initiated polymer (Fig. 4*a*) we expect the four quartets to be of equal weight, but for the other two (Figs. 4*b* and 4*c*) we may expect different degrees of bias towards the isotactic triad and away from the syndiotactic triad.[7]

Numbering the peaks in the ten-line spectrum from 1 to 10 (downfield to upfield) we see that the intensities of lines 7 and 9 rise and fall together and likewise for lines 8 and 10. Furthermore the separation of lines 7 and 9 and of lines 8 and 10 is 14 Hz, corresponding to the expected numerical value of the geminal coupling constant J_{AB}. Lines 7 and 9 are thus derived from the downfield group B line in III and lines 8 and 10 from the upfield group B line in III. Now we have already seen that the polysulfide prepared by $CdCO_3$ initiation is likely to contain a higher proportion of isotactic structures compared with that prepared by $ZnCO_3$ initiation; in the corresponding polysulfones, lines 7 and 9 are strongest for the polymer made from the $CdCO_3$-initiated polysulfide. Hence we may assign the downfield group B line to the isotactic dyad structure and the upfield group B line to the syndiotactic dyad structure. This is the same order as for the group A lines in the polysulfide.

The relative proportions of the isotactic and syndiotactic dyad structures, derived from the relative intensities of the 7, 8, 9, 10 lines (B pro-

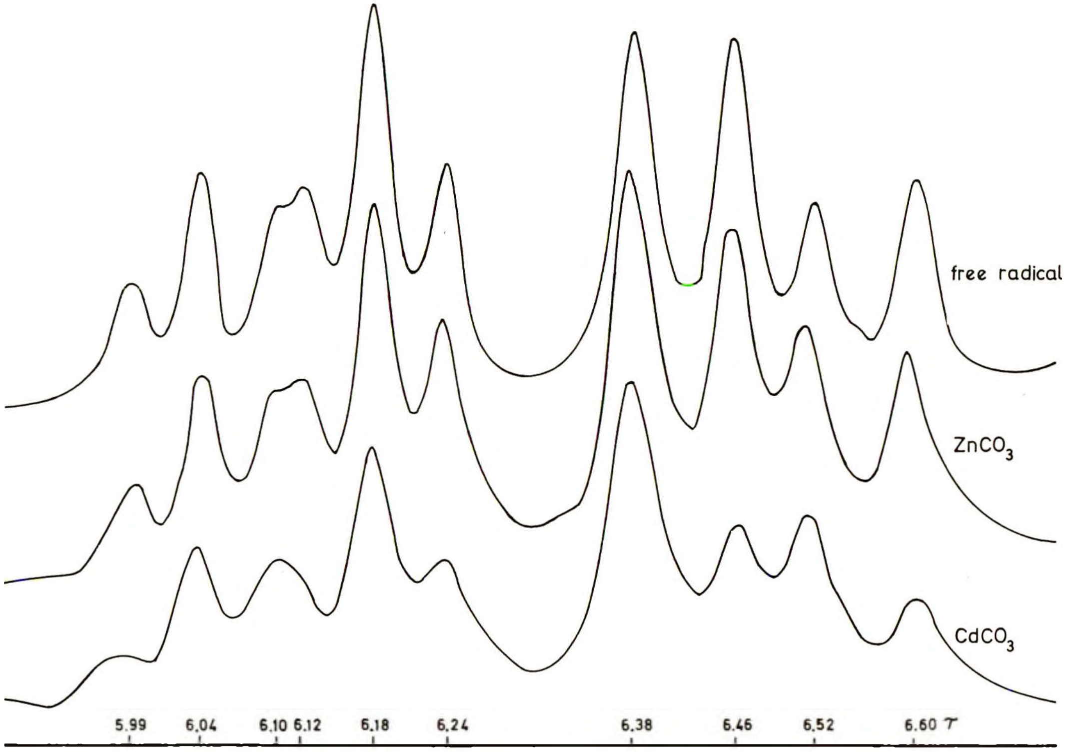

Fig. 4. 100 MHz NMR spectra of [$CH_2CD(CH_3)SO_2$] prepared by three methods: (*a*) free radically initiated copolymerization of propene-2-d_1 and sulfur dioxide; (*b*) via $ZnCO_3$-initiated polymerization of propene-2-d_1 sulfide; (*c*) via $CdCO_3$-initiated polymerization of propene-2-d_1 sulfide. Solvent DMSO-d_6. Computer-averaged spectra: (*a*) 40 scans; (*b*) 40 scans; (*c*) 30 scans.

TABLE I
Proportions of Dyad Structures in Polysulfides and Polysulfones of Propene-2-d_1

	From A components of polysulfide spectra		From B components of polysulfone spectra	
Catalyst	Isotactic, %	Syndiotactic, %	Isotactic, %	Syndiotactic, %
$CdCO_3$	65	35	67	33
$ZnCO_3$	52	48	57	43
Free radical	—	—	50	50

tons) in the polysulfone spectra, are in reasonable agreement with the relative proportions derived from the downfield lines (A protons) in the spectra of the polysulfides,[7] as shown in Table I.

Assignment of group A lines in III

There remains the question of the assignment of the three group A lines to the four triad structures. Numbering the lines in the spectrum of III from 1 to 5 (downfield to upfield) there are four possible ways of pairing the three group A lines with the two group B lines, as shown in Table II.

TABLE II
Possible Combinations P, Q, R, S, of Group A and Group B Lines

P	Q	R	S
1,4	1,5	1,4	1,5
2,4	2,5	2,5	2,4
2,5	2,4	2,5	2,4
3,5	3,4	3,4	3,5

In principle it is possible to decide which combination is correct by comparing the experimental spectrum of IV with that calculated from the frequencies of lines 1 to 5 in III, and the coupling constant $J_{AB} = -14.0$ Hz, adjusting the relative proportions of the four triads to give the best fit.

The predicted line positions for the 10-line spectrum are unfortunately very similar for all four combinations, the correlations being as shown in Table III.

TABLE III
Possible Correlations between Peaks in Spectrum of III and Peaks in Spectrum of IV

5-line spectrum of III		10-line spectrum of IV
1,4	→	1,4,7,9
1,5	→	1,4,8,10
2,4	→	2,5,7,9
2,5	→	2,5,8,10
3,5	→	3,6,7,9
3,5	→	3,6,8,10

TABLE IV

Intensities for AB Quartets Calculated from the Positions in the 5-Line Spectrum (6.06, 6.12, 6.19, 6.43, 6.51 τ) and $J_{AB} = -14.0$ Hz (Normalized to 100 for Each Quartet)[a]

Combination	A,B pairing in 5-line spectrum	10-line spectrum										Total
		1	2	3	4	5	6	7	8	9	10	
P	1,4	16.1			33.9			33.9		16.1		100
	2,4		14.7			35.3		35.3		14.7		100
	2,5		16.5			33.5			33.5		16.5	100
	3,5			15.0			35.0		35.0		15.0	100
Q	1,5	17.5			32.5				32.5		17.5	100
	2,5		16.5			33.5			33.5		16.5	100
	2,4		14.7			35.3		35.3		14.7		100
	3,4			12.4			37.6	37.6		12.4		100

[a] Outer line intensity = $25\{1 - J_{AB}/[J_{AB}^2 + (\nu_A - \nu_B)^2]^{1/2}\}$; inner line intensity = $25\{1 + J_{AB}/[J_{AB}^2 + (\nu_A - \nu_B)^2]^{1/2}\}$.

Tickling experiments, which reveal the peaks forming part of a given quartet, were unsuccessful because the lines were too broad. The choice between combinations P, Q, R, and S of Table II must therefore rest on a comparison of intensities.

First we may note that in combination S, the double pair 2,4 will give rise to lines 2, 5, 7, 9 in the 10-line spectrum of IV. Neither of the other pairs, 1,5 and 3,5, in this combination will give rise to lines in the 2, 5, 7, 9 positions in the spectrum of IV and we may therefore expect that, if this combination is not to be excluded, lines 2 and 9 will be of equal intensity; likewise for lines 5 and 7 (since an AB quartet has a symmetrical intensity distribution). Inspection of Fig. 4 shows that this is clearly not the case; compare for instance lines 5 and 7 in the bottom spectrum. Similarly for combination R, lines 2 and 10 should be of equal intensity; also lines 5 and 8. Again this is not so; compare for instance lines 5 and 8 in the bottom spectrum of Figure 4. We may thus rule out combinations R and S, and it remains to choose between P and Q.

The calculated intensities for each quartet are shown in Table IV.

The experimental intensities, determined by means of a Du Pont curve resolver, are shown in Table V normalized to 100 for each complete spectrum.

The observed ratios of intensities of lines 7 and 9 (1.91, 2.15, 2.45) and of lines 8 and 10 (1.67, 1.72, 1.80) for the three polymers (in the order listed in Table V), do not compare very well with those calculated either for combination P (2.40–2.11 for lines 7 and 9; 2.03–2.33 for lines 8 and 10) or for combination Q (2.40–3.03 for lines 7 and 9; 1.86–2.03 for lines 8 and 10), and for both combinations the trends are as expected only for one pair of lines. This suggests that the individual intensities of lines 7, 8, 9, 10 in Table V are subject to an error of the order of ±1. This is not surprising, since it is difficult to match the observed spectrum precisely by means of the curve resolver.

With this limitation in mind, the proportions of the four quartets giving the closest fit to the experimental intensities were determined by matching successively to lines 6, 8, 5, 7 (combination P) or to lines 6, 7, 5, 8 (combination Q). For both combinations the best fit was obtained with proportions corresponding closely to those expected from a one-parameter model. Thus if the probability of an isotactic dyad placement is σ, the proportions of i, h_i, h_s, and s triads are σ^2, $\sigma(1 - \sigma)$, $(1 - \sigma)\sigma$, and $(1 - \sigma)^2$, respectively. The appropriate weightings of the four quartets for each combination are indicated in footnote b of Table VI. As a final basis for attempting to choose between combinations P and Q, σ was adjusted to give the smallest root-mean-square deviation from the observed intensities as shown in Table VI.

For each of the three polymers, combination P gives marginally the better fit, and the σ values agree quite closely with those derived from the polysulfide spectra (Table I). The value $\sigma = 0.50$ for the free radically initiated polymer and the equal weighting of the four quartets is in accord with the spectrum of III.

TABLE V
Experimental Intensities for the 10-Line Spectrum in Poly(propene-2-d_1 sulfone)

Polymer	10-line spectrum 1	2	3[a] 4[a]	5	6	7	8	9	10	Total
$CdCO_3$[b]	3.8	9.5	11.6	16.5	8.6	21.8	10.5	11.4	6.3	100
$ZnCO_3$[b]	4.0	8.4	12.5	16.6	8.5	18.9	14.1	8.8	8.2	100
Free radical[c]	4.4	8.4	12.7	15.9	8.5	17.9	16.0	7.3	8.9	100

[a] Not estimated separately because of overlap.
[b] Denotes catalyst used to prepare the polysulfide from which the polysulfone was made.
[c] Free radically initiated copolymerization of propene + SO_2.

TABLE VI
Calculated Intensities (%) for the 10-Line Spectrum in Poly(propene-2-d_1 Sulfone) on the Basis of Best Fit of a Single-Parameter (σ) Model

Polymer[a]	Combination[b]	Best σ	10-line spectrum 1	2	3 4	5	6	7	8	9	10	$(\overline{d^2})^{1/2}$ [c]
$CdCO_3$	P	0.64	3.7	8.1	11.3	18.9	8.0	22.3	12.4	9.7	5.6	1.3
"	Q	0.64	4.0	8.1	10.4	18.9	8.6	23.2	11.9	8.8	6.1	1.4
$ZnCO_3$	P	0.55	4.0	7.7	12.3	17.3	8.7	19.1	15.5	8.4	7.0	0.70
"	Q	0.55	4.3	7.7	11.3	17.3	9.4	20.0	14.9	7.5	7.6	0.90
Free radical	P	0.51	4.0	7.7	12.3	17.3	8.7	17.7	16.8	7.8	7.7	0.75
" "	Q	0.50	4.4	7.8	11.2	17.2	9.4	18.2	16.5	6.8	8.5	0.80

[a] As in Table V.
[b] Weightings for P: 2, 4 σ^2; 1, 4 and 3, 5 $\sigma(1-\sigma)$; 2, 5 $(1-\sigma)^2$. For Q: 2, 4 σ^2; 1, 5 and 3, 4 $\sigma(1-\sigma)$; 2, 5 $(1-\sigma)^2$.
[c] d = (observed intensity) − (calculated intensity).

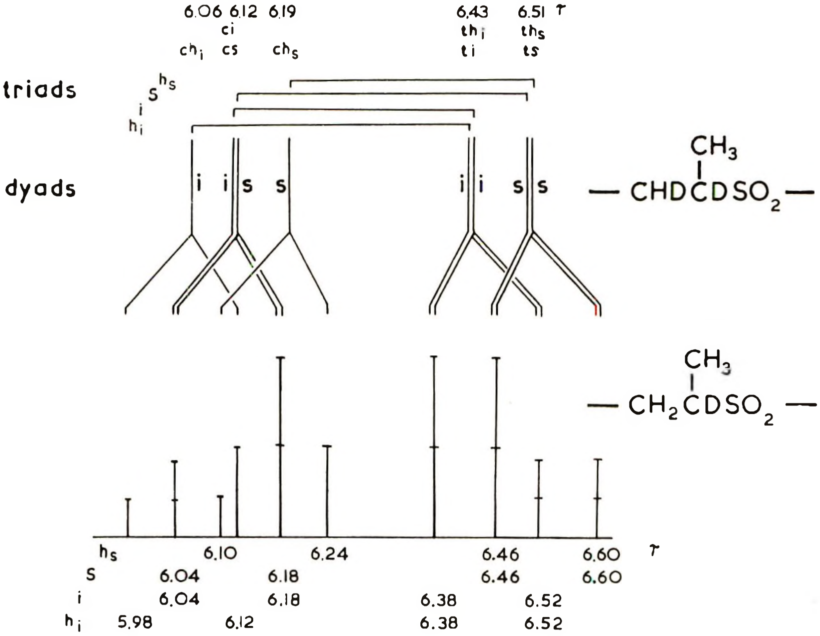

Fig. 5. Diagram showing the complete assignment of the five-line main-chain proton spectrum of poly(propene-1,2-d_2 sulfone), and the relationship between the spectra of III and IV for the free radically initiated polymer.

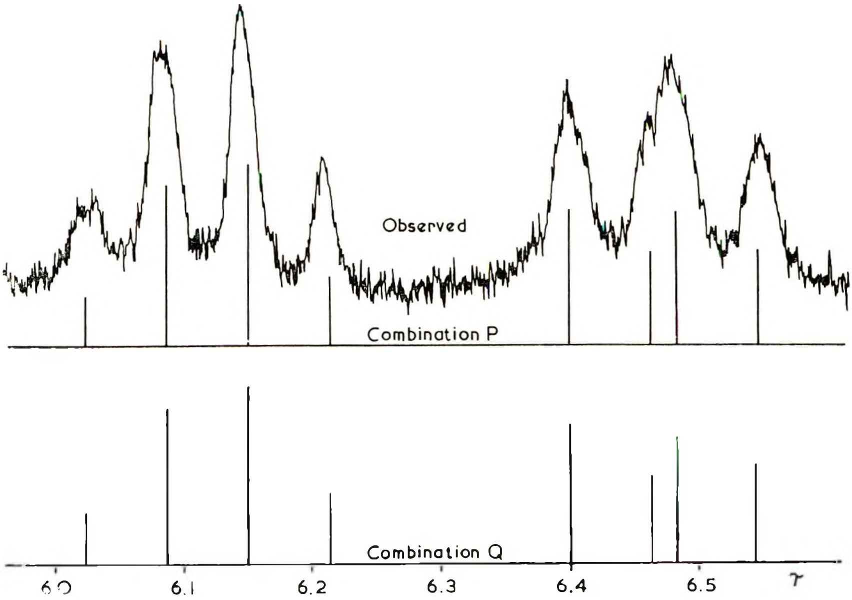

Fig. 6. Comparison of experimental 220 MHz spectrum for the free radically initiated polymer IV, with that calculated from 100 MHz spectrum assuming (*a*) combination P (*b*) combination Q, and equal proportions of the four quartets.

Assuming that combination P is correct, the assignment of the group A lines in the spectrum of III can now be made. The most abundant quartet in the spectrum of IV prepared via $CdCO_3$ initiation is derived from lines 2 and 4 in the spectrum of III (see footnote to Table VI). These lines therefore contain the *i* triad. Likewise, the least abundant quartet, derived from lines 2 and 5, corresponds to the *s* triad. Line 1 is coupled with line 4 which is therefore the h_i triad, and line 3 is coupled with line 5 which is therefore the h_s triad. The complete assignment is shown in Figure 5. (That given previously[18] is incorrect.) It may be noted that if combination Q were correct, the only effect on the assignment would be to interchange the h_i and h_s lines. However, apart from the fact that combination P fits the results somewhat better than combination Q, the former seems intrinsically more probable because of the more systematic pairings of the lines. It may also be noted that with combination P the average line position for isotactic dyads in group A (6.09τ) is downfield from the average line position for syndiotactic dyads in group A (6.155τ). This difference is of about the same magnitude and in the same direction as that for the group B lines (0.08τ). The difference is considerably larger than that observed for the group A lines in the polysulfide (0.03τ), presumably as a result of the greater bond anisotropy of the sulfone groups[17] compared with the sulfide.

The 220 MHz Spectrum of IV

In an attempt further to confirm the interpretation outlined above we have compared the calculated and experimental 220 MHz spectra of the free radically initiated polymer IV as shown in Figure 6. However, discrimination between combinations P and Q can not be made on this basis. It will be noticed that there is a greater degree of overlap in the 220 MHz spectrum than in the 100 MHz spectrum.

Interpretation of Spectrum of I

The B part of the spectrum of the undeuterated polymer, shown in Figure 1*a*, can now be readily interpreted in terms of two quartets, derived from $\tau_B = 6.43$ (isotactic dyad) and $\tau_B' = 6.51$ (syndiotactic dyad). The B lines lie at 6.34, 6.44, 6.49 and 6.59τ and the B′ lines at 6.41, 6.51, 6.56 and 6.66τ, the splitting constants in each case being $S_{AB} = 15$ Hz, $S_{BC} = 10$ Hz. As with the polysulfide,[7] S_{AB} is a little bigger than $-J_{AB}$ (14 Hz). By analogy with the polysulfide we may expect J_{BC} to be about 0.5 Hz smaller than S_{BC}. Its magnitude indicates that the conformation about the main-chain C—C bond is again predominantly *trans*. It has also been shown that the preferred conformation about the central C—C bond in 1,2-di-*n*-propylsulfonylethane is *trans*.[18]

We thank the Science Research Council for a postdoctoral fellowship to M. N.; Mr. R. Spratt for the 100 MHz spectra, Dr. J. K. Becconsall for the 220 MHz spectrum, and Dr. W. Cooper and Dr. F. A. Bovey for helpful discussions.

References

1. P. R. Sewell, in *Annual Review of NMR Spectroscopy*, E. F. Mooney, Ed., Academic Press, New York–London, 1968, p. 165.
2. K. H. Hellwege, U. Johnsen, and K. Kolbe, *Kolloid-Z.*, **214**, 45 (1966).
3. K. C. Ramey and N. D. Field, *J. Polym. Sci., B*, **2**, 461 (1964).
4. H. Tani, N. Oguni, and S. Watanabe, *J. Polym. Sci. B*, **6**, 577 (1968).
5. J. Schaefer, *Macromolecules*, **2**, 533 (1969).
6. H. Tani and N. Oguni, *J. Polym. Sci. B*, **7**, 803 (1969).
7. K. J. Ivin and M. Navrátil, *J. Polym. Sci. B*, **8**, 51 (1970); *J. Polym. Sci. A-1*, in press.
8. V. S. Foldi and W. Sweeny, *Makromol. Chem.*, **72**, 208 (1964).
9. J. W. Smith, *Electric Dipole Moments*, Butterworths, London, 1955, p. 230.
10. P. S. Skell and R. G. Allen, *J. Amer. Chem. Soc.*, **81**, 5383 (1959).
11. H. L. Goering and D. W. Larsen, *J. Amer. Chem. Soc.*, **81**, 5937 (1959).
12. G. Natta, M. Farina and M. Peraldo, *J. Polym. Sci.*, **43**, 142 (1960).
13. E. Lombardi, A. Segre, A. Zambelli, A. Marinangeli, and G. Natta, in *Macromolecular Chemistry, Prague 1965* (*J. Polym. Sci. C*, **16**), O. Wichterle and B. Sedlácek, Eds., Interscience, New York, 1967, p. 2539.
14. T. Yoshino, H. Kenjo, and K. Kuno, *J. Polym. Sci. B*, **5**, 703 (1967).
15. T. Yoshino, J. Komiyama, and M. Shinomiya, *J. Amer. Chem. Soc.*, **86**, 4482 (1964).
16. W. Fowells, C. Schuerch, F. A. Bovey, and F. P. Hood, *J. Amer. Chem. Soc.*, **89**, 1396 (1967).
17. W. M. Ritchey and F. J. Knoll, *J. Polymer Sci. B*, **4**, 853 (1966).
18. A. H. Fawcett, K. J. Ivin, M. Navrátil, and N. A. Walker, paper presented at International Symposium on Macromolecular Chemistry, Toronto, Canada, 1968, paper A4.4.

Received May 12, 1970

JOURNAL OF POLYMER SCIENCE: PART A-1 VOL. 8, 3391-3403 (1970)

Effects of Mercaptides on Anionic Polymerization. II. Polymerization of Acrylonitrile Initiated by Mercaptides*

TAKUJI HIRAHARA and YUJI MINOURA, *Research Institute for Atomic Energy, Osaka City University, Osaka, Japan*

Synopsis

The polymerization of acrylonitrile by the several alkali metal mercaptides was investigated. The initiation reaction was found spectroscopically and by the sodium fusion method to proceed in a Michael-like form similar to a cyanoethylation reaction. From the results of the copolymerization of acrylonitrile and methyl methacrylate by the mercaptides, it was found that the mercaptides behaved as the anionic initiators. The effects of the counterions on the rate of polymerization were found to increase with increasing the electropositivities in the order of Li < Na < K. A negative overall activation energy was obtained, −2.2 kcal/mole, in the temperature region of −30°C to +20°C. The catalytic reactivities of the mercaptides were smaller than those of the corresponding oxygen analogs, except in the case of the phenyl substituent. Only in the case of the phenyl substituent, thiophenoxide was found to be much more effective than phenoxide, phenyl-SNa ≫ phenyl-ONa. The catalytic reactivities of the various sodium mercaptides were also determined to follow not only the basicities of the nucleophiles, but also the polarizabilities as follows: *tert*-butyl-SNa ≈ *n*-dodecyl-SNa > phenyl-SNa > *n*-octyl-SNa > isopropyl-SNa > *n*-propyl-SNa > ethyl-SNa. The enhanced reactivity of thiophenoxide in spite of the low pK_a value was attributed to the higher polarizability based on the low α effect.

INTRODUCTION

Many studies concerning the catalytic activities of the anionic initiators have been reported, and now in many cases catalytic activities of the anionic initiators are thought to depend mainly on the basicities of the parent compounds of the initiators.

Wooding and Higginson first examined the polymerization of acrylonitrile, methyl methacrylate, styrene, and butadiene by the various organosodium compounds.[1]

Morton and Grovenstein[2] observed the order of reactivity for the initiation of styrene polymerization by organo-sodium compounds.[2] In this case, relative reactivities were as follows:

---

* This work was presented at the annual meeting, Chemical Society of Japan, Tokyo, April 1967, and at the 16th annual conference of the Society of Polymer Science Japan, Fukuoka, October 1967.

$\text{Am—Na} > C_6H_5CH_2Na > CH_2{=}CHCH_2Na > CH_2{=}CHNa > C_6H_5Na$

In still another series of polymerization reactions induced by organometallic initiators with a different monomer, virtually the same reactivity order was observed for the organic moiety.[3]

Zilkha and co-workers studied the polymerization of acrylonitrile by several alkali metal aldoxides in a nonpolar medium,[4–6] and reported that catalytic activities were dependent on the basicity of the parent alcohol. They also determined the relative reactivities of anionic initiators for the polymerization of acrylonitrile, methyl methacrylate, and styrene in *N*,*N*′-dimethylformamide at 0°C.[7]

Vogl studied the reactivity for the polymerization of *n*-butylaldehyde by the various alkoxides[8] and proposed three conditions important for the initiator effectiveness: (1) sufficient solubility in the reaction medium; (2) ability to add to the carbonyl double bond; (3) ability of the carbonyl adduct to propagate polymerization.

From the initiation reaction, Hsieh determined the relative reactivities of several organolithium compounds for the polymerization of butadiene, isoprene, and styrene.[9–11]

Waack and Doran also reported on the polymerization of styrene by the several organolithium compounds in tetrahydrofuran medium and determined the reactivity order:[12] butyl $\gg$ benzyl $\approx$ allyl $>$ vinyl $\approx$ phenyl. They suggested that the order was not consistent with the basicity order. Recently, they made progress further in their study of reactivity of anionic initiators and classified in view of the styrene type of the organolithium compounds:[13] alkyl > benzyl > allyl > phenyl > vinyl > triphenylmethyl; from the structure type, the order appears to be alkyl > charge delocalized > sp^2 hybridized.

Hopff and co-workers, however, observed in their study of the anionic polymerization of diethyl methylenemalonate by the several amines, that catalytic activity of the amines for the monomer was completely unrelated to with the basicities of the amines.[14]

In this respect the studies of the additional activity of $CH_2{=}CHLi$ to 1,1-diphenylethylene[15] and the order of additional reactivities of several carbanions to 1,1-diphenylethylene[16] (benzyl-Li > i-PrLi > *n*-BuLi > EtLi > PhLi) have resulted in useful contributions.

The order of the anionic initiators classified by Tsuruta[17] and the study of the activity of ionic initiators by Kamio[18] also presented much available suggestions.

The effects of the counterions on the initiator reactivity have been also studied by many workers. In general, it is thought that the counterions do not affect the ability to initiate the polymerization, though they affect considerably influences on the rate of polymerization and the stereoregularity of the polymer. For instance, the effects of the counterions on initiator reactivity for a series of alkali and alkaline earth amides in the polymerization of methyl methacrylate in liquid ammonia are shown by the following order:[19] $KNH_2 > NaNH_2 > LiNH_2 > Ca(NH_2)_2 > Sr(NH_2)_2 > Ba(NH_2)_2$.

In our previous paper, we reported the effects of several mercaptides on the overall rate and the polymer tacticity in the butyllithium-initiated polymerization of methyl methacrylate in toluene at −30°C, under conditions in which the monomer did not polymerize with mercaptides alone.[20]

In this paper, the modes of polymerization of acrylonitrile catalyzed by mercaptides having somewhat lower pK_a values than the general anionic initiators were studied, and the relative reactivities of the several mercaptides were determined. A comparison of the reactivities of the mercaptides with the oxygen analogs was also made. The factors that determine the catalytic reactivities of the anionic initiators are also discussed.

EXPERIMENTAL

Reagents

Mercaptans. Commercially available products were distilled immediately before use. The middle fractions, whose boiling points were in good agreement with the values reported in the literature were used:[21] ethylmercaptan, bp 35°C; *n*-propylmercaptan, bp 67.0°C; isopropylmercaptan, bp 52.5–53°C; *tert*-butylmercaptan, bp 64.0°C; thiophenol, bp 86°C/5 mm Hg; *n*-octylmercaptan, bp 77–78°C/10 mm Hg; *n*-dodecylmercaptan, bp[22] 111–112°C/3 mm Hg.

Tetrahydrofuran. A good grade of commercial ether was refluxed overnight over sodium and then distilled. The middle fraction was redistilled immediately before use after refluxing over sodium and benzophenone till dark blue color developed.[23]

Diethyl Ether. Commercially available ether was repeatedly shaken with dilute ferrous sulfate solution and then water. It was distilled over sodium wire after drying over calcium chloride and refluxing with sodium wire.

Acrylonitrile. Commercially available monomer was washed successively with 10% sodium hydroxide solution to remove the inhibitor and then water. The monomer was dried with anhydrous calcium chloride and then distilled under argon; the middle fraction was collected and stored in the dark. This fraction was freshly distilled immediately before use over calcium hydride at 73–74°C under an argon atmosphere.

Mercaptides. Alkali metal mercaptides were prepared in a three-necked flask equipped with a stirrer, an argon gas inlet and a condenser protected by a calcium chloride tube, by the addition of corresponding mercaptans to freshly cut sodium in dry ether as solvent, under an argon atmosphere. After refluxing and vigorous stirring for about 10–20 hr the solvent was distilled off under a stream of argon.[24,25] The mercaptides were stored under an argon atmosphere until used.

Phenol. Commercially available product was distilled at 61.0°C under a pressure of 9 mm Hg. Other alcohols used here were purified in the same way described in our previous paper.[20]

Alkoxides. The alkoxides used in this paper were all prepared in the same manner as the mercaptides.

Polymerization

The polymerizations were carried out in sealed glass tubes as described in our earlier paper.[20] In all experiments traces of moisture and air were vigorously excluded.

Sulfur Analysis

The sulfur analysis in the lower molecular weight polymer obtained by sodium thiophenoxide initiator was accomplished qualitatively by the sodium fusion method.[26]

Spectral Measurement

Ultraviolet spectra of the oligomer obtained were recorded on a Hitachi-EPS-2 type spectrometer.

The measurements of infrared spectra were carried out on a Hitachi-Perkin-Elmer 337 double-beam spectrometer over the region of 4000–600 cm^{-1}.

RESULTS AND DISCUSSION

The addition reaction of the mercaptans to acrylonitrile is known to be a cyanoethylation reaction. The mercaptans readily add to acrylonitrile similarly to alcohols in a Michael-like form to yield β-cyanoethyl sulfide, as shown in eq. (1).[27–30] The reaction is also known to proceed especially easily under base-catalyzed conditions, even below 50°C.

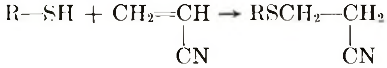

$$R{-}SH + CH_2{=}\underset{\substack{|\\ CN}}{CH} \rightarrow RSCH_2{-}\underset{\substack{|\\ CN}}{CH_2} \tag{1}$$

In general, the reaction is often utilized advantageously for the quantitative analysis of acrylonitrile by use of dodecyl mercaptan, which has especially high additional reactivity.[31]

We extended this reaction to the polymerization of acrylonitrile using alkali metal mercaptides. To confirm the initiation reaction of the polymerization, oily oligomer was obtained by using an excess of sodium thiophenoxide to acrylonitrile in diethyl ether solvent at a room temperature in an argon atmosphere under a vigorous stirring.

The presence of phenyl nuclei in the low molecular weight polymer was recognized by the ultraviolet and infrared spectra shown in Figures 1 and 2; sulfur included in the oligomer was qualitatively determined by the sodium fusion method.

The copolymerization of acrylonitrile and methyl methacrylate cat-

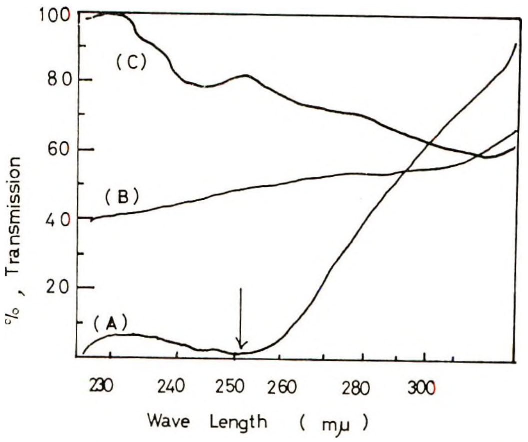

Fig. 1. Ultraviolet spectra of oily oligomers of AN obtained by sodium thiophenoxide in THF solvent: (*A*) with phenyl-SNa catalyst; (*B*) with BuLi; (*C*) with Na metal. [oligomer] = ca. 10^{-4} mole/l. in methanol at room temperature. The arrow denotes the band due to $\pi \rightarrow \pi^*$ transition of phenyl group.

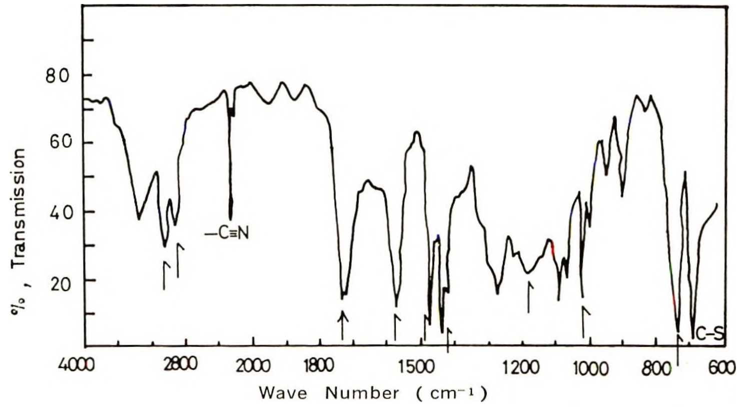

Fig. 2. Infrared spectrum of oily oligomer of AN obtained with sodium thiophenoxide in THF Solvent: (↾) bands due to the phenyl group; (↑) band due to a substantial amount of cyclic *β*-keto ester.[31]

alyzed by sodium thiophenoxide was also investigated in *N,N*-dimethylformamide medium at 0°C; results are presented in Table I.

From these results the initiation of polymerization of acrylonitrile by the alkali metal mercaptides is concluded to proceed in a fashion similar to the cyanoethylation reaction, seen in eq. (2).

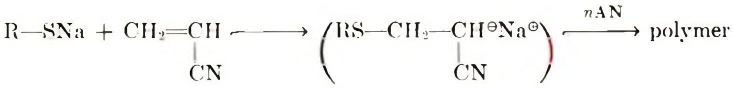

$$\text{R—SNa} + \underset{\displaystyle \text{CN}}{\text{CH}_2\text{=}\underset{|}{\text{CH}}} \longrightarrow \left(\text{RS—CH}_2\text{—}\underset{\displaystyle \text{CN}}{\underset{|}{\text{CH}^{\ominus}\text{Na}^{\oplus}}}\right) \xrightarrow{n\text{AN}} \text{polymer} \qquad (2)$$

The polymerization of acrylonitrile by the mercaptides occurred in both nonpolar solvents such as benzene and toluene and in polar solvents, such as tetrahydrofuran, dimethylformamide, dimethyl sulfoxide, dimethoxy-

TABLE I
Copolymerization of Acrylonitrile (AN) and Methyl Methacrylate (MMA) Initiated by Sodium Thiophenoxide in *N*,*N*'-Dimethylformamide at 0°C. [AN] = 3.04 mole/l., [C_6H_5SNa] = 2.40 × 10^{-2} mole/l.

[MMA], mole/l.	Conversion, %	AN in the copolymer, mole-%
0.94	28.9	98.0
1.87	18.9	98.0
4.87	8.1	>94[a]

[a] Three replicates.

ethane, and diglyme, but in view of the low solubility of the mercaptides and the polymer for some of these solvents, *N*,*N*'-dimethylformamide was generally used.

The time–conversion curves obtained for the polymerization of acrylonitrile initiated by sodium thiophenoxide in *N*,*N*'-dimethylformamide at 0°C are shown in Figure 3.

The initial rate of polymerization was found to follow a first-order dependence on concentration of the mercaptide. The initial rate of polymerization was also found to follow a first-order dependence on the concentration of monomer. The relationship between ln ($[M]_0/[M]$) and the polymerization time is shown in Figure 4, in which the first-order rate constant, k = 2.05 × 10^{-2}/min., is obtained.

The ability to initiate the polymerization of acrylonitrile depended only on the organic moiety for the alkali metals examined and was notaffected by the counterions, but the rate of polymerization increased with in

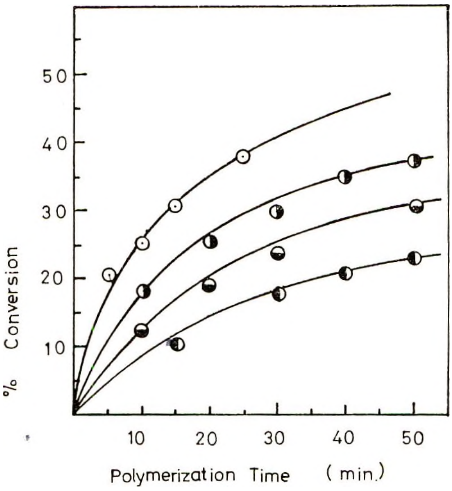

Fig. 3. Polymerization of acrylonitrile by sodium thiophenoxide at 0°C in DMF solvent and at various phenyl-SNa concentrations and [AN] = 4.56 mole/l.: (⊙) [Phenyl-SNa] = 8.0 × 10^{-3} mole/l.; (◑) 6.0 × 10^{-3} mole/l.; (◒) 5.0 × 10^{-3} mole/l.; (◐) 4.0 × 10^{-3} mole/l.

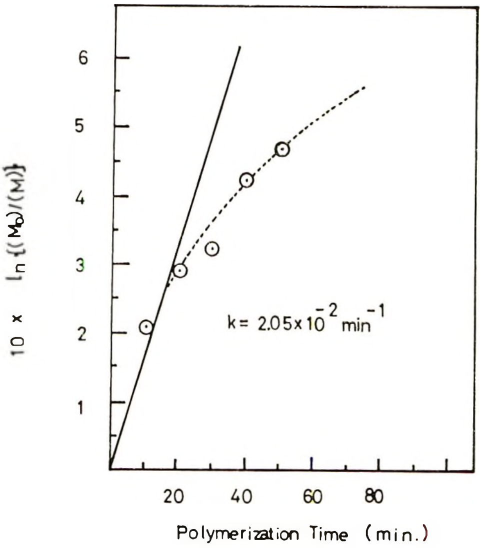

Fig. 4. Relationship between ln ([M$_0$]/[M]) and polymerization time for AN polymerization by sodium thiophenoxide in DMF solvent at 0°C; [AN] = 4.56 mole/l.; [Phenyl-SNa] = 6.0 × 10^{-3} mole/l.

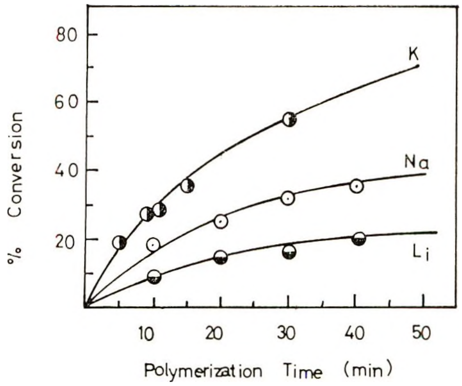

Fig. 5. Effect of counterions on reactivity of thiophenoxide for AN polymerization in DMF solvent at 0°C: (◑) K; (⊙) Na; (◒) Li. [AN] = 4.56 mole/l.; [thiophenoxide] = 6.0 × 10^{-3} mole/l.

creasing electropositivity of the counterions in the order, Li < Na < K, as shown in Figure 5.

Interestingly, when tetrahydrofuran was used as a solvent, however, lithium salt did not initiate the polymerization at a low concentration of the salt ([phenyl-SLi] <1.5 × 10^{-2} mole/l.) but at a higher concentration ([phenyl-SLi] >2.0 × 10^{-2} mole/l.), the ability to initiate the polymerization of the monomer increased rapidly, as shown in Figure 6.

In the cases of potassium and sodium salts, such phenomena were not observed.

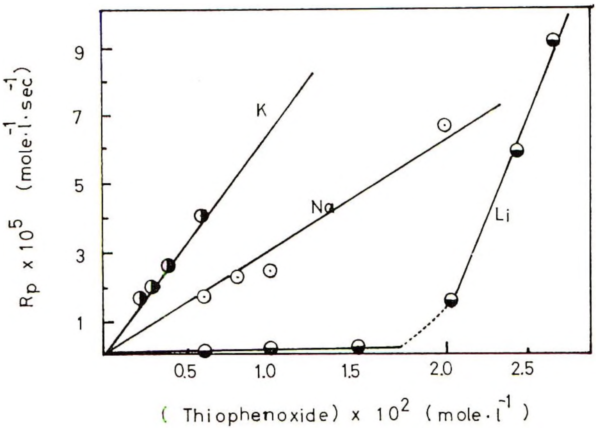

Fig. 6. Effect of counterions on rate of polymerization in THF solvent at 0°C: (◑) phenyl-SK; (⊙) phenyl-SNa; (◒) phenyl-SLi. [AN] = 3.04 mole/l.

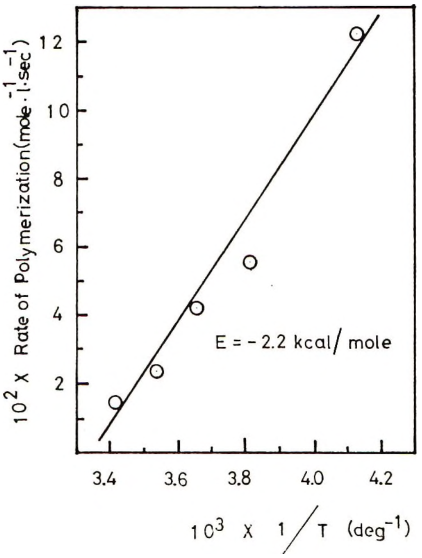

Fig. 7. Relationship between rate of polymerization and temperature for polymerization of AN by phenyl-SNa in DMF solvent in temperature region of −30°C to +20°C; [AN] = 4.56 mole/l.; [phenyl-SNa] = 6.0 × 10^{-3} mole/l.

Organolithium compounds such as butyllithium and ethyllithium are well known to form association complexes in tetrahydrofuran.[33-35]

The results stated above suggest the presence of such association phenomena also for the lithium thiophenoxide in the solvent, and formation of relatively stable associates at a low concentration of the salt. The associates formed in the process were not further studied. The polymerization of acrylonitrile initiated by sodium thiophenoxide was carried out in the temperature region of +20 to −30°C in dimethylformamide; the Arrhenius plot is shown in Figure 7.

The rate of polymerization increased with decreasing temperature in the range studied. From the plot, an apparently negative activation energy, −2.2 kcal/mole, was obtained. No polymerization occurred, however, at −78°C under otherwise parallel conditions.

It is quite reasonable, therefore, to assume the presence of an optimum temperature for the polymerization of acrylonitrile by the mercaptides between −30 and −78°C. Generally, when a negative activation energy is observed, the potential-energy barrier for any elementary process cannot be negative. The negative activation energy, therefore, indicates some complexity of the polymerization process. The reasons for the phenomenon are fully discussed by Shimomura and co-workers.[36] They suggested that at least three possibilities should be considered. The hypothesis most probable in view of other findings is as follows.[37]

One of the reagents, A, forms a mixture of two species, that is A′ and A″, which coexist in a rapidly established equilibrium. The overall reaction is determined, therefore, by two simultaneous reactions

$$A' + B \xrightarrow{k'} C \tag{3}$$

$$A'' + B \xrightarrow{k''} C \tag{4}$$

in conjugation with the equilibrium

$$A' \overset{K_s}{\rightleftarrows} A'' \tag{5}$$

The above rearrangement may or may not involve solvent. The apparent rate constant k of such reaction is given by

$$k = \gamma k' + (1 - \gamma)k'' \tag{6}$$

$$= k'/(1 + K_s) + K_s k''/(1 + K_s) \tag{7}$$

where γ and $(1 - \gamma)$ represent, respectively, the fractions of A′ and A″ at equilibrium.

For $k' \ll k''$ and for a not too small K_s, this approximates to

$$k = K_s k''/(1 + K_s) \tag{8}$$

An apparent negative activation energy is observed if ΔH_s is negative and E'' sufficiently low.

They also proposed a second hypothesis supporting the first: The rate of an ionic reaction depends significantly on solvent, and a large change may be observed when the condition is modified. Temperature affects the properties of solvents, and the transition states of the polymerization become progressively more solvated as the temperature is lowered. An increase in the degree of solvation of the transition states results in a gradual lowering of the potential-energy barrier. The enhanced reactivity at low temperature is, thus, attributed to the presence of a highly reactive, thermodynamically distinct species, the proportion of which increases with decreasing polymerization temperature.

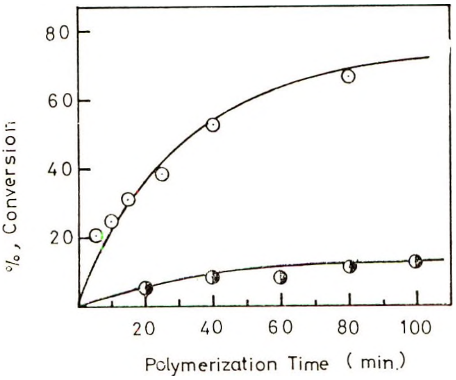

Fig. 8. Relative reactivity of thiophenoxide to phenoxide for acrylonitrile polymerization in DMF solvent at 0°C: (⊙) phenyl-SNa, (◑) phenyl-ONa. [AN] = 4.56 mole/l.; [Catalyst] = 8.0×10^{-3} mole/l.

It would be reasonable to assume the presence of different types of active sites, that is, a solvent-separated ion pair and a contact ion-pair species also, for the polymerization of acrylonitrile initiated by the mercaptides in dimethylformamide.

A comparison of the relative reactivities of the mercaptides with the corresponding oxygen analogs were made. In general, the alkoxides were found to be much more effective than the corresponding mercaptides, and when the alkoxide or phenoxide was used, almost explosive polymerization occurred under the conditions given in Figure 8.

In the case of the phenyl substituent, however, the mercaptide was much more effective than the phenoxide, as shown in Figure 8.

In general the additional reactivities of the nucleophiles are determined according to the following conditions:[38] (a) basicity of the nucleophile, (b) polarizability of the nucleophile, (c) α-effect.

Nucleophiles having higher additional reactivities form a large amount of active species in the initiation reaction, and thus the reactivity in the polymerization is enhanced. The pK_a values of the alcohols are much higher than those of the corresponding mercaptans. In the cases of alkyl substituents only the inductive effect influences the polarizability, and the C—O bounds of the alkoxides consist of $2p\pi$–$2p\pi$ interaction; on the other hand, the C—S bonds of the mercaptides are $2p\pi$–$3p\pi$, which is unstable compared to $2p\pi$–$2p\pi$ interaction. The C—S bonds are thus more polarizable than the corresponding C—O bonds.[39] As can be seen from the refractive indices n_D, however, the difference between them in the polarizability is only slight, in spite of the large difference in the pK_a values; for example, for C_2H_5SH, pK_a 10.50 (in H_2O, at 20°C),[40] n_D^{20} 1.4311;[41] for C_2H_5OH, pK_a 18 (in H_2O, at 20°C),[42] n_D^{20} 1.36.[43]

The relative reactivity is, therefore, determined nearly by the pK_a values only. In the case of the phenyl substituent, however, α-effect must be also considered. The negative charge on the oxygen of the phenoxide is

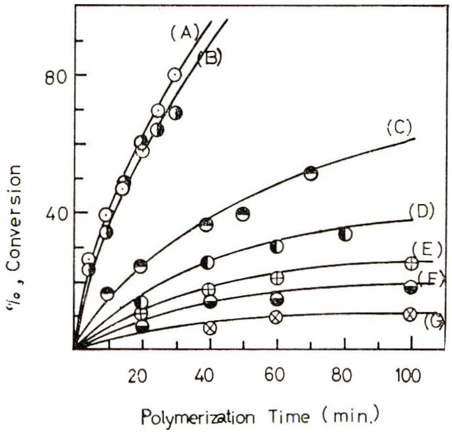

Fig. 9. Relative reactivities of several mercaptides for AN polymerization in DMF solvent at 0°C: (*A*) *tert*-Bu-SNa (⊙); (*B*) *n*-dodecyl-SNa (◑); (*C*) phenyl-SNa (◓); (*D*) *n*-octyl-SNa (◐); (*E*) isopropyl-SNa (●); (*F*) *n*-propyl-SNa (◒); (*G*) ethyl-SNa (⊗). [AN] = 4.56 mole/l.; [mercaptide] = 6.0×10^{-3} mole/l.

well known to mesomerize with the lone pairs on the phenyl nuclei as shown in eq. (9):

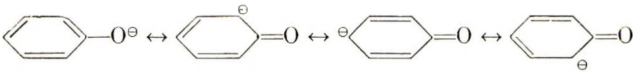

(9)

On the other hand, the C—S bond of thiophenoxide is unstable compared to the C—O bond, as already stated above. Therefore the negative charge on sulfur can not strongly interact with the lone pairs on the phenyl nuclei and thus the C—S bond is highly polarizable.

The highly enhanced reactivity of thiophenoxide compared to phenoxide is thus attributed to the high polarizability of the sulfur anion. The comparison of the relative reactivities of thiophenoxide with phenoxide is one of the most typical examples that does not depend on the pK_a values only.

The relative reactivities of the several sodium mercaptides for the polymerization of acrylonitrile in dimethylformamide at 0°C were also determined.

As shown in Figure 9, the reactivity decreases in the order: *tert*-butyl-SNa ≈ *n*-dodecyl-SNa > phenyl-SNa > *n*-octyl-SNa > isopropyl-SNa > *n*-propyl-SNa > ethyl-SNa.

In the cases of the alkyl substituents the polarizabilities are determined by the inductive effect. The order is, therefore, dependent both on the pK_a values of the parent mercaptans and the polarizabilities, except in the case of thiophenoxide.

The enhanced reactivity of thiophenoxide in spite of the low pK_a value is attributed to the high polarizability as may be seen from the low α-effect as already stated above. Edwards[44,45] tried to determine quantitatively the effects of the basicity and the polarizability on the nucleophilic reaction, and the following relationship was obtained when the steric hindrance was neglected:

$$\log (k/k_0) = \alpha E_n + \beta H \qquad (10)$$

where (k/k_0) denotes a relative (to water) rate or equilibrium constant and E_n denotes a nucleophilic constant characteristic of an electron donor and is obtained from the electrode potentials; H is the relative basicity of the donor to protons and is expressed as $H = pK_a + 1.74$. α and β are substrate constants obtained experimentally. By extending the relationship further, the relative reactivity of the anionic initiators could be quantitatively estimated. In the determination of the relative reactivity of the anionic initiators, however, the effects of the association phenomena and the steric hindrance must be also taken into consideration as was suggested independently by Waack and Steveson[15] and Grovenstein and Wentworth[16] in studies on addition of $CH_2{=}CH_2Li$, and some carbanions to 1,1-diphenylethylene.

References

1. N. S. Wooding and W. C. E. Higginson, *J. Chem. Soc.*, **1952,** 774.
2. A. A. Morton and E. Grovenstein, Jr., *J. Amer. Chem. Soc.*, **74,** 5434 (1952).
3. K. Yoshida and T. Morikawa, *Sci. Ind. Osaka*, **27,** 80 (1953).
4. A. Zilkha, B. Felt, and M. Frankel, *J. Chem. Soc.*, **1959,** 928.
5. A. Zilkha and B. Feit, *J. Appl. Polym. Sci.*, **5,** 251 (1961).
6. B. Feit and A. Zilkha, *J. Appl. Polym. Sci.*, **7,** 289 (1963).
7. A. Ottolenghi, S. Barzakay, and A. Zilkha, *J. Polym. Sci. A*, **1,** 3643 (1963).
8. O. Vogl, *J. Polym. Sci. A*, **2,** 4607 (1964).
9. H. L. Hsieh, *J. Polym. Sci. A*, **3,** 153 (1965).
10. H. L. Hsieh, *J. Polym. Sci. A*, **3,** 163 (1965).
11. H. L. Hsieh, *J. Polym. Sci. A*, **3,** 173 (1965).
12. R. Waack and M. A. Doran, *Polymer*, **2,** 365 (1961).
13. R. Waack and M. A. Doran, *J. Org. Chem.*, **32,** 3395 (1967).
14. H. Hopff, H. Lüssi, and S. Allisson, *Makromol. Chem.*, **44–46,** 95 (1961).
15. R. Waack and P. E. Steveson, *J. Amer. Chem. Soc.*, **87,** 1183 (1965).
16. E. Grovenstein, Jr., and G. Wentworth, *J. Amer. Chem. Soc.*, **89,** 1852 (1967).
17. T. Tsuruta, in *Syntheses of High Polymers*, T. Tsuruta, Ed. Kagakudojin, Kyoto, Japan, 1961, Chap. 4, p. 54.
18. K. Kamio, *Nippon Kagaku Zasshi*, **84,** 565 (1963).
19. W. E. Goode, W. H. Snyder, and R. C. Fettes, *J. Polym. Sci.*, **42,** 367 (1960).
20. T. Hirahara, T. Nakano, and Y. Minoura, *J. Polym. Sci. A-1*, **6,** 485 (1968).
21. R. B. Wagner and H. D. Zook, *Synthetic Organic Chemistry*, Wiley, New York, 1961, Chap. 31, pp. 778–786.
22. C. R. Noller and J. J. Gordon, *J. Amer. Chem. Soc.*, **55,** 1091 (1933).
23. D. E. Paul, D. Lipkin, and S. I. Weissman, *J. Amer. Chem. Soc.*, **78,** 116 (1956).
24. P. Claesson, *J. Prakt. Chem.* [2], **15,** 196 (1877).
25. J. C. Sheehan and G. D. Daves, Jr., *J. Org. Chem.*, **29,** 2006 (1964).
26. L. F. Fieser, *Experiments in Organic Chemistry*, 3rd ed., Heath, Boston, p. 228.
27. C. D. Hurd and L. E. Gershbein, *J. Amer. Chem. Soc.*, **69,** 2328 (1947).
28. M. W. Harman (to Monsanto Chemical Co.), U. S. Pat. 2,413,917 (1947).
29. J. L. Szabo and E. T. Stiller, *J. Amer. Chem. Soc.*, **70,** 3667 (1948).
30. L. Rapoport, A. Smith, and M. S. Newman, *J. Amer. Chem. Soc.*, **69,** 693 (1947).

31. D. W. Beesing, W. P. Tyler, D. M. Kuitz, and S. A. Harrison, *Anal. Chem.*, **21,** 1073 (1949).

32. W. E. Goode and F. H. Owens, *J. Polym. Sci.*, **47,** 75 (1960).

33. G. Witting, F. Meyer, and G. Lange, *Ann.*, **571,** 167 (1951).

34. F. J. Welch, *J. Amer. Chem. Soc.*, **81,** 1345 (1959).

35. K. K. O'Driscoll, R. J. Boudreau, and A. V. Tobolsky, *J. Polym. Sci.*, **31,** 115 (1958).

36. T. Shimomura, K. J. Tölle, J. Smid, and M. Szwarc, *J. Amer. Chem. Soc.*, **89,** 796 (1967).

37. T. E. Hogen-Esch and J. Smid, *J. Amer. Chem. Soc.*, **88,** 307 (1966).

38. J. O. Edwards and R. G. Pearson, *J. Amer. Chem. Soc.*, **84,** 16 (1962).

39. A. B. Burg, *Organic Sulfur Compounds*, N. Kharasch, Ed., Pergamon Press, New York, 1961, Vol. I, p. 30.

40. J. B. Conant and G. W. Wheland, *J. Amer. Chem. Soc.*, **54,** 1212 (1932).

41. E. C. H. Hunter and J. R. Partington, *J. Chem. Soc.*, **1931,** 2062.

42. M. Schlosser, *Angew. Chem.*, **76,** 124 (1964).

43. *The Merck Index of Chemicals and Drugs*, 7th ed. Merck & Co. Inc., 1960, p. 28.

44. J. O. Edwards, *J. Amer. Chem. Soc.*, **76,** 1540 (1954).

45. J. O. Edwards, *J. Amer. Chem. Soc.*, **78,** 1819 (1956).

Received February 3, 1970
Revised April 23, 1970

JOURNAL OF POLYMER SCIENCE: PART A-1 VOL. 8, 3105-3115 (1970)

Synthetic Thermally Reversible Gel Systems. VI

HOWARD C. HAAS, RUBY L. MacDONALD, and ALAN N. SCHULER, *Research Laboratories, Polaroid Corporation, Cambridge, Massachusetts 02139*

Synopsis

Forming and conditioning thermally reversible aqueous gels of polyacrylylglycinamide (PAG) at various temperatures has little effect on either the melting point (T_m) of the gels or the heat of crosslinking (ΔH_c) except at temperatures where partial hydrolysis can occur. This is added evidence that unlike with gelatin, crystallite formation does not play a role in gel formation. For unfractioned PAG, the linear relationship between the logarithm of molecular weight and $1/T_m$ predicted and observed for gelatin gels, does not hold. With mixed gelatin-PAG gels, a gelatin/PAG ratio of ≥ 4 completely inhibits the formation of a PAG gel network. At lower gelatin/PAG ratios, the PAG network forms, and if gelatin is considered as an inert diluent, normal values for the melting points and ΔH_c for PAG gels are observed. At a gelatin/PAG ratio of 4, the presence of PAG reduces the ΔH_c for the gelatin gel by inhibiting the formation of as large or as ordered crystallite crosslinks. To reconcile the problem of aggregation preceding gelation one can assume that $\bar{M}_w$ of an aggregate is a linear function of C^2. If this is done, the same relationship which normally relates C with T_m is obtained. The equilibrium swelling of PAG films in water at 25°C is markedly molecular weight-dependent and can vary from below 5 to about 40 wt-% polymer at equilibrium. It has been found that long-term dark storage of dry samples of PAG under ambient temperature conditions results in pronounced decreases in the intrinsic viscosities of their aqueous solutions. It is speculated that this results from weak links, perhaps peroxy, in the polymer backbone. The possible relationship of this phenomenon to the slow stage of the viscosity deterioration of aqueous polyacrylamide solutions is pointed out. The higher viscosity of low $\overline{\text{DP}}$ PAG in $2M$ NaCNS compared to H_2O and the larger percentage increase of $[\eta]$ with increasing temperature in the latter, verify the greater solvent power of $2M$ aqueous thiocyanate for PAG. At a concentration level of 3%, aqueous PAG solutions are almost Newtonian whereas at higher concentrations (5%), the viscosity decreases appreciably with increasing rates of shear. The copolymerization of AG with isopropylacrylamide has been studied and the somewhat unusual results discussed. Copolymers containing an AG mole fraction greater than 0.40 do not exhibit a cloud point up to 100°C. If the isopropylacrylamide mole fraction approaches 0.60, the solutions do not gel down to 0°C. This ability to prepare copolymers over a narrow composition range that neither gel or undergo phase separation in the temperature range 0-100°C is probably related to the random distribution of monomer units in the copolymer backbone.

Some years ago we reported on the synthesis[1] of acrylyl (AG) and methacrylylglycinamide (MG) whose homopolymers and many copolymers yield thermally reversible aqueous gels. Subsequent papers in this series dealt with the properties of polyacrylylglycinamide (PAG), its solutions and thermally reversible gels,[2–4] and the persulfate-initiated polymerization kinetics of AG.[5]

In this paper we would like to discuss briefly a variety of different subjects related to PAG. Aqueous gels of PAG were conditioned at different temperatures and the effect of temperature on melting points and the heat of crosslinking, ΔH_c, determined. Mixed PAG–gelatin gels have been studied in an attempt to obtain additional insight into gel structure. Some high shear rheological measurements on aqueous PAG solutions and the temperature dependence of the intrinsic viscosity in water and $2M$ NaCNS are also reported. Observations have been made on the long-term storage stability of PAG. In attempts to synthesize polymers whose solutions gel on cooling and undergo phase separation on heating, *N*-isopropylacrylamide–AG copolymers were prepared, evaluated, and a copolymer composition–temperature phase diagram constructed.

Aqueous PAG Gels

X-ray diffraction and other studies have shown that gelatin gels contain crystallites[6–8] and that these are probably related to the thermally reversible crosslinks making up the gel network. Experimental values for $-\Delta H_c$ ranging from 50 to 220 kcal/mole of crosslinks[9] confirm the complex nature of the crosslinks and imply that numerous peptide groups are involved in a single crosslink. Conditioning[9] gelatin gels at temperatures not far below their melting point improves their perfection and both raises the melting points and the values for $-\Delta H_c$. Thermodynamic analysis[3] and a DTA measureable exothermic heat of gel reorganization preceding gelatin gel fusion[4] give added evidence that the crosslinks are made up of small crystallites.

There are implications in the literature[8] that crystallinity is a requisite for the phenomenon of thermally reversible gelation. We are not in accord with this idea. Equilibrium swelling and modulus measurements,[3] values for $-\Delta H_c$ of between 5 and 12 kcal/mole[2,3] and the absence of DTA-detectable fusion endotherms[5] support our contention that aqueous thermally reversible PAG gels are noncrystalline in nature.

To pursue this subject a little further, aqueous gels of PAG were prepared, conditioned at different temperatures and the melting points measured. In the first experiment, aqueous solutions of five PAG samples (50 g/l.) of different molecular weights were cooled to 3°C and 15°C, held at these temperatures for 18 hr and the gel melting points measured by the method of Haas et al.[2] These are recorded in Table I.

Unlike gelatin, the differences in melting points between gels conditioned at 3 and 15°C are very small. If anything, the gels conditioned at the higher temperature show somewhat lower fusion points which is opposite to the expected direction if crystalline crosslinks are involved. If it is assumed that some reasonably constant $\overline{M}_w/\overline{M}_n$ ratio exists for these five samples and log $\overline{M}_w$ is plotted against $1/T$, there is a drastic deviation from linearity. The linearity of this relationship has been suggested by Eldridge and Ferry and shown to hold for gelatin gels.[9]

TABLE I
Melting Points of Aqueous PAG Gels

Sample	$\bar{M}_n \times 10^{-3}$	Melting point, °C	
		3°C conditioning	15°C conditioning
1	27.6	25.3	23.5
2	40.2	40.6	40.8
3	78.1	64.0	—
4	332.6	71.7	71.0
5	944.0	78.6	78.0

In the past we have been concerned with large variations in Huggins' k' values and suspect that this is related to various molecular weight distributions and extents of branching among the different PAG samples. This may also be the reason for the nonlinearity of the log M-inverse temperature plot. In a second experiment, gels of high $\overline{\text{DP}}$ PAG were formed and conditioned at 5°C and at a much higher temperature, 50°C for 18 hr. The melting point data are given in Table II.

TABLE II
Melting Points of Aqueous PAG Gels

Concn, g/l.	Melting point, °C	
	5°C conditioning	50°C conditioning
30	67.4	75.8
40	74.3	80.0
50	78.2	83.3
60	81.9	85.8
70	84.5	87.0
ΔH_c, kcal/mole	−13.3	−15.8

From the usual log C versus $1/T$ plots,[9] values for ΔH_c of −13.3 kcal/mole and −15.8 kcal/mole are obtained for the gels conditioned at 5 and 50°C, respectively. The value of −13.3 kcal/mole is within experimental error of the normally observed range of −5 to −12 kcal/mole. In contrast to the gels conditioned at 5°C, the gels conditioned at 50°C liberate ammonia when treated in the cold with dilute alkali, showing that partial hydrolysis has occurred during the 18-hr period at 50°C. We believe that this accounts for the higher melting points, since we have previously shown[2] that introduction of small amounts of acrylic acid into PAG by copolymerization raises the melting points of the aqueous gels. Here again, past thermal history does not seem to have any major effect on gel properties; this would not be the case if crystallite formation was involved. We do not wish to imply that conditioning PAG gels at a temperature near the melting point cannot result in a gel closer to equilibrium (lower free energy) which would have a slightly larger number of reversible crosslinks per unit volume of gel and consequently a slightly higher melting point.

Aqueous PAG–Gelatin Gels

Polyacrylylglycinamide and gelatin are compatible in concentrated aqueous solutions.[1] With many gelatins, but not all, PAG is apparently compatible even in dry film form. For the following experiments, a PAG sample of $[\eta] = 1.0$ dl/g ($2M$ NaCNS at 25°C) and $\bar{M}_n$ of 4.3×10^5 was employed. An Atlantic gelatin having a Bloom of 225 and a pH = 4.60 was used. For the first experiment, weight percent mixtures of the two polymers were prepared varying from 0% PAG to 0% gelatin. Solutions of these mixtures were then made (50 g/l.), the solutions cooled to 21.2°C and then stored at this temperature for 18 hr. The melting points of the resulting gels, determined as before, are recorded in Table III.

TABLE III
Melting Points of Aqueous PAG-Gelatin Gels

Gelatin/PAG (w/w)	PAG, g/l.	Melting point, °K
1/0	0	304.0
8/2	10	303.0
6/4	20	327.9 (54.9°C)
4/6	30	345.5
2/8	40	350.8
0/1	50	357.5

As the ratio of PAG to gelatin increases, the melting points of the mixed gels are seen to increase. If gelatin is considered to be an inert diluent, a ΔH_c of -7.3 kcal/mole of crosslinks is obtained from the slope of a plot of log [PAG] versus $1/T$. This value is characteristic for aqueous PAG gels. At a concentration of 10 g PAG/l. (gelatin/PAG ratio of 4), there appears to be considerable interference by the gelatin with the PAG network, as evidenced by the low melting point of 30°C. At higher PAG concentrations, the noticeable network appears to revert to one of PAG since the melting points are comparable to those of PAG gels in the absence of gelatin. There seems to be little interaction, reinforcement, or cocrystallization of gelatin and PAG, since these might be expected to raise the melting points of the gels at the low PAG end and also raise the value of $-\Delta H_c$. In a second experiment, for the same samples of PAG and gelatin used for the data of Table III, heats of crosslinking were measured for gelatin gels and for gelatin–PAG gels containing a gelatin/PAG ratio of 4. The gels were quenched at 4°C and conditioned at this temperature for 18 hr. The gel melting points are given in Table IV.

A value for ΔH_c of -80 kcal/mole falls within the range normally found for gelatin gels. From the melting points of the gelatin–PAG gels, it is seen that as long as the gelatin/PAG ratio is about 4, there are few PAG–PAG interactions, regardless of the absolute amount of PAG present. [Compare a melting point of 54.9°C (Table III) with one of 31° (Table IV) both at a PAG content of 20 g/l.] Although there is some scatter

TABLE IV
Melting Points of Aqueous Gelatin and 4/1 Gelatin-PAG Gels

Gelatin concn, g/l.	Melting point, °K	4/1 Gelatin-PAG concn, g/l.	Melting point, °K
20	299.5	20	298.5
40	301.2	40	300.5
60	302.0	60	301.7
80	302.5	80	302.0
100	303.1	100	304.0 (31.0°C)
ΔH_c, kcal/mole	−80		−62

in plots of log C versus $1/T$ for 20% PAG–gelatin gels, there is little doubt that the value of $-\Delta H_c$ for gelatin has been reduced. This is true whether or not PAG is treated as an inert diluent in computing the values of C. The lower value for $-\Delta H_c$ is not totally unexpected and could result from PAG impurities in the gelatin crystallite crosslink or from the inability of gelatin to form as large or as perfect crystallite crosslinks in the presence of PAG because of the lower mobility of the gelatin segments. We favor the latter possibility, since the log C versus $1/T$ plot shows a steeper slope than expected solely from depressions of the gel melting points.

The large difference in melting points of the gelatin and PAG gels discussed above which allow a study of mixed gels is probably ascribable to differences in molecular weight of the polymers involved. From Table I, a PAG gel (50 g/l.) having an $\bar{M}_n$ of 27.6×10^3 has a melting point of about 25°C. Gelatin gels having $\bar{M}_w$ between 50 and 60×10^3 at about 50 g/l. have similar melting points (see Table I of reference 9). Furthermore, by using the data of Eldridge and Ferry[9] to evaluate the constant in their derived relationship for gelatin gels

$$\log M_w = \Delta H_c/16RT + \text{constant} \tag{1}$$

at a given gelatin concentration, it can be easily shown that gelatin gels from high molecular weight gelatin should have melting points comparable to those from PAG of similar molecular size.

Considering that gelatin and undoubtedly PAG also form aggregates in solution and that it is these aggregates that link together later to give the gel, it is somewhat confusing to consider gelation in terms of the molecular weight of the molecularly dispersed polymeric specie. More important would be the molecular weight of the aggregate at the point of incipient gelation or the molecular weight of the freed aggregate at the moment the gel network is broken by raising the temperature. Eldridge and Ferry state that at the gel point the relationship

$$fm_{\text{cl}} = C/2\bar{M}_w \tag{2}$$

will hold. Here, f is a coefficient, m_{cl} is the concentration of crosslinks in moles per liter at the gel point, the fm_{cl} product is the concentration of noncyclic crosslinks at the gel point, and C is the concentration of polymer (in gram per liter). Instead of $\overline{M}_w$, one can consider the aggregate molecular weight which must be a function of C^2 (i.e., aC^2). If this substitution is made, and the result combined with an equilibrium constant for the binary association of free crosslinking loci, m_i, one obtains

$$K = m_{\text{cl}}/m_i^2 \tag{3}$$

$$K = 1/2aCfm_i^2 \tag{4}$$

Putting this expression in logarithmic form, differentiating with respect to temperature, and combining the result with van't Hoff's law, yields

$$-d \ln C/dt = \Delta H_c/RT^2 \tag{5}$$

which is the same expression as that obtained by Eldridge and Ferry. Like these authors, it is assumed that $d \ln m_i/dT$ and $d \ln f/dT$ equal zero. Although the difference in approach may seem trivial, it makes clear the unimportance of the molecular weight of the totally dissociated species in the derivation of expression (5) or its integrated form.

In the case of water-soluble polymers like PAG which dissolve if heat is supplied but which form thermally reversible gels, the extent of equilibrium swelling in H_2O at 25°C is very molecular weight-dependent. This is illustrated by the data of Table V.

TABLE V
Equilibrium Swelling of PAG Films in H_2O at 25°C

$[\eta]$ (2M NaCNS, 25°C), dl/g	$\overline{M}_n$	PAG, wt-% at equilibrium
0.31	5×10^4	5.2 (approx.)
0.64	1.9×10^5	19.7
2.50	2.7×10^6	36.0

Storage Stability and Rheology

We have found that dry samples of PAG stored at room temperature in brown bottles for prolonged periods of time (1–3 years) can undergo substantial decreases in intrinsic viscosity. At present, the cause of this deterioration is unknown. Although no germicidal reagent was present, it seems unlikely that in the dry form the polymer would be subject to attack by bacteria or fungi. Acrylamide[10,11] and AG[12] both undergo base-catalyzed polymerizations which involve hydrogen transfer. This reaction results in peptide groups in the polymer backbone which may be subject to hydrolytic or enzymatic attack. PAG prepared by radical initiation,[12] however, has been shown to yield only glycine upon hydrolysis, and this implies the absence of backbone amide groups in these polymers. Thermogravimetric analysis[3] of PAG has shown decomposition to begin at 260°C. However, when a sample of PAG was heated for 4 hr at 150°C under vacuum,[2] a decrease in the intrinsic viscosity in water from 4.05 to 2.60 was observed. It would seem therefore that there are a few weak links in the PAG backbone, perhaps, of the oxygen copolymer type, —$(M)_x$—O—O—$(M)_y$—, which undergo slow decomposition in the dry solid. Oxygen copolymers, of course have been reported for vinyl acetate[13] and other vinyl monomers.[14, 15] The decrease in molecular weight of dry PAG samples on storage may be related to the slow stage of the viscosity loss of aqueous polyacrylamide solutions.[16]

The deterioration of PAG on storage has caused us to report some erroneous viscosity measurements in paper 2 of this series (unpublished). Therein we reported that intrinsic viscosities are lower in 2*M* NaCNS than in H_2O. This is true only in the case of high molecular weight PAG, where the presence of NaCNS breaks up soluble aggregates. For PAG polymers of low $\overline{DP}$, where aggregation in dilute solution is not a problem, higher $[\eta]$ values are obtained in 2*M* NaCNS because of expansion of the random coil when intramolecular bonds are disrupted. This is amply illustrated by the data of Table VI, which describes the preparation of two samples of PAG and the results of viscosity measurements made shortly after polymer preparation. The polymers of Table VI were isolated by precipitation into methanol and purified by reprecipitation from water into methanol.

TABLE VI
Intrinsic Viscosities of PAG Homopolymers

Sample	Preparation	Temp, °C	H_2O		2M NaCNS	
			$[\eta]$, dl/g	k'	$[\eta]$, dl/g	k'
1	3 g AG, 27 ml H_2O, 4 ml isopropanol, 8 mg $K_2S_2O_8$; 65°C, 2 hr	25	0.153	0	0.310	0.9
		35	0.184	0	—	—
		40	0.209	0	0.335	0.6
		45	0.219	0	0.352	0.3
2	3 g AG, 30 ml H_2O, 1 ml isopropanol, 4 mg $K_2S_2O_8$; 65°C, 1 hr	25	6.2	0	2.5	0.9

A larger percentage increase in the $[\eta]$ in H_2O with increasing temperature and the higher viscosity (for sample 1) in the thiocyanate are added evidence that thiocyanate solution is a somewhat better solvent for PAG than H_2O. The η_{sp}/c for H_2O have zero slope in the range 25–45°C and hence a Huggins k' value of approximately zero. For thiocyanate solutions, the large decrease in k' with increasing temperature is also very unusual. The effects of temperature on k' are generally not very marked except in cases of polymer association which we do not believe is a factor with PAG in thiocyanate solution. (For stiff chain polymers, k' sometimes decreases with increasing temperature, but this also seems inapplicable.)

The viscosity of aqueous PAG solutions was determined as a function of shear at a temperature (81°C) considerably above the gel point and at concentrations of 3 and 5 wt.-% PAG. A polymer having $[\eta] = 0.93$

dl/g in 2*M* NaCNS at 25°C was used. Measurements were made on a Hoake Rotovisko instrument with the use of the NV cup attachment. The results are plotted in Figure 1. At the 3% concentration level, the shear dependence of viscosity is small, but at 5% the PAG solution is distinctly non-Newtonian, showing shear-thinning characteristics. Gelatin solutions ranging from 1.9 to 16.6 g/100 ml, measured over the temperature range 42–51°C and a pH range of 3.4–6.6 show viscosities which are virtually independent of shear rate.[17]

AG–Isopropylacrylamide Copolymers

Poly-*N*-isopropylacrylamide is a polymer which is soluble in cold water but which undergoes phase separation[18] when the temperature is raised to about 31°C. Aqueous PAG solutions, of course, form thermally reversible gels when the temperature is lowered below the gel point. We thought it might be interesting to see if copolymers of the two monomers could be produced which, in aqueous solution, gel on cooling and undergo phase separation on heating.

N-isopropylacrylamide (NIA) recrystallized from benzene–hexane and having a melting point of 64°C was used. The copolymerizations with AG described in Table VII were conducted at 25°C in sealed, evacuated glass test tubes. All copolymerization tubes contained in addition to the monomers, 16 ml of H_2O, 0.4 ml of isopropanol, and 5 mg of $K_2S_2O_8$. Conversions to polymer ranged from 10 to 20%. Isolation and purification methods varied with the particular copolymer, but involved either precipitation from water into methanol or acetone or the phase separation from H_2O with increasing temperature.

A plot of M_2 versus m_2 is presented in Figure 2. The data are interesting. The dotted curve would require values of approximately $r_1 = 3$ and $r_2 = 2$. This means that NIA free radical prefers to add NIA monomer and that

TABLE VII
Copolymerization of NIA (M_1) and AG (M_2)

						Characteristics of aqueous 10 wt-% copolymer solution	
Polymerization	AG, g	NIA, g	M_2[a]	N, %[b]	m_2[a]	Phase separation temp, °C	Gelation temp, °C
A	1.000	2.648	0.250	13.85	0.139	35–36	None
B	1.000	1.639	0.350	15.21	0.273	62–63	None
C	1.500	2.153	0.381	15.63	0.316	67–69	None
D	1.000	1.078	0.450	15.91	0.343	98–99 (?)	None
E	2.200	1.942	0.500	17.39	0.497	None	43

[a] M_2 represents the mole fraction of monomer 2 (AG) in the monomer mixture; m_2 is the mole fraction of monomer 2 in the copolymer.

[b] Nitrogen analysis of the copolymers by Clark Microanalytical Lab., Urbana, Ill.

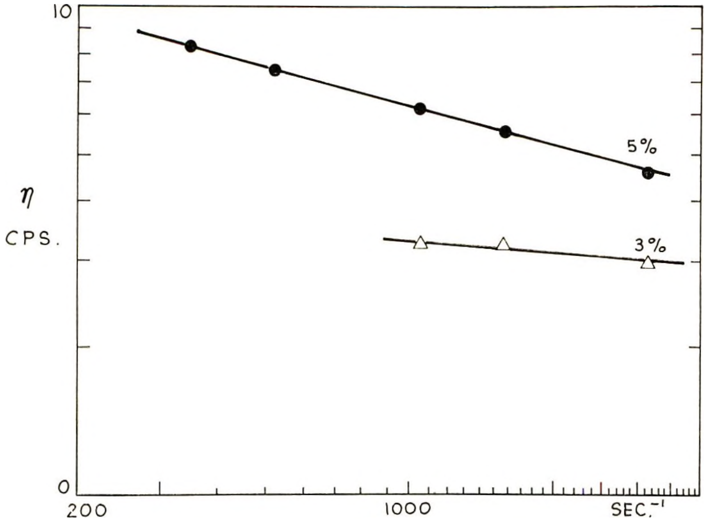

Fig. 1. Shear dependence of viscosity of aqueous PAG solutions, 81°C.

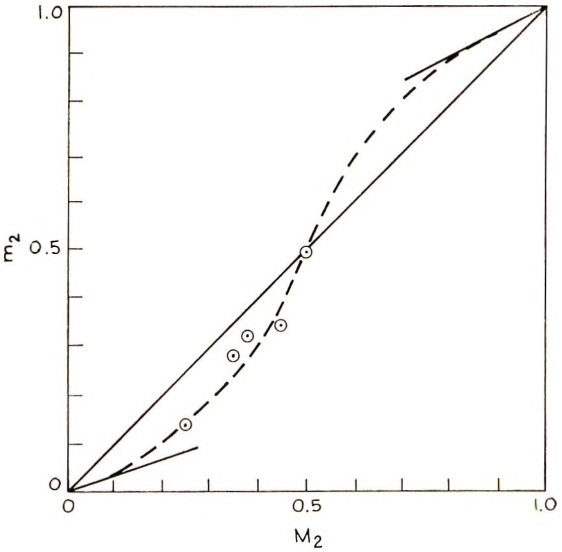

Fig. 2. Copolymerization of NIA(M_1) and AG(M_2).

AG free radical prefers to add AG monomer; the system is thus tending toward independent but concurrent polymerization of the two monomers. This is conceivable in a system of the AG–NIA type, where clustering in solution of AG monomer might occur by hydrogen bonding and clustering of NIA monomer (where hydrogen bonding is sterically hindered) by hydrophobic interactions of the isopropyl groups. However, no totally independent concurrent free-radical polymerizations are known and in fact there are few if any systems for which it has been definitely established that

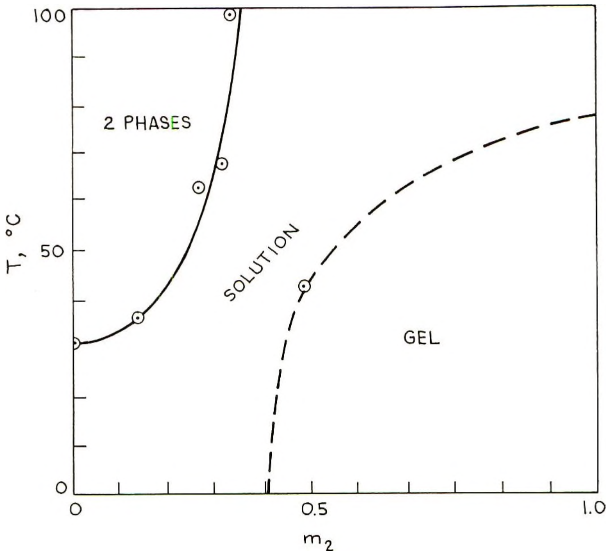

Fig. 3. Phase diagram (0–100°C) for the system NIA–AG copolymers and water.

the r_1r_2 product is significantly greater than unity. Q and e values of 0.81 and -0.46, respectively, for AG[2] and $Q = 0.40$ and $e = +0.47$ for NIA[19] certainly would not lead to the experimental copolymerization data for the AG–NIA system. We will leave this question in abeyance until more expanded copolymerization data are available. For the time being and for the discussion which follows we will assume the data are best approximated by a 45° line ($r_1 = 1$, $r_2 = 1$) which implies identical Q and e values for each monomer and equivalent reactivities of each monomer for each radical.

Solutions of the copolymers in water (10% by weight) were prepared, and their ability to undergo phase separation by slowly raising the temperature was investigated. Solutions of copolymers having a mole fraction of AG of approximately 0.40 or more do not show a cloud point up to 100°C. Similarly, it appears that when the mole fraction of NIA exceeds approximately 0.60, the solution will not gel down to 0°C. There is undoubtedly a narrow range of copolymer composition in this region where neither phase separation or gelation occurs between 0 and 100°C. Copolymer sample D is essentially a sample having these characteristics. The solution does not gel and it is a very borderline situation with regard to phase separation at 98–99°C. The phase diagram for 10 wt.-% solutions is illustrated in Figure 3. The sol–gel line is dotted, since the gel melting points are molecular weight-dependent. The ability to form copolymers which neither gel or have cloud points probably is related to the highly random placement of the two monomers in the copolymer backbone.

The authors wish to thank Mr. Paul Lubin for his help in carrying out a portion of the experimental work.

References

1. H. C. Haas and N. W. Schuler, *J. Polymer Sci. B*, **2**, 1095 (1964).
2. H. C. Haas, R. D. Moreau, and N. W. Schuler, *J. Polym. Sci.*, *A-1*, **5**, 915 (1967).
3. H. C. Haas, C. K. Chiklis, and R. D. Moreau, *J. Polym. Sci.*, *A-1*, **8**, 1131 (1970).
4. H. C. Haas, M. J. Manning, and M. H. Mach, *J. Polym. Sci.*, *A-1*, **8**, 1725 (1970).
5. H. C. Haas, R. L. MacDonald, and A. N. Schuler, *J. Polym. Sci.*, *A-1*, **8**, 1213 (1970).
6. K. Herrmann, O. Gerngross, and W. Abitz, *Z. Physik. Chem.*, **B10**, 371 (1930).
7. H. Boedtker and P. Doty, *J. Phys. Chem.*, **58**, 968 (1954).
8. H. Morawitz, *Proc. Paint Res. Inst.*, **38**, 59 (1966).
9. J. E. Eldridge and J. D. Ferry, *J. Phys. Chem.*, **58**, 992 (1954).
10. D. S. Breslow, G. E. Hulse, and A. S. Matlack, *J. Amer. Chem. Soc.*, **79**, 3760 (1957).
11. A. Leoni, S. Franco, and G. Polla, *J. Polym. Sci. A-1*, **6**, 3187 (1968).
12. Y. Iwakura, F. Toda, Y. Torii, and R. Sekii, *J. Polym. Sci. A-1*, **5**, 1585 (1967).
13. C. E. Baines, R. M. Elofson, and G. D. Jones, *J. Amer. Chem. Soc.*, **72**, 210 (1950).
14. J. Polacek, I. Kossler, and J. Vodehnol, *J. Polym. Sci. A*, **3**, 2511 (1965).
15. C. H. Bamford and P. R. Morris, *Makromol. Chem.*, **87**, 73 (1965).
16. W. P. Shyluk and F. S. Stow, Jr., *J. Appl. Polym. Sci.*, **13**, 1023 (1969).
17. H. G. B. de Jong, H. R. Kruyt, and J. Sens, *Kolloid Beih.*, **36**, 429 (1932).
18. M. Heskins and J. E. Guillet, *J. Macromol. Sci. (Chem.)*, **A2**, 1441 (1968).
19. Dr. C. Chiklis (Polaroid Corp.), private communication.

Received February 11, 1970

JOURNAL OF POLYMER SCIENCE: PART A-1 VOL. 8, 3417–3427 (1970)

Viscous Flow and Structure of Linear Polymers

G. M. BARTENEV, *Polymer Physics Research Laboratory, V. I. Lenin State Pedagogical Institute, Moscow, U.S.S.R.*

Synopsis

The viscosity of linear polymers obeys the logarithmic additivity rule. This is associated with the fact that the activation energy of the viscous flow within certain limits of parameters changes does not depend on temperature, stress, molecular weight, and content of active filler. The mechanism of viscous flow of linear polymers is associated with the reversible destruction of an unstable supramolecular structure typical of the polymers in the state of viscous flow. The effect of shear stress on the viscosity of linear polymers does not obey the Eyring equation. It is supposed that the effect of shear stress on viscosity is associated with the peculiar mechanism of the destruction of the supramolecular structure. At higher rates of viscous flow of the polymer, the activation energy can decrease as a result of the deep destruction of the supramolecular structure. This is a reversible process, as after removal of stress the supramolecular structure slowly reverts to its original state.

The viscous flow of linear polymers is characterized by the following distinctive properties: (1) high viscosity due to the high molecular weight of the polymers; (2) independence of the temperature coefficient of viscosity of molecular weight and stress; (3) a peculiar role of the stress high enough to reduce viscosity during processing; (4) a peculiar role of high elastic deformation occurring in viscous polymer flow.

Linear polymer melts having molecular weights greater than their critical ones are systems with very pronounced properties of non-Newtonian high-viscosity fluids. The viscosity of these systems is called structural viscosity and depends on shear stress, decreasing with increasing stress. The mechanism of viscous flow of the linear polymers considered below deals mainly with a less studied aspect of this complicated phenomenon: the effect of shear stress on viscous flow.

Rule of Logarithmic Additivity

From the investigations of Fox and Flory[1] of the effect of temperature and molecular weight on the viscosity of polyisobutylene as well as from the investigations by Bartenev and co-workers[2–6] of the effect of shear stress and active fillers on the viscosity of rubbery polymers, it follows that all the unbranched linear polymers having a molecular weight in excess of the critical one M_c obey the rule of logarithmic additivity of viscosity:

$$\log \eta = \log C + \log \eta_1(T) + \log \eta_2(P) + \log \eta_3(M) + \log \eta_4(\varphi) \qquad (1)$$

which can be expressed in a more concise form, where η_i are dimensionless functions of parameters T, P, M, and φ:

$$\eta = C\eta_1(T)\eta_2(P)\eta_3(M)\eta_4(\varphi) \tag{2}$$

where C is a constant characterizing the structure of polymer chains and having the dimension of viscosity, T is the absolute temperature, P is the shear stress, M is the mean molecular weight, and φ is the fraction volume of active filter.

The temperature dependence of the polymer viscosity is well studied and expressed by equation

$$\eta_1(T) = e^{U/kT} \tag{3}$$

where k is the Boltzman constant, U is the activation energy of the polymer viscous flow, which practically is the constant of the given polymer and which does not depend on stress and molecular weight (contour length of macromolecule). In a physical sense, the independence of molecular weight consists in the statistical independence of separate segments of a linear macromolecule.

The form of the function $\eta_2(P)$ and the mechanism of the dependence of viscosity on shear stress are discussed below. In the case of linear polymers,[7] for all $M > M_c$ the function $\eta_3(M)$ is equal to

$$\eta_3(M) = (M/M_c)^n \tag{4}$$

where $n = 3.5$. The function $\eta_4(\varphi)$ is expressed by a complex dependence on the volume fraction of active filler φ, but with small quantities of filler (as much as 10% by volume or $\varphi = 0.1$)

$$\eta_4(\varphi) = 1 + a\varphi \tag{5}$$

where the value of the dimensionless constant a depends on the behavior of filler and polymer. The value $a = 5$–10 is most typical of linear rubbery polymers.[6] Further, the effect of fillers will not be considered, because this problem is a subject of special consideration.

The rule of logarithmic additivity is applicable within a certain range of changes of temperature, stress, and molecular weight. At higher temperatures and stresses, deviations from this rule can take place because of the transition towards "chemical" flow or to chemical destruction of a polymer. The rule of logarithmic additivity means that when linear polymers flow, temperature and stress effects on viscosity are independent of each other. From this rule it follows, in particular, that the activation molecular mechanism of flow expressed by the function $\eta_1(T)$, does not undergo any changes with changing stress and molecular weight.

Effect of Shear Stress on the Viscosity of Linear Polymers

The effect of shear on viscosity is of prime importance in polymer processing, as the rheological properties determine the behavior of the material in many processes. This is associated with the fact that the polymers, being anomalous viscous systems, are characterized by a much greater increase of the shear rate with increasing stress than that resulting from the Newtonian law of viscous flow. In other words, the function $\eta_2(P)$ in eq. (2), and, consequently, the viscosity η essentially depends on shear stress.

It is observed that with lower molecular weights and higher temperatures the dependence of viscosity on shear stress gradually disappears, i.e., a transition to Newtonian flow with a constant viscosity is observed. Practically, this is realized in polymers having a molecular weight below the critical one. This simple case is not realized in polymers of high molecular weights.

In our papers[2,4] dealing with polyisobutylene it was established that this linear polymer is characterized by the following dependence of viscosity on shear stress:

$$\eta = \eta_0 e^{-\alpha P} \tag{6}$$

where the shear stress $P \geqslant 0$, and η_0 and α are constants. Consequently, $\eta_2(P) = \exp\{-\alpha P\}$, and with $\varphi = 0$, eq. (2) takes the form

$$\eta = C(M/M_c)^n \exp\{(U/kT) - \alpha P\} \tag{7}$$

The analysis of the data given in previous papers[8,9] on several linear polymers leads to the conclusion that the linear high polymers obey eq. (6). Consequently, rheologically, they may be classified into a special class of polymers, as their properties are different from those of low molecular polymers as well as linear branched polymers. For the former, $\alpha = 0$, and they are Newtonian fluids; for the latter, α is not constant.

As it is seen from the data given in Figures 1 and 2, not only polyisobutylene, but also other linear polymers obey to eq. (6) and are characterized by the independence of α of temperature. The independence of

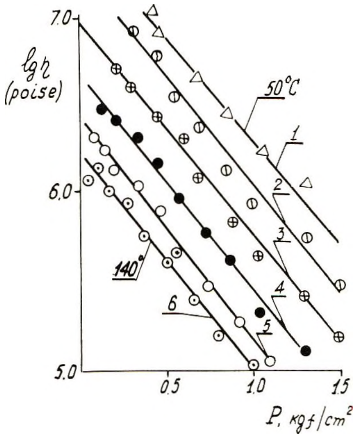

Fig. 1. Relations between the logarithm of viscosity and shear stress for natural rubber at different temperatures: (*1*) 50°C; (*2*) 60°C; (*3*) 80°C; (*4*) 100°C; (*5*) 120°C; (*6*) 140°C.

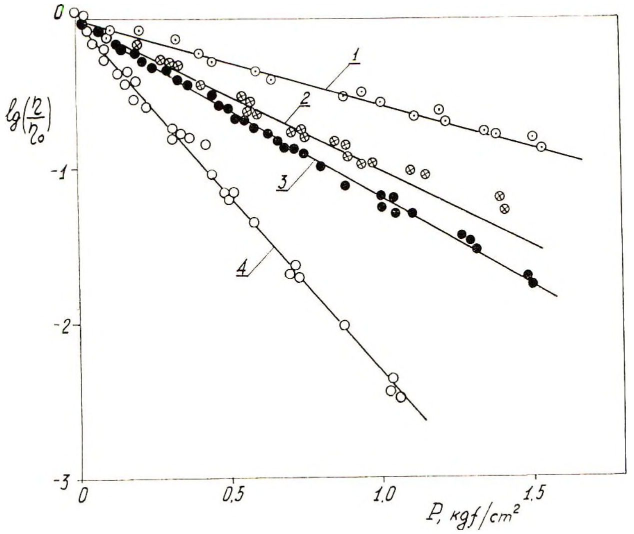

Fig. 2. Relation between the logarithm of relative viscosity and shear stress: (*1*) linear polyethylene with molecular weight of 92,000 in the temperature range 163–274°C; (*2*) weakly branched polyethylene with molecular weight of 178,000 in the temperature range 151–264°C;[8] (*3*)natural rubber in the temperature range 50°–140°C;[9] (*4*) polyisobutylene, with molecular weight of 900,000 in the temperature range of 20–140°C.[4, 14]

this constant of temperature can be illustrated by an example of the dependence of the logarithm of viscosity on shear stress for natural rubber (Fig. 1). The plot of these dependences is based on data given in a paper of Saunders and Treloar.[9] As it is seen, the experimental straight lines are parallel for all temperatures from 50°C to 140°C.

Table I summarizes the critical molecular weight, according to Bueche,[7] mean molecular weight, activation energy, constant α, and logarithm of constant C for certain polymers. It is seen from this table that the

TABLE I
Rheological Constants of Several Linear Polymers

Polymer	Molecular weight M	Critical molecular weight M_c	U, kcal/mole	α, cm²/kg	log C (poise)
Polyethylene					
Linear	92,000	2,000	6.8	1.3	−5.1
Weakly branched	178,000	—	9.8	2.8	—
Strongly branched	—	—	12.9	Depends on stress	—
Natural rubber	200,000	17,000	8.1	2.8	−1.7
Polyisobutylene					
Low molecular	60,000	17,000	13.4	2.0	−5.3
High molecular	900,000	17,000	13.4	5.5	−5.5

constant α depends on the molecular weight and the structure of the polymer chains. It must be expected that with $M < M_c$, $\alpha = 0$ and $n = 1$. Therefore, for low molecular polymers, eq. (7) takes a more simple form

$$\eta = C(M/M_c) \exp \left\{ \frac{U}{kT} \right\} \tag{7a}$$

where the activation energy U will decrease when the molecular weight approaches that typical of monomers.

Structure of Linear Polymers

It is known from papers by Kargin et al. that amorphous polymers are characterized by a supramolecular structure.[10] Since the van der Waals forces are responsible for molecular order in linear polymers, supramolecular structures in amorphous polymers must be weak and readily damaged by the effect of heat motion and stress. The level of molecular order in a linear polymer depends on temperature. The lower the temperature, the more pronounced is the supramolecular structure. Near the glass transition temperature, the forming of the polymer structure practically ceases because of the loss of molecular mobility.

At high temperatures (in the state of viscous flow), ordered structures become unstable and are readily destroyed, due to the lessening of molecular interaction between polymer chains and to the increased intensity of heat motion. Here, certain processes of molecule orientation appear to continue, and temporary ordered microregions ("microbundles" or microassembly or microblock) appear, instead of bundles whose length is much greater than that of molecules. The former, by their nature, resemble regions of short-range order in fluids but differ from them by higher stability and greater order due to the fact that the chain segments in microblocks are oriented primarily parallel to each other. The ordered microregions comprise structures which undergo continuous destruction in one place and formation in another place. The time of their life at high temperatures is short compared to the time of observation, but is much longer than that of the transition of free segments (not entering into microblocks) from one equilibrium location to another. Within a sufficiently long observation time, both the structure of the crystalline polymers melts and the structure of the amorphous polymers at high temperatures are accepted, on the average, as a structure of random chains. That is why under certain test conditions, for example, in tests of the thermodynamical (equilibrium) properties of network polymers, the model of random chains remains valid.

In general, the structure of rubbery polymers can, in first approximation to the real pattern, be represented as consisting of two regions: one, comprising free segments whose heat motion is quasi-independent; and another, microblocks or a molecular-ordered structure having ordered microregions of a fluctuating nature arranged throughout its entire volume.

A redistribution of the number of segments between the ordered and disordered regions of the polymer takes place with changing temperature and stress. The viscous flow of the linear polymer under the effect of stress follows the pattern of continuous destruction and rearrangement of the supramolecular structure. The greater the stress and the rate of viscous flow, the higher the rate and the degree of destruction.

Different Mechanisms of Non-Newtonian Flow

For a simple system comprising one type of kinetic unit, Eyring[11] proposed the equation

$$\eta(P) = \eta(0)\,\frac{z}{Shz} \tag{8}$$

where the parameter $z = \omega P/kT$ is the magnitude proportional directly to shear stress and to volume element ω accounted for by one kinetic unit of flow, and inversely proportional to absolute temperature; $\eta(0)$ is the viscosity at shear stress P approaching zero ("zero" viscosity). It depends on molecular weight and is a function of temperature

$$\eta(0) = Ae^{U_0/kT} \tag{9}$$

Within the range of low shear stresses the viscosity becomes Newtonian, as at $z \ll 1$, $Shz \cong z$, and $\eta = \eta(0)$.

Physically, the mechanism of the effect of shear stress on viscosity consists, according to Eyring, in the fact that the activation energy in the non-Newtonian region decreases with increasing shear stress, from a certain law.

From eqs. (8) and (9) it follows that at high stresses ($z \gg 1$) the structural viscosity obeys to equation

$$\eta(P) \cong A\,\exp\left\{(U_0 - \omega P)/kT\right\} \tag{10}$$

where $U_0 - \omega P = U$ is an activation energy depending on shear stress, and ω is the volume of a kinetic unit that can, for different systems, be an atom, a molecule, a colloid particle, or a segment of a macromolecule.

The Eyring mechanism of non-Newtonian flow does not presuppose any changes in the system structure at the transition from rest to flow; therefore the structural parameters A and U_0 in the process of flow are considered to be constant.

The shear stress or the rate of shear deformation can not only decrease the activation energy (from the Eyring mechanism), but also lead to a distruction of the structure and to a decrease in the viscosity, and the higher the rate of the flow, the greater the degree of destruction and the lower the viscosity. The processes of structure destruction appear to be pronounced in thixotropic dispersion systems. These systems are studied in most detail by Rehbinder and his colleagues.[12–15]

If the supramolecular structure of the polymer is destroyed, then, contrary to the Eyring mechanism, it should be taken into account that the "zero" activation energy U_0 in eq. (10) is not constant but changes at the transition from rest to flow.

The structure of any system is always rearranged during flow. In the case of the Eyring mechanism, the structure as a whole remains the same (original) during the process of rearrangement, and, therefore, after removal of the stress, the system practically regains instantly its original structure and physical properties. In the case of the Rehbinder mechanism, the structure changes, and its recovery time, after removal of stress, will be the thixotropic recovery time. The structure will be different immediately after removal of stress, approaching only gradually the original one. From the standpoint of thixotropy the Eyring mechanism can be observed in its pure form in a system which has a thixotropic recovery time equal to zero. In the other extreme case, when this time is very long, we deal with systems which are incapable of regaining their structure after its destruction.

Two common mechanisms of structural destruction are observed: energy-based and entropy-based. This classification in understandable, if we proceed from the general equation of viscosity proposed by Eyring:[11,16]

$$\eta = A_0 e^{-S/k} e^{U/kT} \tag{11}$$

where S is the entropy of the activation and U is the activation energy of the flow process.

The first mechanism applies to the case when the activation energy changes along with the change of the structure, while the entropy of activation practically remains unchanged. This mechanism is typical of the dispersion structures. The second mechanism applies to the case when the entropy of the activation changes along with the change of the structure, with the activation energy being unchanged. This mechanism is typical of linear polymers.

In the case of the entropy mechanism the entropy increases as a result of the transition from an ordered to a random structure in the process of the destruction of the supramolecular structures. In particular, let us suppose a linear dependence,

$$S = S_0 + bP$$

we obtain

$$\eta = B \exp \{(U/kT) - \alpha P\} \tag{12}$$

where $B = A_0 e^{-S_0/k}$ and $\alpha = b/k$.

The viscosity of the linear polymers obeys well the empirical equation (7). As it is seen, this equation coincides with eq. (12).

Flow Mechanism of Linear Polymers

The flow of the linear polymer can be presented as a result of the rearrangement of the supramolecular structure under the effect of heat motion and external loads. Even in the absence of external loads the system ap-

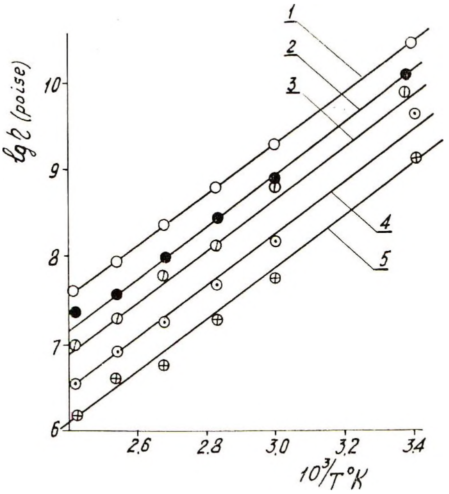

Fig. 3. Temperature dependences of the viscosity of polyisobutylene at different shear stresses, according to the authors' data: (*1*) 0; (*2*) 0.17 kg/cm²; (*3*) 0.31 kg/cm²; (*4*) 0.52 kg/cm²); (*5*) 0.73 kg/cm².

pears to have interior processes of destruction and formation of local ordered microregions. A certain concentration of elements of the supramolecular structure corresponds to each temperature.

The entropy mechanism of the structural viscosity of linear polymers has been proposed and expounded.[2,3] The molecular nature of the mechanism is as follows. During flow, the supramolecular structure of the polymer undergoes destruction reversibly, and it is greater, the higher the shear stress. The destruction of the structure occurs so that the polymer chain segments, which are elements of supramolecular structures (microblocks), break away one at a time. The activation energy of the transition of the

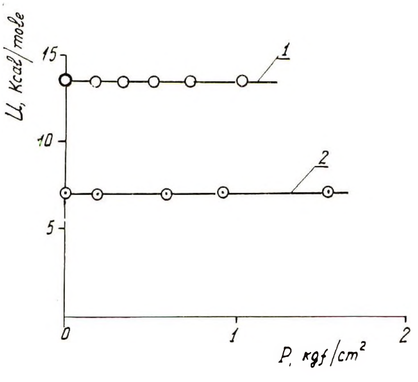

Fig. 4. Invariance of the activation energy of the viscous flow: (*1*) polyisobutylene in the stress range of 0.005–1.1 kg/cm² and at a rate of deformation from 10^{-5} to 10 sec^{-1}; (*2*) linear polyethylene in the stress range of 0–1.5 kg/cm² and a rate of deformation from 0 to 1600 sec^{-1}.

segments to the free state is therefore equal to that of polymer flow. The separation of segments from microblocks occurs due to the effect of heat motion, whereas the stress is not great enough to have a substantial effect on the breaking away of segments. Therefore the activation energy must be constant in a certain range of stresses.

The probability of the reverse process, i.e., transition of segments from the free state to the ordered one, depends on the stress value and decreases with increasing shear stress, as the latter readily carries away the separated segments and, thereby, hinders the reverse process or adhesion of free segments to microblocks. As a result the average number of free segments increases with increasing stress, and the viscosity decreases.

Thus, the shear stress results in the indirect rather than direct destruction of the supramolecular structure, as the effect of the stress appears to diminish the probability of the recovery of the structure. The activation energy does not depend on stress, because it is determined not by the average number of elements of the supramolecular structure, but by their nature. Hence, it follows that the stress has effect not on the energy, but on the entropy of the activation during flow.

The temperature dependence of the viscosity of polyisobutylene at different shear stresses (Fig. 3) can, experimentally, bear out the independence of the activation energy of stress. In Figure 3 the slope of all the straight lines is the same.

The invariance of the activation energy of the viscous flow of polyisobutylene and the melting of linear polyethylene in the range of low stresses is seen from Figure 4. For polyethylene the activation energy is calculated from data obtained by Shott and Kaghan.[8]

It is natural to expect that at higher rates of viscous flow incident to the full destruction of the supramolecular structure, the activation energy will, with increasing shear stress, decrease to a level characteristic of the heat motion of free segments. This phenomenon was observed by the authors for divinyl rubber (Fig. 5). We observed, in a certain range of stresses, two states of the polymer: one with a mildly disrupted and another with a heavily disrupted supramolecular structure. The former state is characterized by an activation energy of viscous flow equal to 5.6 kcal/mole, and the latter by an activation energy of 2 kcal/mole.

Let us return now to eq. (10) in connection with the experimental data given. By comparing the experimental data it is easy to conclude that eq. (10) does not cover the observed decrease of the viscosity (Fig. 2), as the activation energy does not change (Fig. 4). The cause of this may be understood, on the basis of numerical calculations.

It is known that one segment of rubbery polymer macromolecules consists of 30–40 carbon atoms in the main valence chain, which corresponds to the length of a chain segment of 35–50 Å. As the distance between the chains in a polymer is about 5 Å, the volume of one segment is 0.9×10^{-21}–1.2×10^{-21} cm^3. The substitution of the segment volume ($\omega = 10^{-21}$ cm^3), which is typical of the polymers, into eq. (10) indicates that this

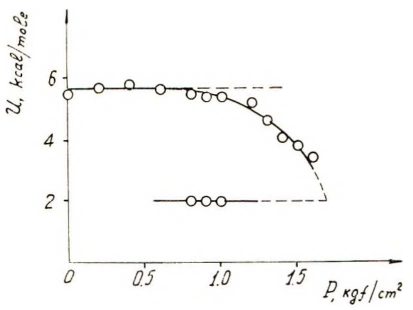

Fig. 5. Effect of shear stress on the value of the activation energy of the viscous flow of divinyl rubber.

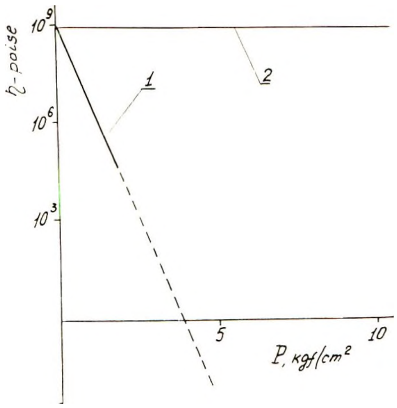

Fig. 6. Dependences of the viscosity of polyisobutylene at 80°C ($\lg \eta_0 = 8.8$) on shear stress, as calculated: (*1*) from the authors' eq. (6), at $\alpha = 5.5$ cm²/kg; (*2*) from the Eyring equation (8) at $\omega = 10^{-21}$ cm³ and $U_0 = 13.4$ kcal/mole.

equation does not at all yield any decrease of the viscosity within the stress range under investigation (Fig. 6). It turns out that $z \ll 1$ and $\eta(P) = \eta(0)$. A decrease of the viscosity, according to eq. (10), will occur, but at much greater stresses being far beyond the limits of stresses. This result substantiates that the Eyring mechanism does not explain the dependence of the polymer viscosity on stress.

It will be very much to the point to note that this conclusion does not touch the diffusion-segmental mechanism of the polymer flow, also proposed by Eyring.

In order that the general diffusion-segmental Eyring mechanism of viscous flow will agree with the flow mechanism associated with the destruction of the supramolecular structure, it should be borne in mind that the destruction and formation of supramolecular structure elements in rubbery polymers in the region of viscous flow proceeds by breaking away or by adhesion of separate segments of linear macromolecules.

References

1. T. G. Fox and P. J. Flory, *J. Amer. Chem. Soc.*, **70,** 2384 (1948).

2. G. M. Bartenev, *Dokl. Akad. Nauk SSSR*, **133,** 88 (1960).

3. G. M. Bartenev, *Vysokomol. Soedin.*, **6,** 2155 (1964).

4. G. M. Bartenev and L. A. Vishitskaya, *Vysokomol. Soedin.*, **6,** 751 (1964).

5. I. V. Zakharenko, F. S. Tolstoukhina, and G. M. Bartenev, *Kolloid. Zh.*, **22,** 168 (1960).

6. G. M. Bartenev and N. V. Zakharenko, *Kolloid. Zh.*, **24,** 121 (1962).

7. F. Bueche, *Physical Properties of Polymers*, Wiley, New York, 1962.

8. H. Shott and W. S. Kaghan, *J. Appl. Polym. Sci.*, **5,** 175 (1961).

9. D. Saunders and L. Treloar, *IRI Trans.*, **24,** 92 (1948).

10. V. A. Kargin and G. L. Slonimskii, *Brief Outlines of the Physico-chemistry of Polymers*, Izdat. Khim., Moscow, U.S.S.R., 1967.

11. H. Eyring, *J. Chem. Phys.*, **4,** 283 (1936).

12. L. A. Abduragimova, P. A. Rehbinder, and N. N. Serb-Serbina, *Kolloid. Zh.*, **17,** 184 (1955).

13. N. V. Mikhailov and A. M. Likhtgeim, *Kolloid. Zh.*, **17,** 364 (1955).

14. L. V. Ivanova-Tchumakova and P. A. Rehbinder, *Kolloid. Zh.*, **18,** 429 (1956).

15. V. A. Fedotova, H. Khadzaeva, and P. A. Rehbinder, *Dokl. Akad. Nauk USSR*, **170,** 1133 (1966).

16. S. Glasstone, K. Laidler, and H. Eyring, *The Theory of Rate Processes*, McGraw-Hill, New York, 1941.

Received February 17, 1970

JOURNAL OF POLYMER SCIENCE: PART A-1   VOL. 8, 3429–3433 (1970)

Photosensitization of Vinyl Polymerization by Uranyl Ions

K. VENKATARAO and M. SANTAPPA, *Department of Physical Chemistry, University of Madras, Madras 25, India*

Synopsis

Monomer acrylamide was used as quencher of uranyl ion fluorescence and Stern-Volmer plots were constructed at three monochromatic wavelengths of exciting radiation. The results indicated that the reaction between excited uranyl ion and monomer is one of energy transfer. The rate parameters $k_p/k_t^{1/2}$ and k_d'/k_i were calculated from the polymerization kinetics at high monomer concentrations. A general mechanism for the photopolymerization of vinyl monomers sensitized by uranyl ions is proposed and discussed.

Introduction

Uranyl ion has been used as a photooxidant[1] and a photoinitiator of vinyl polymerization.[2] We reported earlier results of photoreduction of uranyl ions by aliphatic alcohols and aldehydes[3] and of photosensitized polymerization of acrylamide and methacrylamide by uranyl ions (paper I in this series).[4] We have also studied the quenching of uranyl ion fluorescence by aliphatic alcohols and aldehydes[5] and concluded that the quenching of fluorescence and electron-transfer reaction were one and the same. It was believed that a study of quenching of uranyl ion fluorescence by monomers would solve the problem of the nature of the primary process in the photoinitiation of polymerization by uranyl ions. As a typical case, acrylamide was used as the quencher of uranyl ion fluorescence. The studies revealed that the primary process is indeed an energy-transfer reaction. Further studies on the polymerization kinetics at high monomer concentrations gave a method for calculating $k_p/k_t^{1/2}$ and k_d'/k_i for acrylamide. A detailed mechanism for the kinetics of photoinitiation of polymerization by uranyl ion is given and discussed.

Experimental

The chemicals used were purified as described in our earlier paper,[3] and the photochemical arrangement along with the reaction cell was also described earlier.[6] The fluorescence quenching studies were made in the same manner as described for the organic reducing agents in our earlier paper.[5] The photopolymerization of acrylamide sensitized by uranyl ions at high monomer concentrations (0.1–1.0M) was done with low light intensities at $\lambda = 436$ mμ and 365 mμ. Diffuse daylight was scrupulously avoided during the experiments.

Results and Discussion

Fluorescence quenching studies were made with 0.01M uranyl perchlorate, 0.1M perchloric acid, and acrylamide (10^{-4}–$10^{-3}M$) at three monochromatic wavelengths of light (436 mμ, 405 mμ, and 365 mμ). The Stern-Volmer plot is linear (Fig. 1) and from the slope and intercept, the value of $k_q/(k_d + k_f) = 717$ was calculated. This indicates that under the experimental conditions with monomer concentrations $\geq 0.1M$, the fluorescence of uranyl ions is quenched up to 98%. Hence, if the primary reaction between excited uranyl ion and the monomer molecule is an elec-

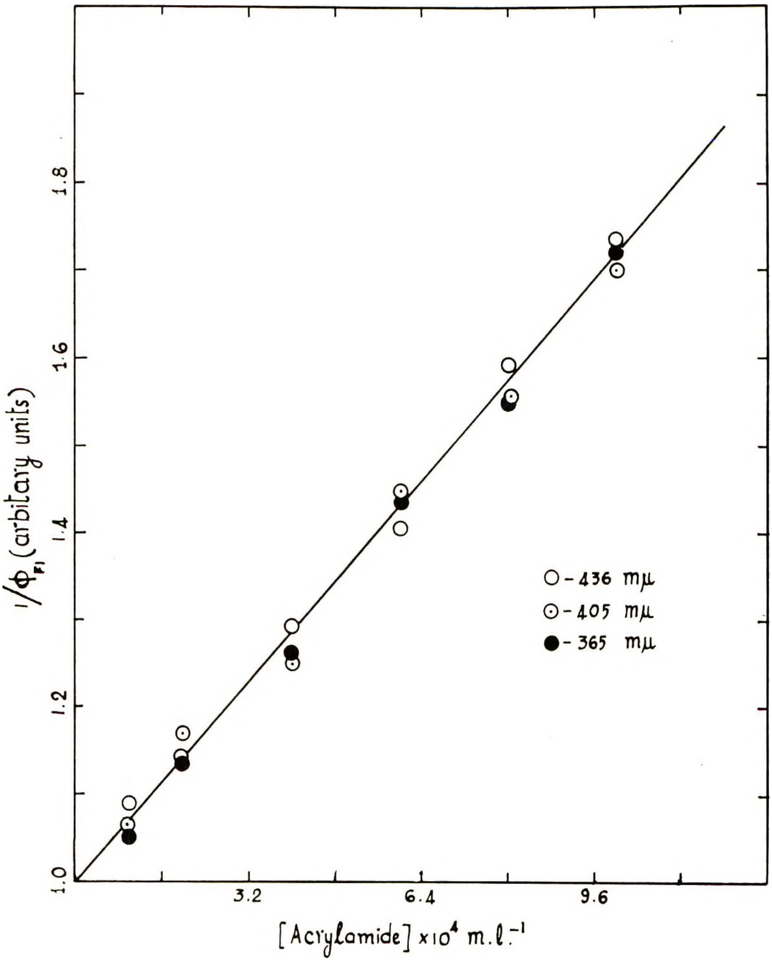

Fig. 1. Stern-Volmer plot for the quenching of uranyl ion fluorescence by acrylamide.

tron-transfer reaction, the rate of initiation should be independent of monomer concentration, and the rate of polymerization R_p should be proportional to [M]. However, our previous studies[4] clearly indicated that the rate of initiation is proportional to $[M]^{1/2}$ and R_p is proportional to $[M]^{3/2}$. This, along with the fact that no reduction of U^{6+} to U^{4+} was observed in the reaction mixture,[4] supports the energy-transfer mechanism proposed by us earlier. Further, it may be seen that, though there is a weak complex formation between uranyl ion and the monomer acrylamide (indicated by the increasing absorbancy of the reaction mixture with increasing [M]), it has no influence over the primary reaction step. Taking into account all these facts, the following improved mechanism is suggested for the photopolymerization of acrylamide by uranyl ions, the system being at a constant pH = 1.0.

$$UO_2^{++} + h\nu \xrightarrow{k\epsilon I} UO_2^{++}{}^* \tag{1}$$

$$UO_2^{++*} \xrightarrow{k_d} UO_2^{++} + \Delta \tag{2}$$

$$UO_2^{++*} \xrightarrow{k_f} UO_2^{++} + h\nu' \tag{3}$$

$$UO_2^{++*} + M \xrightarrow{k_q} UO_2^{++} + M^* \tag{4}$$

$$M^* + M \xrightarrow{k_i} 2R_1 \tag{5}$$

$$M^* \xrightarrow{k_d'} M + \Delta' \tag{6}$$

$$R_1 + M \xrightarrow{k_p} R_2 \tag{7}$$

$$\vdots$$

$$\cdots\cdots$$

$$\cdots\cdots$$

$$\cdots\cdots$$

$$R_{r-1} + M \xrightarrow{k_p} R_r \tag{8}$$

$$R_r + R_s \xrightarrow{k_t} P_r + P_s \tag{9}$$

Here R_r is the polymer chain radical with chain length r and P_r is the polymer with chain length r. The above mechanism assumes that the reaction between UO_2^{++*} and monomer gives an excited monomer molecule through energy transfer, which reacts with another monomer molecule to give two free radicals [step (5)]. The visible spectrum of uranyl ion in the region 360–500 mμ, was attributed to the excitation from a ground singlet to lowest triplet states, by De Jaeger and Govers[7] ($^3\pi_{0u} \leftarrow {}^1\Sigma^+{}_{0g}$, $^3\pi_{1u} \leftarrow {}^1\Sigma^+{}_{0g}$ and $^3\pi_{2u} \leftarrow {}^1\Sigma^+{}_{0g}$). Krongauz[8] observed that in the photosensitized polymerization of methyl methacrylate participation of monomer triplet in the initiation reaction with triplet state energy level between 2.2 and 2.5 eV (495–500 mμ) was possible. Methyl methacrylate was also found to quench the fluorescence of uranyl ions similar to acrylamide. It may therefore be assumed that with acrylamide also there is a probability of transfer of excitation energy from uranyl ion triplets to monomer triplet to produce an excited monomer molecule. More information with regard to the exact nature of the excited monomer triplet and its reaction with another monomer molecule cannot be gained from our fluorescence or kinetic studies alone, though it may be supposed that M* is in the form of a transient diradical (because of the spin uncoupling of a π bond) which extracts an electron from another monomer molecule to produce two monoradical ions whose charges may be neutralized by counterions in the solution. From the mechanism proposed above, expressions for rate of polymerization R_p easily follow:

$$R_p = \frac{\sqrt{2}\, k_p k_\epsilon^{1/2} I^{1/2} [\mathrm{M}]^{3/2}}{k_t^{1/2}\{(k_d'/k_i) + [\mathrm{M}]\}^{1/2}} \tag{10}$$

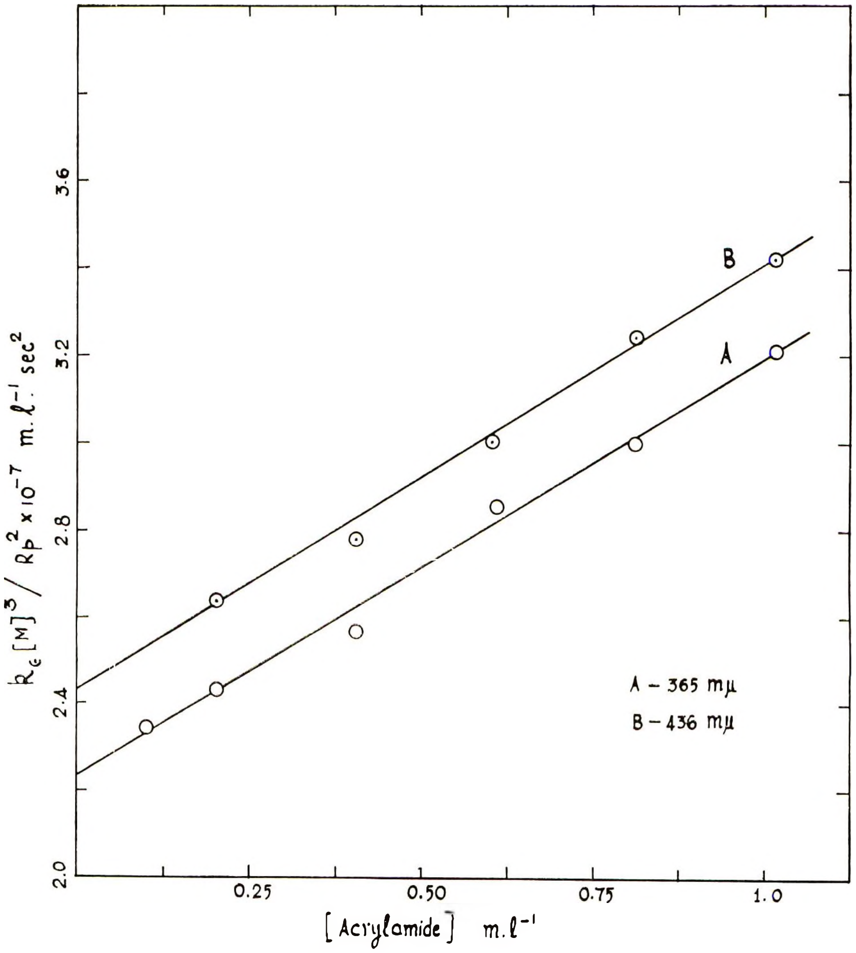

Fig. 2. Plot of $k_\epsilon[\mathrm{M}]^3/R^2_p$ vs. [M]: (A) = 365 mμ, intensity = 1.26 × 10^{-7} $Nh\nu$/l. sec; (B) = 436 mμ, intensity = 1.148 × 10^{-8} $Nh\nu$/l. sec.

$$\frac{1}{R_p^2} = \frac{k_t k_d'}{2k_p^2 k_i k_\epsilon I[\mathrm{M}]^3} + \frac{k_t}{2k_p^2 k_\epsilon I[\mathrm{M}]^2} \tag{11}$$

$$k_\epsilon[\mathrm{M}]^3/R_p^2 = (k_t k_d'/2k_p^2 k_i I) + (k_t[\mathrm{M}]/2k_p^2) \tag{12}$$

Since the absorbancy of the reaction mixture increases with increasing [M] (0.1–1.0 M), the k_ϵ values were computed independently for each [M] used. At high [M], $k_\epsilon[\mathrm{M}]^3/R_p^2$ was plotted against [M] (Fig. 2). From the slope and intercept values, $k_p/k_t^{1/2}$ and k_d'/k_i values were calculated. The values are for 436 mμ, $k_p/k_t^{1/2} = 2.096$, $k_d'/k_i = 2.46$; for 365 mμ, $k_p/k_t^{1/2} = 2.123$; $k_d'/k_i = 2.538$. These $k_p/k_t^{1/2}$ values agree very well with those given by Natarajan and Santappa.[9] The effect of H^+ ion on R_p can still be explained by the formation of monomer cations:

$$\mathrm{M} + \mathrm{H}^+ \rightleftarrows \mathrm{MH}^+ \tag{13}$$

Our thanks are due to the C.S.I.R., New Delhi for providing a Senior Research Fellowship to one of us (K. V. R.) during the tenure of which this work was carried out.

References

1. R. L. Belford and E. Rabinowitch, *Spectroscopy and Photochemistry of Uranyl Compounds*, Pergamon Press, Oxford, 1965.
2. V. Mahadevan and M. Santappa, *J. Polym. Sci.*, **50**, 361 (1961).
3. K. Venkatarao and M. Santappa, *Z. Physik. Chem.* (Frankfurt), **54**, 101 (1967).
4. K. Venkatarao and M. Santappa, *J. Polym. Sci. A-1*, **5**, 637 (1967).
5. K. Venkatarao and M. Santappa, *Z. Physik. Chem.* (Neue Folge), **66**, 308 (1969).
6. K. Venkatarao and M. Santappa, *J. Mysore Univ. Sect. B*, **21**, 51 (1968).
7. S. De Jaeger and T. Govers, *Nature*, **205**, 900 (1965).
8. V. A. Krongauz, *Teor. Eksper. Khim., Akad. Nauk Ukr. SSR*, **1**, 47 (1965).
9. L. V. Natarajan and M. Santappa, *J. Polym. Sci. A-1*, **6**, 3245 (1968).

Received September 9, 1969
Revised November 18, 1969

JOURNAL OF POLYMER SCIENCE: PART A-1 VOL. 8, 3435–3442 (1970)

Copolymerization of Styrene and Butadiene in Emulsion. I. Composition of the Latex Particles

G. M. BURNETT, G. G. CAMERON, and P. L. THORAT,
Department of Chemistry, University of Aberdeen,
Old Aberdeen, Scotland

Synopsis

The composition of the latex particles during intervals I and II of the emulsion polymerization of styrene and butadiene (initial weight ratio 71 parts butadiene:29 parts styrene) has been determined at 5, 15, and 25°C. The monomer content of the latex particles diminishes linearly with conversion. The composition ratio (weight styrene: weight butadiene inside the particles divided by weight styrene:weight butadiene in the binary phase) also decreases with conversion, the decrease being particularly marked as the end of interval II is approached. It is shown that the assumptions embodied in the theory of Medvedev et al. are incorrect. The results are compared with the recent theories of Gardon.

INTRODUCTION

The progress of most emulsion polymerizations can be differentiated into three distinct intervals. During interval I, active latex particles are formed which provide the sites for propagation. In interval II no new latex particles are formed, and the system comprises three phases: monomer droplets which contain free monomer and act as reservoirs, latex particles in which polymerization proceeds, and the aqueous phase. The end of interval II and the beginning of interval III coincide with the disappearance of the monomer droplets, and at this point the remaining free monomer is all dissolved in the latex particles. An important assumption of the well-known Smith-Ewart theory[1] is that during interval II the monomer:polymer ratio in the latex particles is virtually constant. It has been shown that for some systems this assumption is not strictly correct, although Gardon[2] has recently pointed out that it is a good approximation. Most of the experimental work relevant to this theory has been concerned with homopolymerizations; there is very little information in the literature on variations with conversion of the monomer and polymer composition of the latex particles for copolymerizations.

The work described in this paper was aimed at clarifying this situation in the case of the commercially important SBR system (initial monomer weight ratio 71 parts butadiene:29 parts styrene). The results provide a practical test of Gardon's[2] predictions regarding the composition of the latex particles in binary emulsion copolymerizations. They are also a necessary precursor to the studies of cross-linking described in Part II of this work.[3]

When two monomers are present, there are immediate problems in analyzing the contents of the latex particles, particularly when one monomer, in this case butadiene, is volatile. For this reason a circuitous method of determining the free butadiene was adopted. This method requires prior knowledge of the reactivity ratios for the copolymerization; the results obtained are dependent to some extent on the values chosen for these parameters.

EXPERIMENTAL

Polymerization

The bottle polymerization method was adopted with a standard 1500-type SBR recipe[4] as shown in Table I. Freshly distilled monomers were used, the butadiene being added in excess and the surplus vented off in a stream of oxygen-free nitrogen. This procedure also removed the air from the bottles. Polymerizations were carried out in a thermostatted water tank. The bottles were rotated end-over-end at 35 rpm. Conversions were determined by the syringe-solids method.

Determination of Styrene:Polymer Ratio in Latex Particles

In these experiments the polymerization was first short-stopped by admitting oxygen. The bottle contents were then divided into two portions

TABLE I
Recipe for Emulsion Copolymerization of Styrene and Butadiene[a]

	Level, phm[a]
Butadiene	71
Styrene	29
p-Menthane hydroperoxide (initiator)[b]	0.06
tert-Dodecyl mercaptan (TDM-modifier)	Variable
Emulsifier	
Water	200
Disproportionated rosin acid soap (Dresinate 214)	5.0
Trisodium phosphate dodecahydrate (buffer)	0.5
Secondary emulsifier (Orotan)	0.1
Activator[b]	
Ferrous sulfate heptahydrate	0.02
EDTA (complexing agent)	0.03
Sodium formaldehyde sulfoxylate	0.05

[a] Figures refer to parts per hundred parts of monomer by weight.

[b] The initiator (I) and activator (A) levels in the above recipe are half those in the standard recipe and are referred to as I/A level of 50/50. Similarly 25/25 refers to half of the above quantities.

one of which was used to determine the conversion. The other portion was poured into a 50-ml polypropylene centrifuge tube fitted with a metal cap and spun at 5000 *g* for 3 min at 0 ± 1°C in a temperature-controlled centrifuge. This operation was carried out as quickly as possible. The emulsion separated into two layers, the upper layer containing monomer from the droplets and the lower aqueous layer containing the latex particles, soap etc.

The aqueous layer was removed by hypodermic syringe via the base of the tube. A weighed portion was dissolved in 250 ml of a benzene–isopropanol mixture (80:20 by volume). This solution was then analyzed for styrene spectrophotometrically by using a Beckmann instrument at 282.5 mμ. Beer's law was valid for this system, and substances other than styrene did not interfere in the measurements. The polymer content of the sample was determined by evaporating a portion of this solution to dryness in a vacuum oven, a correction being applied for the solids such as soap etc. from the original recipe. A satisfactory alternative procedure for the polymer estimation was to evaporate the benzene–isopropanol solution to a small volume and to precipitate the polymer in excess isopropanol. Agreement between the two methods was excellent. During the centrifugation no attempt was made to estimate the butadiene. However, the butadiene loss was kept to a minimum to guard against disruption of the latex, and while the quantitative retention of the butadiene was impossible, the losses prior to and during centrifugation were small.

It was found that no polymer could be obtained from the upper monomer layer, confirming that all the polymer was in aqueous portion and that none was formed in the monomer droplets.

Copolymer Composition

The styrene content of the copolymers was determined spectrophotometrically at 262 mμ in chloroform by the method of Meehan.[5] The fraction x of styrene in the copolymer is given by

$$x = (E_C - E_B)/(E_S - E_B)$$
$$= 0.462\, E_C - 0.0185$$

in which E_C, E_S, and E_B are the specific extinction coefficients of the copolymer, pure polystyrene, and pure polybutadiene, respectively. The butadiene content was found by difference.

RESULTS

The weight ratios of styrene:polymer in the latex particles at 5, 15, and 25°C are plotted in Figure 1, which shows that at a given conversion this ratio increases with increasing polymerization temperature, and at a given temperature decreases with increasing conversion.

The variation of cumulative copolymer composition with temperature and conversion is shown in Figure 2. Temperature variation within the

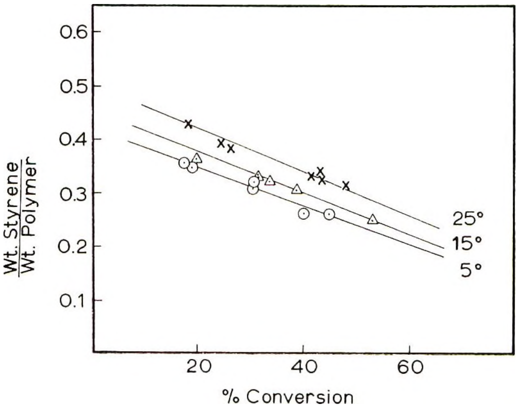

Fig. 1. Weight ratio of monomeric styrene to polymer in the latex particles as a function of conversion.

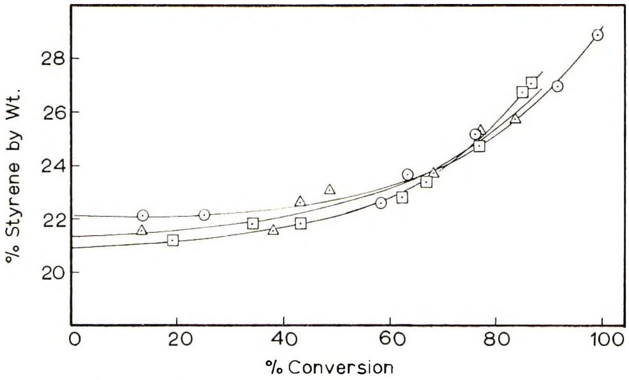

Fig. 2. Styrene in the copolymer as a function of conversion: (⊙) 5°C; (△) 15°C; (⊡) 25°C.

present range has a comparatively minor effect on composition, but an increase in temperature lowers slightly the styrene content of the polymer formed initially.[6] As has been previously observed,[4] the styrene content increases slowly with conversion at first but much more rapidly beyond 60% conversion. In the present context the incremental copolymer composition is more important than the average or cumulative composition. The incremental and cumulative composition are linked by the equation of Wall:[7]

$$[\bar{\bar{g}}] = [\bar{g}] + W \frac{d[\bar{g}]}{dW} \qquad (1)$$

where $[\bar{g}]$ is the weight average property, in this case composition, as a function of conversion, W. The incremental composition $[\bar{\bar{g}}]$ is calculated by applying eq. (1) to the smoothed curves in Figure 1. The results of this operation are shown in Figure 3. It is noticeable that the cumulative and

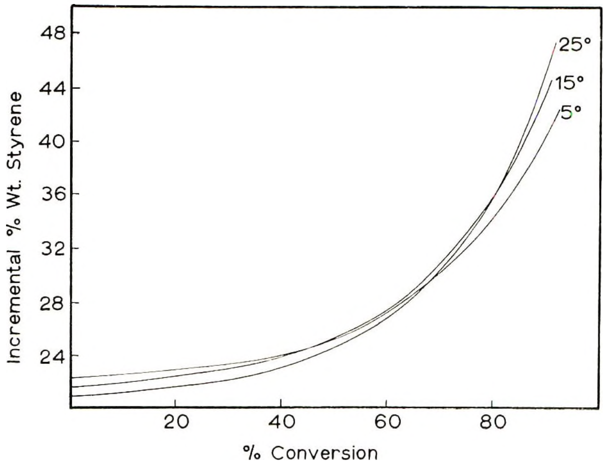

Fig. 3. Incremental content of styrene in the copolymer as a function of conversion.

incremental compositions diverge as polymerizations proceeds. Thus at 100% polymerization the average copolymer composition is the same as the initial feed (29% styrene), while the final increment formed contains over 40% styrene.

DISCUSSION

The copolymer composition equation is

$$\frac{dM_1}{dM_2} = \frac{[\mathrm{M}_1]}{[\mathrm{M}_2]} \left\{ \frac{r_1([\mathrm{M}_1]/[\mathrm{M}_2]) + 1}{([\mathrm{M}_1]/[\mathrm{M}_2]) + r_2} \right\}$$

where r_1 and r_2 are the reactivity ratios of monomers 1 and 2 (styrene and butadiene, respectively), $[\mathrm{M}_1]/[\mathrm{M}_2]$ the molar feed ratio of monomers, and dM_1/dM_2 the monomer ratio in the increment of copolymer formed. Therefore knowing r_1 and r_2 and the incremental composition of the copolymer as a function of conversion, as in Figure 3, the molar feed ratio of the monomers in the latex particles as a function of conversion can be calculated.

Ideally r_1 and r_2 should be the "true" values applicable to bulk homogeneous polymerization, since the situation in the latex particles approximates to a micro-bulk copolymerization. Reactivity ratios from emulsion copolymerization based upon overall monomer composition are not necessarily the same as the "true" values, except at very low conversions, since the overall free monomer ratio may not correspond to that within the growing particles. Unfortunately, there are few reliable data on bulk copolymerization in the literature, and in many cases where an emulsion system has been employed the conversion is not stated explicitly. The reactivity ratios used in the present calculations were obtained by interpolation of the data referred to by Orr and Williams.[6] These are likely to be the most reliable and form a straight line plot of log r versus $1/T$. The interpolated values of r_1 and r_2 respectively, at 5, 15, and 25°C are: 0.440, 1.400; 0.476, 1.413; and 0.490, 1.420. The temperature dependence of reactivity ratios is small. The incremental monomer feed ratios $[M_1]/[M_2]$ in the latex particles were calculated using the above reactivity ratios and the incremental copolymer composition curves in Figure 3. The monomer feed ratio together with the styrene:polymer ratios from the smoothed curves in Figure 1, yield the ratio of total weight of monomers:total weight of polymer in the latex particles during the course of the polymerization. The data from these calculations are shown in Figure 4, which also includes

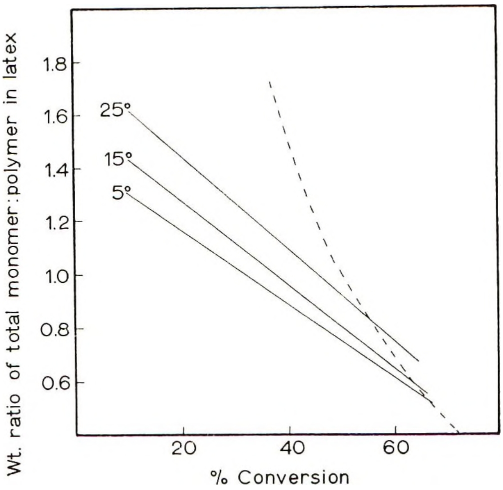

Fig. 4. Weight ratio of total free monomer to polymer in the latex particles as a function of conversion: (---) weight ratio if all free monomers were present in latex particles throughout polymerization.

the theoretical curve that would result if all the unpolymerized monomers were located within the latex particles. The points of intersection of the extrapolated polymer curves therefore indicate the conversion at which the monomer droplets disappear, i.e., the end of interval II of the polymerization. This point is reached between 55 and 65% conversion, in good agreement with previous results.[8] Figure 4 also suggests that the end of interval II occurs at a lower conversion as the temperature is increased. The monomer:polymer ratio decreases continuously during interval II in agreement with the prediction of Gardon.[2] The decrease corresponds to a decrease in the volume fraction of the monomer of approximately 20 to 30%. Bearing in mind that part of this decrease is probably attributable to progressive crosslinking of the polymer in the latex particles with increasing conversion,[2] these figures are in reasonable agreement with Gardon's suggested maximum of 25%.[2]

From the data just discussed it is a simple step to calculate the monomer ratio in the monomer droplets and compare this with the corresponding figure within the latex particles, to obtain the composition ratio K, given by:

$$K = \frac{\text{(styrene:butadiene in latex particles)}}{\text{(styrene:butadiene outside latex particles)}}$$

The variation of K with conversion at the three temperatures is shown in Figure 5. At zero conversion, K should be close to unity. The small deviations from unity shown in Figure 5 are not significant and result from errors in extrapolating the curves in Figure 2 to zero conversion and, to a smaller extent, from uncertainties in the reactivity ratios. The most significant feature of these curves is the steady decrease in K with conversion and the much more rapid drop as the end of interval II is approached. This is more clearly seen in the 25°C curve and arises from the more rapid loss of butadiene from the monomer droplets and their relative enrichment in styrene. Thus at 50% conversion at 25°C the weight ratio of styrene:butadiene in the monomer droplets is 2.17, while the corresponding ratio within the latex particles is 0.49. Our results, particularly at 25°C, do not agree entirely with Gardon's prediction that K should not vary by more than about 40% during intervals I and II, unless the last 15% of conversion in this interval is neglected. Beyond about 40% conversion, the factor which most influences variations in K in our calculations is the styrene:polymer ratio from Figure 1. Differences in copolymer composition and reactivity ratios with temperature play a comparatively minor role. Thus, the dotted curve in Figure 5 was calculated by using the reactivity ratios and the polymer composition curve corresponding to experiments at 15°C and the styrene:polymer curve for 25°C. It may be that under the conditions of our experiments diffusion effects do play a part, while in this respect, Gardon's calculations apply to an idealized system.

In their theory of emulsion polymerization, Medvedev et al.[9,10] assumed that all the unconverted monomer is absorbed into the latex particles from

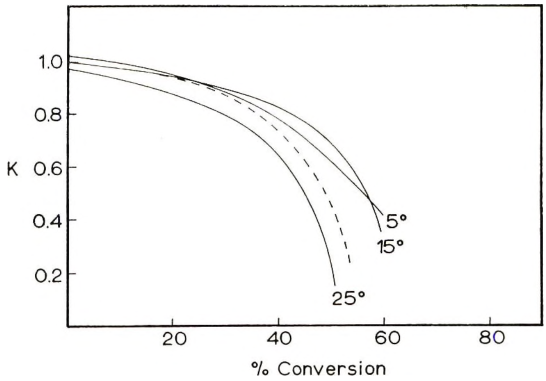

Fig. 5. Composition ratio K = wt. styrene: wt. butadiene in particles/wt. styrene: wt. butadiene in binary phase as a function of conversion: (---) from reactivity ratio and composition at 15°C and styrene:polymer curve at 25°C.

the beginning of the reaction, that the surface area between the latex particles and the aqueous phase is constant throughout the reaction and that the rate of polymerization is controlled by diffusion of monomer to the surface of the particles. In his recent series of papers, Gardon has criticized these assumptions[2] on the grounds that they would hold only if the latex particles absorbed very large quantities of monomer. Indeed, below 10% conversion a swell ratio larger than ten would be required and from both practical and theoretical considerations this is highly improbable. The swell ratios of the latex particles obtained in the present work never exceeded three, even below 10% conversion. This futher substantiates Gardon's view that Medvedev's assumptions are unrealistic.

We are indebted to the International Institute of Synthetic Rubber Producers for a generous grant in support of this work.

References

1. W. V. Smith and R. H. Ewart, *J. Phys. Chem.*, **16,** 592 (1948).
2. J. L. Gardon, *J. Polym. Sci. A-1,* **6,** 2859 (1968).
3. G. M. Burnett, G. G. Cameron, and P. L. Thorat, *J. Polym. Sci. A-1,* **8,** 3435–3442 (1970).
4. E. W. Duck, in *Encyclopedia of Polymer Science and Technology,* H. F. Mark, N. G. Gaylord, and N. M. Bikales, Eds., Interscience, New York, 1967, Vol. 5, p. 840.
5. E. J. Meehan, *J. Polym. Sci.*, **1,** 175 (1946).
6. R. J. Orr and H. L. Williams, *Can. J. Chem.*, **29,** 270 (1951).
7. F. T. Wall, *J. Amer. Chem. Soc.*, **67,** 1929 (1945).
8. W. D. Harkins, *J. Amer. Chem. Soc.*, **69,** 1428 (1947); *J. Polym. Sci.*, **5,** 217 (1950).
9. G. D. Berezhnoi, P. M. Khomikovsnii, and S. S. Medvedev, *Vysokomol. Soedin.*, **2,** 141 (1960).
10. S. S. Medvedev, *Proceedings of the International Symposium on Macromolecular Chemistry, Prague* **1957,** Pergamon Press, New York, 1958, pp. 174–190.

Received February 17, 1970
Revised April 15, 1970

JOURNAL OF POLYMER SCIENCE: PART A-1 VOL. 8, 3443-3453 (1970)

Copolymerization of Styrene and Butadiene in Emulsion. II. Relative Rates of Crosslinking and Propagation

G. M. BURNETT, G. G. CAMERON, and P. L. THORAT, *Department of Chemistry, University of Aberdeen, Old Aberdeen, Scotland*

Synopsis

For the styrene–butadiene emulsion copolymerization (71 parts butadiene:29 parts styrene) the ratio of the rate coefficients for crosslinking, k_x, and propagation, k_p, have been determined at 5, 15, and 25°C by using an adaption of the method of Morton and co-workers. These ratios yield a value of 4.85 kcal/mole for the difference in activation energy between crosslinking and propagation, $E_x - E_p$. Since the relative frequency of crosslinking and propagation depends upon the copolymer composition, and hence upon the free monomer ratio and the temperature, the range of application of these data is more limited than in a simple homopolymerization.

INTRODUCTION

The kinetics of crosslinking and propagation reactions during the polymerization of a diene have been derived by Flory,[1] who showed that the relative rates of crosslinking and propagation are given by

$$d\nu/d\alpha = 2(k_x/k_p)[\alpha/(1-\alpha)] = 2K[\alpha/(1-\alpha)] \qquad (1)$$

where ν is the proportion of crosslinked units, α the fractional conversion, and k_x and k_p the rate coefficients for crosslinking and propagation, respectively. Morton and co-workers[2,3] have adapted eq. (1) to homopolymerizations of dienes in emulsion where the ratio $[\alpha/(1-\alpha)]$ is replaced by the polymer:monomer ratio in the latex particles. By using Bardwell and Winkler's relationship[4] to calculate weight-average degree of polymerization, $\bar{Y}_w$, of the primary polymer chains at the gel point, Morton and co-workers were able to determine the difference between the energies of activation for crosslinking and propagation, $E_x - E_p$. With this information it is possible to calculate K, the relative crosslinking rate constant, at any temperature and thus obtain a value for $\bar{Y}_w$ at the gel point, i.e., the weight-average degree of polymerization required for gelation. In the commercial polymerization of dienes where gelation is undesirable this knowledge is of considerable value.

In the present paper Morton's approach is extended to cover the copolymerization of styrene and butadiene. The appearance of a second monomer, however, poses serious problems. For example the term $[\alpha/(1-\alpha)]$ in eq. (1) has to be replaced by $[\alpha_{BD}/(1-\alpha)]$ where α_{BD} represents the fraction of copolymerized monomers which is butadiene. Also the rate coefficients k_p and k_x are now composite quantities, since there are several propagation steps, as in any copolymerization, and at least two crosslinking steps. The frequency with which these various steps occur is dependent upon the relative monomer concentrations, and since concentrations vary with conversion a further limitation is imposed. Fortunately, in the case of the styrene–butadiene emulsion system, the composition of the copolymer and hence the monomer ratio at the locus of polymerization, i.e., within the latex particles, do not vary greatly until beyond about 50% conversion of monomer to polymer.

Thus, the object of the work reported here was to evaluate *K* for the styrene–butadiene copolymerization (71 parts butadiene:29 parts styrene by weight) at the temperatures 5, 15, and 25°C. For this purpose the data on polymer:monomer ratio in the latex described in Part I of this work[5] were employed, and additional experiments were conducted to determine the mercaptan regulating index and the gel point conversions.

EXPERIMENTAL

Polymerizations

The basic recipe, the bottle polymerization and sampling techniques were as described in Part I.[5] In order to reduce the risk of anomalies due to large variations in rates at the three temperatures, the initiator/activator levels (I/A) were adjusted to give approximately the same rates of polymerization—about 10%/hr. At 5, 15, and 25°C the I/A levels (see Part I, Table I) required to achieve this rate were 50/50, 25/25, and 16/16, respectively.

Mercaptan Analysis

The residual mercaptan [*tert*-dodecyl mercaptan (TDM)] in the latex was determined by amperometric titration with silver nitrate using a mercuric iodide cell, of the type described by Morton and Salatiello,[2] as emf source.

Vistex Determination

The gel points were determined by measuring the limiting viscosity number, $[\bar{\eta}]$, by the Vistex technique. A 1–1.5 ml portion of latex was dissolved in 100 ml of benzene–isopropanol mixture (80:20 by volume of Analar grade solvents). Viscosities were measured at 30°C in a suspended-level dilution viscometer. Successive dilutions were made with pure benzene and $[\bar{\eta}]$ was obtained from these data by the standard procedure.[6] As observed by Morton and Salatiello[2] there was a sharp change in slope of the Vistex plot ($\ln \eta_r/c$ versus c) beyond the gel point. The values of [$\bar{\eta}$] obtained from the Vistex plots agreed closely with values obtained from conventional viscometry on the purified dried polymer.

RESULTS AND DISCUSSION

Rates of Polymerization

The conversion versus time plots for the polymerizations with an I/A level of 50/50 are shown in Figure 1. At 5°C the curve is close to linear

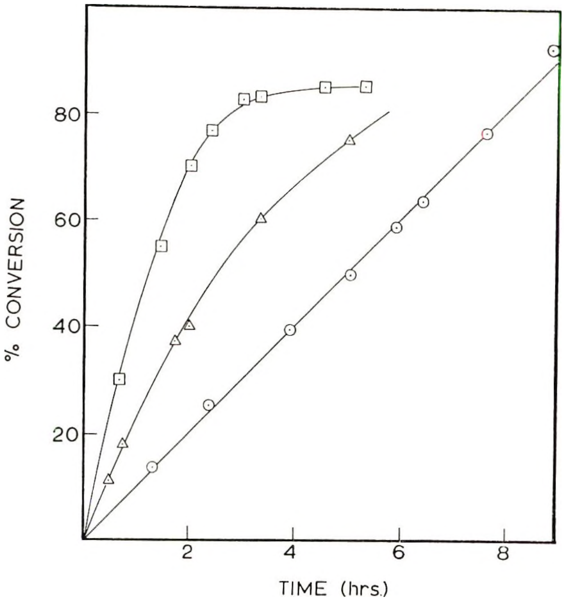

Fig. 1. Conversion of monomers vs. time: (⊙) 5°; (△) 15°; (⊡) 25°C. I/A level at 50/50 of standard recipe.[5]

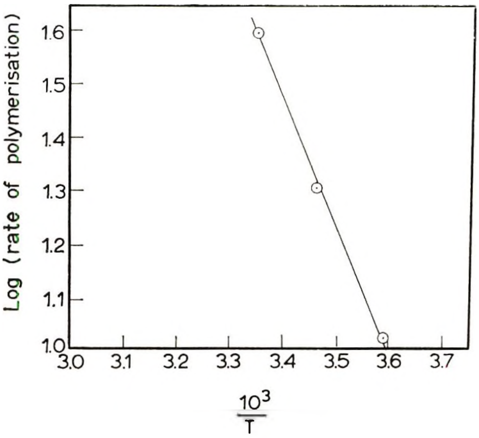

Fig. 2. Arrhenius plot of zero-order rates of polymerization from Fig. 1.

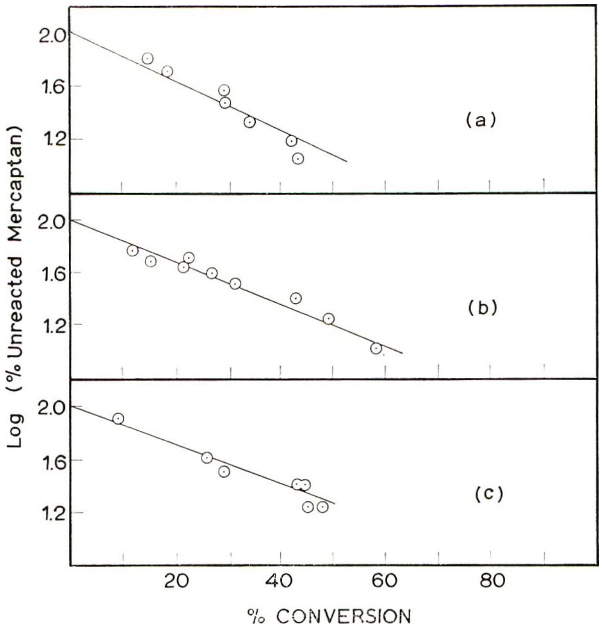

Fig. 3. Mercaptan disappearance curves: (*a*) 5°C, I/A = 50/50, initial TDM 0.22 phm; (*b*) 15°C, I/A = 25/25, initial TDM 0.22 phm; (*c*) 25°C, I/A = 16/16, initial TDM 0.22 phm.

over the complete conversion range studied. At 25°C, by contrast, there is an abrupt decrease in rate around 80% conversion. From the slopes of the approximately linear parts of the curves in Figure 1, the Arrhenius plot in Figure 2 was constructed and gave an overall energy of activation for the process of 10.3 kcal/mole. From the rates of polymerization at 5 and 15°C with I/A at 25/25, the energy of activation was 10.6 kcal/mole. These values agree quite well with the figure 9.7 kcal/mole obtained by Brown and Winkler[7] for a similar redox system.

Mercaptan Disappearance

Figure 3 shows the disappearance curves for TDM at the three temperatures. Up to about 50% conversion the disappearance is first-order, in line with previous observations. From the slopes of the lines in Figure 3 the regulating indices were calculated. The regulating index r is related to the mercaptan content by the relationship

$$r = (2.303/\alpha) \log (R_0/R_1) \tag{2}$$

where R_0 is the initial mercaptan concentration and R_1 the concentration at conversion α. In this manner the values of r for TDM were 4.14, 3.68, and 3.20 at 5, 15, and 25°C, respectively. The value of r at 5°C agrees closely with that quoted by Duck.[8] An Arrhenius plot for the regulating indices (Figure 4) gives a value of 2.1 kcal/mole, which represents the difference in

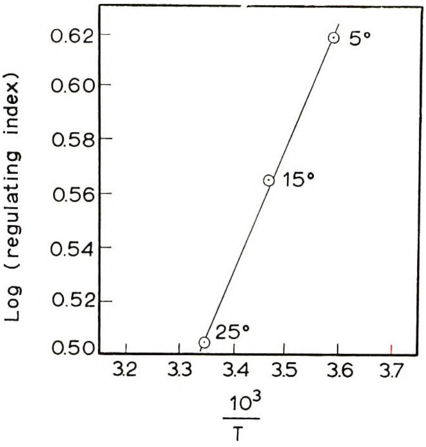

Fig. 4. Arrhenius plot of regulating index for TDM from Fig. 3.

activation energies for propagation and transfer, $E_p - E_{tr}$. This figure agrees well with the literature value of 2.0 kcal/mole at 30°C.[9] These data provide values of r at any temperature for this system, but it is undesirable to extrapolate much beyond the temperature limits of this study, since it is known[9] that $E_p - E_{tr}$ can change at higher temperatures, presumably due to loss of mercaptan by reactions other than transfer.

Determination of Gel Point

In order to apply Bardwell and Winkler's equations to calculate $\bar{Y}_w$ of the primary chains at the gel point two conditions must be satisfied: (a) the calculations must be applied at conversions within the first-order part of the mercaptan disappearance curves, and (b) transfer with mercaptan must be the predominant process controlling primary chain length.

The first condition is satisfied simply by adjusting the TDM levels to give a gel point below 50% conversion. In the present work it was

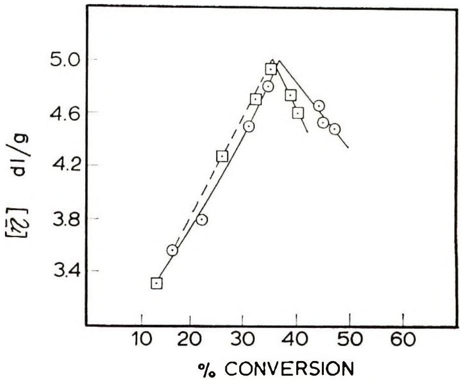

Fig. 5. Limiting viscosity number [η] from Vistex determinations as a function of conversion at 5°C and TDM 0.04 phm: (⊙) I/A = 50/50; (□) /IA = 16/16.

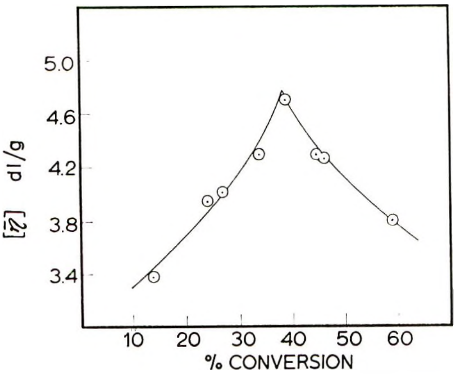

Fig. 6. Limiting viscosity number [η] from Vistex determinations as a function of conversion at 15°C, TDM 0.051 phm, I/A = 25/25.

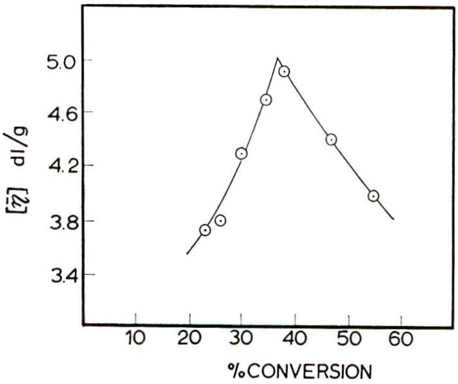

Fig. 7. Limiting viscosity number [η] from Vistex determinations as a function of conversion at 25°C, TDM 0.0647 phm, I/A = 16/16.

found that TDM levels of 0.040, 0.051, and 0.065 phm at 5, 15, and 25°C, respectively, gave gel points at 36–39% conversion. Curves showing limiting viscosity number (from Vistex determinations) as a function of conversion under the above conditions are shown in Figures 5, 6, and 7. The gel point conversions were taken from the maxima in the curves in the usual way.

To satisfy the second condition it has to be shown that termination of macroradicals by initiator radicals is a relatively infrequent process. This was done in two ways. In the first approach two runs at 5°C were conducted with TDM levels of 0.040 phm in each but in one case the I/A level was 50/50 and in the other it was 16/16. If primary radical termination is significant, then the degree of polymerization and the viscosity of the products from the second run should be much higher than from the first. It can be seen from Figure 5 that up to the gel point the limiting viscosity numbers lie very close together and that the gel points are the same within experimental error. In the second approach the viscosity-average molecular weights $\bar{M}_v$ calculated on the basis of Bardwell and Winkler's theory were compared with the experimental values of $\bar{M}_v$. According to Bardwell and Winkler,[4] in a system in which transfer with mercaptan is the predominant process controlling primary chain length, the weight-average degree of polymerization, $\bar{Y}_w$ is given by

$$\bar{Y}_w = 2(e^{r\alpha} - 1)/\alpha r^2 R_0 \tag{3}$$

where α, r, and R_0 have their previous significance, and $\bar{Y}_v$ is related to $\bar{Y}_w$ by

$$\bar{Y}_v = (1.85/2.00)\ \bar{Y}_w \tag{4}$$

Values of $\bar{Y}_v$ calculated from eqs. (3) and (4) for runs at 5 and 25°C are shown in Table I. Experimental values of $\bar{Y}_v$ were calculated from the

TABLE I
Viscosity-Average Degrees of Polymerization of Primary Chains $\bar{Y}_v$

Temperature, °C	I/A level	TDM, phm	Conversion, %	$\bar{Y}_v$ Observed	$\bar{Y}_v$ From mercaptan consumption [eqs. (3) and (4)]
5	50/50	0.04	20	7269	5450
5	50/50	0.04	30	9138	7044
5	50/50	0.04	35	10247	8000
25	16/16	0.065	20	6514	4025
25	16/16	0.065	30	8600	4827
25	16/16	0.065	35	9970	5235

values of $[\eta]$ (from the Vistex measurements) by using the relationship[10]

$$[\eta] = 1.80 \times 10^{-4}(65\ \bar{Y}_v)^{0.76} \tag{5}$$

where the figure 65 represents the average molecular weight of the structural unit of the copolymer up to 40% conversion. Experimental values of $\bar{Y}_v$ are also shown in Table I. In all cases the experimental value of $\bar{Y}_v$ is greater than the calculated value. This situation is strong evidence against non-mercaptan termination. If termination by primary radicals had been significant there should have been a large discrepancy in the other direction. The measured values of $\bar{Y}_v$ are somewhat higher than the primary values, since the latter do not take account of the crosslinking.[2,3]

The conclusion that non-mercaptan termination is insignificant in the present redox system does not agree with Brown and Winkler's findings.[7] It is worth pointing out that the recipe used in the present work differed from that employed by Brown and Winkler, who used cumene hydroperoxide as initiator, a mixture of tertiary mercaptans as modifier, and dextrose as reducing agent. Also, in the present work the I/A levels, particularly at higher temperatures, were much lower than those used by Brown and Winkler. This last point is probably the main contributing factor to the differences between the two reports.

Calculation of the Relative Crosslinking Rate Constant

From the data presented in Part I of this work the ratio of copolymerized butadiene:total free monomer in the latex particles was calculated. This ratio was a function of conversion and fitted an equation of the form:

$$\alpha_{BD}/(1 - \alpha) = A + B\alpha^2$$

where A and B are constants at a fixed temperature (Table II). It follows that for this system eq. (1) should be modified to

TABLE II
Variation of Ratio $[\alpha_{BD}/(1 - \alpha)]$ (Moles of Copolymerized Butadiene:Moles of Total Free Monomers in Latex Particles) with Temperature and Conversion

Temperature, °C	A and B in $[\alpha_{BD}/(1 - \alpha)] = A + B\alpha^2$	
	A	B
5	0.6743	2.346
15	0.6200	2.271
25	0.5504	1.900

$$\frac{d\nu}{d\alpha} = 2K[A + B\alpha^2] \tag{6}$$

At the gel point $\nu/\alpha = \rho = 1/\bar{Y}_{wg}$, since the density ρ of crosslinked units, is equal to the reciprocal weight average degree of polymerization of the primary chains at the gel point. Thus, at the gel point, eq. (6) can be integrated between the limits $\alpha = 0$ and $\alpha = \alpha_g$, yielding

$$\nu/\alpha = 1/\bar{Y}_{wg} = 2K[A + (B/3)\alpha^2_g] \tag{7}$$

Since A + (B/3) and α_g have been determined experimentally and $\bar{Y}_{wg}$ calculated from eq. (3), K can be obtained at the three temperatures 5, 15,

TABLE III
Calculation of Relative Crosslinking Rate Constant K

	At 5°C	At 15°C	At 25°C
Regulating index, r	4.14	3.68	3.20
TDM charge R_0, moles/mole monomer $\times 10^4$	1.250	1.577	2.000
Gel point conversion, α_g	0.37	0.37	0.38
Weight-average degree of polymerization at gel point $\bar{Y}_w \times 10^{-3}$	9.148	7.347	6.090
$K \times 10^5$	7.0	9.4	12.65
$E_x - E_p$, kcal/mole		4.85	

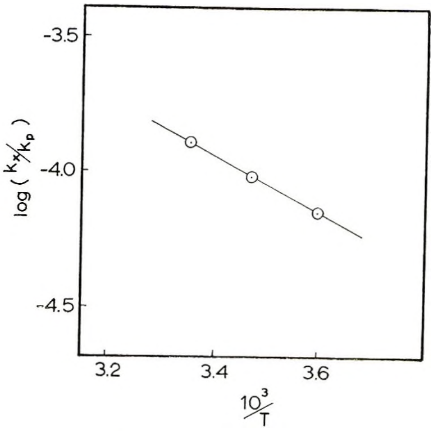

Fig. 8. Arrhenius plot for the relative crosslinking rate constant $K = k_x/k_p$ from eq. (7).

and 25°C. The relevant data are summarized in Table III. Since $K = k_x/k_p$, an Arrhenius plot for K yields the difference in activation energy for crosslinking and propagation, $E_x - E_p$. Thus from Figure 8, $E_x - E_p$ is 4.85 kcal/mole. It is noteworthy that, unlike the simple case of butadiene,[2] $\bar{Y}_{ug}$ is now a function of the gel point conversion and not a constant at a fixed temperature.

In theory it should be possible to deduce K at any temperature from Table III and Figure 8. There are, however, practical limitations to this procedure, particularly when lengthy extrapolations are necessary. As was mentioned earlier, k_x and k_p are composite quantities in this instance and are not rate "constants" in the normally accepted sense. Thus, attack on copolymerized butadiene units can occur at internal or pendant double bonds and may involve either a styrene- or a butadiene-ended macroradical. k_x therefore depends on polymer structure and composition. This means that extrapolation outside the temperature range 5–25°C to obtain values of K is valid only provided polymer structure and composition vary in the same manner outside this temperature range as they do within it.

Similar reasoning shows that both k_x and k_p are functions of conversion, and the values of K in Table III must therefore be averages over the conversion range studied, i.e, 0–40%. Up to 50% conversion, however, the composition of the copolymer varies very little[5]—within 1 or 2%—and any variation in K is likely to be very small. Beyond 50% conversion the average styrene content of the copolymer increases rapidly, and K must also change.

It is clear that the values of the relative crosslinking rate constant in Table III apply only to the copolymerization with a styrene:butadiene ratio of 29:71. In order to deduce K at any temperature and any initial monomer ratio it would be necessary to plot $E_x - E_p$ and A_x/A_p as functions of monomer ratio, A_x and A_p being the appropriate frequency factors. At this time there are only the present data ($E_x - E_p$, 4.85 kcal/mole and

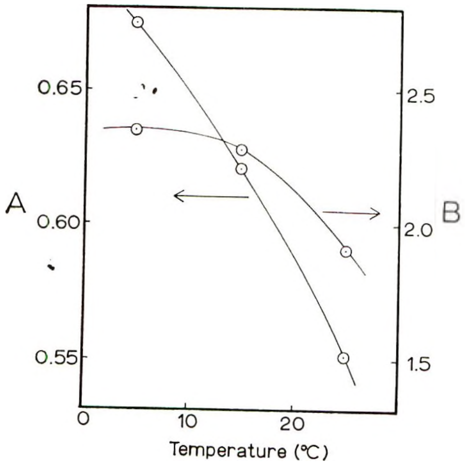

Fig. 9. Parameters A and B from eq. (7) as functions of temperature.

A_x/A_p, 0.45) and those of Morton et al.[2] for pure butadiene ($E_x - E_p$, 7.5 kcal/mole and A_x/A_p, 15.8), and more data for different monomer ratios are required to complete the picture.

Morton and Salatiello[2] have pointed out that the practical value in obtaining K is that it can be used to relate quantitatively gel point and mercaptan charge at any temperatures by using eqs. (1) and (3). In the case of butadiene this procedure is relatively simple, since the polymer:-monomer ratio $[\alpha/(1 - \alpha)]$ is virtually constant. With the styrene-butadiene copolymerization, however, the appropriate parameter is $[\alpha_{BD}/(1 - \alpha)]$ which varies with conversion, as in eq. (7), as well as with temperature. The constants A and B in eq. (7) must therefore be known at the required temperature. Figure 9 shows A and B plotted as functions of temperature. Since there are only three points on each diagram the curves are not too well defined. Interpolation with either curve should be satisfactory, but extrapolation of B to temperatures above 25°C is dubious. Since current commercial practice is concentrated on low-temperature polymerization in these systems, this is not a serious limitation.

The above discussion shows that, while Morton's approach can be applied to copolymerizations, there are certain severe limitations on the quantitative use that can be made of the data. At present these can only be used for semiquantitative predictions when conditions lie beyond the range of the present studies. Further studies outside this range would clearly extend the usefulness of these results.

We are indebted to the International Institute of Synthetic Rubber Producers for a generous grant in support of this work.

References

1. P. J. Flory, *J. Amer. Chem. Soc.*, **69**, 2893 (1947).
2. M. Morton and P. Salatiello, *J. Polym. Sci.*, **6**, 225 (1950).

3. M. Morton and W. E. Gibbs, *J. Polym. Sci. A*, **1**, 2679 (1963).

4. J. Bardwell and C. A. Winkler, *Can. J. Res.*, **B27**, 116, 128, 139 (1949).

5. G. M. Burnett, G. G. Cameron, and P. L. Thorat, *J. Polym. Sci.* **A-1**, **8**, 3435 (1970).

6. D. A. Henderson and N. R. Legge, *Can. J. Res.*, **B27**, 666 (1949).

7. R. M. Brown and C. A. Winkler, *Can. J. Chem.*, **31**, 13 (1953).

8. E. W. Duck, in *Encyclopedia of Polymer Science and Technology*, H. F. Mark, N. G. Gaylord, and N. M. Bikales, Eds., Interscience, New York, 1967, Vol. 5, p. 811.

9. F. A. Bovey, I. M. Kolthoff, A. I. Medalia, and E. J. Meehan, *Emulsion Polymerization* (*High Polymers*, Vol. IX), Interscience, New York, 1955, p. 123.

10. W. G. Mochel and J. B. Nichols, *Ind. Eng. Chem.*, **43**, 154 (1951).

Received February 17, 1970

JOURNAL OF POLYMER SCIENCE: PART A-1 VOL. 8, 3455–3460 (1970)

Copolymerization of Styrene and Butadiene in Emulsion. III. Crosslinking Studies by Partial Conversion Properties

G. M. BURNETT, G. G. CAMERON, and P. L. THORAT,
Department of Chemistry, University of Aberdeen,
Old Aberdeen, Scotland

Synopsis

Crosslinking in the styrene–butadiene emulsion copolymerization (21 parts styrene: 79 parts butadiene) prior to gelation has been studied by means of partial conversion number-average molecular weights at 5, 15, and 25°C. It is shown that the macromolecular population begins to diminish at progressively lower conversions as the reaction temperature is increased. This is attributed to the relative increase in crosslinking over propagation as the reaction temperature is increased and also to the decrease in mercaptan regulating index with increasing temperature.

INTRODUCTION

In part II[1] of this work the relative crosslinking rate constant K for the styrene–butadiene (21 parts styrene:79 parts butadiene by weight) system was derived at 5, 15, and 25°C. K increases with temperature, showing that crosslinking becomes relatively more frequent as the temperature is increased. An alternative way of looking at crosslinking up to the gel point is to examine the changes in macromolecular population of the system with conversion. In a polymerization involving a diene, initiation and transfer tend to increase the macromolecular population while crosslinking tends to reduce it. Thus the rate of change of macromolecular population with respect to conversion is a sensitive guide to the balance between these opposing processes.

Changes in macromolecular population during polymerization are conveniently followed by employing Wall's concept of partial conversion properties. The partial-conversion number-average molecular weight, $\overline{\overline{M}}_n$, is related to the rate of change in macromolecular population dN/dW by

$$1/\overline{\overline{M}}_n = dN/dW \tag{1}$$

where N is the number of moles of macromolecules in the system and W is the weight of polymer produced. If the number-average molecular weight, $\overline{M}_n$ can be measured during the course of polymerization dN/dW can be calculated from the relationship derived by Wall

$$dN/dW = [\bar{M}_n - W(d\bar{M}_n/dW)]/\bar{M}_n^2 \qquad (2)$$

Provided the macromolecular population is increasing with conversion, dN/dW will be positive. However, as soon as crosslinking dominates the process, the molecular population will diminish and dN/dW will become negative.

Wall's approach has been applied by Burnett and co-workers to elucidate crosslinking reactions in the copolymerization of styrene and methyl methacrylate with poly(ethylene fumarate),[3,4] while Wall and co-workers[5] conducted similar studies with GR-S formation at 50°C. So far, only one brief report[6] on similar work on low-temperature redox-initiated emulsion polymerization of styrene and butadiene has appeared. Since current commercial practice is concentrated on low-temperature polymerization, a more detailed investigation along these lines may have some practical significance. It is also of interest to observe whether the partial-conversion properties correlate with the relative crosslinking rate constants at different temperatures.

EXPERIMENTAL

Polymerization and sampling techniques were as described previously.[1,7]

Number-average molecular weights were obtained by osmometry in toluene at 37°C by using a Mechrolab 501 high-speed osmometer with Ultracella "allerfeinst" grade membranes.

Viscosity measurements were done in a suspended-level dilution viscometer with benzene as solvent at 30°C.

The polymer samples for characterization were precipitated in methanol. After filtration, the samples were washed three times with hot distilled water and three times with methanol. The final methanol wash contained 0.1% antioxidant (2,6-di-*tert*-butyl-*p*-cresol). Samples were dried and stored in the dark under vacuum at room temperature.

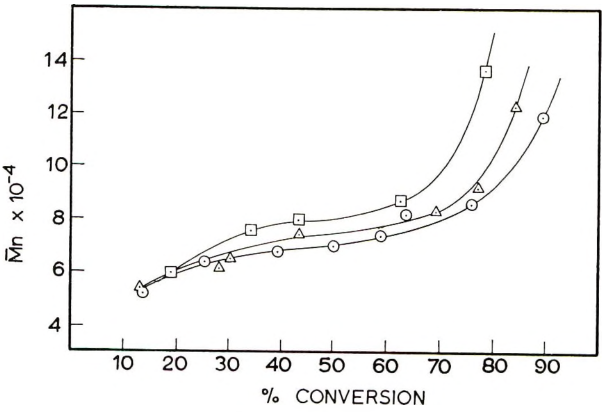

Fig. 1. Number-average molecular weights $\bar{M}_n$ vs. conversion: (⊙) 5°C, I/A = 50/50; (△) 15°C, I/A = 25/25; (⊡) 25°C, I/A = 16/16. TDM 0.22 phm.

RESULTS AND DISCUSSION

The curves of $\bar{M}_n$ versus conversion for runs at 5, 15, and 25°C are shown in Figure 1. In each run the initial modifier concentration [*tert*-dodecyl mercaptan (TDM)] was the same (0.22 phm), but the initiator/activator levels (I/A) were adjusted to give approximately the same rate of polymerization. The three curves have the same overall shape and show the typical rapid rise in the later stage of polymerization due to crosslinking.

From the smoothed curves in Figure 1, dN/dW at conversion intervals was calculated by using eq. (2). Figure 2 shows the plots of dN/dW for the three runs. Up to about 50% conversion there are no dramatic changes in dN/dW, and the positive values of this parameter show that the macromolecular population is increasing with conversion. Beyond about 50%

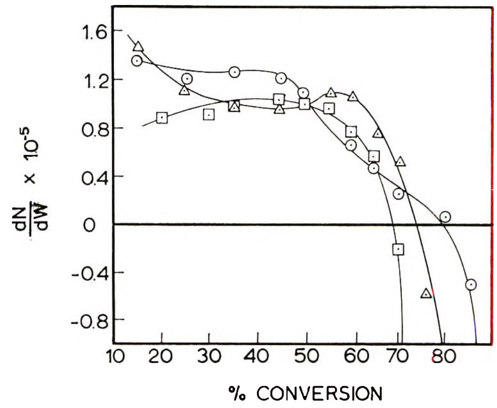

Fig. 2. dN/dW vs. conversion from smoothed curves in Fig. 1: (⊙) 5°C; (△) 15°C; (⊡) 25°C.

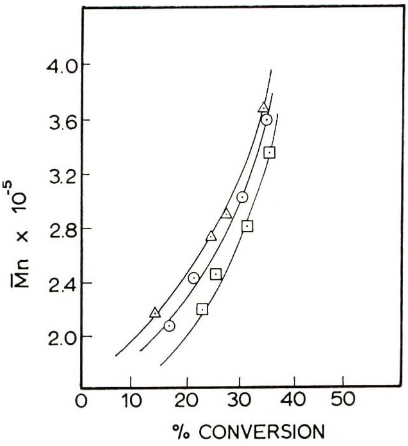

Fig. 3. Number-average molecular weights $\bar{M}_n$ vs. conversion: (⊙) 5°C, I/A = 50/50, TDM 0.04 phm; (△) 15°C, I/A = 25/25, TDM 0.051 phm; (⊡) 25°C, I/A = 16/16 TDM 0.065 phm.

conversion the curves begin to drop, showing that the initial rate of increase in the population is not sustained. dN/dW eventually cuts the zero line and becomes negative above about 70% conversion. The crossover point occurs at the conversion where crosslinking and the creation of new macromolecules are balanced, and beyond this point the molecular population is diminishing. The crossover point occurs at lower conversions as the reaction temperature is increased, and the steepness of the fall in dN/dW occurs in a similar manner. These trends are exactly what would be anticipated from the fact that K increases with temperature. The relative rates of mercaptan disappearance also contribute to these curves. The fact that the regulating index decreases with increasing temperature[1] means that, at a constant initial TDM level, the higher the temperature, the greater the average degree of polymerization of the primary chains at a given conversion, and hence the fewer crosslinks per primary chain required to form infinite networks. It is therefore the combination of two factors: longer primary chains and relatively more rapid crosslinking, which leads to the earlier dominance of crosslinking at higher temperatures.

These experiments were conducted with the same initial modifier levels at all three temperatures. In the experiments designed for calculation of K,[1] however, the rates of polymerization were approximately the same but the modifier levels were adjusted to give the same gel point at each temperature. Curves of $\overline{M}_n$ versus conversion for these runs are shown in Figure 3. For all three runs, the crossover points (Fig. 4) are the same, 31–32% within experimental error, while the corresponding gel points were at 37–38% conversion.[1] The occurrence of the gel point at a slightly higher conversion than the crossover point of dN/dW has been observed before. The difference arises because infinite networks cannot form until after crosslinking has begun to reduce the macromolecular population.[6]

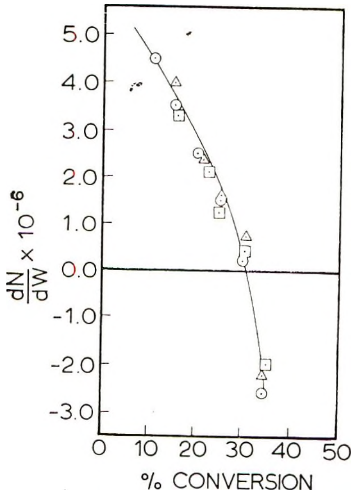

Fig. 4. dN/dW vs. conversion from smoothed curves in Fig. 3: (⊙) 5°C; (△) 15°C; (⊡) 25°C.

The foregoing discussion shows the sensitivity of the parameter dN/dW to crosslinking and its potential as a tool for studying the effects of polymerization variables on crosslinking. Evaluation of $\bar{M}_n$, however, is still a relatively lengthy procedure and requires more expensive and complex equipment than is needed for viscosity measurements. It is therefore relevant to enquire if the same sensitivity can be achieved with simple viscometry.

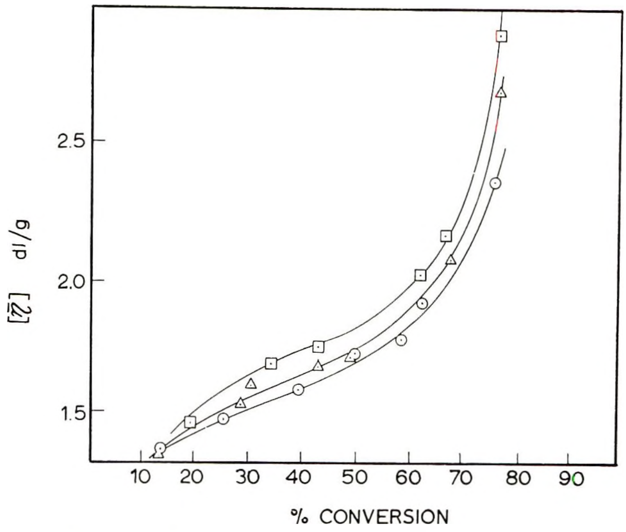

Fig. 5. Intrinsic viscosities [$\bar{\eta}$] as a function of conversion for runs in Fig. 1: (⊙) 5°C; (△) 15°C; (⊡) 25°C.

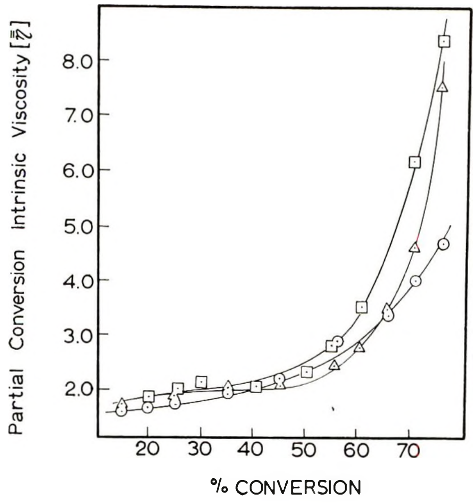

Fig. 6. Partial-conversion intrinsic viscosities [$\bar{\eta}$] as a function of conversion from smoothed curves in Fig. 5: (⊙) 5°C; (△) 15°C; (⊡) 25°C.

Wall[2] has also defined the partial conversion intrinsic viscosity, $[\bar{\bar{\eta}}]$, as

$$[\bar{\bar{\eta}}] = [\bar{\eta}] + W\,(d[\bar{\eta}]/dW) \tag{3}$$

where $[\bar{\eta}]$ is the cumulative intrinsic viscosity and W the fractional conversion. $[\bar{\bar{\eta}}]$ can be calculated from plots of $[\bar{\eta}]$ versus conversion.

Plots of $[\bar{\eta}]$ and $[\bar{\bar{\eta}}]$ versus conversion for the runs in Figure 1 are shown in Figures 5 and 6, respectively. The curves in Figure 5 are similar in shape to those in Figure 1. The absence of maxima indicate that the gel point was not reached. The curves in Figure 6 show a rapid rise with conversion, the rise being more marked as the polymerization temperature is increased. This presumably reflects the relative importance of crosslinking as the temperature increases. The curves reveal little more than this, however, so that for crosslinking studies prior to gelation, partial-conversion number-average molecular weights are likely to be more informative.

We are indebted to the International Institute of Synthetic Rubber Producers for a generous grant in support of this work. We are grateful to Mrs. A. J. R. Dewar for much of the characterization work.

References

1. G. M. Burnett, G. G. Cameron, and P. L. Thorat, *J. Polym. Sci. A-1*, **8**, 3443 (1970).
2. F. T. Wall, *J. Amer. Chem. Soc.*, **67**, 1929 (1945).
3. G. M. Burnett, J. N. Hay, and J. D. B. Smith, *J. Polym. Sci. A*, **2**, 5111 (1964).
4. G. M. Burnett, J. N. Hay, and J. D. B. Smith, Soc. Chem. Ind. Monograph No. 20, London, 1966, p. 261.
5. F. T. Wall and L. F. Beste, *J. Amer. Chem. Soc.*, **69**, 1761 (1947).
6. G. M. Burnett, G. G. Cameron, A. Dukiet, and J. M. Pearson, *Chem. Ind.* (London), **1968**, 1518.
7. G. M. Burnett, G. G. Cameron, and P. L. Thorat, *J. Polym. Sci. A-1*, **8**, 3435 (1970).

Received February 17, 1970
Revised April 15, 1970

JOURNAL OF POLYMER SCIENCE: PART A-1 VOL. 8, 3461-3481 (1970)

Direct Rotating-Sector Studies of the Systems: Styrene–Methyl Methacrylate and Styrene–Methyl Acrylate

J. P. MARANO, JR.,* L. H. SHENDALMAN,† and C. A. WALKER,
Department of Engineering and Applied Science, Yale University,
New Haven, Connecticut 06520

Synopsis

The rotating-sector technique was applied directly in a study of two copolymerization systems: styrene–methyl methacrylate and styrene–methyl acrylate. The two coupled rate expressions which describe the change in radical concentrations for two-component polymerizations degenerate into a single expression identical in form to the radical expression for a homopolymerization when the ratio of the radical concentrations under intermittent illumination is assumed constant and equal to the ratio under steady illumination. Numerical solutions of the complete rate expression by use of constants from the literature confirm that this assumption is valid for a rotating-sector experiment. The overall lifetimes of these two-component systems were defined and measured experimentally as a function of monomer composition and then compared with lifetimes calculated by using literature rate constants. The agreement was satisfactory. The direct application of the technique to the two-component system provides an independent experiment which for some systems seems to be more sensitive to the value of the cross-termination constant than the usual steady-state method.

Introduction

A basic understanding of the kinetics of vinyl copolymerization systems requires a knowledge of the rate of change of concentrations of the chemical species in each step of the chain mechanism. In the study of the kinetics of each system a steady-state experiment will not yield sufficient information to determine all the individual rate constants of the chain mechanism.

The classical copolymerization mechanism is shown in eqs. (1)–(9).

Initiation:

$$M_1 \xrightarrow{R_{i_1}} M_1^* \tag{1}$$

$$M_2 \xrightarrow{R_{i_2}} M_2^* \tag{2}$$

---

† Present address: Esso Research and Engineering Company, Linden, New Jersey 07036.

* Present address: Union Carbide Corporation, Chemicals and Plastics, South Charleston, West Virginia 25303.

Propagation:

$$M_1^* + M_1 \xrightarrow{k_{p_{11}}} M_1^* \tag{3}$$

$$M_1^* + M_2 \xrightarrow{k_{p_{12}}} M_2^* \tag{4}$$

$$M_2^* + M_2 \xrightarrow{k_{p_{22}}} M_2^* \tag{5}$$

$$M_2^* + M_1 \xrightarrow{k_{p_{21}}} M_1^* \tag{6}$$

Termination:

$$M_1^* + M_1^* \xrightarrow{k_{t_{11}}} \text{stable products} \tag{7}$$

$$M_2^* + M_1^* \xrightarrow{k_{t_{12}}} \text{stable products} \tag{8}$$

$$M_2^* + M_2^* \xrightarrow{k_{t_{22}}} \text{stable products} \tag{9}$$

Here, M_1, M_2 are monomers; $k_{p_{xy}}$ is the propagation constant for free radical x reacting with monomer y; $k_{t_{xy}}$ is the termination constant of free radical x reacting with free radical y; R_{i_1}, R_{i_2} are the rates of initiation of M_1 and M_2, respectively.

This mechanism indicates that in addition to the rate of initiation, at least seven velocity constants must be determined. The velocity constants of this mechanism have been determined in the past by first performing steady-state and non-steady-state experiments on each homopolymerization and then performing composition and steady-state rate measurements on the copolymerization. The non-steady-state homopolymerization experiments allow the homopropagation and homotermination constants of each comonomer to be exclusively and separately known. The composition studies on the copolymerization allow the ratio of the homopropagation to cross-propagation constants to be determined, and the steady-state rate measurements allow a ratio of the cross-termination to the homoterminations constants to be determined.

These experiments on the comonomers and copolymer are sufficient to determine all the individual rate constants of the classical copolymerization model. This scheme of study lacks versatility, however, and is not applicable to all vinyl copolymerization systems. If, for example, one of the comonomers does not homopolymerize, the homopropagation and termination constants for this component cannot be determined. This is the case when carbon monoxide, sulfur dioxide, or another nonpolymerizing substance is used as a comonomer. Also, for certain vinyl polymerization systems difficulties are encountered in the use of composition studies to determine the reactivity ratios, and it is therefore advantageous to have another method of determining these constants.

It is understandable how an additional independent experiment could be very useful in the determination of these sometimes indeterminable quantities. This work proposes copolymerization systems to be studied by the direct application of a non-steady-state technique and describes the direct application of what is felt to be the simplest and most reliable non-steady-state technique to the copolymer system.

A well-established technique for determining the lifetime* of a homopolymerization chain radical and therefore the velocity constant for the termination step is the rotating sector technique. This periodic illumination method was first suggested by Briers, Chapman, and Walters in 1926,[2] and its application to the study of chain reaction kinetics is described by Noyes and Leighton.[3] Since the method is adequately described elsewhere,[4] a full description will not be given here. It suffices to say that the equations which are necessary for the determination of the lifetime of a chain radical have only been developed for the case where the proposed reaction model degenerates into a simple chain transfer mechanism. This simple transfer mechanism is adequate for describing homopolymerization kinetics[5–14] For such systems, the eq. (10) adequately described the homopolymerization chain radical concentration:

$$d[M_1^*]/dt = R_i - 2k_{t_{11}}[M_1^*]^2 \tag{10}$$

where $[M_1^*]$ denotes the concentration of free radicals, $k_{t_{11}}$ is the termination constant, and R_i is the overall rate of initiation.

It can easily be shown that the average lifetime is

$$\tau = \frac{[M_1^*]_s}{2k_{t_{11}}(M_1^*)_s^{\,2}} \tag{11}$$

or

$$\tau = (2k_{t_{11}}R_{i_0})^{-1/2} \tag{12}$$

where $(M_1^*)_s$ is the steady-state concentration of M_1^* (free radical from M_1) and R_{i_0} is the steady-state rate of initiation.

Many workers[1,2,15,16] have given solutions of eq. (10) for the conditions imposed upon it by the rotating-sector experiment. This allows the intermittent illumination experiment to be used for the determination of the velocity constants of the chain mechanism. Mathematical descriptions have been proposed with solutions found for variations of the simple chain-transfer mechanism[9,17–25] and though some of these point toward[17,21] the direct application of the technique to a two-component polymer system, an adequate treatment has been neglected until recently.[26] The solution of the system of differential equations which results from the well established model for copolymerizations[1,27–29] is a drawback in the direct application of the pulsed illumination technique. The appropriate rate expressions for the model shown in eqs. (1)–(9) are given in eqs. (13)–(16).

For the radical from M_1:

---

* "The average lifetime of an active center is the average time from the creation or initiation, of a radical chain to its ultimate annihilation, disregarding possible intervening transfer processes. This lifetime must equal the population of chain radicals divided by their rates of destruction."[1]

$$d[\mathrm{M}_1^*]/dt = R_{i1} - k_{p12}[\mathrm{M}_1^*][\mathrm{M}_2] + k_{p21}[\mathrm{M}_2^*][\mathrm{M}_1] - 2k_{t11}[\mathrm{M}_1^*]^2 - k_{t12}[M_1^*][M_2^*] \quad (13)$$

For the radical from M_2:

$$d[\mathrm{M}_2^*]/dt = R_{i2} + k_{p12}[\mathrm{M}_1^*][\mathrm{M}_2] - k_{p21}[\mathrm{M}_2^*][\mathrm{M}_1] - 2k_{t22}[\mathrm{M}_2^*]^2 - k_{t12}[\mathrm{M}_1^*][\mathrm{M}_2^*] \quad (14)$$

For M_1:

$$d[\mathrm{M}_1]/dt = -k_{p11}[\mathrm{M}_1^*][\mathrm{M}_1] - k_{p21}[\mathrm{M}_2^*][\mathrm{M}_1] \quad (15)$$

For M_2:

$$d[\mathrm{M}_2]/dt = -k_{p12}[\mathrm{M}_1^*][\mathrm{M}_2] - k_{p22}[\mathrm{M}_2^*][\mathrm{M}_2] \quad (16)$$

Where, $[\mathrm{M}_1]$, $[\mathrm{M}_2]$ are concentration of M_1 and M_2, respectively; $[\mathrm{M}_1^*]$, $[\mathrm{M}_2^*]$ are concentration of free radicals from M_1 and M_2, respectively, R_{i2}, R_{22} are initiation rates; $k_{p_{xy}}$ and $k_{i_{xy}}$ denote propagation and termination constants, respectively.

A discussion of the solution of these equations under the conditions imposed by the rotating sector experiment will be given later. It is first necessary to develop the expression for the lifetime of the chain.

Lifetimes of Copolymer Systems

In this section a discussion of the rotating sector method for the copolymerization system will be presented. It should be noted that these considerations should apply to chain reactions in general.

In general it can be shown for a system with N types of radicals that[26]

$$\tau = \frac{\sum_{i=1}^{N} \alpha_{i1}}{R_{i0}^{1/2}\left(2\sum_{i=1}^{N}\sum_{j=1}^{N} k_{tij}\,\alpha_{i1}\,\alpha_{j1}\right)^{1/2}} \quad (17)$$

where

$$\alpha_{ij} = [\mathrm{M}_i^*]/[\mathrm{M}_j^*] = k_{p_{ji}}[\mathrm{M}_i]/k_{p_{ij}}[\mathrm{M}_j]$$

For the two-component system, eq. (17) becomes

$$\tau R_{t0}^{1/2} = \frac{(1/k_{p12}) + [(1/k_{p21}) - (1/k_{p12})]x_2}{[a_1 + (2b - 2a_1)x_2\,(a_1 - 2b + a_2)x_2^2]^{1/2}} \quad (18)$$

where

$$a_1 = 2k_{t11}/k_{p12}^2$$

$$a_2 = 2k_{t22}/k_{p21}^2$$

$$b = k_{t12}/k_{p12}k_{p21}$$

and x_2 denotes the mole fraction of M_2.

It is interesting to note the derivative of $\tau\sqrt{R_{i0}}$ with respect to x_2 indicates a minimum (maximum), other than at the end points, occurs in the interval $0 \leq x_2 \leq 1$ when

$$\frac{x_2}{1 - x_2} = \left(\frac{k_{p21}}{k_{p12}}\right)\frac{2k_{t11} - k_{t12}}{2k_{t22} - k_{t12}} \tag{19}$$

if $\psi \neq 1$,* where $\psi = k_{t12}/2k_{t11}{}^{1/2}k_{t12}{}^{1/2}$.

If equation (19) is substituted into eq. (18), it will be seen that for the extrema ($\psi \neq 1$)

$$\tau R_{i0}{}^{1/2} = \sqrt{2}\left[\frac{(k_{t11} + k_{t22} - k_{t12})}{(4k_{t11}k_{t22} - k_{t12})}\right]^{1/2} \tag{20}$$

For $\psi = 1$, the minimum (maximum) of the function in the interval, 1 to 0 must be at the beginning or end of that interval, that is $x_2 = 1$ or $x_2 = 0$. For this case it can be shown that eq. (18) becomes

$$\tau R_{i0}{}^{1/2} = \frac{1 + (k_{p12}/k_{p21} - 1)x_2}{\sqrt{2}k_{t11}{}^{1/2} + (\sqrt{2}k_{t22}{}^{1/2}k_{p12}/k_{p21} - \sqrt{2}k_{t11}{}^{1/2})x^2} \tag{21}$$

If an experimental extrema can be found, eqs. (19) and (20) would be excellent aids in these investigations. Noting also that at the zero intercept

$$\tau R_{i0}{}^{1/2} = (2k_{t11})^{-1/2} \tag{22}$$

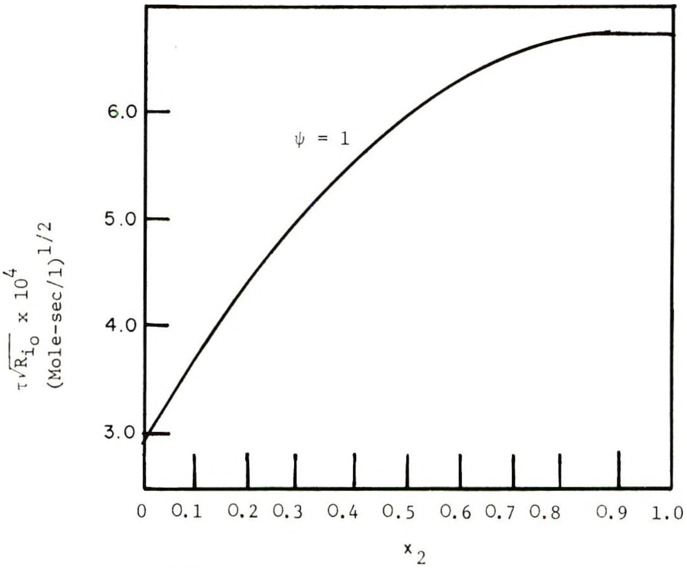

Fig. 1. Calculated $\tau\sqrt{R_{i0}}$ as a function of the mole fraction of *p*-methoxystyrene for the styrene–*p*-methoxystyrene system at 25°C.

---

* Since $x_2/(1 - x_2) > 0$, it is required that $\psi \neq 1$.

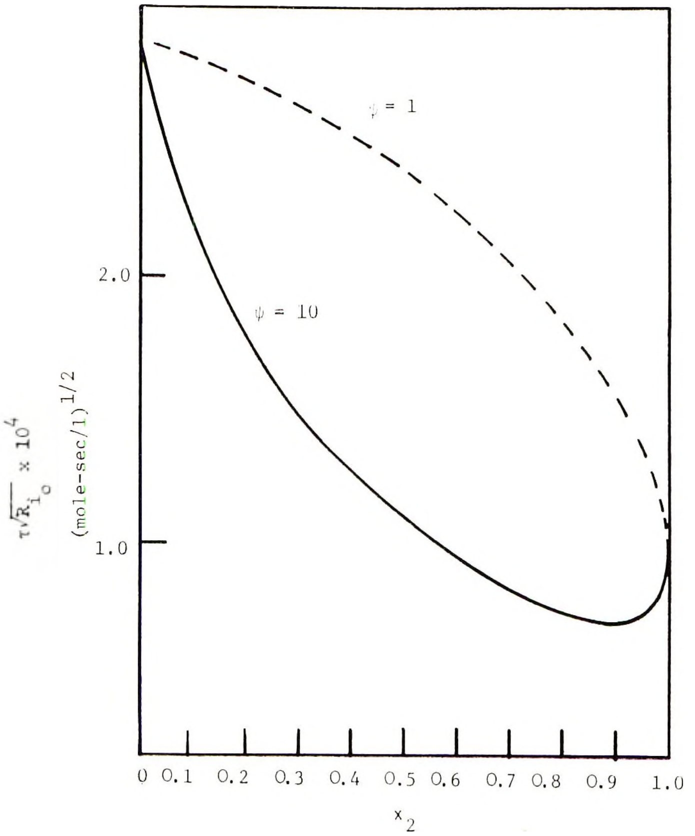

Fig. 2. Calculated $\tau\sqrt{R_{i_0}}$ as a function of the mole fraction of methyl methacrylate for the styrene–methyl methacrylate system at 25°C.

and at the $x_2 = 1$ intercept

$$\tau R_{i_0}^{1/2} = (2k_{t_{22}})^{-1/2} \tag{23}$$

the investigation of eq. (18) should be very fruitful. In theory, eqs. (19) and (20) could be used to determine all the termination constants and the ratio $k_{p_{21}}/k_{p_{12}}$. If also a steady-state analysis is made on the homopolymers the ratio r_1/r_2 could be determined. At any rate, it is seen that these expressions may be used in a variety of ways in the determination of the individual constants, in these experiments.

Figures 1–3 show plots of eq. (18) for various systems. The constants used to calculate these curves are taken from Burnett and Melville[30] and are shown in Table I. Figure 1 shows the styrene–p-methoxystyrene system for which $\psi = 1$ while in Figures 2 and 3 the curve $\psi = 1$ is plotted as a dotted line to show how the styrene–methyl methacrylate, styrene–methyl acrylate systems deviate from the ideal case ($\psi = 1$). (The termination constants used to calculate these curves were all assumed to be due to combination.)

TABLE I

Reaction Velocity Constants for Polymerization Systems, M_1 = Styrene[a]

					$k_{t11} \times 10^{-6}$ [b]		$k_{t22} \times 10^{-6}$ [b]			
M_2	k_{p11}	k_{p22}	k_{p12}	k_{p21}	Combination	Disproportionation	Combination	Disproportionation	$k_{t12} \times 10^{-6}$	$1/\alpha$ ($[M_1] = [M_2]$)[c]
Methyl methacrylate	39.5	273.0	77.0	585.0	12.0	6.0	93.2	46.6	350	7.599
p-Methoxystyrene	39.5	2.92	34.0	3.54	12.0	6.0	2.12	1.06	($\psi = 1$)	0.1039
Methyl acrylate	39.5	270.0	53.4	3600.0	12.0	6.0	110.0	55.0	1100	67.5

[a] Data of Burnett and Melville.[30]

[b] For comparisons made in this work the termination constants as listed must be divided by two; as written they are defined by $\tau^{-1} = \sqrt{R_{i_0} k_t}$, while the convention used in this work is $\tau^{-1} = \sqrt{R_{i_0} 2k_t}$.

[c] $\alpha = (M_2^*)_s/(M_1^*)_s$.

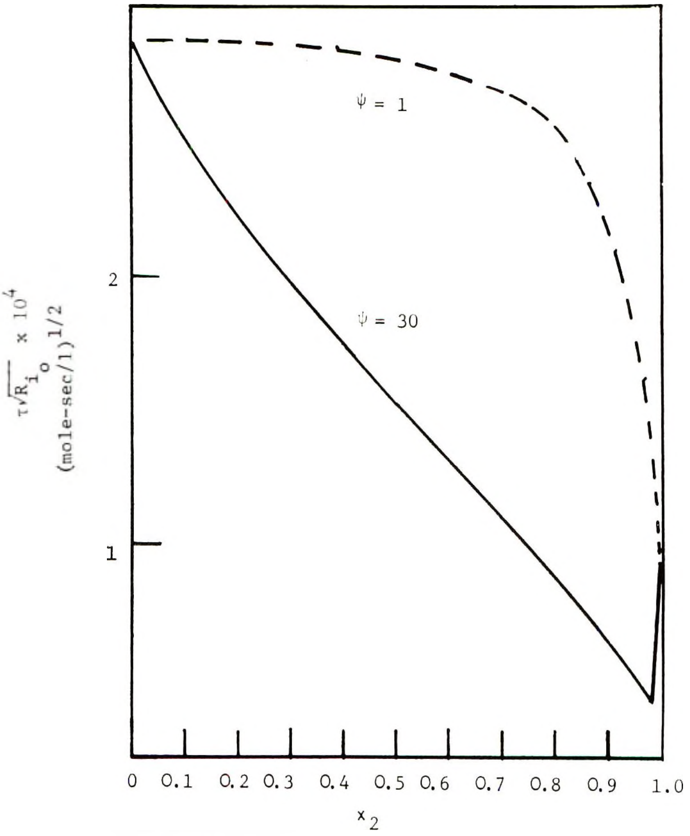

Fig. 3. Calculated $\tau\sqrt{R_{i_0}}$ as a function of the mole fraction of methyl acrylate in the styrene-methyl acrylate system at 25°C.

The definition of τ given by eq. (18) is an appropriate lifetime for the two two-component polymerization system described by the mechanism given in eqs. (1)–(9). However, to apply the sector technique to experimental copolymer systems with the intention of generating meaningful results requires the set of differential equations (13)–(16) to be solved under nonsteady-state conditions. Since this set of equations did not appear to have a simple analytical solution; a numerical solution was simulated on an IBM 7094 Computer.

In the steady-state solution of these equations it is common practice to assume that the rates of change of concentrations of M_1^* and M_2^* are so small that they can be considered to be zero, and it is a consequence of the long-chain assumption (and estimated fact) that the numerical values of $k_{p_{12}}$ $[M_1^*]$ $[M_2]$ and $k_{p_{21}}$ $[M_2^*]$ $[M_1]$ are much larger than the numerical values of $R_{i_{10}}$, $k_{t_{12}}$ $[M_1^*]$ $[M_2^*]$, and $2k_{t_{11}}$ $[M_1^*]^2$. Hence it follows that the algebraic sum of the two largest terms must also be near zero and α_{12} is, therefore a constant (for small conversions). In the case of intermittent illumination, it appears possible that $d[M_1^*]/dt$ and $d[M_2^*]/dt$ will still be numerically small. In this case, then, it might be that the rates of the cross-propagation steps would still be nearly equal. If this is the case, it would lead to a considerable simplification of the equation for intermittent illumination. This reasoning is not unlike that of Burns and Dainton[21] in their consideration of what might be considered a simplification of the set of equations, eqs. (13)–16). The assumption was therefore tested by a computer simulation of three copolymerizations for which rate constants were available. The simulations of eqs. (13)–(16), were quite successful and, as will be seen later, show α_{12} to be a constant during intermittent illumination. This leads to an analytical solution of the copolymer equations for the non-steady-state conditions of a rotating-sector experiment.

By using a square-wave initiation rate response and applying a fourth-order Runge-Kutta Gill numerical-integration technique, the rates of reaction of the copolymer systems, styrene–methyl methacrylate, styrene–methyl acrylate and styrene–*p*-methoxystyrene were determined numerically by using values of the velocity constants found in the literature (Table I). The simulations show that during the pseudo-steady-state period, inherent to the experimental technique, the ratio of the free radical species was constant to a high degree of approximation. Figure 4 shows a typical simulation run. It is seen the ratio $[M_1^*]/[M_2^*]$ is a constant and equal to the value it would attain in a steady-state experiment after only one

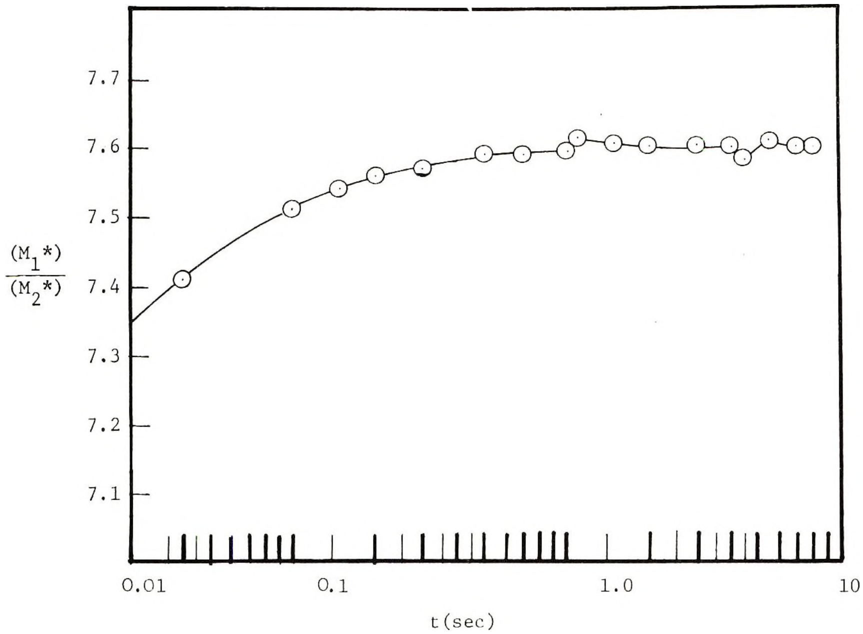

Fig. 4. Plot of the ratio $[M_1^*]/[M_2^*]$ as a function of time during intermittent illumination determined by a computer simulation of a 50% styrene–methyl methacrylate copolymer system, where the flash period is 4 sec (r = 3) and the lamp is on at t = 0.

flash cycle. It was found that after a number of flash cycles the ratio $[M_1^*]/[M_2^*]$ becomes nearly constant for all the conditions and systems tested.

Use of the assumption

$$[M_1^*]/[M_2^*] = [M_1^*]_s/[M_2^*]_s$$

causes the sum of equations. (13) and (14) to degenerate into the form given by eq. (10) when $k_{t_{11}}$ is replaced by an effective termination constant. The theoretical treatment given by Melville[4] and Noyes[3] can therefore be

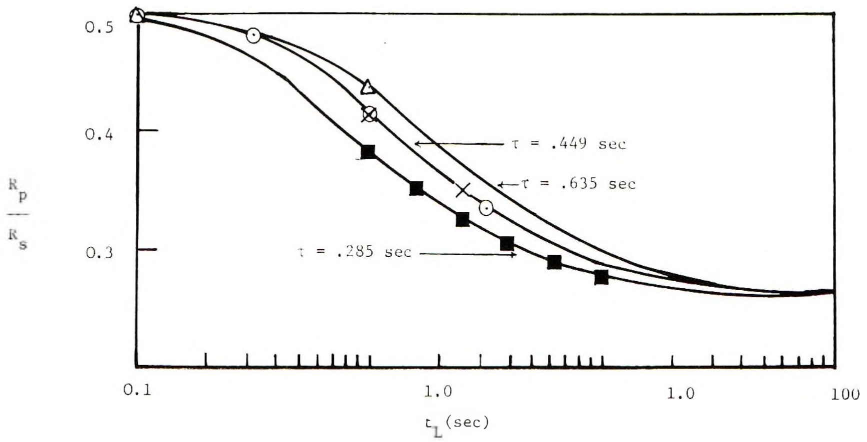

Fig. 5. Plots of the ratio of the rate of reaction under intermittent illumination to that under steady illumination as a function of t_L, as determined by a computer simulation of the styrene–methyl methacrylate polymerization system: (——) data of Burnett and Melville;[2] (⊙) run 1-A; (△) run 1-B; (×) run 1-C; (■) run 1-D.

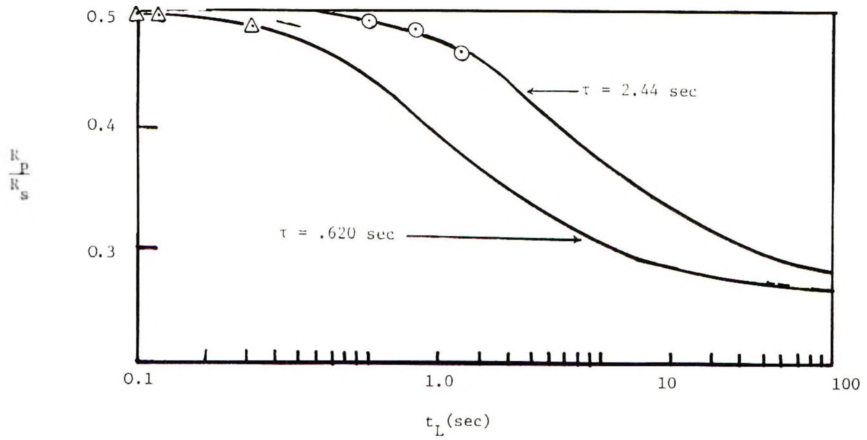

Fig. 6. Plots of the ratio of the rate of reaction under intermittent illumination to that under steady illumination as a function of t_L, as determined by computer simulation: (⊙) data of Burnett and Melville;[2] (⊙) styrene–p-methoxystyrene· (△) styrene–methyl acrylate.

applied directly to copolymer systems when their lifetime is redefined by eq. (18). Further, it is easily seen

$$\frac{R_p}{R_s} = \frac{\overline{\{d([\mathrm{M}_1] + [\mathrm{M}_2])/dt\}_p}}{\{d([\mathrm{M}_1] + [\mathrm{M}_2])/dt\}_s} = \frac{\overline{[\mathrm{M}_1{}^*]}}{[\mathrm{M}_1{}^*]_s} = \frac{\overline{[\mathrm{M}_2{}^*]}}{[\mathrm{M}_2{}^*]_s} \tag{24}$$

where

$R_p = \overline{\{d([\mathrm{M}_1] + [\mathrm{M}_2])/dt\}_p}$ = average rate of copolymerization during pulsed illumination

$R_s = \{d([\mathrm{M}_1] + [\mathrm{M}_2])/dt\}_s$ = average rate of copolymerization during steady illumination

Additional proof for the validity of the analytical solution can be generated by determining the ratio of the average rate of copolymerization under intermittent illumination to the rate under steady illumination at various flash periods. These ratios were determined numerically for the conditions listed in Table II and are shown in Figures 5 and 6 and Tables III–V for various light times (t_L). A comparison of these values with the t_L/τ values given by Melville[2] also shown in Figures 5 and 6, allow lifetimes to be determined. These lifetimes determined by the computer simulation are shown in Tables III–V for each value of t_L used. Also shown in these

TABLE II
Computer Simulations

Run no.	System[a]	Pulse period time range, sec	Styrene, %	Over-all Rate of initiation $R_i \times 10^8$ mole/l.-sec	Individual initiation rates[b]
1-A	S-MM	0.126–12.6	50	6	$R_{i1_0} = R_{i2_0}$
1-B	S-MM	0.4, 4	50	3	$R_{i1_0} = R_{i2_0}$
1-C	S-MM	4, 10	50	6	$R_{i1_0} = 0$; $R_{i2_0} = 6 \times 10^{-8}$ mole/l.-sec
1-D	S-MM	4–40 sec	10	6	$R_{i2_0} = 5.4 \times 10^{-8}$ mole/l.-sec $R_{i1_0} = 0.6 \times 10^{-8}$ mole/l.-sec
2	S-pM	4–10	50	6	$R_{i1_0} = R_{i2_0}$
3	S-MA	0.4, 1.26	50	6	$R_{i1_0} = R_{i2_0}$

[a] S-MM = styrene–methyl methacrylate; S-pM = styrene–*p*-methoxystyrene; S-MA = styrene–methyl acrylate.

[b] R_{i1_0} = steady-state rate of initiation of M_1; R_{i2_0} = steady-state rate of initiation of M_2.

TABLE III

Computer Simulation Lifetimes for Styrene–Methyl Methacrylate System

Run no.	Styrene, $[M_1]$, %	$R_{i_0} \times 10^8$, mole/l.-sec	t_L,[a] sec	R_p/R_s[b]	t_L/τ	$[\overline{M}_1{}^*]_p/[M_1{}^*]_s$	$[\overline{M}_2{}^*]_p/[M_2{}^*]_s$	τ, sec	τ_c (calcd), sec
1-A[c]	50	6.0	1.26	0.48100	0.68	0.48096	0.48105	0.463	0.449
			4.00	0.41419	2.23	0.41415	0.41424	0.448	
			12.60	0.33699	7.00	0.33695	0.33704	0.450	
1-B[e]	50	3.0	1.0	0.43925	1.58	0.43922	0.43928	0.633	0.635
1-C[d]	50	6.0	1.0	0.41423	2.23	0.41374	0.41473	.448	0.449
			2.5	0.35023	5.60	0.34975	0.35074	.449	
1-D[c]	10	6.0	1.000	0.38131	3.5	0.38046	0.38148	0.286	0.285
			1.585	0.35105	5.5	0.35021	0.35122	0.288	
			2.500	0.32579	8.6	0.32495	0.32596	0.290	
			3.975	0.30568	14.0	0.30485	0.30584	0.284	
			6.30	0.29025	22.5	0.28942	0.29042	0.280	
			10.00	0.27865	35.0	0.27782	0.27882	0.286	

[a] Light time of square-wave illumination pulse.

[b] $R_p/R_s = d([M_1] + [M_2])_p/d([M_1] + [M_2])_s$.

[c] $R_{i1_0} = R_{i2_0}$.

[d] $R_{i1_0} = 0$, $R_{i2_0} = 6 \times 10^{-8}$ mole/l.-sec.

[e] $R_{i1_0} = 0.6 \times 10^{-8}$ mole/l.-sec; $R_{i2_0} = 5.4 \times 10^{-8}$ mole/l.-sec.

TABLE IV
Computer Simulation Lifetimes for Styrene–*p*-Methoxystyrene System[a]

t_L, sec	R_p/R_s	t_L/τ	$[M_1^*]_p/$ $[M_1^*]_s$	$[M_2^*]_p/$ $[M_2^*]_s$	τ, sec
1.00	0.49357	0.40	0.49459	0.49236	2.50
1.585	0.48427	0.62	0.48529	0.48306	2.54
2.500	0.46629	1.02	0.46731	0.46509	2.45

[a] 50% Styrene; $R_{i0} = 6.0 \times 10^{-8}$ mole/l. sec; $R_{i1_0} = R_{i2_0}$; τ_c (calcd) = 2.44 sec.

TABLE V
Computer Simulation Lifetimes for Styrene–Methyl Acrylate System[a]

t_D, sec	R_p/R_s	t_L/τ	$[M_1^*]_p/$ $[M_2^*]_s$	$[M_2^*]_p/$ $[M_2^*]_s$	τ, sec
0.126	0.49781	0.20	0.49773	0.49793	0.63
0.315	0.48894	0.50	0.48885	0.48906	0.63

[a] 50% Styrene; $R_{i0} = 6.0 \times 10^{-8}$ mole/l. sec; $R_{i1_0} = R_{i2_0}$; τ_c (calcd) = 0.620 sec.

tables is τ_c, a value for the lifetime determined by using eq. (18). Agreement between the value of τ determined numerically and the value calculated from eq. (18) is found to be excellent.

It should also be noted (see Tables III–V)

$$\frac{\{d([M_1] + [M_2])/dt\}_p}{\{d([M_1] + [M_2])/dt\}_s} = [M_1^*]/[M_1^*]_s = [M_2^*]/[M_2^*]_s \qquad (25)$$

as predicted earlier.

The immediate conclusion is that for all practical purposes the copolymer rate expressions degenerate into a form similar to the homopolymer expression and by merely changing the definition of τ to that given by eq. (18) the rotating sector theory and technique can be meaningfully applied to the two component system.

The validity of these ideas can also be shown by experimentation which is the subject of the next section.

Experimentation

To demonstrate the validity and utility of the non-steady-state application of the sector technique to copolymer systems laboratory experiments were conducted. Since the purpose of this work was to demonstrate the method and not to generate new raw data, the often investigated styrene–methyl methacrylate copolymer system was chosen for the demonstration along with some rough experiments conducted on the stryene-methyl acrylate system.

Lifetime studies on the initial monomer fractions of 50, 90, and 100 mole-% methyl methacrylate in styrene were made. Monomer compositions of 23% and 50% methyl acrylate in styrene were also studied. The three concentration levels for methyl methacrylate were chosen because accord-

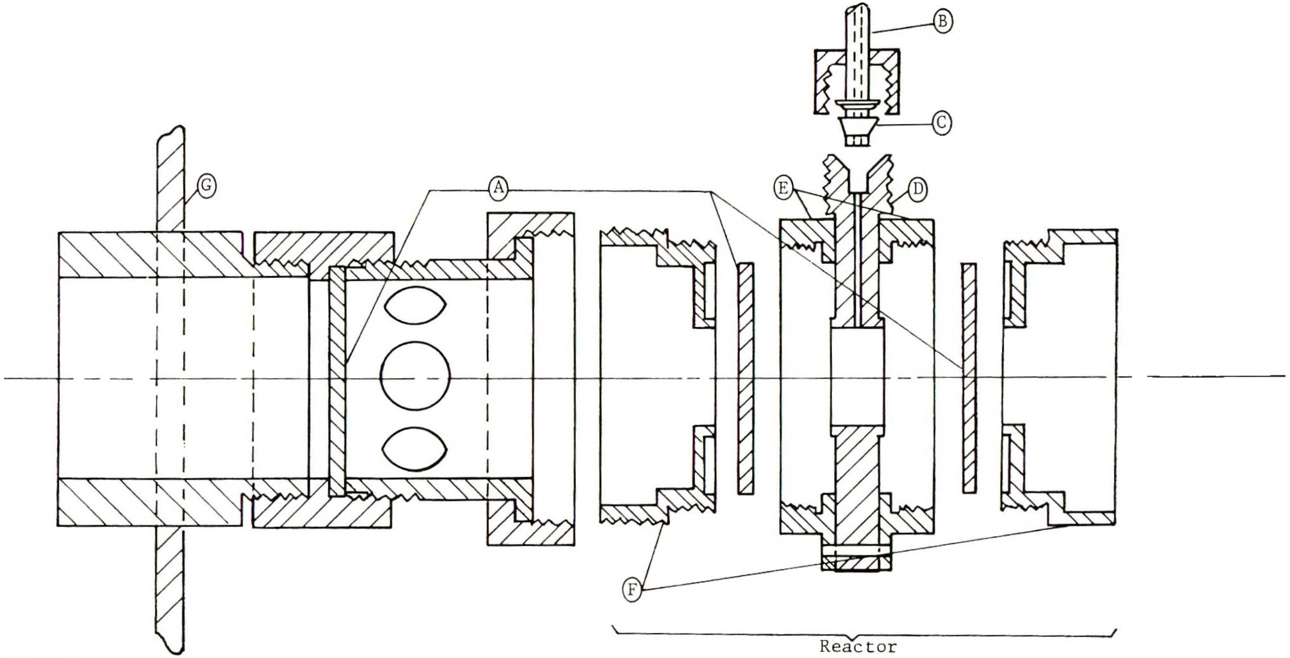

Fig. 7. Reactor and mounting assembly: (A) quartz windows; (B) capillary tube; (C) Swagelok ferrules; (D) Teflon main body; (E) brass flanges; (F) brass window nuts; (G) temperature bath wall.

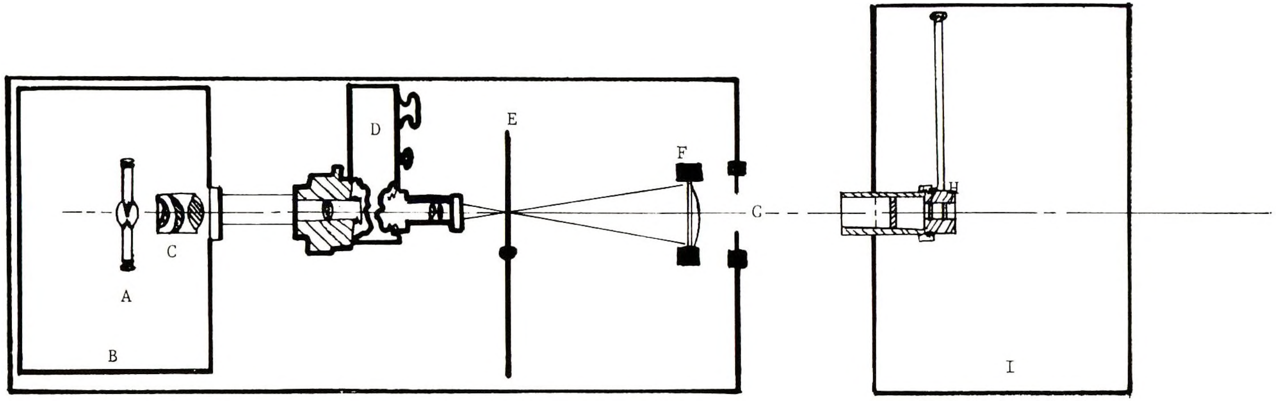

Fig. 8. System for measuring reaction rate: (A) lamp; (B) lamp housing; (C) collimating lens system; (D) monochromator and focusing system; (E) chopping disk; (F) collimating condenser lens; (G) iris diaphragm and camera shutter; (H) reactor assembly; (I) constant-temperature bath.

ing to available rate data and our estimates, the system would show a minimum in lifetime in this region. All the bulk polymerization experiments were conducted at 25°C with azobisisobutyronitrile as the photoinitiator.

Apparatus

A special type of dilatometer reactor was used to measure the change in reactant concentration with time.[21] This reactor, shown in Figure 7, is made of Teflon, brass, and quartz. The light path for the reactor was 1.22 cm and the volume was 9.63 cc.

The height of liquid in the capillary tube was measured with a cathetometer. ($\approx$0.00013% conversion based on styrene could be detected.)

The optical system is shown in Figure 8. The light source was a 500-W high-pressure mercury arc lamp which was filtered by a Schoeffel prism monochromator adjusted to 3650 Å with a half band width of 450 Å. All lenses and windows used in the system were of quartz. The cooling bath (10 gal) was mounted onto an adjustable rotary table for easy positioning of the reactor and maintained to a constant temperature of 25°C by using a temperature controller with a 0.001°C sensitivity.

The lamp intensity was monitored during the experiments by a photoresistor (Clairex 960-CLS)–digital ohm meter system which was calibrated with a potassium ferrioxalate actinometer.[31–33] In addition, the pulse time period for the intermittent illumination experiments was monitored by a photoresistor, triggering device connected to an electronic timer.

For the pulsed illumination runs the beam was chopped at its narrowed point ($\approx$1 mm) by a 7-in. blackened aluminum disk which had a 90° slot cut from it. This system gives a maximum deviation from a square wave of 0.2% at an infinitely long time period.[15,26] (Note: the error decreases for finite time periods.) The speed of chopping was controlled by a variable speed motor fitted with a feedback control system.

Purification

The monomers (Matheson Coleman and Bell) were first freed of inhibitors, prepolymerized, distilled at reduced pressure (20 mm) and then introduced into a high vacuum system constructed of Pyrex #2103 buret tubing. Here, the monomers were freed of oxygen by repeated freezing, pumping, thawing, and refreezing and then distilled under vacuum into a mixing chamber. The amount of each monomer distilled was determined by the volume change in the burets. The reactor into which was weighed the desired amount of initiator (azobisisobutyronitrile) was attached to the mixing chamber in such a way that inversion of the entire system would cause the contents of the mixing chamber to fill the reactor.

Rate of Reaction

Several steady-state, pulsed, and dark rates were measured for each filling of the reaction vessel. A least-squares best fit of the change in capillary height with time was determined for each run, and the average of the steady-state runs was then taken as the appropriate steady-state height change. The average of the dark rate runs was taken as the dark rate.

Discussion of the Results

The ratios of the pulsed to steady-state runs for various t_L for three monomer compositions (50, 90, 100% methyl methacrylate) are shown in Figures 9–11. Since the ratio of the dark to the steady rate was relatively large, lifetime measurements were made using the equation given by

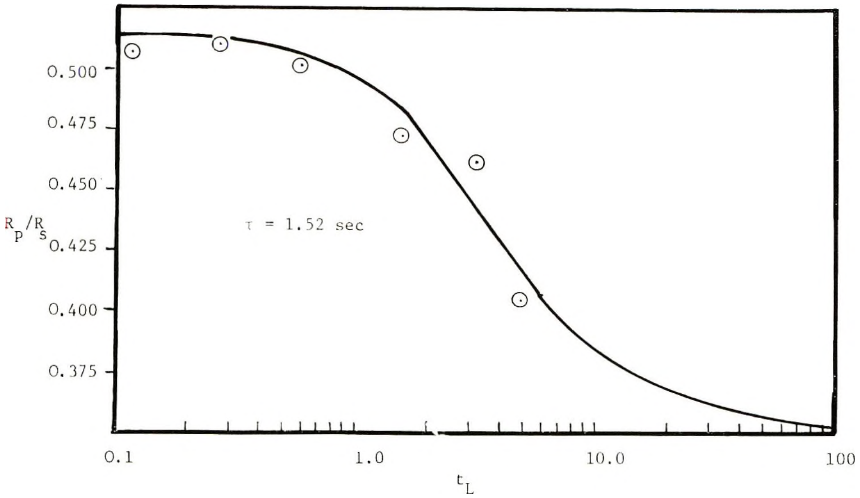

Fig. 9. Experimental R_p/R_s as a function of t_L for 100% methyl methacrylate at a measured dark ratio of 0.137.

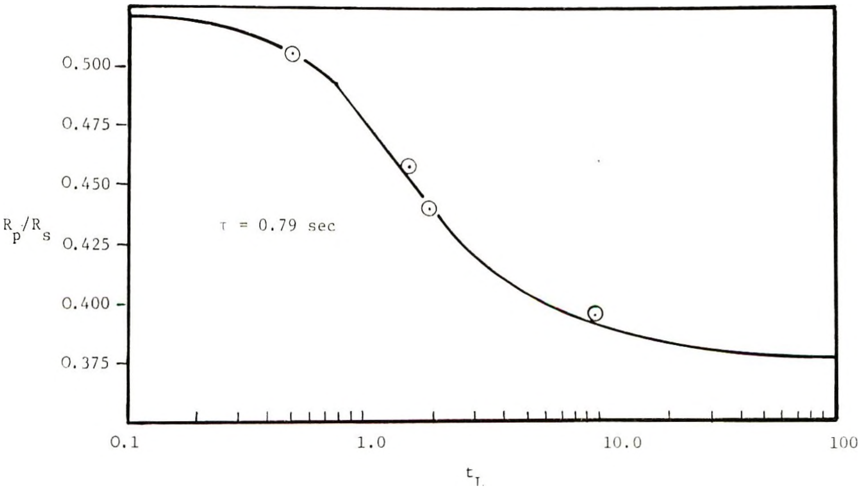

Fig. 10. Experimental R_p/R_s as a function of t_L for 90% methyl methacrylate–styrene at a measured dark ratio of 0.169.

Matheson[9] which takes into account a dark rate. Plots of this equation for various dark ratios encountered in these experiments are shown in Figure 12. The displacement of these curves and experimental curves (Figs. 9–11) allow the lifetime to be determined.

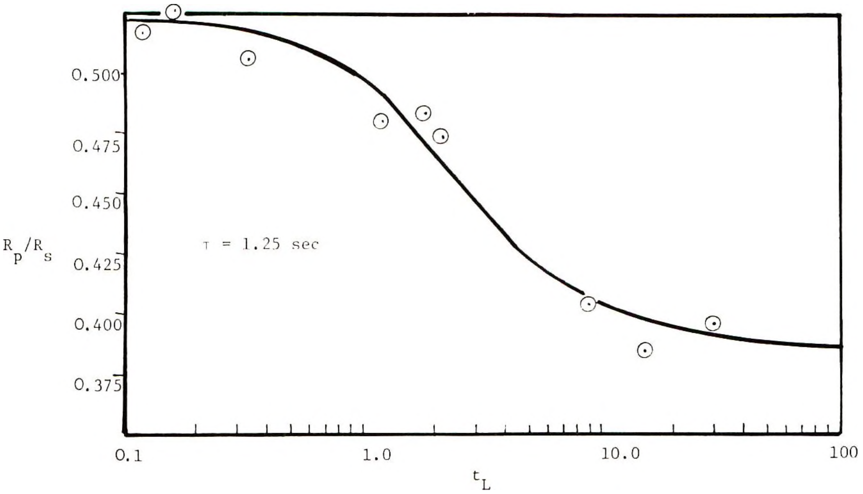

Fig. 11. Experimental R_p/R_s as a function of t_L for 50% methyl methacrylate–styrene at a measured dark ratio of 0.180.

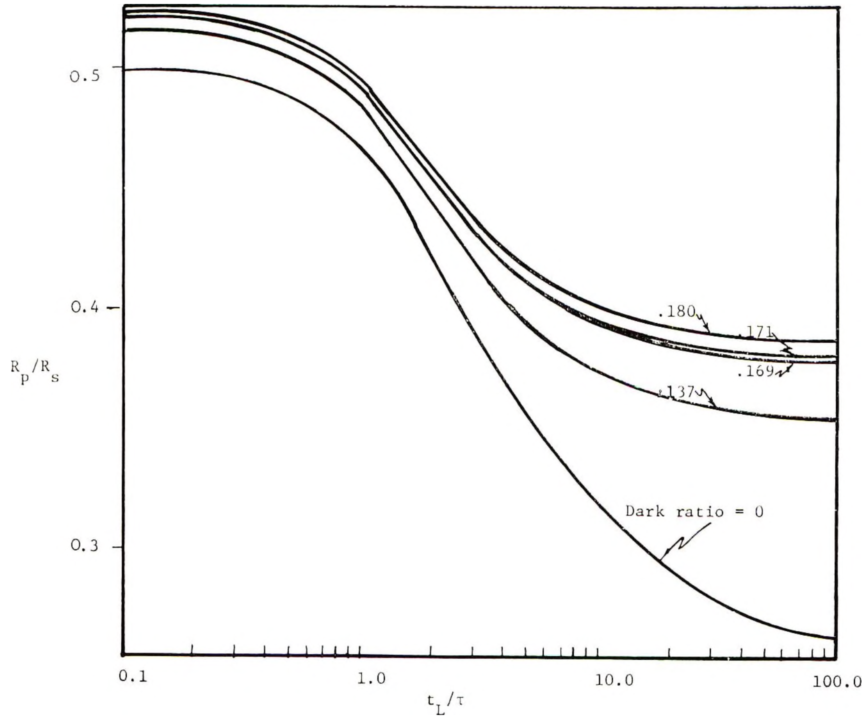

Fig. 12. Curves of R_p/R_s as a function of t_L/τ for various dark ratios.

The initiation rate for each run was estimated by using the equation

$$R_{i_0} = 2\Phi\mu C_s I_0 \qquad (26)$$

where Φ denotes efficiency, μ is the absorption coefficient (determined on the natural logarithm), C_0 is the concentration of the initiator (azobisisobutyronitrile), and I_0 is the incident radiation intensity.

Equation (15) is valid for small absorption (< 10%) which is the case for these experiments. The efficiency of the photoinitiation of azobisisobutyronitrile has been determined by Bukhart[34] and we assume his value of 0.158 is appropriate for our system. Bevington[35,36] has demonstrated that for this initiator in the styrene–methyl methacrylate system the thermal efficiency is independent of monomer composition. Assuming this is also true for the photo-efficiency and using the value for the photoefficiency determined by Bukhart, the data of Marano 26 are shown in Figure 13.

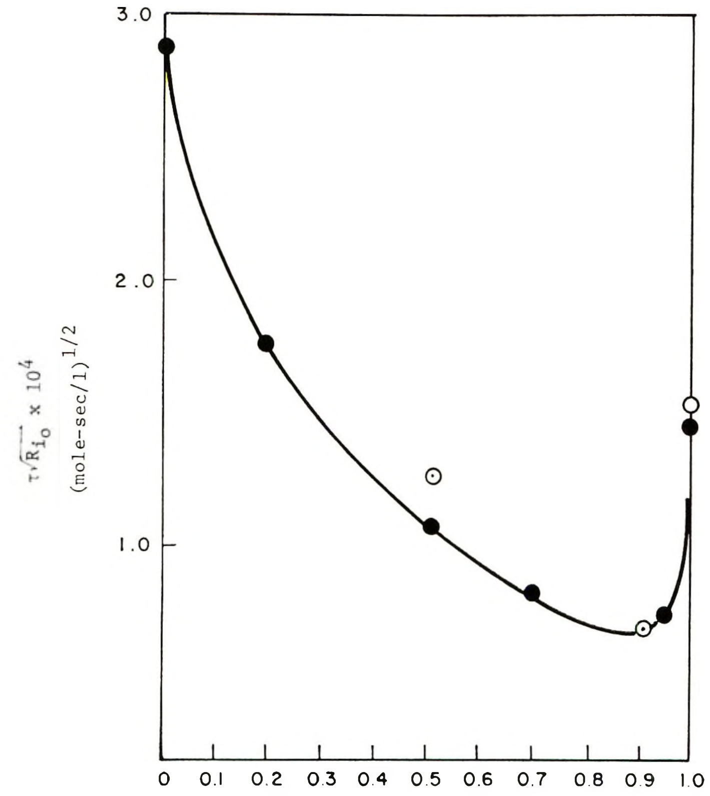

Fig. 13. Experimental and calculated $\tau\sqrt{R_{i_0}}$ as a function of the mole fraction methyl methacrylate for the styrene–methyl methacrylate system at 25°C. (●) calculated; (⊙) experimental data. The constants used in these calculations are taken from Table I. Styrene was taken as combination termination while methyl methacrylate as disproportionation. This has been shown to be the case by Bevington.[36] In this respect the calculated plot of Fig. 13 differs from the calculated plot of Fig. 2 where all combination was assumed.

Along with the experimental data a plot of eq. (18) is shown. This plot was constructed by using values of the rate constants taken from the literature and shown in Table I. It is seen the agreement between the experimental data and the calculated plot is excellent.

Experiments were also performed on the styrene methyl acrylate system at two levels of concentration (50 and 77% styrene). The stringent purification used on the styrene-methyl methacrylate system was not followed for these experiments, however, the agreement of the experimental data with the calculated curves was within the estimated experimental error.[26]

Conclusion

The results of the computer simulations and the excellent agreement of the experimental work with calculations based on previous literature values for the rate constants show the ideas generated in this work and that the assumptions used are valid.

To summarize it has been shown: (1) the conditions (repeated pulse of illumination) of the rotating-sector technique force the ratio of radical concentrations to become constant and equal to the steady-state illumination value; (2) the copolymer rate expressions degenerate into the form of the homopolymer equation because of (1); (3) the rotating-sector technique can be successfully applied to two-component polymerization systems; (4) by lifetime versus monomer composition, alone, all the termination constants and the ratio of the cross-propagation constants can be determined.

It is believed that the direct application of the technique to two-component polymerization or even multicomponent polymerization systems can provide an extra experimental tool to use in sorting out the various velocity constants. It may yield intrinsically accurate crosstermination constants for some systems and could prove to be very valuable in applications involving copolymer systems where one of the two monomers does not homopolymerize.

The authors wish to gratefully acknowledge the financial support of the American Chemical Society—Petroleum Research Fund in the form of a graduate fellowship for J. P. M.

This paper is based in part on a paper presented at the Third Joint IIQPR-AIChE Meeting, San Juan, Puerto Rico, May 1970.

References

1. P. J. Flory, *Principles of Polymer Chemistry*, Cornell Univ. Press, Ithaca, N. Y., 1953.
2. F. Briers, D. L. Chapman, and E. Walters, *J. Chem. Soc.*, **1926,** 568 (1926).
3. W. A. Noyes and P. A. Leighton, *The Photochemistry of Gases*, Reinhold, New York, 1937.
4. G. M. Burnett and H. W. Melville, *Technique of Organic Chemistry*, Vol. VII, S. L. Friess and A. Weissberger, Eds., Interscience, New York, 1953, pp. 133–170.
5. G. M. Burnett and H. W. Melville, *Proc. Roy. Soc.* (London), **A189,** 456 (1947).
6. B. R. Chinmayanandam and H. W. Melville, *Trans. Faraday Soc.*, **50,** 73 (1954).

7. H. Kwart, H. S. Broadbent, and P. D. Bartlett, *J. Amer. Chem. Soc.*, **72**, 1060 (1950).
8. M. H. Mackay and H. W. Melville, *Trans. Faraday Soc.*, **45**, 323 (1949).
9. M. S. Matheson, E. E. Auer, E. B. Bevilacqua, and E. J. Hart, *J. Amer. Chem. Soc.*, **71**, 497 (1949).
10. M. S. Matheson, E. E. Auer, E. B. Bevilacqua, and E. J. Hart, *J. Amer. Chem. Soc.*, **71**, 2610 (1949).
11. M. S. Matheson, E. E. Auer, E. B. Bevilacqua, and E. J. Hart, *J. Amer. Chem. Soc.*, **73**, 1691 (1951).
12. M. S. Matheson, E. E. Auer, E. B. Bevilacqua, and E. J. Hart, *J. Amer. Chem. Soc.*, **73**, 1700 (1951).
13. M. S. Matheson, E. E. Auer, E. B. Bevilacqua, and E. J. Hart, *J. Amer. Chem. Soc.*, **73**, 5395 (1951).
14. H. W. Melville and L. Valentine, *Trans. Faraday Soc.*, **46**, 210 (1950).
15. R. M. Felder, *AIChE Symp. Ser., Nuclear Eng.*, **62**, 12 (1966).
16. F. B. Hill, *AIChE J.*, **10**, 166 (1964).
17. J. Adam, S. Dusoleil, and P. Goldfinger, *Bull. Soc. Chim. Belg.*, **65**, 912 (1956).
18. W. G. Barb, *Proc. Roy. Soc.* (London), **A212**, 66, 177 (1952).
19. W. G. Burns, R. Barker, B. A. Lewis, and E. J. York, *Trans. Faraday Soc.*, **61**, 2686 (1965).
20. W. G. Burns and F. S. Dainton, *Trans. Faraday Soc.*, **46**, 411 (1950).
21. W. G. Burns and F. S. Dainton, *Trans. Faraday Soc.*, **48**, 39 (1952).
22. F. S. Dainton, D. A. Lomax, and M. Weston, *Trans. Faraday Soc.*, **53**, 460 (1957).
23. S. Dusoleil, P. Goldfinger, A. M. Mahieu-Van der Auwerd, G. Martens, and D. Van der Auwerd, *Trans. Faraday Soc.*, **57**, 2197 (1961).
24. O. K. Rice, *J. Chem. Phys.*, **10**, 440 (1942).
25. A. Shepp, *J. Chem. Phys.*, **24**, 939 (1955).
26. J. P. Marano, Jr., Thesis, Yale University, New Haven, Conn., 1969.
27. H. W. Melville, B. Noble, and W. F. Watson, *J. Polym. Sci.*, **2**, 229 (1947).
28. C. Walling, *J. Amer. Chem. Soc.*, **71**, 1930 (1949).
29. M. Boudart, *Kinetics of Chemical Processes*, Prentice-Hall, Englewood Cliffs, N.J., 1968.
30. G. M. Burnett and H. W. Melville, *Chem. Rev.*, **54**, 225 (1954).
31. C. G. Hatchard and C. A. Parker, *Proc. Roy. Soc.* (London), **A235**, 518 (1957).
32. C. A. Parker, *Proc. Roy. Soc.* (London), **A220**, 104 (1954).
33. C. A. Parker, *Trans. Farady Soc.*, **50**, 1213 (1954).
34. R. D. Bukhart, *J. Phys. Chem.*, **70**, 605 (1966).
35. J. C. Bevington, H. W. Melville, and R. P. Taylor, *J. Polym. Sci.*, **14**, 463 (1954).
36. J. C. Bevington, H. W. Melville, and R. P. Taylor, *J. Polym. Sci.*, **12**, 449 (1954).

Received February 10, 1970
Revised May 20, 1970

JOURNAL OF POLYMER SCIENCE: PART A-1 VOL. 8, 3483-3493 (1970)

Radiation-Induced Polymerization of 3,3,4,4,5,5,5-Heptafluoropentene-1 at High Pressure

DANIEL W. BROWN, ROBERT E. LOWRY, and LEO A. WALL
Polymer Chemistry Section, U.S. Department of Commerce
National Bureau of Standards Washington, D.C. 20234

Synopsis

A study was made of the radiation-induced polymerization under pressure of 3,3,4,4,5,5,5-heptafluoropentene-1. Polymerization rates increase with pressure (activation volume equals −11 cc/mole) and temperature (activation enthalpy equals 6.5 kcal/mole) in liquid phase. At 13800 atm and 25°C, freezing occurs; the polymerization rate in the solid is very small. In liquid phase polymerization can continue for many hours after the irradiation is terminated. An active species is formed by radiation which initiates polymerization in the dark period.

Introduction

Some time ago several radiation-induced polymerizations of 3,3,4,4,5,5,5-heptafluoropentane-1 were carried out at high pressure.[1] Subsequently, a study was made of the copolymerization of this pentene with tetrafluoroethylene.[2] Incidental to this it was found that the liquid-phase polymerization of the pentene continued for hours after removal of the sample from the radiation source. It was also found that the pentene froze at some pressures in the experimental range; freezing considerably reduced the polymerization rate. These effects have been studied further and the results are reported herein.

Experimental

The pentene was purchased from Peninsular Chem Research, Gainesville, Florida. It was quite pure as judged by boiling point; analysis by vapor-phase chromatography revealed less than 0.1% impurities. Before use it was treated with Ascarite, dried over phosphorus pentoxide, and degassed.

Equipment and techniques were as described earlier.[3] Steel vessels were used except when glass tubes are specified. The radiation source was ^{60}Co. Polymer yields were established by evaporating the monomer after polymerization and weighing the recovered monomer and residue separately. The intrinsic viscosities were determined as before[4] in hexafluorobenzene at 29.7°C.

Results

In Figure 1 the specific volume of the pentene at 24°C is plotted versus pressure. The isobaric volume change at 13800 atm indicates that freezing occurs. This was never observed without first superpressing the pentene by about 1500 atm. Slightly above or below the equilibrium pressure the transition runs very slowly even with crystals present. Initially, data were taken without appreciation of the very low rate of equilibration, and the transition did not appear to be isobaric.[5] At 1 and 11,000 atm the pentene freezes at −135° and 0°C, respectively.

Without irradiation no polymer was found when the pentene was held for 24 hr at 22°C at pressures of 10000, 13500, or 15500 atm. Thus, the rate of thermal polymerization is very small. Exposure to γ-radiation at high pressure readily gives polymer, which was always completely dissolved in the monomer. Figure 2 shows the polymer yield after different irradiation times at pressures of 5000, 10000, and 13500 atm. In this and succeeding figures the numbers associated with the points are the intrinsic viscosities of the polymer in deciliters/gram.

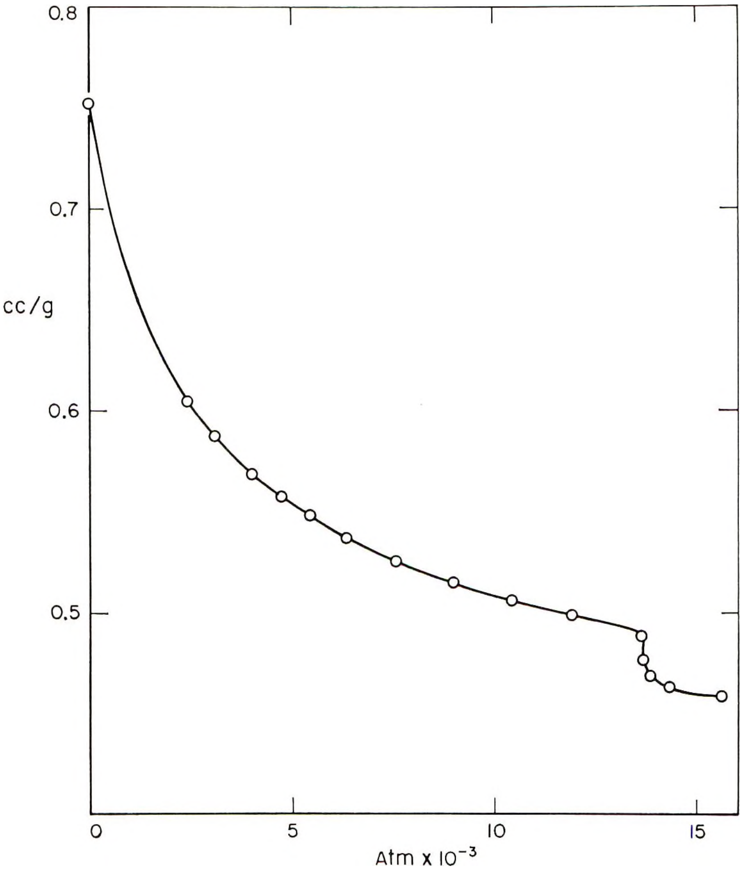

Fig. 1. Specific volume of 3,3,4,4,5,5,5-heptafluoropentene-1 at 24°C vs. pressure.

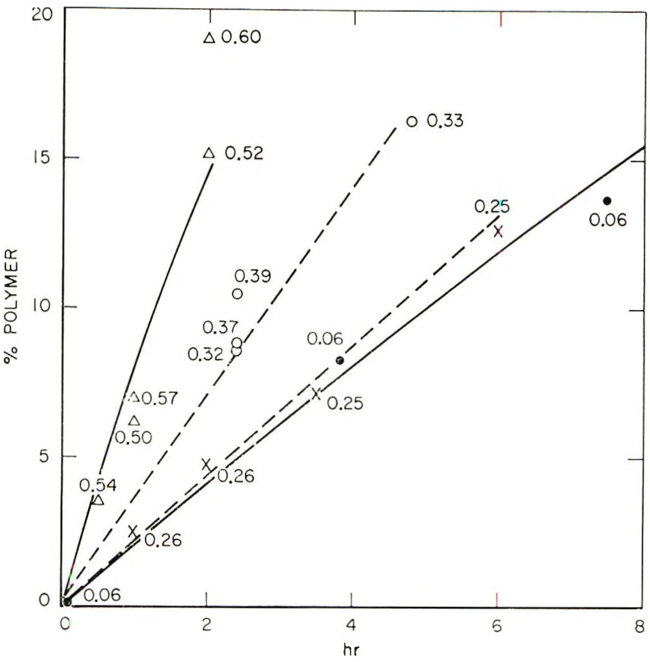

Fig. 2. Polymer yield vs. time in source at 22°C, no storage. Lines are for first-order disappearance of monomer: (△) 13500 atm, 38000 rad/hr, $k_1 = 0.079$ hr^{-1}; (○) abscissa, hr × 0.1, 10000 atm, 2000 rad/hr, $k_2 = 0.0038$ hr^{-1}, dashed line; (×) 10000 atm, 38000 rad/hr, $k_3 = 0.023$ hr^{-1}, dashed line; (●) abscissa, hr × 0.1, 5000 atm, 38000 rad/hr, $k_4 = 0.0021$ hr^{-1}. Numbers near points are intrinsic viscosities.

Of particular interest is the question of rate acceleration. If the aftereffects mentioned above are associated with long-lived propagating species, their number should increase with total dose and rate acceleration should occur. Lines drawn on this plot are calculated for first-order monomer disappearance for the rate constants specified. Rate accelerations should appear as increasingly large upward deviations of the experimental points from the lines at high polymer yields. At 5000 and 10000 atm no such trend is observed. The deviations from these lines and the results of the three replicate runs at 10000 atm indicate the degree of precision in the measurements. A questionable case is at 13500 atm, where one 2-hr point is about 30% higher than the line. As a result of the short reaction time, the scatter at this pressure is greater than at 5000 and 10000 atm.

Intrinsic viscosities are substantially independent of time at each pressure and radiation intensity. This is contrary to the anticipated behavior if long-lived propagating species are present. The size of these species, and hence the intrinsic viscosity would increase with conversion unless monomer transfer interfered with the process.

Despite the absence of thermal polymerization or rate acceleration during irradiation, significant after effects do occur in liquid phase. Table I compares polymer yields and intrinsic viscosities obtained after 1-hr irradia-

TABLE I

Polymerization at 22°C of 3,3,4,4,5,5,5-Heptafluoropentene-1 with and without 24 hr Storage After 1 hr Irradiations at 38000 rads/hr

Pressure, atm		Polymer, %		[η], dl/g	
Stored	Not stored	Stored	Not stored	Stored	Not stored
0.7	0.7	0.03	~0.005	Not determined	
5000	5000	0.90	0.16	0.12	0.06
9800	10200	10.1	2.5	0.43	0.26
13000	13600	31.5, 26.4	6.2, 7.0	0.73, 0.63	0.50, 0.57
15400[a]	15400[a]	0.10	0.08	0.26	0.25

[a] Monomer had crystallized.

tions with and without subsequent 24-hr storage. The pressures are arithmetic means of initial and final values. The maximum conversion (31.5%) resulted in a pressure drop of 1500 atm at substantially constant volume. Thus, conditions are not truly isobaric. At pressures of 13500 atm or less there is about a fivefold increase in conversion on 24 hr storage. Intrinsic viscosities also increased considerably. In the solid phase at 15500 atm no significant storage effect is observed.

At 0.7 atm (autogenous pressure) the yields are low and only oils are obtained. More convincing evidence of induced activity at this pressure was desired. To obtain this a pentene sample was irradiated at 0.7 atm for one hour and brought to 13500 over a period of 1 hr. It was pressurized slowly in order to minimize compressive heating. After 24 hr storage the polymer content was 6.8%. Several similar experiments testing further ideas were carried out; results are in Table II. Here it is seen that when

TABLE II

Polymerization of 3,3,4,4,5,5,5-Heptafluoropentene-1 during Storage at 13500 atm after 1 hr Irradiations at 38000 rads/hr at Autogenous Pressure (22°C, 24 hr Storage)

Irradiation	Transfer	Polymer, %	[η], dl/g
Steel	None	6.8	0.83
Glass	Poured	0.78	0.87
Glass	Condensed	0	—
Glass[a]	Poured[b]	0.43	0.50

[a] 1.5 mole-% dry O_2 added before irradiation.

[b] O_2 removed before transfer.

the pentene was irradiated in the bomb much more polymer formed during storage than when the pentene was irradiated in a glass vessel and subsequently poured through a preevacuated space into the bomb. This transfer, of course, required additional time and took place in light so considerations besides the difference in container are involved. Transfer of the pentene by condensing the vapor into the bomb after irradiating liquid pentene in glass resulted in no polymer formation on high-pressure storage.

We thought that the active species had low volatility and were largely left behind. To test this idea a glass tube containing the pentene was given 38,000 rads, opened in the absence of air, and the pentene removed by evaporation at −40°C; tetrafluoroethylene was condensed onto the residue at −196°C and the tube resealed. Within 20 min after being warmed to room temperature a small amount of polytetrafluoroethylene had precipitated; after an additional 2 hr period little additional polymer was obtained. The final polymer yield was 0.1%. No polytetrafluoroethylene formed in a tube that had been evacuated, irradiated, charged with tetrafluoroethylene, and held at room temperature as a blank. Qualitatively, the same observations were made with an additional pair of tubes.

From the above it seems clear that a polymerization initiator of low volatility forms when 3,3,4,4,5,5,5-heptafluoropentene-1 is irradiated. Presumably the active species are radicals since polytetrafluoroethylene forms best via radical reactions. The catalyst has not been identified. Our initial speculation was that a peroxide, perhaps polymeric, formed from residual oxygen. In the last experiment in Table II, oxygen was purposely added before irradiation and removed prior to storage, with the idea of increasing peroxide formation and so, the polymer yield on storage. In-

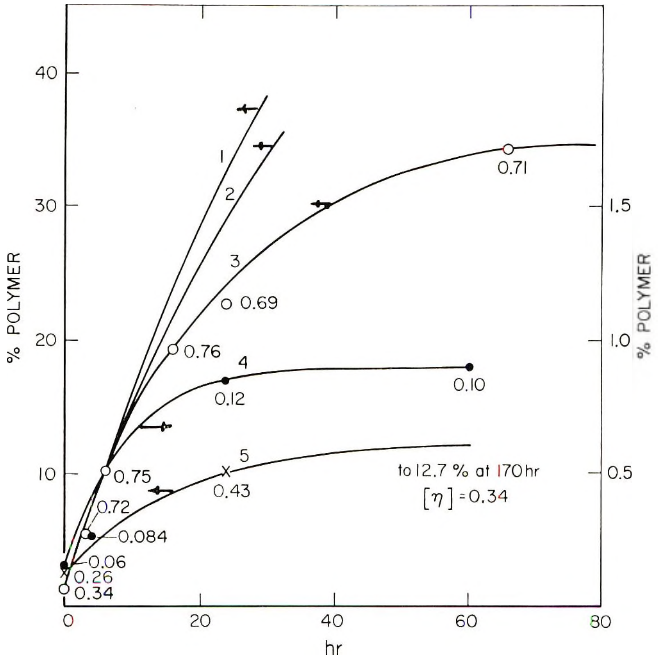

Fig. 3. Polymer yield vs. storage time (22°C, 1 hr irradiation at 38000 rad/hr): (*1*) first-order, $k = 0.0156$ hr^{-1}; (*2*) second-order, $k = 1.59 \times 10^{-3}$ l./mole-hr; (*3*) eq. (1), $k_1 = 0.074$ hr^{-1}, $2k_2[C_0]^{1/2}/(k_1k_4)^{1/2} = 0.44$; (*4*) eq. (1), $k_1 = 0.23$ hr^{-1}, $2k_2[C_0]^{1/2}/(k_1k_4)^{1/2} = 0.0074$; (*5*) eq. (1), $k_1 = 0.11$ hr^{-1}, $2k_2[C_0]^{1/2}/(k_1k_4)^{1/2} = 0.11$. Left ordinate: (○) irradiation at 5000 atm, storage at 13500 atm, (×) 10000 atm; right ordinate: (●) 5000 atm. Numbers near points are intrinsic viscosities.

stead, a decrease resulted. Another negative result involved rapidly opening a bomb that had been irradiated for 1 hr at 13500 atm, withdrawing some of the monomer–polymer mixture, diluting it with hexafluorobenzene, and determining the solution viscosity at various times. One would expect that if polyperoxides had been present there would have been a viscosity drop; none was observed.

A *G* value (yield per 100 eV absorbed) of about 0.2 was found for conversion of pentene to oil in an irradiation in glass for 24 hr at 10^5 rad/hr. The oil contains several components, none of which were identified. Presumably, some components are inactive so the *G* value for catalyst formation must be less than 0.2 in an irradiation of this duration.

Additional experiments were performed to elucidate the kinetics of the after effect. Figure 3 shows the polypentene yield as a function of storage time. For irradiations at 5000 atm, storage was at 13500 or at 5000 atm. For the former case the intercept at zero time is the polymer yield found after bringing an irradiated sample to 13500 atm and reducing the pressure immediately. Other intercepts were results of experiments without storage at the same pressure (Fig. 2). The intrinsic viscosities reach limiting values quickly. These are higher than any obtained at the same pressure without storage even at much lower radiation intensity. The lines in Figure 3 are calculated for mechanisms discussed below.

Table III gives polymer yields and intrinsic viscosities obtained in samples stored for 3 hr at 13500 atm after different irradiation periods at 5000 atm. The yield goes up markedly for irradiation times between 0.24 and 4 hr. Very little polymer formed during storage after the 0.25 hr irradiation. Intrinsic viscosities do not change despite the marked changes in average rate. This implies that transfer controls the molecular weight in this range of polymerization rates.

TABLE III

Effect of Irradiation Time on the Polymerization during Storage (3 hr, 13500 atm) of 3,3,4,4,5,5,5-Heptafluoropentene-1 (Irradiations at 5000 atm, 38000 rad/hr)

Time, hr	(Time -0.25),$^{1/2}$ hr$^{1/2}$	Polymer, %	[η], dl/g
0	—	0	—
0.25	0	0.084	—
0.5	0.5	4.25	0.68
1.0	0.87	5.52	0.72
4.0	1.94	14.9	0.68

Results without storage are thought interpretable in terms of a common kinetic mechanism. The rate constant was calculated from each conversion. The logarithms of these are plotted versus pressure in Figure 4. Representative intrinsic viscosities are given. Rate maxima occur near the freezing pressure at 22°C and at 0°C. Addition of 1,1-difluoroethane prevents freezing and rates appear characteristic of unfrozen monomer.

At 22°C the lines for different radiation intensities are approximately parallel, indicating that the rates differ by about the same factor at each pressure. This factor is 4.4–5.8 between pressures of 5000 and 13000 atm. The square root of the intensity ratio is 4.5, indicating proportionality between it and the rate.

Figure 5 is a modified Arrhenius plot. Rates increase and intrinsic viscosities decrease as temperature increases. The latter implies that transfer becomes more important at high temperature.

In separate experiments, water, ammonia, and air were added to the pentene before polymerization at 10000–13500 atm. Radiation doses were about 10^5 rads. Water had no appreciable effect. Ammonia and air both

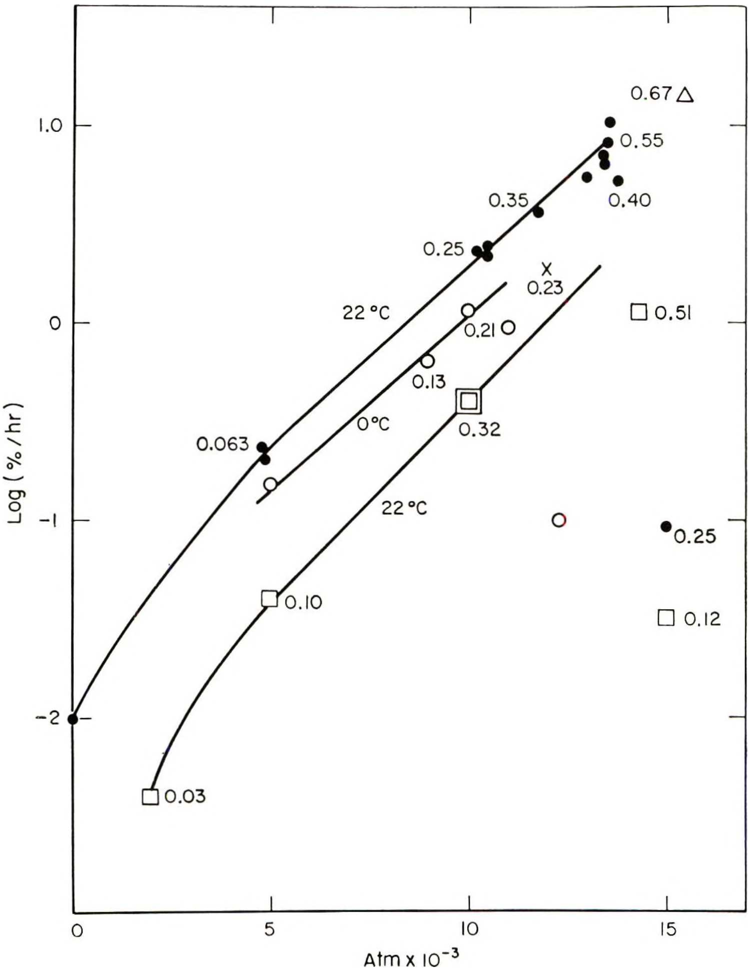

Fig. 4. Polymerization rate vs. pressure: (●) 22°C, 38000 rad/hr; (△) 22°C, 38000 rad/hr, 20 mole % CH_3CHF_2; (○) 0°C, 38000 rad/hr; (×) 0°C, 38000 rad/hr, 20 mole-% CH_3CHF_2; (□) 22°C, 2000 rad/hr. Lines end at freezing pressures. Numbers near points are intrinsic viscosities.

caused a twofold rate reduction compared with results without additives. The intrinsic viscosities were one third below normal with air but were normal with ammonia. With the latter, slightly yellow polymer was obtained. Water, ammonia, and air strongly inhibit anionic, cationic, and free-radical chain reactions, respectively, at low pressures. Since none was very effective, it is possible that one or more of these may not function in the same way at high pressure.

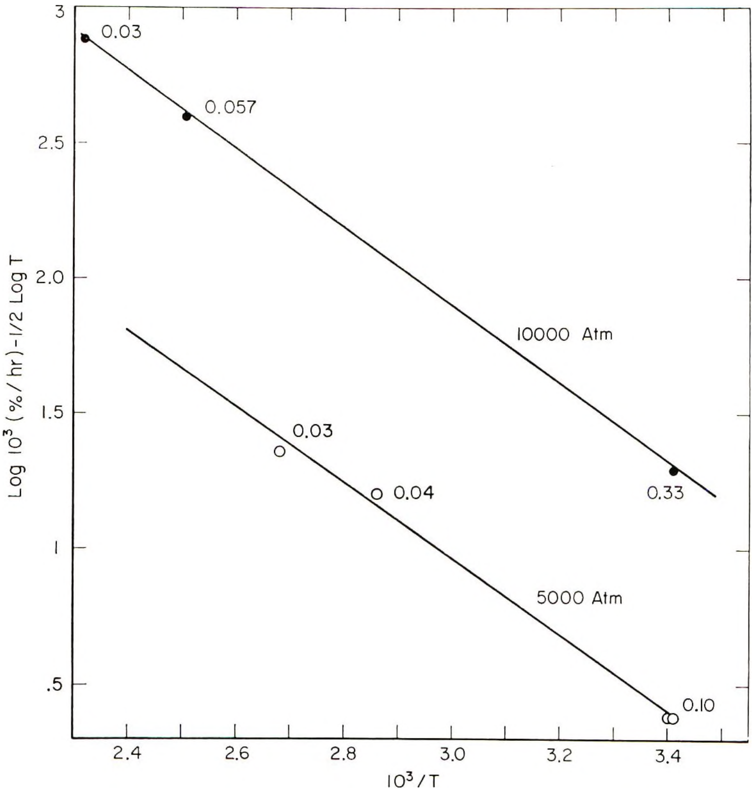

Fig. 5. Modified Arrhenius plot, rates at 2000 rad/hr: (○) 5000 atm; (●) 10000 atm. Numbers near points are intrinsic viscosities.

Discussion

The kinetics of "dead end polymerization" as developed by Tobolsky[6] account satisfactorily for the variation of polymer yield with storage time (Fig. 3). The mechanism follows.

Initiation:

$$C \xrightarrow{k_1} 2R$$

$$dR/dt = 2k_1[C]$$

Propagation:

$$R_n + M \xrightarrow{k_2} R_{n+1}$$

$$-dM/dt = k_2[M]\left(\sum_1^{\infty}[R_n]\right)$$

Termination:

$$R_n + R_m \xrightarrow{k_4} P_{n+m}$$

$$-dR/dt = 2k_4\left(\sum_1^{\infty}[R_n]\right)^2$$

Here [C] is the concentration of a catalyst, in our case formed during the radiation period. It is assumed to decompose to form radicals. In the storage period these are the only polymerization initiators. When [C] approaches zero, the polymerization stops, hence the name, "dead end polymerization." [R] and [M] are the concentrations of radicals and monomer respectively; the k's are rate constants and t is time. Application of the steady state assumption leads to [6]

$$\ln\frac{[M_0']}{[Mt]} = \frac{2k_2[C_0]^{1/2}}{(k_1k_4)^{1/2}}\,(1 - e^{-k_1t/2}) \qquad (1)$$

Here $[M_0']$ is the monomer concentration at the start of the storage period. It is less than $[M_0]$, the value without polymer, by the appropriate intercept in Figure 3. For storage at 13500 atm the intercept is 1.4%, so $[M_0'] = 0.986[M_0]$. $[M_t]$ is the monomer concentration on opening the bomb, which is also expressed as a fraction of $[M_0]$. $[C_0]$ is the concentration of catalyst at the start of the storage period. Although unknown, it should be the same in all samples with the same prestorage history. In effect, k_1 and $2k_2[C_0]^{1/2}/(k_1k_4)^{1/2}$ are constants for each reaction prehistory and may be calculated from any two experimental conversions. By using conversions at 6 and 66 hr in eq. (1), one obtains values of 0.074 hr^{-1} and 0.44 for k_1 and $2k_2[C_0]^{1/2}/(k_1k_4)^{1/2}$, respectively, at 13500 atm. Line *3* in Figure 3 is generated if these constants are used in eq. (1). The agreement of values on line *3* with experimental conversions at times of 3, 16, and 24 hr is excellent. The conversion at infinite time is predicted to be 36.7%. Lines *1* and *2* are those obtained if monomer disappears during storage by first- and second-order kinetics, respectively, with rate constants determined from the conversion after 6 hr storage. These lines indicate much more polymer at times greater than 6 hr than observed; at infinite time the conversion would be complete.

For storage at 10000 and 5000 atm, values of k_1 calculated from eq. (1) are 0.11 and 0.23 hr^{-1}, respectively. Thus k_1 appears to increase as pressure decreases. The short time (about 20 min) during which polytetrafluoroethylene accumulated in the experiments at autogenous pressure is consistent with this.

Longer irradiation times should lead to larger $[C_0]$, so more polymer will be formed in the same storage time. Data in Table III demonstrate this.

If $[C_0]$ is proportional to irradiation time, one expects from eq. (1) that the polymer yield in such experiments will go up about as the square root of the effective radiation time since $\ln([M_0']/[M_t])$ is proportional to $[C_0]^{1/2}$ and is approximately equal to the yield for small yields. In column 2 of Table III are listed these square roots if the effective radiation time is taken to be the excess over 0.25 hr because an induction period is indicated. A plot of these numbers versus polymer yield scatters somewhat but might be taken as indicating proportionality. An accurate calculation would require allowance for catalyst decomposition during irradiation, determination of $[M_0']$ for each irradiation time, and characterization of the induction period. The last two have not been done.

If C is formed at a rate proportional to intensity, radicals from C should form during irradiation at a rate $2k_1[C] = 2FG_cI[1 - e^{-k_1t}]$ where F is a factor converting G_cI into the same units as $k_1[C]$, I is the radiation intensity, and G_c is the G value for catalyst formation. Values of k_1 between 0.23 and 0.074 hr^{-1} imply appreciable rate changes over the first 10–30 hr of irradiation. That no definite polymerization rate changes were observed during irradiation implies that G_c is much smaller than G_R, the value for direct formation of radicals from the pentene, by the following reasoning. The upper limit for $2k_1[C]$ is $2FG_cI$; radicals form directly from the pentene at a rate FG_RI. The polymerization rate goes as the square root of the sum of these two rates. Thus the maximum factor by which C's decomposition can accelerate the polymerization rate is $[1 + (2G_c/G_R)]^{1/2}$. If G_c is 10% of G_R, only a 10% rate rise would be obtained.

If this argument is valid the initiation step during irradiation is effectively:

$$M \xrightarrow{FG_RI} R$$

with

$$dR/dt = FG_RI$$

Propagation and termination are as above. The polymerization rate in the source is then:

$$-(dM/Mdt) = (FG_RI/2k_4)^{1/2}k_2$$

The isothermal pressure dependence (Fig. 4) and the isobaric temperature dependence (Fig. 5) of (dM/Mdt) give the overall activation volume and enthalpy, respectively.[1] Between 5000 and 13000 atm values are about −11 cc/mole at 22°C and 6.5 kcal/mol (27 kJ/mole), respectively. Previously a value for the activation enthalpy at 15000 atm of 11.4 kcal/mole was reported.[1] Crystallization at this pressure would have occurred at one of the two temperatures used, making this value inapplicable to one phase. By assuming G_R the overall free energy of activation may be calculated [1]. If G_R equals four this is 11.5 kcal/mole (48 kJ/mole) at 5000 atm and 22°C. The entropy of activation is −16 cal/mole-degree (−67 J/mole-degree).

This study was supported by the Army Research Office, Durham, North Carolina.

Certain commercial materials and instruments were identified in this paper in order to adequately specify the experimental procedure. In no case does such identification imply recommendation or endorsement by the National Bureau of Standards, nor does it imply that the material or equipment identified is necessarily the best available for the purpose.

References

1. D. W. Brown, paper presented at American Chemical Society Meeting, Atlantic City, 1965; *Polym. Preprints,* **6,** 965 (1965).
2. D. W. Brown, R. E. Lowry, and L. A. Wall, *J. Polym. Sci. A1,* **8,** 2441, (1970).
3. L. A. Wall, D. W. Brown, and R. E. Florin, paper presented at American Chemical Society Meeting, Chicago, September 1961; *Polym. Preprints,* **4,** No. 2, 366 (1961).
4. D. W. Brown and L. A. Wall, *J. Polym. Sci. A-1,* **6,** 1367 (1968).
5. D. W. Brown, R. E. Lowry, and L. A. Wall, paper presented at American Chemical Society Meeting, New York, 1969; *Polym. Preprints,* **10,** 1395 (1969).
6. A. V. Tobolsky, *J. Amer. Chem. Soc.,* **80,** 5927 (1958).

Received May 4, 1970

JOURNAL OF POLYMER SCIENCE: PART A-1 VOL. 8, 3495–3501 (1970)

Quaternary Ammonium Polymers from 1,4-Diaza[2.2.2]bicyclooctane

J. C. SALAMONE and B. SNIDER, *Macromolecular Research Center, Institute of Science and Technology, The University of Michigan, Ann Arbor, Michigan 48105*

Synopsis

Menschutkin reactions of 1,4-diaza[2.2.2]bicyclooctane with various α,ω-dibromoalkanes and α,α'-dibromoxylenes have been studied in two solvent systems and at different temperatures. It was found that quaternary ammonium polymers could easily be prepared from this rigid, bicyclic, ditertiary amine.

Introduction

In recent years there has been considerable interest in the syntheses and properties of cationic polyelectrolytes. Polycations have been reported to exhibit certain biological properties, such as acting as bacteriocidal and antiheparin agents,[1] and they are currently finding application in various commercial processes.[2] These polyions are also of interest in solvolytic rate studies in which they greatly affect the reaction rates of ionic reagents.[3,4]

The preparations of quaternary ammonium polymers derived from various Menschutkin reactions have been reported by several workers.[1,5–12] Marvel et al. have found that an ω-haloalkyl dialkyl amine of type I, where, typically, X is a bromo group and R is a methyl group, can condense with itself, when m = 7–10, to yield a polycation (II) which contains the positively charged site in the polymer backbone.[5,6]

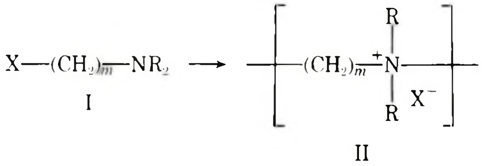

$$\underset{\text{I}}{X{-}(CH_2)_m{-}NR_2} \longrightarrow \underset{\text{II}}{\left[-(CH_2)_m-\overset{\displaystyle R}{\underset{\displaystyle R}{\overset{+}{N}}}- \; X^- \right]} \qquad (1)$$

The products were reported to be hygroscopic, and they varied in physical appearance from viscous liquids to powdery solids. The molecular weights of these polyions were calculated to be from 3350 to 28,000. When m was from 4 to 6, a variety of cyclic, low molecular weight salts was obtained,[13] although when m was 3, a polymeric quaternary salt was formed.[7,8] The latter polymer presumably resulted from a rearrangement of an unstable four-membered ring, whereas when ethyl, propyl, or butyl groups were used for the latter reaction, only the corresponding four-membered cyclic salts were obtained.

The Menschutkin reaction between a diprimary alkyl halide and a di-tertiary amine has also been reported to yield polymeric, quaternary salts (III).[9–12] Polyions of structures II and III have been

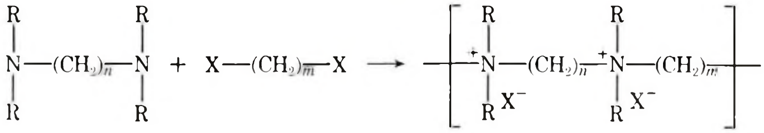

$$\mathrm{R_2N{-}(CH_2)_n{-}NR_2} + \mathrm{X{-}(CH_2)_m{-}X} \longrightarrow \left[\overset{+}{\mathrm{N}}\mathrm{R_2}{-}(\mathrm{CH_2})_n{-}\overset{+}{\mathrm{N}}\mathrm{R_2}{-}(\mathrm{CH_2})_m\right] \; 2\mathrm{X^-} \qquad (2)$$

III

termed ionene polymers because of the presence of ionic amine units in the polymer backbone.[1] The ionene polymers prepared by reaction (2) are of considerable interest, since the electrostatic and hydrophobic characteristics of the ionene can be altered by a variation of either n or m.

Reaction (2) was initially studied by Kern and Brenneisen.[9] They were able to obtain hygroscopic, polymeric salts varying in molecular weight from 3,000 to 10,000 where R = methyl, X = bromo, n = 2 or 3, and m = 3, 5, or 10. Rembaum et al. have recently reported that for the reaction (2), where R was typically a methyl group and X was a bromo group, polymers with a weight-average molecular weight of 10,000–15,000 were usually obtained when n and m were greater than three.[1] When n and m were less than three, either cyclic compounds or unexpected linear compounds normally resulted. Other investigators have also reported the preparations of cyclic compounds in similar reactions.[13–16]

In order to reduce the possibility of cyclization and also to obtain a high nucleophilicity of a di-tertiary amine, we have investigated quaternization reactions of the rigid, bicyclic, ditertiary amine 1,4-diaza[2.2.2]bicyclooctane (DABCO, IV) with normal, primary, aliphatic dibromides or with xylylene dibromides to yield ionene polymers of structure (V). The bicyclic ditertiary amine DABCO is

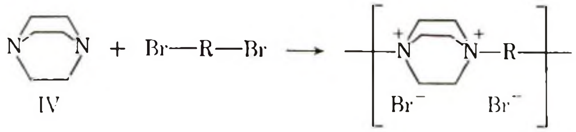

(3)

IV

V

analogous to the acyclic ditertiary amine N,N,N',N'-tetramethylethylenediamine. However, because of its rigid structure, the nitrogen lone-pair electrons should be fully exposed. This would be expected to enhance the nucleophilicity of DABCO relative to its nonrigid analog in much the same fashion as has been noted in the greater reactivity of the bicyclic amine quinuclidine with methyl iodide, in comparison to the reactivity of triethylamine.[17] Although there apparently have been no reported examples of the nucleophilicity of DABCO relative to its analog N,N,N',N'-tetramethylethylenediamine in a quaternization reaction, this effect has been clearly revealed in a hydrolytic reaction.[18]

Based on these effects, it was anticipated that ionene polymers could readily be prepared from DABCO. Furthermore, the utilization of this diamine could lead to a polycation with a higher positive charge density than that prepared from previously reported Menschutkin reactions, since the rigid structure in the former case would lead to a greater proximity of positively charged sites.

Experimental

The experimental procedures employed were similar to those previously reported.[1,11,12] The solvent systems investigated were dimethylformamide (DMF)–methanol (MeOH) (1:1 by volume) and dimethyl sulfoxide (DMSO). The general procedures were: to 10 ml of solvent was added 0.01 mole of the α,ω-dibromide and 0.01 mole of DABCO. The reactions in DMF–MeOH were performed at room temperature, normally for two weeks, whereas the reactions in DMSO were performed at 70°C for 24 hr. Water (up to 10 ml) was added during the course of all reactions, except for 1,10-dibromodecane and 1,12-dibromododecane in DMSO solution, in order to maintain a homogeneous system. The reaction contents were then transferred to dialysis tubing. After dialysis with 50% ethanol–water and then water, the solutions were lyophilized. All the ionene polymers prepared were water-soluble, except that from 1,12-dibromododecane. The ionene polymer from 1,10-dibromodecane yielded a turbid solution in water. The lyophilized products remained solid after exposure to air, even after a period of several days. However, they apparently retain a water content of approximately 8%, but do not become tacky. The elemental analyses of the ionene prepared from DABCO and the various dibromides in DMF–MeOH are listed in Table I.

Results and Discussion

These reactions were performed in two solvent systems and at different temperatures. In previous investigations it was reported that the rates of ionene formation were more rapid in solvents of higher dielectric constant and at higher temperature.[1,10] It was also found that although the rate was faster at higher temperature, the specific viscosity of the solution was less than that obtained at 25°C, indicating that a termination step was involved. This termination step could presumably involve the formation of stable cyclic compounds or the reaction of the dibromide with the solvent (DMF).

For the DABCO system, formation of cyclic compounds would be difficult because of the rigidity of the diamine. The formation of a possible trimeric ring from the reaction of DABCO and 1,3-dibromopropane at 70°C in methanol for 6 hr has previously been suggested.[19] However, it seems quite likely that this is an ionene polymer which, of course, would have the same elemental composition as that of a cyclic structure.

TABLE I
Elemental Analyses of Ionene Polymers from DABCO and Various Dibromides

Dibromide reagents		Elemental composition			
		C, %	H, %	N, %	Br, %
1,3-Dibromopropane	Calcd	34.42	5.78	8.92	50.88
	Found	34.14	5.94	8.87	50.70
1,4-Dibromobutane	Calcd	36.61	6.14	8.54	48.71
	Found	36.34	6.03	8.46	47.87
1,5-Dibromopentane	Calcd	38.62	6.48	8.19	46.71
	Found	38.37	6.62	8.08	46.84
1,6-Dibromohexane	Calcd	40.47	6.79	7.87	44.87
	Found	39.75	7.04	7.64	45.07
1,8-Dibromooctane	Calcd	43.77	7.35	7.29	41.59
	Found	43.40	7.50	7.08	41.35
1,10-Dibromodecane	Calcd	46.62	7.82	6.80	38.76
	Found	46.43	8.08	6.57	38.49
1,12-Dibromododecane	Calcd	49.10	8.24	6.36	36.29
	Found	49.06	8.45	5.97	36.32
α,α′-Dibromo-*o*-, *m*-, and *p*-xylene	Calcd	44.70	5.36	7.45	42.49
	Found (*o*)	44.41	5.48	7.46	42.24
	Found (*m*)	44.53	5.37	7.47	42.41
	Found (*p*)	44.38	5.70	7.03	42.64

The yields and intrinsic viscosities of the polycations which were prepared in DMF–MeOH and DMSO are reported in Tables II and III respectively. The intrinsic viscosities were determined in 0.4*M* KBr, where possible, in order to compare these values to previously reported values of the nonrigid ionenes.[1,10,11] It is noted that the yields of the ionenes prepared from the dibromoalkanes in DMF–MeOH are somewhat lower than those prepared in DMSO, whereas the yields of the ionenes from the xylyl-

TABLE II
Syntheses of Ionene Polymers in DMF–MeOH[a]

Dibromide reagents	Yield, %	[η], dl/g[b]
1,3-Dibromopropane	2.2	0.13[c]
1,4-Dibromobutane	3.8	0.25[c]
1,5-Dibromopentane	13.7	0.16
1,6-Dibromohexane	38.9	0.20 0.21[c]
1,8-Dibromooctane	18.5	0.18
1,10-Dibromodecane	18.4	0.18
1,12-Dibromododecane	23.4	0.18
α,α′-Dibromo-*o*-xylene	46.7	0.04[c]
α,α′-Dibromo-*m*-xylene	50.6	0.04
α,α′-Dibromo-*p*-xylene	60.4	0.05

[a] Reaction for 2 weeks at 22°C, except for 1,8-dibromooctane and 1,12-dibromododecane (3 weeks).

[b] Obtained in 0.4*M* KBr in 1:1 DMF–water, except where otherwise indicated.

[c] Obtained in 0.16*M* KBr in 1:1 DMF–water.

TABLE III
Syntheses of Ionene Polymers in DMSO[a]

Dibromide reagents	Yield, %	$[\eta]$, dl/g[b]
1,3-Dibromopropane	11.1	0.09
1,4-Dibromobutane	23.5	0.17[c]
1,5-Dibromopentane	11.4	0.15
1,6-Dibromohexane	27.5	0.18
1,8-Dibromooctane	35.4	0.18
1,10-Dibromodecane	39.8	0.17
		0.16[d]
1,12-Dibromododecane	70.0	0.25[d]
α,α'-Dibromo-*o*-xylene	0	—
α,α'-Dibromo-*m*-xylene	0	—
α,α'-Dibromo-*p*-xylene	11.7	0.03

[a] Reaction conditions: 24 hr at 70°C.
[b] Obtained in aqueous 0.4*M* KBr, except where otherwise indicated.
[c] Obtained in aqueous 0.2*M* KBr.
[d] Obtained in 0.4*M* KBr in 1:1 DMF–water.

ene dibromides for the former solvent system are considerably larger than those obtained for the latter solvent system. In fact, only a negligible amount (ca. 2–3 mg) of solid could be obtained from the reactions with α,α'-dibromo-*o*- and *m*-xylenes in DMSO. This result could perhaps be caused by a Kornblum oxidation of the xylylene dibromides in the reaction system of DABCO and DMSO.[20]

The intrinsic viscosities of the ionene polymers prepared from both solvent systems were reasonably similar. Several of the ionenes prepared from DMF–MeOH were found to be insoluble in aqueous 0.4*M* KBr, a solvent system utilized by Rembaum et al.[1,10,11] Consequently, these polymers were studied in 0.4*M* KBr in 1:1 DMF–water. In general, the intrinsic viscosities increased slightly with increasing chain length of the dibromoalkane. It is found that the ionene polymers prepared from DABCO and 1,4-dibromobutane or 1,6-dibromohexane have intrinsic viscosities three to four times those of the corresponding ionenes prepared from its nonrigid analog, *N,N,N',N'*-tetramethylethylenediamine.[11] This result was anticipated because of the greater nucleophilicity of the bicyclic amine.

In regard to the intrinsic viscosities of the ionenes from the xylylene dibromides, it is noted that these values are considerably lower than those from the dibromoalkanes. Although the xylene dibromides could be expected to react at a higher rate than the aliphatic dibromides, the lower viscosities of their ionene polymers can perhaps be accounted for by the increased rigidity or steric hindrance which results during polymer formation, particularly for the ortho and meta isomers.

The preparation of ionene polymers from DABCO and dibromomethane or 1,2-dibromoethane[21] was also attempted. Under the conditions described in the experimental section for the other dibromoalkanes in DMF–MeOH or in DMSO, no polycationic products resulted. From the former solvent system, crystals of 1-bromomethyl-4-aza-1-azoniabicyclo[2.2.2]octane bromide (VI) and 1,2′-bromoethyl-4-aza-1-azoniabicyclo[2.2.2]octane bromide (VII) were obtained in moderate yield from reaction with dibromomethane and 1,2-dibromoethane, respectively.

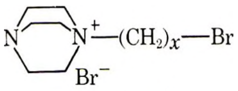

VI, $x = 1$
VII, $x = 2$

The melting points, infrared spectra, and NMR spectra of the resulting compounds were compared to those of independently prepared VI and VII,[19] and no significant differences were detected.

It is interesting to note that these monobromide salts could be isolated. This probably reflects a decreased nucleophilicity of the second nitrogen after the first is quaternized. An effect of this type could be related to the large difference in pK_a values between the monocation of DABCO (pK_a 3.6) and the neutral form (pK_a 8.8).[18]

In a second attempted polymerization, compounds VI and VII were heated at 125°C in DMF for 3 days, with no observable increase in solution viscosity. After dialysis of the reaction mixture, no polymeric products were obtained. These results are consistent with those of Rembaum et al., who also have had difficulties in preparing ionenes of a high density of positive charge.[1,10,11]

We hope to report in the near future the effect of these cationic polyelectrolytes on the reaction rates of low molecular weight reagents.

The authors are grateful to Professor C. G. Overberger for his support and encouragement of this work.

References

1. A. Rembaum, W. Baumgartner, and A. Eisenberg, *J. Polym. Sci. B*, **6**, 159 (1968), and references cited therein.
2. For a review see "Symposium on Polymeric Cations," in *Polym. Preprints*, **10**, No. 2, (1969).
3. H. Morawetz, C. G. Overberger, J. C. Salamone, and S. Yaroslavsky, *J. Amer. Chem. Soc.*, **90**, 651 (1968), and references cited therein.
4. H. Morawetz, *Svensk Kem. Tidskr.*, **79**, 309 (1967).
5. C. F. Gibbs, E. R. Littman, and C. S. Marvel, *J. Amer. Chem. Soc.*, **55**, 753 (1933).
6. M. R. Lehman, C. D. Thompson, and C. S. Marvel, *J. Amer. Chem. Soc.*, **55**, 1977 (1933).
7. C. F. Gibbs and C. S. Marvel, *J. Amer. Chem. Soc.*, **56**, 725 (1934).
8. C. F. Gibbs and C. S. Marvel, *J. Amer. Chem. Soc.*, **57**, 1137 (1935).
9. W. Kern and E. Brenneisen, *J. Prakt. Chem.*, **159**, 193 (1941).
10. A. Rembaum, *J. Macromol. Sci.*, **A3**, 87 (1969).
11. H. Noguchi and A. Rembaum, paper presented at 158th National Meeting, American Chemical Society, New York, N. Y., Sept. 1969; *Polym. Preprints*, **10**, No. 2, 718 (1969).
12. H. Noguchi and A. Rembaum, *J. Polym. Sci. B*, **7**, 383, 395 (1969).

13. E. R. Littman and C. S. Marvel, *J. Amer. Chem. Soc.*, **52,** 287 (1930).
14. L. Knorr and P. Roth, *Ber.*, **39,** 1425 (1906).
15. J. I. G. Cadogan, *J. Chem. Soc.*, **1955,** 2971.
16. S. M. McElvain and L. W. Bannister, *J. Amer. Chem. Soc.*, **76,** 1126 (1954).
17. H. C. Brown and N. R. Eldred, *J. Amer. Chem. Soc.*, **71,** 445 (1949).
18. A. J. Kirby and W. P. Jencks, *J. Amer. Chem. Soc.*, **87,** 3209 (1965).
19. T. P. Abbiss and F. G. Mann, *J. Chem. Soc.*, **1964,** 2248.
20. W. W. Epstein and F. W. Sweat, *Chem. Rev.*, **67,** 247 (1967).
21. The preparation of this quarternary polymer has recently been reported.[22] However, employing this preparation we find that the reaction only gives monomeric salt VII.
22. J. W. Bayer and E. Santiago, U. S. Patent No. 3,489,663 (1970).

Received May 6, 1970

JOURNAL OF POLYMER SCIENCE: PART A-1 VOL. 8, 3503-3510 (1970)

Catalysis of Olefin Isomerizations by Boron Trifluoride*

J. M. ROBERTS, Z. KATOVIC, and A. M. EASTHAM,
Division of Applied Chemistry, National Research Council of Canada, Ottawa 7, Canada

Synopsis

The kinetics of isomerization of butenes by boron trifluoride with acetic acid or methanol as cocatalysts have been re-examined. The results, over a wide concentration range, and at temperatures from −20 to +20°C, are consistent with previous data, but it is shown that the previously suggested mechanism cannot apply. By using deuterated acetic acid as cocatalyst it has been found that isomerization exactly parallels protonation, which is consistent with a mechanism involving a classical carbonium ion.

Our earlier studies of the isomerization of 2-butenes by boron trifluoride were interpreted in terms of the mechanism,

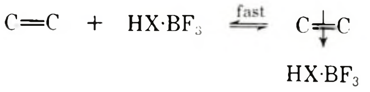

$$C{=}C + HX{\cdot}BF_3 \overset{\text{fast}}{\rightleftharpoons} \underset{\substack{\downarrow \\ HX\cdot BF_3}}{C{=}C} \qquad (1)$$

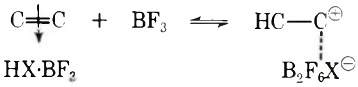

$$\underset{\substack{\downarrow \\ HX\cdot BF_2}}{C{=}C} + BF_3 \rightleftharpoons \underset{\substack{\vdots \\ B_2F_6X^{\ominus}}}{HC{-}C^{\oplus}} \qquad (2)$$

where HX, the "cocatalyst" or proton source, may be water, methanol, or acetic acid. In order to explain the observed nonlinear dependence of the rate in olefin concentration, it was postulated that the equilibrium constant for reaction (1) was of such magnitude that complex formation approached completion (i.e., approached the concentration of HX) at the higher olefin concentrations employed in the experiments. It follows from this assumption that the complex ought to be sufficiently stable to be detected, but this has not proved to be true. In Figure 1 are shown some measurements of the partial pressure of butene (0.1 mole/l.) over solutions of $BF_3\cdot CH_3COOH$ in ethylene chloride; catalyst concentrations are high so some polymerization occurs, but it is clear from extrapolation of the measurements to zero time that there is no large and rapid uptake of butene

---

* Presented at the IUPAC Symposium on Macromolecular Chemistry, Budapest, Hungary, August 1969.

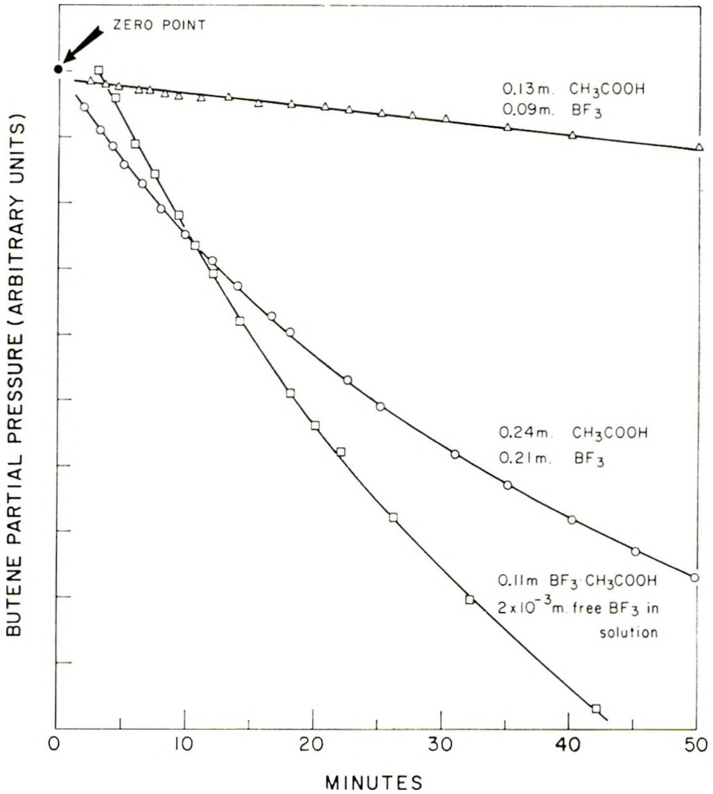

Fig. 1. Partial pressure of butene over solutions of BF_3·acetic acid in ethylene dichloride.

as required by the mechanism. We have therefore been forced to conclude that the postulated complex cannot exist in sufficient concentration to account for the kinetics.

Since the above mechanism is untenable and since we have no acceptable alternative for it, we have felt it desirable to re-examine and extend the measurements on which it was based. In particular, we wished to avoid the correction factor used to assess the medium effect when varying the olefin concentration; this was accomplished by employing mixtures of butene and butane such that the total hydrocarbon content of the solutions was always 1.0 mole/l. The measurements have been extended to a considerably wider range of concentrations and to the three temperatures 20, 0, and −20°C. In addition, we have attempted to establish clearly the relationship between protonation and isomerization by studying the two processes simultaneously using deuterioacetic acid as cocatalyst.

Experimental

The kinetic measurements were carried out essentially as previously described.[1,2] The presence of butane, especially when butane/butene is greater than nine, interferes with the estimation of butene-1 but not of *cis*-

or *trans*-butene-2. Small amounts of *trans* isomer in large amounts of *cis*-butene are easily separated, but small amounts of *cis* isomer tend to be obscured by the tail of a large *trans* peak in the chromatogram; there is thus greater uncertainty in the results when the *trans* isomer is used as starting material.

Measurements of vapor pressure of butenes over solutions of catalyst were made with butene mixtures corresponding closely to the equilibrium composition (75% *trans*, 22% *cis*, 3% butene-1). Pressures were determined with a constant-volume manometer, and readings were taken for at least 45 min. The catalyst solution was brought to 20.0°C and then the butene forced rapidly into the measuring flask from a side arm. In all cases the pressure obtained by extrapolating to zero time was within 2% of the pressure measured in the absence of catalyst, and was usually much closer.

Deuterioacetic acid, CH_3COOD of 99.8% isomer purity was prepared for us by Dr. L. C. Leitch. The deuterium content of the mixed butenes was obtained by mass spectrometry with an accuracy of better than 5% for each component, C_4H_7D and $C_4H_6D_2$. The isomer composition was obtained, as usual, by gas–liquid chromatography. Both deuterium content and isomer composition were determined on at least three samples from each reaction mixture.

Results

The observed initial rates of isomerization of *cis*- and *trans*-butene-2 at the three temperatures are shown in Figure 2. The catalyst throughout was 1.0×10^{-3} mole/l. of $CH_3COOH \cdot BF_3$ and 2.0×10^{-3} mole/l. of free, dissolved, BF_3. Hydrocarbon concentration (butene + butane) was 1.0 mole/l.; the solvent was ethylene dichloride. The results are generally very similar to those previously reported; exact comparison is possible only at 1.0 mole/l. of butene because most of the present reaction mixtures contain butane, but at that point agreement is excellent for experiments with *cis*-butene, rather poor for those with *trans*-butene. (It was noted above that analytical difficulties arise with the *trans* isomer; also the back reaction is more important with this isomer, since equilibrium is reached when the *trans* concentration is still 75%.)

The rate decreases slowly with decreasing temperature. The effect is roughly consistent with an activation energy of 5–6 kcal/mole but undoubtedly is due to a number of factors such as changes in dielectric constant and equilibrium constants, as well as to activation energy, so has little real significance. Its main interest here lies in its similarity to the temperature dependence of polymerization,[3] suggesting the possibility of a common rate-controlling step.

The rate seems to become increasingly independent of olefin concentration as the temperature is decreased. This point too, is of interest in connection with the polymerization kinetics which approach first-order dependence in monomer.[3,4] If monomer were involved in the initiation, one

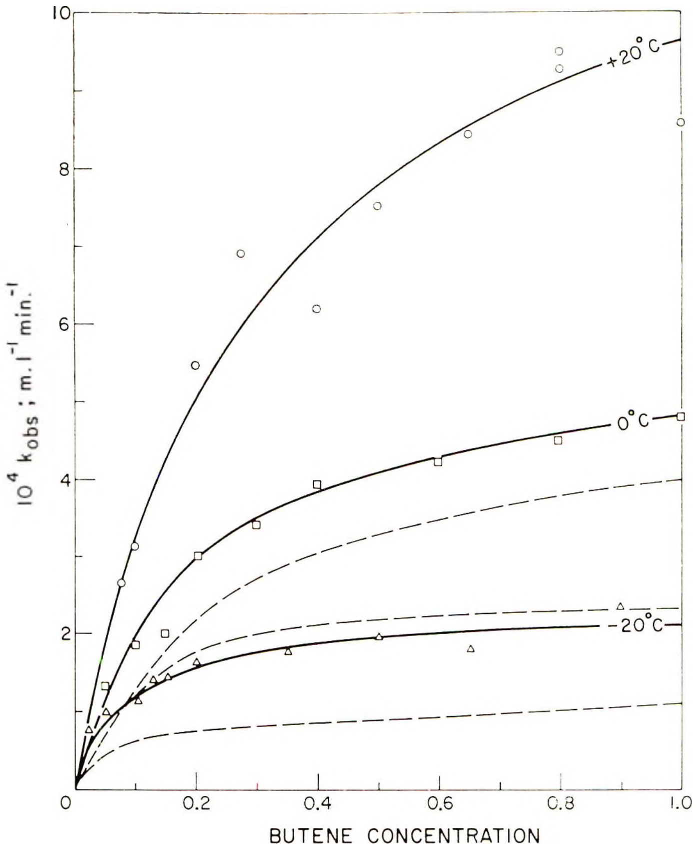

Fig. 2. Rate of isomerizations of butenes by boron trifluoride·acetic acid in ethylene dichloride solution: (——) *cis*-butene; (--) *trans*-butene.

might expect to find that the order in monomer, in the rate expression for monomer consumption during polymerization, was greater than one, so again one may suspect a relationship between the isomerization and initiation processes.

The effect of cocatalyst concentration on the rate of isomerization was reexamined at 20°C with the use of solutions containing equal amounts of butane and butene (0.5 mole/l.) and a constant excess of free boron trifluoride in solution (i.e., excess over that required to form the 1:1 complex with cocatalyst) of 1.5×10^{-3} mole/l. The results are shown in Figure 3 and provide an excellent illustration of the difficulties in this field; the measurements were made with great care and cover a concentration change of nearly one hundredfold, yet are quite inadequate to define unambiguously the nature of dependence of the rate of cocatalyst concentration. The solid line in the figure represents a half-order dependence and the dotted line a first-order dependence with intercept; the zero point on the scale has been shifted as shown, on the assumption that the blank, determined in the

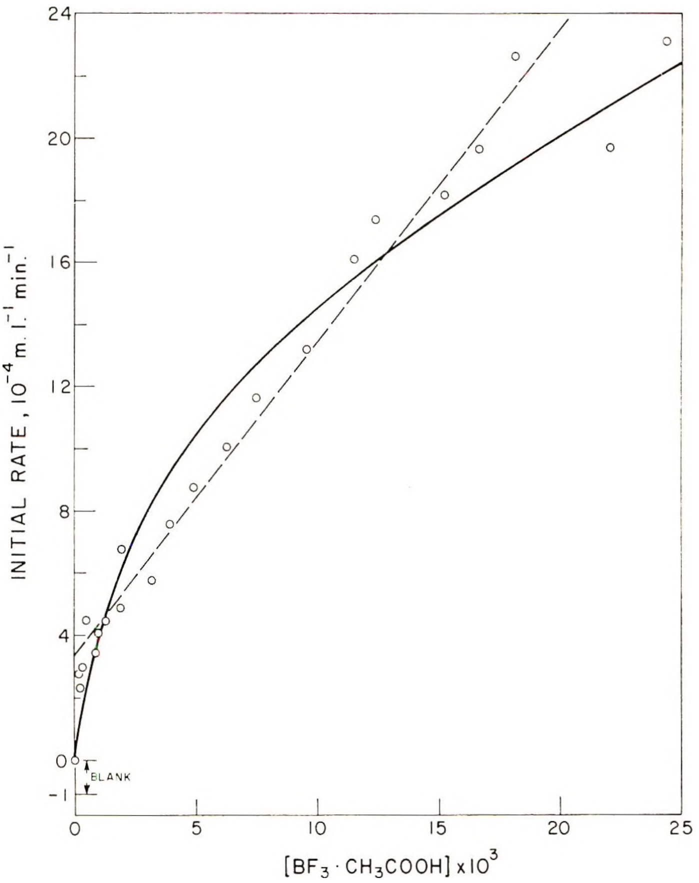

Fig. 3. Dependence of the rate of isomerization of *cis*-butene-2 on cocatalyst concentration. Butene and butane concentrations, each 0.5 mole/l.; free BF_3 in solution, 1.5 $\times$ 10^{-3} mole/l.

absence of cocatalyst, applies at all cocatalyst concentrations. In our earlier work, over a smaller concentration range, we had concluded that the reaction was of the first order in cocatalyst but it now seems more probable that the reaction approaches first order only above about 10^{-3} mole/l. cocatalyst, and that a change in kinetics may occur at lower concentrations. A shift from a free ion to an ion-pair mechanism or some similar equilibrium process could perhaps account for the results.

The results with methanol as cocatalyst, over a shorter concentration range, are entirely consistent with the results for acetic acid (Fig. 4). Again they suggest a first-order dependence above about 10^{-3} mole/l., with a change in kinetics below this point. We should point out here that methanol is from two to five times as effective as acetic acid as a cocatalyst; we previously reported erroneously that it was about equally effective.

Throughout these studies it has been assumed that isomerization proceeds through a classical carbonium ion and hence is directly related to the usually

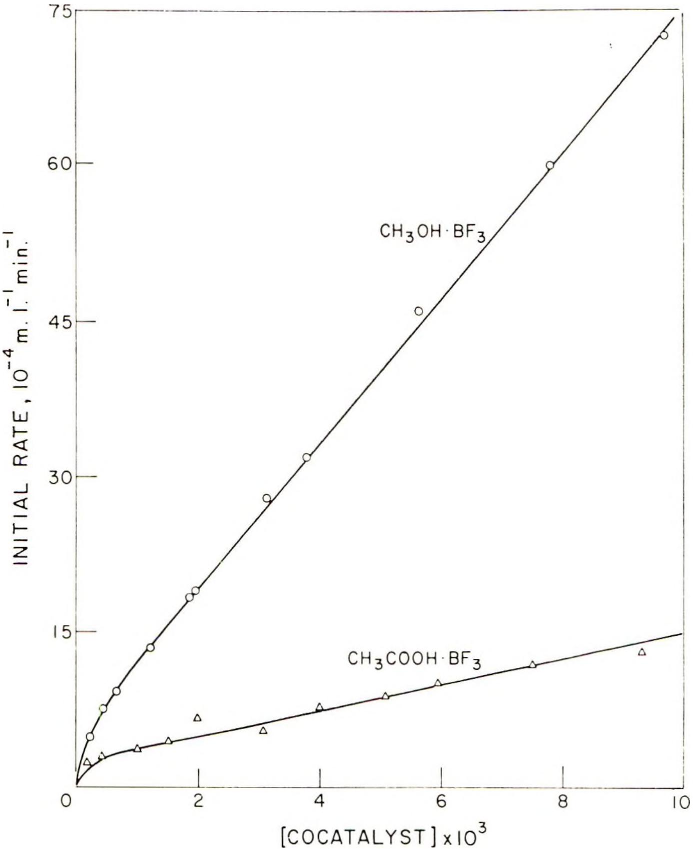

Fig. 4. Dependence of the rate of isomerization on cocatalyst concentration; *cis*-butene-2; free BF_3, 1.5 × 10^{-3} mole/l.

accepted mechanism for initiation of polymerization. However it is at least conceivable that the rearrangement could occur without complete development of the ion: the catalyzing proton could be lost again before becoming covalently bonded to carbon. A view of this kind is consistent with the fact that isomerization is much more rapid than initiation of polymerization of butene-2, and with the observation that deprotonation seems to occur much more rapidly from the butene-2 ion (I), if it is formed, than from the oligomer ion (II), in spite of their similarity in structure (stabilization of the ion II by rearrangement to a tertiary ion is not believed to be a dominant process).

$CH_3—CH_2—\overset{+}{C}H—CH_3$
I

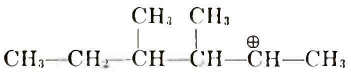
$CH_3—CH_2—\underset{}{\overset{\overset{CH_3}{|}}{C}H}—\overset{\overset{CH_3}{|}}{C}H—\overset{\oplus}{C}H—CH_3$
II

In an effort to obtain more information on this point we have measured the rate of deuteration of butenes during the isomerization, using deuterioacetic acid (CH_3COOD) as cocatalyst.

The measurements present a few problems which are easily understood in terms of the classical mechanism.

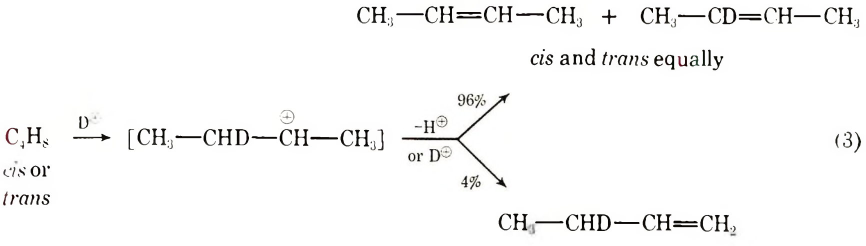

$$\underset{cis\text{ or }trans}{C_4H_8} \xrightarrow{D^{\oplus}} [CH_3-CHD-\overset{\oplus}{C}H-CH_3] \xrightarrow[\text{or }D^{\oplus}]{-H^{\oplus}} \begin{cases} \xrightarrow{96\%} CH_3-CH=CH-CH_3 + CH_3-CD=CH-CH_3 \quad \textit{cis}\text{ and }\textit{trans}\text{ equally} \\ \xrightarrow{4\%} CH_3-CHD-CH=CH_2 \end{cases} \qquad (3)$$

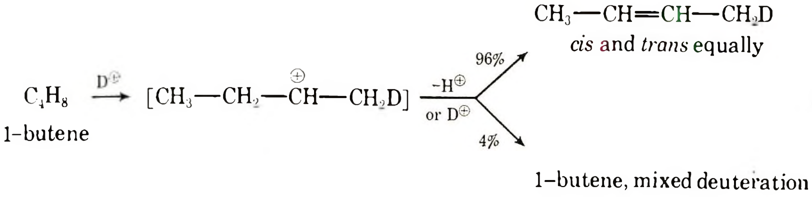

$$\underset{\text{1-butene}}{C_4H_8} \xrightarrow{D^{\oplus}} [CH_3-CH_2-\overset{\oplus}{C}H-CH_2D] \xrightarrow[\text{or }D^{\oplus}]{-H^{\oplus}} \begin{cases} \xrightarrow{96\%} CH_3-CH=CH-CH_2D \quad \textit{cis}\text{ and }\textit{trans}\text{ equally} \\ \xrightarrow{4\%} \text{1-butene, mixed deuteration} \end{cases} \qquad (4)$$

From earlier work we know that the reaction intermediate decomposes to approximately equal amounts of the *cis* and *trans* isomers (48% of each) and a small amount (3–4%) of 1-butene. The rate of isomerization of the *cis* or *trans* isomer is thus about half the rate of protonation, whereas the rate of isomerization of 1-butene should roughly equal the rate of protonation. However, when deuterons replace protons a serious complication arises because of the difference in the rate of expulsion of the two species. The effect is not very important when butene-1 is used as the starting isomer because, as seen in eq. (4), 96% of the product in this case is formed by proton expulsion only. It is important with the *cis* and *trans* isomers, where 96% of the product is formed by expulsion of either a proton or deuteron from the —CHD— group [eq. (3)]; little can be said about the

TABLE I

Relative Rates of Isomerization and Deuteration[a]

Monomer	[CH_3COOD], mole/l.	Rate of isomerization × 10^4 mole/l.-min	Rate of deuteration × 10^4, mole/l.-min	Ratio
Butene-1	0.278	1.5	1.6	0.94
	0.233	2.1	2.4	1.15
	0.173	4.2	4.2	1.00
	0.157	7.8	7.6	1.03
cis-Butene-2	0.187	19[b]	11.4	1.7
	0.233	9.2	5.5	1.7
	0.279	4.8	3.35	1.4

[a] [Butene] = [BF_3] = 0.116 mole/l.; 20°C.

[b] The rate of isomerization of *cis* isomer is taken as twice the rate of formation of the *trans* isomer (see text).

relative rates of the expulsions other than that the k_H/k_D ratio should be less than 8.

In order to avoid scrambling effects and formation of multideutero products, it is necessary to measure initial rates before much of the deuterioacetic acid is converted to the proton acid. This condition requires a fairly slow reaction rate and a large amount of acetic acid-*d*, so it was necessary to reduce the boron trifluoride concentration below that of the cocatalyst. In this respect therefore, the experiments were not carried out under the exact conditions employed for the study of isomerization and polymerization and one can only hope that the mechanism remains unchanged; the fact that the relative rates of formation of the isomers is about the same in the two series of experiments is encouraging. The results are shown in Table I.

The results for butene-1 seem to show clearly that isomerization exactly parallels protonation and hence that a mechanism based on a classical carbonium ion is acceptable. The results for the *cis* isomer are consistent with this conclusion if the k_H/k_D ratio is assigned the reasonable value of 1.5.[5]

One further point of interest may be mentioned. It is generally believed that the principal molecular weight-limiting process in cationic olefin polymerizations is the so-called "monomer transfer" process, in which a proton from the growing chain is transferred to monomer, thus terminating one chain and initiating another. If our observations on the relative rates of isomerization and polymerization are valid, monomer transfer is perhaps more properly described as monomer termination. This concept of proton transfer from ion to monomer raises the interesting question as to whether isomerization might not occur by a chain process in which the proton is transferred repeatedly from one olefin molecule to another. The present results seem to rule out this possibility.

The experimental results reported here show a number of characteristics consistent with the view that isomerization is indeed closely related to initiation of polymerization. It is clear that a mechanism such as that represented by eqs. (1) and (2) cannot account for the results, no matter what values are assigned to the constants, and unfortunately we are unable to suggest a suitable alternative. It is very evident that we require data which are more accurate by an order of magnitude and which can be extended to much lower concentrations of catalyst.

References

1. J. M. Clayton and A. M. Eastham, *J. Chem. Soc.*, **1963**, 1636.
2. A. M. Eastham, *J. Amer. Chem. Soc.*, **78**, 6040 (1956).
3. T. Szell and A. M. Eastham, *J. Chem. Soc. B.*, **1966**, 30.
4. H. R. Allcock and A. M. Eastham, *Can. J. Chem.*, **41**, 932 (1963).
5. V. J. Shiner, Jr., *J. Amer. Chem. Soc.*, **75**, 2925 (1953).

Received August 15, 1969
Revised April 30, 1970

JOURNAL OF POLYMER SCIENCE: PART A-1 VOL. 8, 3511-3527 (1970)

Thermal Degradation of Polymers with Phenylene Units in the Chain. IV. Aromatic Polyamides and Polyimides

G. F. L. EHLERS, K. R. FISCH, and W. R. POWELL,
Air Force Materials Laboratory,
Wright-Patterson Air Force Base, Ohio 45433

Synopsis

The breakdown mechanism of an aromatic polyamide and four polyimides has been studied under vacuum in the temperature range of 375–620°C, by using techniques described earlier, involving collection and analysis of volatile products as well as analyses of residues at different temperatures. The decomposition of the polyamide up to 375°C yielded predominantly carbon dioxide, while between 375 and 450°C about equal amounts of carbon dioxide and carbon monoxide formed. Hydrogen is the major product between 450 and 550°C, along with hydrogen cyanide, methane, and carbon monoxide. The major reaction at the lower temperatures seems to be the cleavage of the linkage between the carbonyl group and the ring, with subsequent formation of a carbodiimide linkage via isocyanate intermediates, and liberation of carbon dioxide. Alternatively, cleavage between the carboxyl and the NH-group leads to the formation of carbon monoxide. Carbon dioxide and carbon monoxide are also the major volatile decomposition products of the polyimides at the lower temperatures. The primary cleavage reaction is believed to be the rupture of the imide ring between a carbonyl and nitrogen, with subsequent formation of isocyanate groups. The latter react with each other to form carbodiimide linkages and carbon dioxide, while the remaining benzoyl radical is the source for carbon monoxide.

INTRODUCTION

While a considerable number of investigations have been concerned with the decomposition of aliphatic polyamides,[1–7] little is known about the decomposition mechanism of aromatic polyamides. Krasnov and coworkers[8,9] subjected polyamides made from *m*- and *p*-phenylenediamine and isophthalic and terephthalic acid to decomposition under vacuum at temperatures between 320 and 530°C. Semi-quantitive mass spectrometric analysis showed carbon dioxide and water as the major volatile products at the lower temperature ranges, along with undetermined amounts of carbon monoxide. At the higher temperatures, benzene and hydrogen cyanide also formed to a considerable extent, along with toluene, benzonitrile, some hydrogen, and the products mentioned before. Ammonia formed at the higher pyrolysis temperatures in the cases of the polymers with the isophathalic acid component. Solid products isolated were the aromatic compounds I–III.

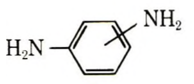

I

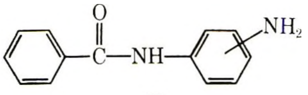

II

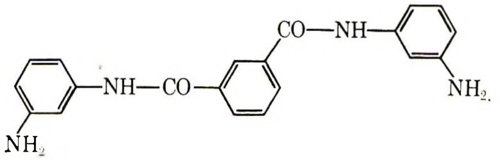

III

The authors concluded that severe hydrolytic reactions of amide bonds occur, with subsequent decarboxylation of the carboxyl endgroups. From the formation of benzonitrile, they assumed that the water for the hydrolytic reactions is formed by dehydration of ammonium salt or amide endgroups [eq. (1)].

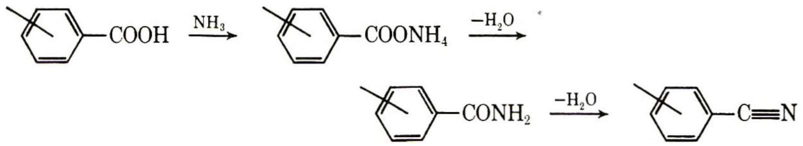

(1)

They also considered the possibility of intermediate isocyanate groups with subsequent formation of a carbodiimide linkage [eqs. (2) and (3)].

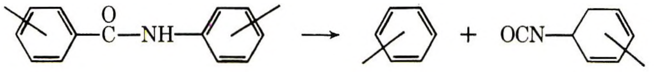

(2)

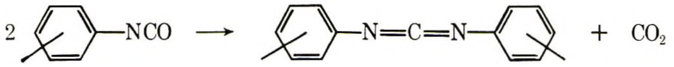

(3)

Other more complex reactions may also occur, as indicated by the presence of hydrogen, carbon monoxide, hydrogen cyanide, and toluene. More recent work[10] involved the study of the decomposition products of aromatic polyamides and -imides under oxidative conditions. The main volatile product was found to be carbon dioxide; other products included carbon monoxide, water and nitrogen.

Studies of the thermal decomposition of polyimides have been reported by Heacock and Berr,[11] who found the following products on vacuum pyrolysis of H-film, at 540°C: benzene (0.7 mole-%), carbon dioxide (35.1 mole-%), carbon monoxide (58.7 mole-%), water (1.2 mole-%), hydrogen (2.6 mole-%), hydrogen cyanide (1.2 mole-%), benzonitrile (0.5 mole-%), and traces of ammonia. About 40–60% of the weight loss consisted of gases; the remainder was liquid and solid product, containing aminophenolic and phthalimide groups. Bruck[12] pyrolyzed H-film under vacuum at 600°C and collected 60.5 mole-% carbon monoxide, 19.0% carbon dioxide, 9% hydrogen, 7.6% water, and smaller amounts of methane, ammonia, hydrogen cyanide, benzene, phenol, and benzonitrile. He attributes carbon dioxide to the hydrolysis and decarboxylation of polyamic acid moieties and assumes that the polyimide group produces only carbon monoxide. From this, he concluded, that H-film contains 22% polyamic acid. Gay and Berr[13] pyrolyzed powdered samples of the polyimide from 4,4′-diaminodiphenyl ether and pyromellitic dianhydride between 400 and 600°C. They found carbon monoxide and carbon dioxide, and above 525°C, hydrogen, to be the major gaseous products. They ascribe carbon dioxide to the presence of isoimide moieties (IV)

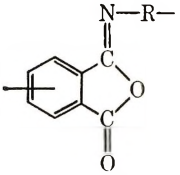

IV

initially present in the polymer as a minor component, while a steady rate of carbon dioxide is generated by isomerization of the imide groups to isoimide groups.

EXPERIMENTAL

Thermogravimetric Analyses

A Chevenard thermobalance was used for tests under nitrogen, at a heating rate of 2.5°C/min and a flow rate of 200 ml/hr. A sample size of 100 mg was used.

Degradation Studies

The results from thermogravimetric analysis were used as a guide to select three decomposition temperatures for the degradation study. The sample was heated stepwise to these temperatures, and volatiles, sublimate, and residues were collected. Details of the procedure and a description of the apparatus used for the decomposition studies have been given earlier.[14–16]

Mass Spectroscopy

The gas samples were analyzed in a Consolidated Electrodynamics Corporation Model 21-103B (modified) mass spectrometer. An ionizing voltage of 70 eV and an ionizing current of 10 μA was used.

Infrared Spectroscopy

Infrared spectra were obtained by use of a Perkin-Elmer infrared recording spectrophotometer, Model 137, and potassium bromide pellets. The polymers and especially the residues were shaken 1–4 min in steel vials in a Wig-L-Bug (Crescent Dental Mfg. Co., Chicago, Ill.) and sifted through brass sieves. The part with a particle size below 75 μ was collected. Depending upon the opacity of the materials, 0.25–0.7% of the polymer in KBr was used.

RESULTS AND DISCUSSION

Description of Polymers

One aromatic polyamide and four polyimides have been subjected to decomposition in this study.

The polyamide (polymer I) received from the Chemstrand Research Center, Inc., Durham, N. C. was a sterically ordered, fully aromatic polyamide whose structure is presumed by the authors to be:

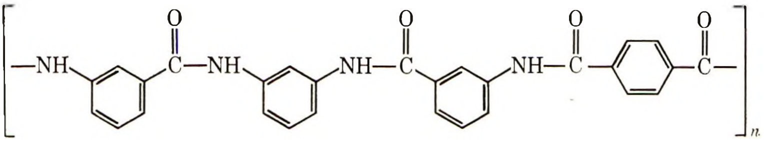

The fluffy, white powder was apparently of high molecular weight, it was, however, insoluble in conventional organic solvents. Studies conducted independently with this polymer[17] showed that it was essentially amorphous. DTA seemed to indicate a second-order transition at 275°C and endotherms at 430 and 460°C related to thermal decomposition. Our own DTA measurements showed a second-order transition at 277°C and an irregular pattern of endotherms and exotherms beginning at 397°C.

The polyimides (Polymers II–V)[18] were yellow to orange films received from Research Laboratories, Westinghouse Electric Corporation. In general, they were prepared by addition of the stoichiometric quantity of an aromatic dianhydride to a solution of an aromatic diamine in dimethylacetamide, keeping the temperature below 50°C, and casting a film from this solution. Dehydration of the polyamic acid to the polyimide was achieved by curing to about 300°C.

Polymer II:

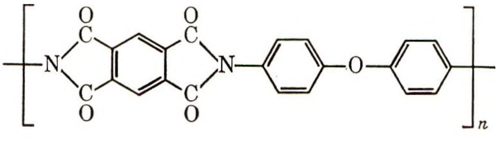

Polymer III:

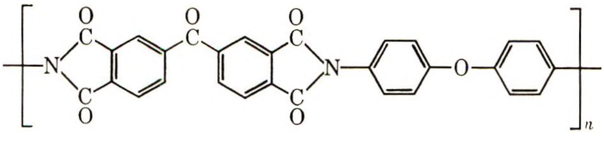

Polymer IV:

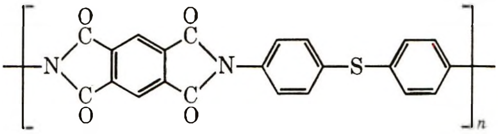

Polymer V:

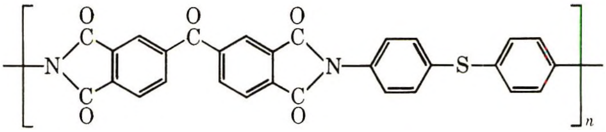

Decomposition of the Polyamide (Polymer I)

Thermogravimetric analysis (Fig. 1) under nitrogen indicated an onset of decomposition at 410°C. An exploratory decomposition run showed that decomposition temperatures of 375, 450, and 550°C adequately covered the major breakdown of the polymer. This preliminary run also indicated that keeping the polymer in an evacuated desiccator for several days was insufficient to remove adsorbed water. Analyses of the polymer gave

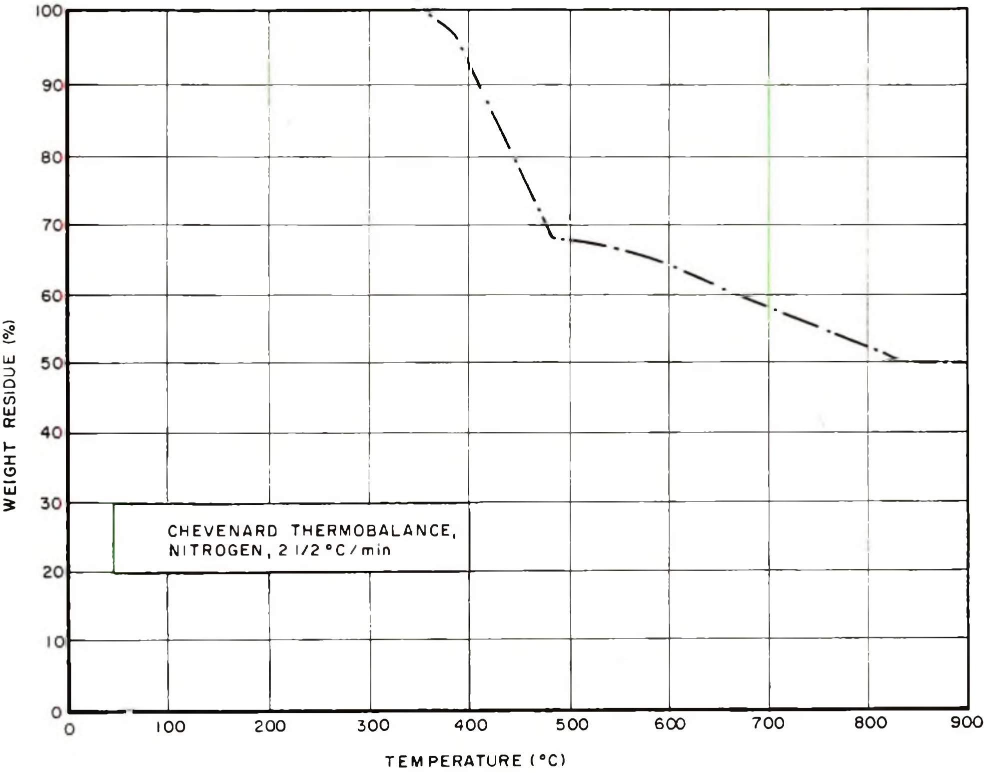

Fig. 1. Thermogravimetric analysis of polymer I.

high values for hydrogen and oxygen and low values for carbon and nitrogen, and the (preliminary) run yielded 8.6, 4.7, and 1.5% water (i.e., moles water/total moles volatiles) at 375, 450, and 550°C, respectively. Drying the polymer at 80°C for 48 hr under vacuum removes practically all of the adsorbed water, and only insignificant amounts were formed during the decomposition, as can be seen in Table I. Table I also shows that

TABLE IA
Analyses of Residues of Polymer I

	C,%	H, %	O, %	N, %
Calcd for $(C_{14}H_{10}O_2N_2)_n$	70.6	4.2	13.4	11.8
Found for polymer	67.5	4.3	13.7	11.2
Found for residue, 375°C	71.4	4.3	10.1	12.0
Found for residue, 450°C	80.0	3.7	1.9	12.2
Found for residue, 550°C	83.4	2.9	2.6	10.0

TABLE IB
Analyses of Volatiles from Polymer I

Temperature range, °C	Volatile products, mole-%								Weight volatiles, %[a]	Total weight loss, %[a]
	$C_6H_5CH_3$	C_6H_6	CO_2	CO	HCN	H_2O	CH_4	H_2		
20–375	—	0.3	86.6	11.5	0.4	0.6	0.1	0.5	9.2	26.5
375–450	0.2	1.7	40.2	44.4	1.5	0.4	1.8	0.8	8.0	22.5
450–550	—	0.8	2.7	8.0	12.4	0.5	9.1	66.5	3.9	5.5

[a] Per cent of starting material.

carbon dioxide is the major volatile decomposition product in the lower temperature range. Between 375 and 450°C the carbon dioxide content decreases, while carbon monoxide reaches a peak, and hydrogen formation is noticeably increased. At the highest temperature range hydrogen is the major product, while some hydrogen cyanide, methane, and carbon monoxide are also formed. Nitrogen is given off only in the form of hydrogen cyanide, and no ammonia is formed. The overall loss of nitrogen is low, which is confirmed by the analytical data of the residues. The infrared spectra (Fig. 2) contribute little to the elucidation of a mechanism. The spectra of the original polymer and the residue at 375°C are almost alike, with the exception of a band in the latter at 700 cm^{-1}; this band may result from monosubstituted aromatic rings (more endgroups). The spectra of the residues at 450 and 550°C are inconclusive with the exception of the above mentioned bands.

As can be seen from the mass balance in Table I, more than half of the weight loss may be attributed to condensables which could not be isolated in sufficient quantity for identification. Friedman,[19] who subjected the same polymer to vacuum pyrolysis up to 1000°C at a rate of 10°C/min

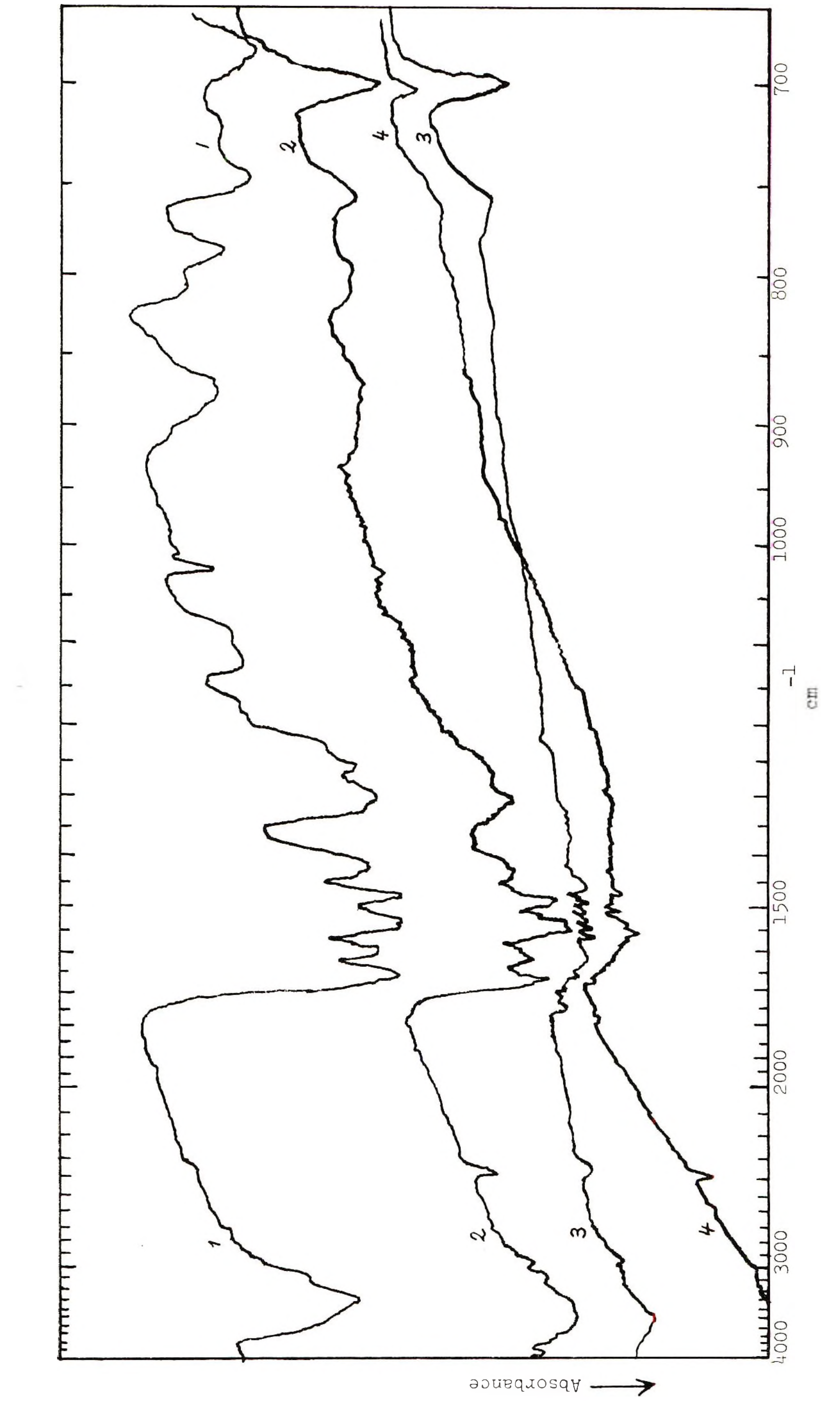

Fig. 2. Infrared spectra of polymer I (*1*) and its residues at (*2*) 380°C, (*3*) 450°C, and (*4*) 550°C.

and who analyzed the effluent gases in a time-of-flight mass spectrometer, found in addition to the products we identified, aniline, benzene, benzonitrile, and also ammonia in sizeable quantities. Smaller amounts of phenylendiamines, diacyanobenzenes, cyanoanilines, phenyl isocyanate, acetylene, and biphenyl have been found. The presence of phenylenediamines, dicyanobenzenes, and cyanoanilines suggests the presence of AA, BB, and AB functional units in the polymer.

One may be inclined to explain the breakdown of aromatic polyamides as being analogous to that of aliphatic polyamides.[7] A rupture of the linkage between the NH-group and the ring may occur first. After abstraction of hydrogen from a ring, an amide endgroup is formed which gives off water to form a nitrile. The water, in turn, hydrolyzes another amide linkage with formation of a carboxyl and an amino end group. The carboxyl group finally decarboxylates to form carbon dioxide as the major volatile decomposition product at lower temperatures.

The following objection can be made against such a mechanism as a major path of breakdown. Since one mole of water is required to form one mole of carbon dioxide, a considerable amount of water must be produced, and a reasonably large part of this would be expected to evolve as free water, as is the case with aliphatic polyamides. However, practically no free water is formed.

It seems to us that the mechanism considered as a possibility by Krasnov and co-workers,[8,9] namely the formation of a carbodiimide linkage via isocyanate groups, has merit. Diphenylcarbodiimide, for example, forms with the evolution of carbon dioxide when phenyl isocyanate is heated to 180°C in a sealed tube. The mechanism which leads to the five major gaseous decomposition products, namely carbon dioxide, carbon monoxide, hydrogen, hydrogen cyanide and methane, and which also accounts for the additional products found by Friedman, can be written as in eqs. (4)–(12).

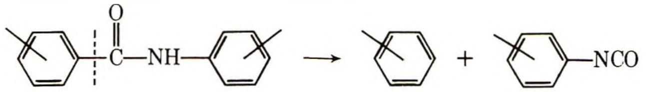

(4)

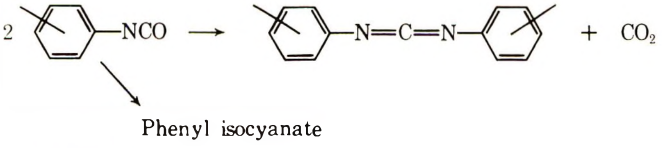

(5)

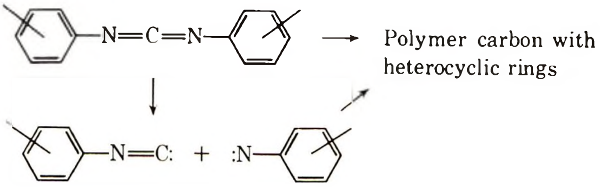

(6)

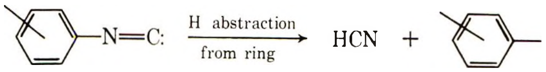

(7)

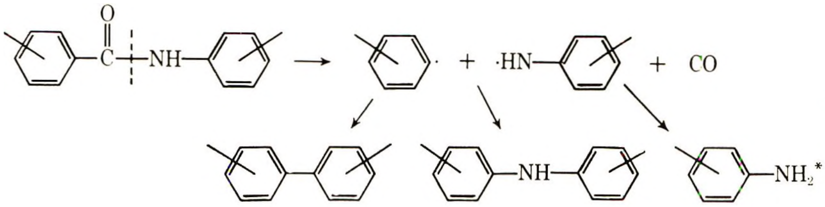

(8)

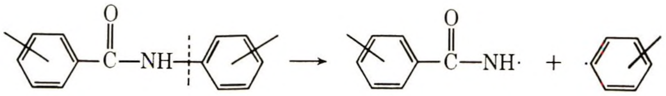

(9)

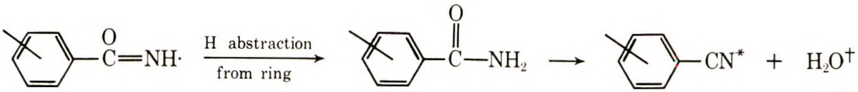

(10)

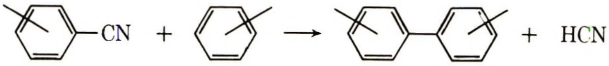

(11)

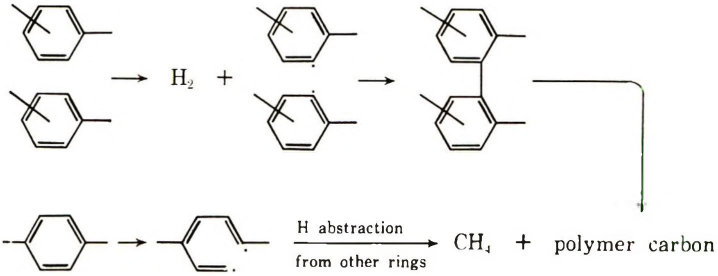

(12)

From the quantities of the volatiles formed at the different temperature levels, it is concluded that the chain cleavage indicated in eq. (4) is the preferred one at the lower temperatures, and those in eqs. (8) (9) occur at successively higher temperatures.

Peculiar is the fact, that Friedman observed "sizeable" amounts of ammonia, while we observed none for the same polymer. Some investigators[2–4,7] studying the decomposition of nylons also found ammonia, while others[1,5,6] did not. A study of this earlier work did not clearly reveal the reason for this discrepancy, and it cannot be said whether the same reasoning would apply to aliphatic and aromatic polyamides. However, temperature, time, and heating rate may be factors of importance, and also the way the volatiles are collected. Hasselstrom and co-workers[2] observed that ammonium carbonate formed during the decomposition of nylon. This may also occur during the decomposition of aromatic polyamides, or, for that matter, during the decomposition of all substances which form carbon dioxide and ammonia simultaneously. Feeding the volatiles continuously into a time-or-flight mass spectrometer may avoid the problem of ammonium carbonate formation. Collecting the gases and analyzing

---

* Possible source for aniline, phenylenediamines, cyanoanilines, benzonitrile, and dicyanobenzenes as found by Friedman.

† May hydrolyze some amide linkages.

them separately may allow the formation of ammonium carbonate which may form a thin layer of sublimate and thus remain undetected.

Decomposition of the Polyimides (Polymers II–V)

The four polyimides are very similar to one another in weight loss curves (Fig. 3) and the kind and amounts of decomposition products (Tables II–V), if the small amount of sulfur-containing decomposition products of polymers IV and V is disregarded. Polymers III and V, with a benzophenone carbonyl, seem to form more carbon monoxide and less carbon

TABLE IIA
Analyses of Residues of Polymer II

	C, %	H, %	O, %	N, %
Calcd for $(C_{22}H_{10}O_5N_2)_n$	69.1	2.7	20.9	7.3
Found for polymer	67.8	2.8	20.1	7.6
Found for residue, 400°C	69.4	2.9	18.9	7.9
Found for residue, 450°C	75.5	3.4	9.9	8.4
Found for residue, 550°C	80.8	2.9	2.5	7.7
Found for residue, 620°C	83.2	2.1	2.6	6.3

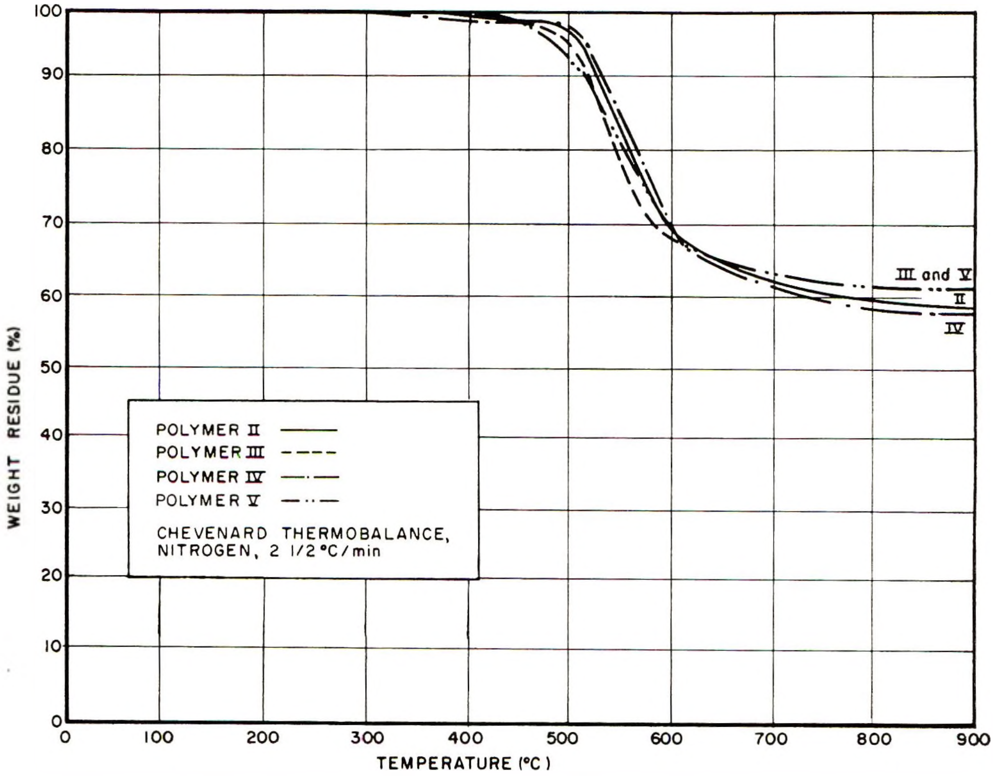

Fig. 3. Thermogravimetric analysis (nitrogen) of polymers II, III, IV, and V.

TABLE IIB

Analyses of Volatiles from Polymer II

Temperature range, °C	Volatile products, mole-%							Weight volatiles, %[a]	Total weight loss, %[a]
	C_6H_6	CO_2	CO	HCN	H_2O	CH_4	H_2		
20–400	0.2	78.0	19.7	0.2	0.5	0.4	1.0	~3.4	3.4
400–450	0.1	43.7	53.0	0.2	—	0.4	2.6	17.4	27.5
450–550	0.2	11.1	46.3	4.3	0.4	5.6	32.1	8.8	9.8
550–620	1.2	1.0	23.6	3.7	0.3	8.6	61.6	4.1	5.1

[a] Per cent of starting material.

TABLE IIIA

Analyses of Residues of Polymer III

	C, %	H, %	O, %	N, %
Calcd for $(C_{29}H_{14}O_6N_2)_n$	71.6	2.9	19.7	5.8
Found for polymer	70.6	3.1	18.8	5.8
Found for residue, 400°C	70.9	2.9	17.8	6.4
Found for residue, 450°C	75.0	3.1	12.4	6.2
Found for residue, 550°C	85.4	2.4	2.3	5.6
Found for residue, 620°C	87.0	1.9	1.5	5.2

TABLE IIIB

Analyses of Volatiles from Polymer III

Temperature °C	Volatile products, mole-%							Weight volatiles, %[a]	Total weight loss, %[a]
	C_6H_6	CO_2	CO	HCN	H_2O	CH_4	CH_4		
20–400	No data, insufficient amounts of volatiles								2.8
400–450	0.2	37.7	60.1	0.3	0.8	0.1	0.8	18.3	18.9
450–550	0.4	20.7	52.3	2.0	0.6	3.8	20.2	~17.3	17.3
550–620	0.2	1.1	21.3	3.0	0.7	9.0	64.7	3.7	4.0

[a] Per cent of starting material.

TABLE IVA

Analyses of Residues of Polymer IV

	C, %	H, %	O, %	N, %	S, %
Calcd for $(C_{22}H_{10}O_4N_2S)_n$	66.3	2.5	16.1	7.0	8.1
Found for polymer		Insufficient material			
Found for residue, 400°C	66.4	2.6	15.4	7.4	7.6
Found for residue, 450°C	70.2	2.8	9.6	7.6	5.8
Found for residue, 550°C	79.0	2.5	1.7	6.9	4.2
Found for residue, 620°C	80.9	1.7	1.3	7.4	3.3

TABLE IVB
Analyses of Volatiles from Polymer IV

Temperature range, °C	Volatile products, mole-%										Weight volatiles, %[a]	Total weight loss, %[a]
	C_6H_6	CS_2	OCS	CO_2	H_2S	CO	HCN	H_2O	CH_4	H_2		
20–400	0.2	—	0.3	82.1	1.1	14.5	0.5	0.4	0.7	0.4	~4.2	4.2
400–450	0.2	—	3.8	41.0	5.9	45.9	1.0	0.8	0.1	1.2	23.4	24.8
450–550	0.4	0.1	1.6	24.7	6.5	49.2	4.8	0.2	1.1	11.4	~12.8	12.8
550–620	0.2	0.1	0.2	2.4	7.9	18.0	9.2	0.4	6.4	55.2	3.4	4.7

[a] Per cent of starting material.

TABLE VA
Analyses of Residues of Polymer V

	C, %	H, %	O, %	N, %	S, %
Calcd for $(C_{29}H_{14}O_5N_2S)_n$	69.3	2.8	15.9	5.6	6.4
Found for polymer	68.3	2.8	16.2	5.6	6.7
Found for residue, 400°C	73.8	3.1	14.2	5.9	4.1
Found for residue, 450°C	70.1	3.0	10.0	5.8	3.8
Found for residue, 550°C	80.5	2.6	2.2	5.5	3.6
Found for residue, 620°C	79.8	2.2	2.2	4.5	3.0

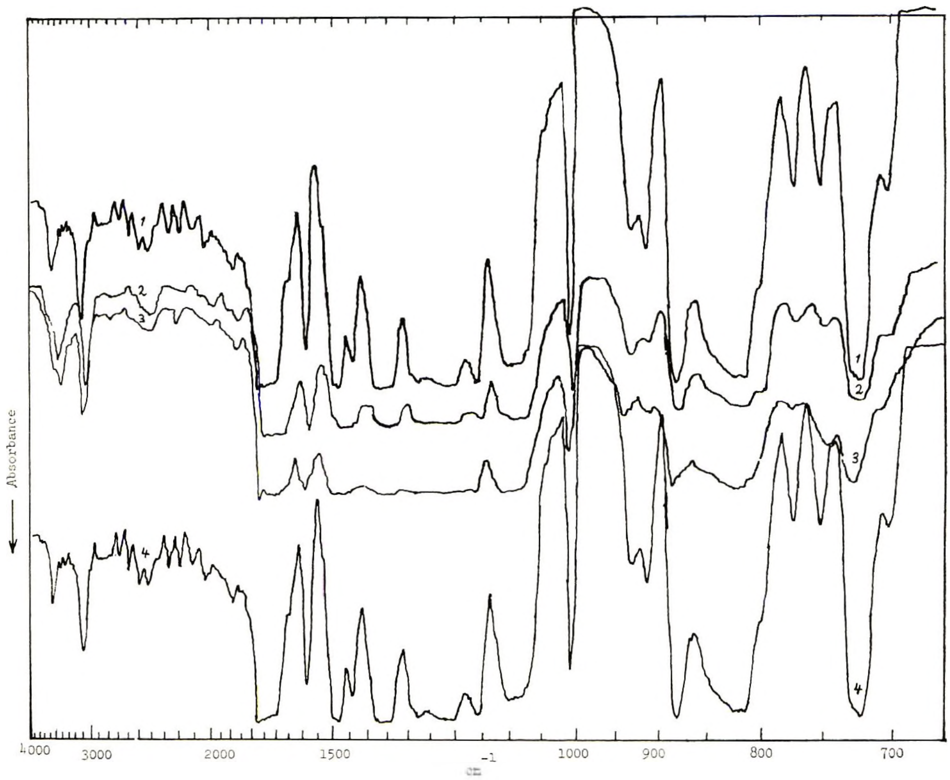

Fig. 4. Infrared spectra of polymer II (*1*) and its residues at (*2*) 400°C, (*3*) 450°C, and (*4*) 550°C.

TABLE VB
Analyses of Volatiles from Polymer V

Temperature range, °C	Volatile products, mole-%									Weight volatiles, %[a]	Total weight loss, %[a]
	C_6H_6	OCS	CO_2	H_2S	CO	HCN	H_2O	CH_4	H_2		
20–400		0.6	64.3	5.2	27.8	0.4	1.0	0.4	0.3	5.4	7.2
400–450	0.4	2.6	26.5	6.4	60.3	0.9	0.5	0.2	2.2	~11.7	11.7
450–550	0.5	0.9	19.1	3.9	48.6	4.4	0.5	2.4	19.7	16.1	20.6
550–620	0.3	0.1	1.3	5.2	12.8	4.9	0.7	8.4	66.3	3.8	5.3

[a] Per cent of starting material.

dioxide than the other two polymers. Those with the sulfide linkage produce some hydrogen sulfide, especially above 400°C, and some carbon oxysulfide with a peak temperature between 400 and 450°C.

The infrared spectra (Fig. 4–7) show a great similarity between the original polymers and the residues at 400°C; as the tables indicate, there is little weight loss up to that point. Changes which occur in the spectra thereafter are the disappearance of bands in the region between 700 and 1200 cm^{-1}. To a large extent, these may be substitution bands which

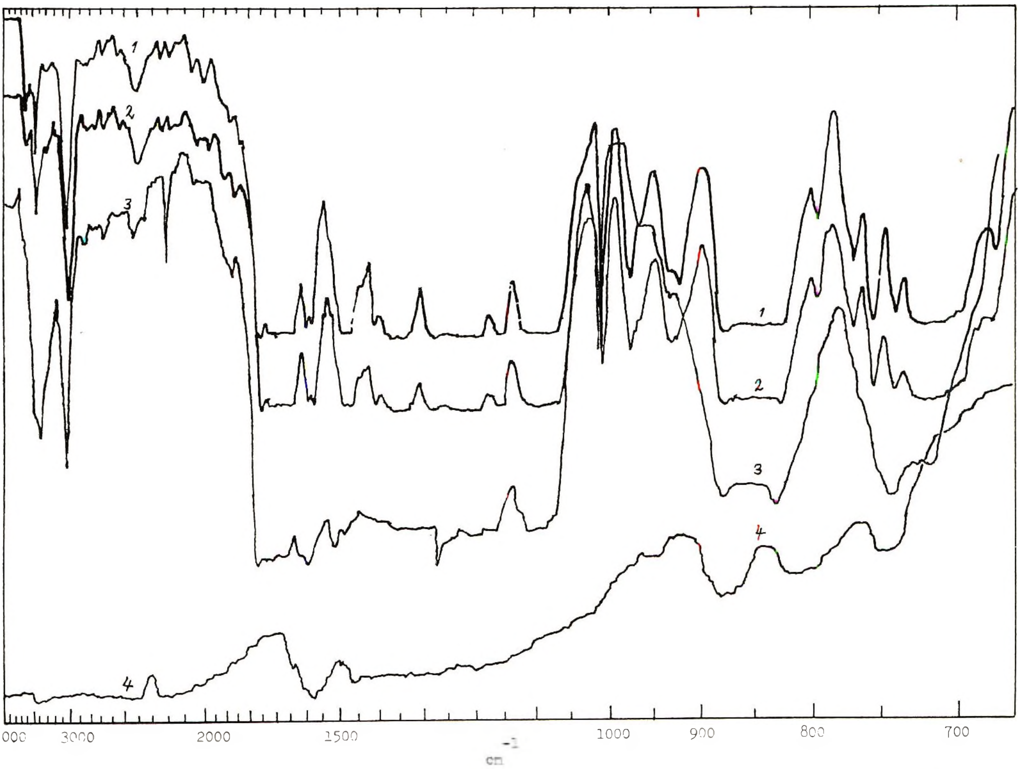

Fig. 5. Infrared spectra of polymer III (*1*) and its residues at (*2*) 400°C, (*3*) 450°C, and (*4*) 550°C.

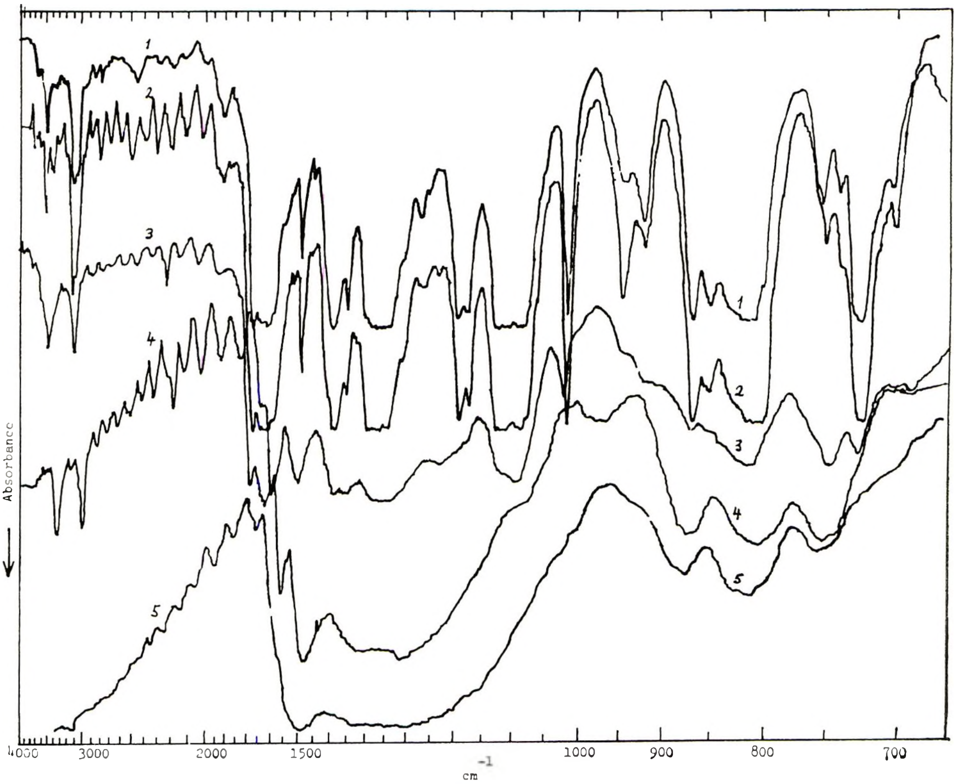

Fig. 6. Infrared spectra of polymer IV (*1*) and its residues at (*2*) 400°C, (*3*) 450°C, (*4*) 550°C, and (*5*) 620°C.

change with bond rupture and crosslinking. The imide band at 1775 cm^{-1} and the imide substitution band[21] at 723 cm^{-1} disappeared at 550°C. In the case of polymer V, the 723 cm^{-1} band had disappeared before 450°C. A new sharp band at 2200 cm^{-1} emerged in the spectra of the residues, especially in the case of polymers III–V. Bands in this region are representative of the C=N stretching vibration, and have been observed with nitriles, isocyanates, and carbodiimides $R_1—N=C=N—R_2$.

In order to propose a breakdown mechanism for the polyimides it becomes necessary to explain the rather unexpected generation of carbon dioxide. Bruck[12] postulates, as has already been pointed out, that carbon dioxide results from the hydrolysis and decarboxylation of polyamic acid groups, whereas carbon monoxide is contributed by the imide group. If this reasoning is applied to the polyimides we evaluated, it would mean that in view of the considerable carbon dioxide evolution, a large amount of polyamic acid should still be present. The analyses of the polymers, however, especially the oxygen analyses, do not confirm this. Furthermore, we would expect that, on heating, the polyamic acids would continue to cyclize rather than to decarboxylate. This, in turn, would generate

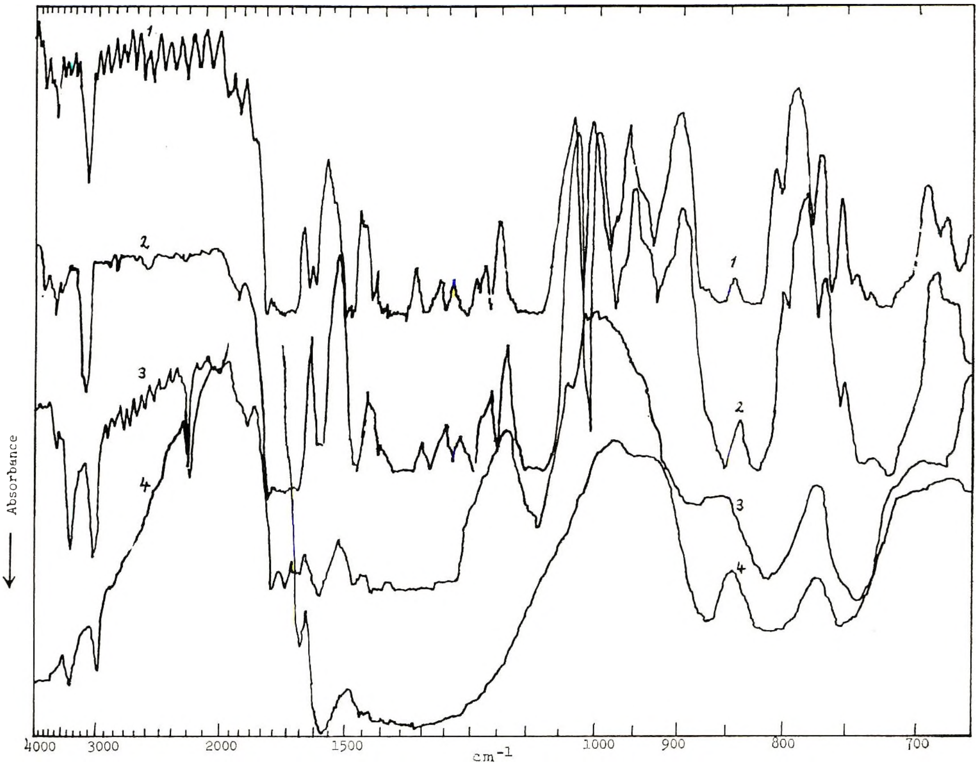

Fig. 7. Infrared spectra of polymer V (*1*) and its residues at (*2*) 400°C, (*3*) 450°C, and (*4*) 550°C

water, which is not found in appreciable quantities. The infrared spectra of our polyimide films did have distinct bands around 3450 cm^{-1}, which may be attributed to NH-stretching frequencies. They are, however, relatively small compared to the rest of the bands and could be indicative of only minor amounts of amide groups in the polymers, as is evident from the results of elemental analysis. It is interesting to note that the relative size of the NH band increases somewhat in the spectra of the 450°C residues. As the mechanism in eq. (13) will show, newly formed amide radicals may abstract hydrogen to yield some NH groups.

Another route for the formation of carbon dioxide, as suggested by Gay and Berr[13] (see Introduction) is the decomposition of isoimide groups believed to be formed through isomerization of the normal imide. A doublet in the infrared band at 10.95 μ (914 cm^{-1}) was attributed to the isoimide. Dine-Hart and Wright[22] prepared polyisoimides and found that they rapidly revert to the more stable imide form on heating. The formation of carbon dioxide from isoimides would, then, require some degree of equilibrium between imide and isoimide at the decomposition temperature.

We believe, that the major decomposition reaction taking place resembles the one postulated for polyamides [eqs. (13)–(15)].

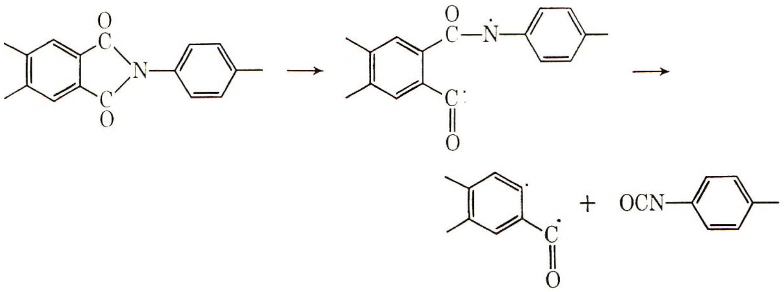

(13)

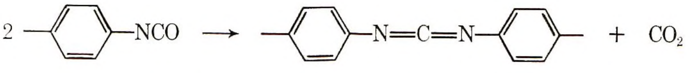

(14)

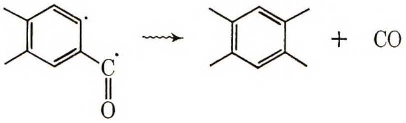

(15)

Evidence for this route is, as mentioned above, the presence of the C=N-stretching frequency, indicative of the isocyanate or carbodiimide linkage, and the increase of the NH-stretching frequency around 3450 cm^{-1} on heating the polymer to 450°C, indicating that the amide radical in eq. (13) forms some CO—NH—linkages through hydrogen abstraction from the ring. Since this hydrogen abstraction is expected to occur only to a limited extent at the relatively low temperature of 450°C, a small increase in the NH bands, as observed, may be indicative of a substantial formation of this radical.

It appears, then, that the major mechanism for the thermal decomposition of aromatic polyamides involves cleavage of the amide linkage as the primary step and formation of carbodiimide moieties and carbon dioxide via isocyanate groups. The polyimides undergo cleavage of the imide ring between a carbonyl and the nitrogen to form, in a second step, an isocyanate and a benzoyl radical. The isocyanate decomposes as explained before via formation of carbodiimide and carbon dioxide, the benzoyl radical yields carbon monoxide.

References

1. B. G. Achhammer, F. W. Reinhart, and G. M. Kline, *J. Res. Nat. Bur. Stand.*, **46,** 391 (1951); *J. Appl. Chem.*, **1,** 301 (1951).
2. T. Hasselstrom, H. W. Coles, C. E. Balmer, M. Hanningan, M. W. Keeler, and R. I. Brown, *Text. Res. J.*, **22,** 742 (1952).
3. I. Goodman, *J. Polym. Sci.*, **13,** 175 (1954).
4. I. Goodman, *J. Polym. Sci.*, **17,** 587 (1955).
5. S. Straus and L. A. Wall, *J. Res. Nat. Bur. Stand.*, **60,** 39 (1958).
6. S. Straus and L. A. Wall, *J. Res. Nat. Bur. Stand.*, **63A**, 269 (1959).
7. B. Kamerbeck, G. H. Kroes, and W. Grolle, "High Temperature Resistance and Thermal Degradation of Polymers," *S. C. I. Monograph No. 13,* **13,** 357 (1961).
8. Y. P. Krasnov, V. M. Savinov, L. B. Sokolov, V. I. Logunova, V. K. Belyakov, and T. A. Polyakova, *Vysokomol. Soedin.*, **8,** 380 (1966).

9. Y. P. Krasnov, V. I. Logunova, and S. B. Sokolov, *Vysokomol. Soedin.*, **8**, 1970 (1966).

10. L. C. Scala, W. M. Hickam, and I. Marschik, *J. Appl. Polym. Sci.*, **12**, 2339 (1968).

11. J. F. Heacock and C. E. Berr, *SPE Trans.*, **5**, 105 (1965).

12. S. D. Bruck, *Polymer*, **6**, 49 (1965).

13. F. P. Gay and C. E. Berr, *J. Polym. Sci. A-1*, **6**, 1935 (1968).

14. G. F. L. Ehlers, K. R. Fisch, and W. R. Powell, *J. Polym. Sci. A-1*, **7**, 2931 (1969).

15. G. F. L. Ehlers, K. R. Fisch, and W. R. Powell, *J. Polym. Sci. A-1*, **7**, 2955 (1969).

16. G. F. L. Ehlers, K. R. Fisch, and W. R. Powell, *J. Polym. Sci. A-1*, **7**, 2969 (1969).

17. H. Romeyn, Jr., AFML-TR-66-250 (1967).

18. J. H. Freeman, L. W. Frost, G. M. Bower, and E. I. Traynor, ASD-TDR-63-555 (1963).

19. H. L. Friedman, H. W. Goldstein, and G. A. Griffith, AFML-TR-68-111 (1968).

20. R. Stollé, *Ber.*, **41**, 1125 (1968).

21. C. E. Sroog, A. L. Endrey, S. V. Abramo, E. C. Berr, W. M. Edwards, and K. L. Olivier, *J. Polym. Sci. A*, **3**, 1373 (1965).

22. R. A. Dine-Hart and W. W. Wright, *J. Appl. Polym. Sci.*, 11, 609 (1967).

Received January 28, 1970

JOURNAL OF POLYMER SCIENCE: PART A-1 VOL. 8, 3529-3532 (1970)

Mechanical Properties of Radiation-Induced Graft Copolymers of Styrene to Polyethylene

SUEO MACHI* and JOSEPH SILVERMAN
Laboratory for Radiation and Polymer Science
Department of Chemical Engineering, University of Maryland,
College Park, Maryland 20742

Synopsis

Measurements were made of the tensile properties of polyethylene-styrene grafts prepared by irradiating polyethylene films in liquid styrene. The films contained true graft and occluded styrene homopolymer. It was shown that yield strength, tensile strength, and initial modulus of elasticity increase while elongation decreases with increasing polystyrene content. The tensile strength and elongation were reduced when the grafted film was soaked in benzene more than 15 hr. The film prepared by a post-irradiation graft gave higher tensile strength and elongation than those of grafts formed by simultaneous irradiation of the film and the monomer. These results indicate that radiation-induced grafting makes the system of polyethylene and polystyrene compatible and potentially useful, provided the samples are not subjected to drastic solvent extraction procedures for the removal of homopolymer.

Several papers[1-7] have been published on the reaction kinetics of radiation-induced grafting of styrene to polyethylene (PE), but only two brief works[1,8] on the mechanical properties of PE-styrene graft have been reported. One paper[1] shows that the tensile strength of the graft prepared by the simultaneous irradiation of the two components decreases with increasing degree of grafting, and the other[8] indicates an increase in tensile strength of the graft prepared by post-irradiation grafting method.

As shown in a previous paper,[9] the deterioration in the properties of polyethylene films prepared by the simultaneous grafting method is due to "bubbles" caused by the prolonged benzene extraction procedure usually employed following grafting. When the grafted film is dried after soaking in benzene for less than 10 hr, it appears to be a homogeneous and compatible system in spite of the presence of considerable amount of occluded styrene homopolymer. In this paper, tensile properties are presented for the irradiated styrene-PE films as a function of polystyrene content and compared with the graft produced by post-irradiation grafting of styrene to PE.

---

* Permanent Address: Takasaki Radiation Chemistry Research Establishment, Japan Atomic Energy Research Institute, Takasaki, Japan.

EXPERIMENTAL

Materials. Dupont low density PE film (additive free, specific gravity = 0.919), 3.8 mil thick, was used in the form of 10 × 90 mm strips. Styrene monomer of commercial grade was washed successively with 10% sodium hydroxide aqueous solution and water, dried with calcium chloride and stored over calcium hydride for a week. The styrene was then distilled over fresh calcium hydride before use.

Irradiation and Grafting. In case of simultaneous irradiation grafting, the strips were immersed in styrene in a glass tube. The styrene was degassed by four cycles of freezing and thawing before the tube was sealed at a pressure of 10^{-5} Torr. Irradiations were carried out at 19°C in the ^{60}Co source of the University of Maryland. For the post-irradiation experiments, the strips were put in a tube and evacuated for 15 hr at 10^{-5} Torr and then sealed off. After irradiating the strips, purified and degassed styrene was introduced into the tube containing the strips through a breakseal. In the interval between irradiation and introduction of monomer, the strips were kept at liquid nitrogen temperature. The post-irradiation grafting reaction was carried out at 23–25°C.

After the reaction, the strips were usually washed with benzene for less than an hour to remove dissolved styrene, dried under vacuum, and weighed. One sample was soaked for 150 hr prior to drying.

Tensile Properties Measurements. The tensile properties of the strips before and after treatment were measured by means of an Instron test machine. Each number reported is the mean of five measurements. The gauge length was 1 in. and the sample was pulled at 1 in. per min.

RESULTS AND DISCUSSION

Stress-strain curves of grafts with different polystyrene (PS) content are illustrated in Figure 1. The physical property measurements are summarized in Table I. The plots of tensile strength, tensile yield, initial mod-

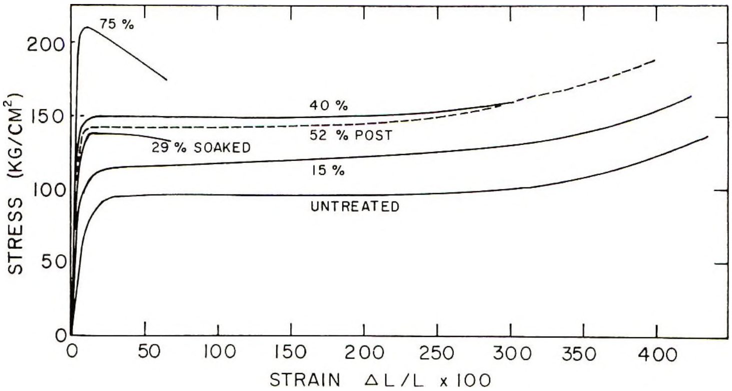

Fig. 1. Stress-strain curves of polyethylene-styrene grafts. Numbers correspond to the sample numbers shown in Table I.

TABLE I
Properties of Polyethylene-Styrene Grafts

Sample number	Polystyrene content (wt%)	Dose (mrad)	Tensile Strength Yield (kg/cm²)	Tensile Strength Break (kg/cm²)	Initial modulus of elasticity (kg/cm²)	Elongation, %
Simultaneous irradiation method						
1	0	0	88	134	1520	436
2	15.4	0.60	113	159	2660	428
3	40.2	0.50	150	161	4090	313
4	75.5	0.90	204	170	6320	65
Sample 3 after 15 hr soak in benzene						
5	28.6	0.50	139	137	3600	66
Post-irradiation method						
6	52.3	1.60	144	181	5190	399

ulus and elongation against PS content are shown in Figure 2. Tensile strength at yield and initial modulus of elasticity increase linearly with polystyrene content up to 75%. Tensile strength at break also increases with PS content, while elongation at break decreases rapidly. It is a general rule that the tensile properties are reduced in a graft of incompatible components. Kargin, however, points out that the physical properties of the graft vary in a less predictable manner in incompatible systems.[10]

The physical blend of PE and PS is an incompatible system. Anderson et al. show that the tensile strength of the blend is reduced by increasing the blended polyethylene fraction.[8] On the other hand, specimens molded from powdery polyethylene grafted with styrene by the post-irradiation grafting method has a higher tensile strength than unmodified polyethylene.[8] The opposite effect has been reported by Ballantine et al.[1] for PE-styrene that

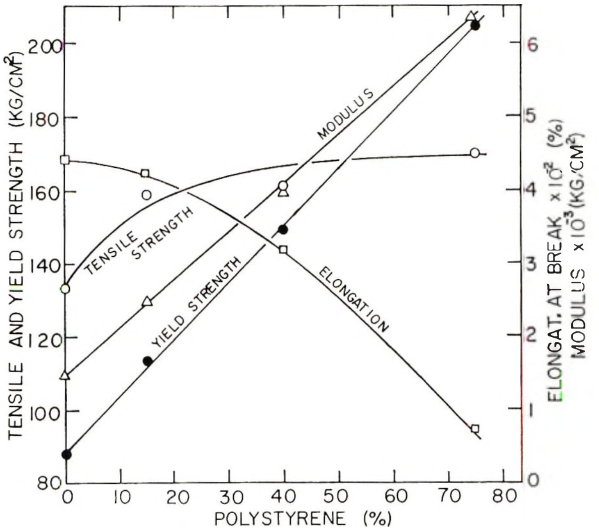

Fig. 2. Relation between tensile properties and polystyrene content.

the tensile strength decreases with increasing PS content. The differences between the behavior of grafts prepared by the simultaneous and post-irradiation methods are not unexpected. The former contains bubbles of occluded styrene homopolymer[4,9] formation in the film.[3,9] On the other hand, there is almost no occluded homopolymer formed in the post-irradiation grafting of styrene to PE[3].

Since then, it was shown in this laboratory that the graft prepared by irradiating PE film in liquid styrene and dried just after irradiation appears to be homogeneous and compatible. The bubbles were found to form and grow as a consequence of soaking in benzene. It was expected that the tensile properties of the grafted film without soaking might be superior in some respects to the original PE.

Figure 2 shows measurements made on unsoaked films. They clearly indicate increases of yield strength, tensile strength, and initial modulus in PE-styrene grafts with considerable amounts of occluded PS. Thus as anticipated, the graft copolymer, PE and occluded PS are compatible, provided that the system is not subjected to prolonged soaking. These facts are also consistent with the observation that blends of graft copolymer and a mixture of polystyrene and polyethylene give improved tensile strength.[8]

When Sample 3 is soaked in benzene for 15 hr, the polystyrene content decreases to 28.6%, bubbles are formed in the film, and the dried sample has a much lower elongation and tensile strength than the original polyethylene.

The polethylene film-styrene graft prepared by pre-irradiation of the film shows more compatible appearance but has mechanical properties similar to films with similar composition prepared by the simultaneous irradiation of monomer and polymer.

The authors would like to express their thanks to Dr. J. Smith of the National Bureau of of Standards for the use of his tensile tester and for useful discussions, and also to the AEC Division of Research for its financial support.

References

1. D. S. Ballantine, A. Glines, D. J. Metz, J. Behr, R. B. Mesrobian, and A. J. Restaino, *J. Polymer Sci.*, **19**, 219 (1956).
2. A. S. Hoffman, E. R. Gilliland, E. M. Merrill, and W. H. Stockmayer, *J. Polymer Sci.*, **34**, 461 (1959).
3. D. S. Ballantine, A. Glines, G. Adler, and D. J. Metz, *J. Polymer Sci.*, **34**, 419 (1959).
4. J. Silverman, S. I. Srinivasan, and D. J. Phalangas, *Industrial Uses of Large Radiation Sources*, IAEA, Vienna, 1963, Vol. 1, p. 245.
5. W. K. W. Chen and H. Z. Friedlander, *J. Polymer Sci. C*, **4**, 1195 (1963).
6. J. Dobo and T. Czvikovszky, *J. Polymer Sci. B*, **2**, 293(1964).
7. T. Takamatsu, T. Konaga, and E. Fukada, *Kobunshi Kagaku*, **24**, 795 (1967).
8. L. C. Anderson, D. A. Roper, and J. K. Rieke, *J. Polymer Sci.*, **43**, 423 (1960).
9. S. Machi and J. Silverman, *J. Polymer Sci. A1*, **7**, 2737 (1969).
10. H. A. J. Bataerd and G. W. Tragear, *Graft Copolymers*, Polymer Reviews Vol. 16, Interscience Publishers, p. 209, (1967).
11. V. A. Kargin, *J. Polymer Sci. C*, **4**, 1601 (1963).

JOURNAL OF POLYMER SCIENCE: PART A-1 VOL. 8, 3533-3541 (1970)

Isomorphous Replacement in Nylon 6 by 4-Aminomethylcyclohexanecarboxylic Acid

FRANK R. PRINCE, ELI M. PEARCE, and ROBERT J. FREDERICKS, *Corporate Chemical Research Laboratory, Allied Chemical Corporation, Morristown, New Jersey 07960*

Synopsis

It was desired to determine the effect of geometric configuration on the ability of 4-aminomethylcyclohexanecarboxylic acid (AMCC) to "isomorphously" replace ε-aminocaproic acid residues in nylon 6. However, we found that *cis*-AMCC isomerized to the more thermodynamically stable *trans* isomer during copolymerization with caprolactam (CL) and also during homopolymerization. A 20/80 *cis/trans* ratio of AMCC residues was found in the 50:50 copolyamides regardless of whether a high-*cis* (72/28) or high-*trans* (15/85) AMCC was used. Powder x-ray diagrams showed similar interplanar spacings for the copolyamides made from both high-*cis* and high-*trans* AMCC. The x-ray study also showed that the nylon 6 lattice can accommodate less than 30 mole-% AMCC residues before a new structure appears. DTA and TGA data of the CL:AMCC copolyamide showed that AMCC raised the melting point, T_g, T_c, and stability of nylon 6.

INTRODUCTION

"Isomorphous" replacement of ε-aminocaproic acid residues in nylon 6 by 4-aminomethylcyclohexanecarboxylic acid (AMCC) has been reported by several authors.[1-4] A plot of melting point versus copolymer composition for the CL-AMCC copolyamides was sigmoidal in shape and this was accepted as evidence of isomorphous replacement. However, Tranter[5] has since disproved the use of melting point versus composition curves as a criterion for isomorphous replacement. He found significant changes in lattice spacings with copolymer composition for some copolyamides even though the melting point curve was linear, and no change in lattice spacings for some copolyamide systems that had eutectic melting point curves. In an excellent review on isomorphism in macromolecules,[6] Allegra and Bassi distinguish true isomorphous replacement from cocrystallization phenomena.

AMCC can exist in both the *cis* and *trans* configurations. To date, the effect of the geometric configuration of AMCC upon its ability to isomorphously replace ε-aminocaproic acid residues in nylon 6 has not been determined. In the cases mentioned above, AMCC was prepared by the catalytic hydrogenation of 4-cyanobenzoic acid or 4-aminomethylbenzoic acid. These are both rigidly planar molecules and would ultimately give a high-*cis* AMCC product.

The effect of monomer geometric configuration upon polymer properties was demonstrated by Muromova and Afanas'eva.[7] They prepared poly-4-aminocyclohexylacetic acid from both the *cis* and *trans* monomer and found that the *trans* polymer was higher melting and more thermally stable than the *cis* polymer. We have made two series of CL–AMCC copolyamides using a high-*cis* AMCC and a high-*trans* AMCC in order to determine the effect of geometric configuration on "isomorphous" replacement in the CL:AMCC copolyamide system. Several of these copolyamides were hydrolyzed and the products analyzed to determine whether any *cis–trans* isomerization occurs during the polymerization.

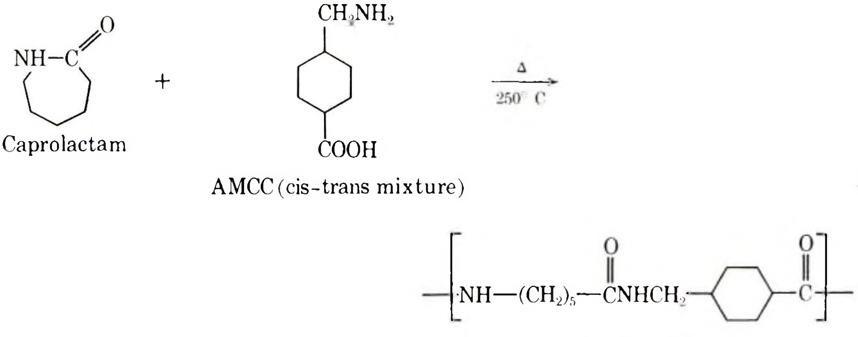

Copolyamide

EXPERIMENTAL

High-*trans* AMCC (85% *trans*) was purchased from Aldrich Chemical. The high-*cis* AMCC (72% *cis*) was synthesized by the hydrogenation of benzylamine-4-carboxylic acid in acetic acid with platinum oxide. This gave AMCC with a melting point of 244°C.

Melt condensation of mixtures of CL and AMCC were carried out at 250°C in sealed tubes in an aluminum heating block. The copolyamides were precipitated from 90% formic acid and water (~85% yield). Reduced viscosities were determined in *m*-cresol. DTA data was obtained on the DuPont 900 differential thermal analyzer and The Perkin-Elmer differential scanning calorimeter. When the samples were heated, quenched, and reheated, the glass transition temperatures (T_g) increased because of the removal of volatiles. In each case, the highest T_g was reported. TGA data were obtained by using the Ainsworth system with an F & M temperature programmer, the samples being heated at 10°C/min in a nitrogen atmosphere. The x-ray diffraction powder patterns were obtained on a Norelco x-ray diffractometer using copper Kα radiation. The per cent crystallinity was determined from these patterns by dividing the area of the crystalline regions by the crystalline plus amorphous area. The nylon 6 and the 90:10 CL–AMCC polyamides were annealed because their glass transition temperatures are below the drying temperature. The copolyamides were hydrolyzed in a sealed tube with 7.2*N* HCl at 110°C for 3 days, 1 ml of HCl being used for every 60 mg of copolyamide. The amino acids were made volatile for gas chromatographic analysis by converting them to methyl ester hydrochlorides through Fischer esterification. The methyl esters were then converted to butyl esters by transesterification with butyl alcohol. The butyl esters were *N*-acetylated by refluxing with trifluoroacetic anhydride and analyzed without purification.

RESULTS AND DISCUSSION

A significant difference in copolymerization rates between *cis*- and *trans*-AMCC with CL was immediately apparent. Copolymerization of the high-*trans* AMCC proceeded very rapidly. The 90:10 and 70:30 CL–AMCC comonomer mixtures became extremely viscous melts in less than 1 hr; the 50:50 mixture copolymerized explosively with spattering and precipitation of solid polymer from the melt in less than 30 min. Similar changes in the corresponding monomer mixtures with *cis*-AMCC required 4 hr at 252°C. More evidence for the faster copolymerization rate of *trans*-AMCC is seen by comparing the reduced viscosities of the copolyamides made with high-*trans* and high-*cis* monomers (Table II). At any given copolymer composition the copolyamide from high-*trans* AMCC has a higher reduced viscosity than the high-*cis* analog, even though the copolymerizations with high-*cis* monomer were allowed to proceed one and a half times as long.

There are two factors which could retard the polymerization of *cis*-AMCC relative to *trans*-AMCC: (1) 1,3-diaxial shielding of either the carboxyl or aminomethyl group, since the *cis* monomer must adopt the equatorial–axial conformation whereas the *trans* AMCC conformer has both groups in equatorial positions where there is no shielding; and (2) isomerization of the *cis* to *trans* isomer before polymerization. If it is difficult for the AMCC monomer to enter the chain in the *cis* configuration, then isomerization would precede copolymerization and therefore account for the slower polymerization rate. This would be similar to the findings of Frunze et al.,[8] who reported that the condensation of *cis*-hexahydroterephthalic acid with hexamethylenediamine resulted in isomerization to the *trans* acid. Activation of the α-cyclohexyl proton by the electron-withdrawing carboxyl group in both these cases would facilitate isomerization of the *cis* monomer to the more thermodynamically stable *trans* isomer. Cyclohexane monomers which do not possess active α-cyclohexyl protons (e.g., bis-aminomethylcyclohexane) would polymerize without isomerization, and in these cases the conformational differences between the *cis* and *trans* isomers would be the dominant factor in effecting polymerization rate differences.

In order to determine if geometric isomerization of AMCC occurred during polymerization, the two 50:50 CL–AMCC copolyamides were hydrolyzed with HCl according to the procedure of Heiheus.[9] The resulting amino acids were made volatile by conversion to their *N*-trifluoroacetyl butyl ester derivatives and the *cis*:*trans* isomer ratios determined by gas

TABLE I
Geometric Composition of Aminomethylcyclohexane-carboxylic Acid Samples and CL–AMCC Copolyamide Hydrolyzates

Sample	HCL-hydrolytic conditions	*cis*, %	*trans*, %	Isomerization, %
High-*trans* AMCC	No	15 ± 2	85 ± 2	—
High-*trans* AMCC	Yes	17 ± 2	83 ± 2	0
50:50 CL–high-*trans* AMCC	Yes	20 ± 2	80 ± 2	~5 (*trans*→*cis*)
High-*cis* AMCC	No	72 ± 2	28 ± 2	—
High-*cis* AMCC	Yes	64 ± 2	36 ± 2	~11 (*cis*→*trans*)
50:50 CL–high-*cis* AMCC	Yes	22 ± 2	78 ± 2	~70 (*cis*→*trans*)
50:50 CL–high-*cis* AMCC[a]	Yes	22 ± 2	78 ± 2	~70 (*cis*→*trans*)

[a] Duplicate run.

chromatographic analysis. The chromatograms showed just three major peaks, one corresponding to aminocaproic acid, and two for the *cis*- and *trans*-AMCC derivatives. The relative ratios were calculated from area per cent, and the results are summarized in Table I.

Gas chromatographic analysis of the hydrolyzate of the 50:50 CL–high-*trans* AMCC copolyamide showed a 20:80 *cis–trans* mixture which suggested a 5% *trans*→*cis* isomerization during polymerization. Analysis of the 50:50 CL–high-*cis* AMCC hydrolyzate showed a 22:78 *cis–trans* mixture which definitely represents a 70% *cis*→*trans* isomerization during polymerization. The *cis*:*trans* ratio of the high-*trans* AMCC monomer was unchanged when subjected to exactly the same hydrolysis conditions as the copolyamides, and the high-*cis* monomer underwent only an 11% *cis*→*trans* isomerization as compared with 70% for the copolyamide. This shows conclusively that a *cis*→*trans* isomerization of AMCC occurs during polymerization at 250°C and approaches an equilibrium 20:80 *cis*:*trans* ratio.

TABLE II
Differential Thermal Analysis Data for Nylon 6 and CL–AMCC Copolyamides

CL, mole-%	AMCC, mole-%	AMCC configuration	η_{sp}/c	T_g, °C	T_c, °C	T_m, °C	Crystallinity, ±5%
100	—	—	1.05	45	75	221	58
90	10	High-*trans*	1.25	58	93	218	38
70	30	"	0.72	90	135	240	21
50	50	"	0.79	115	165	355	30
90	10	High-*cis*	1.08	60	95	216	45
70	30	"	0.65	80	130	238	20
50	50	"	0.53	105	160	350	34

Differential Thermal Analysis

DTA data (Table II) clearly show that glass transition temperatures (T_g), crystallization temperatures (T_c), and the melting points of the CL–AMCC copolyamide increased with increasing AMCC content. The similarities in T_g, T_c, and T_m for the corresponding copolyamides made from high-*cis* and high-*trans* AMCC is apparent. These similarities are not incidental but occur because the polymer structure is identical in both cases. Any small differences in properties can probably be attributed to molecular weight difference between high-*trans* and high-*cis* copolyamides.

Thermogravimetric Analysis

Thermal degradation studies of the copolymers were made by measuring the weight loss in a nitrogen atmosphere at a programmed heating rate of 10°C/min. Weight loss data (Table III) at 400 and 450°C showed that polymer stability increases with increasing AMCC content. All of the CL–AMCC copolymers have their catastrophic weight loss above 400°C and show a stepwise degradation due to moisture, solvent, or other impurities.

TABLE III
Thermogravimetric Analysis Data for Nylon 6
and CL–AMCC Copolyamides

	Weight loss, %				
Polymer	At 300°C	At 350°C	At 400°C	At 450°C	At 500°C
Nylon 6	0.3	1.4	8.4	68	91
90:10 CL–high-*trans* AMCC	1.3	2.4	9.0	48	93
70:30 "	1.9	2.5	7.0	49	93
50:50 "	2.6	3.2	5.7	39	95
90:10 CL–high-*cis* AMCC	2.7	3.3	9.8	61.5	92
70:30 "	1.4	2.4	8.3	51	91
50:50 "	1.9	2.1	7.3	52	94

X-Ray Diffraction

To determine the concentration of AMCC residues in nylon 6 which can be tolerated before lattice distortion develops, the x-ray diffraction powder patterns of the CL–AMCC copolyamides were obtained. By determining the onset of lattice distortion for both the high-*cis* and the high-*trans* copolyamides one can establish whether or not one geometric configuration of AMCC residues can be more readily accommodated by the nylon 6 lattice than the other.

Figures 1–6 are representative of the powder patterns obtained. The data obtained from these patterns are summarized as follows. (1) There was no difference in the interplanar spacings of a CL–AMCC copolyamide

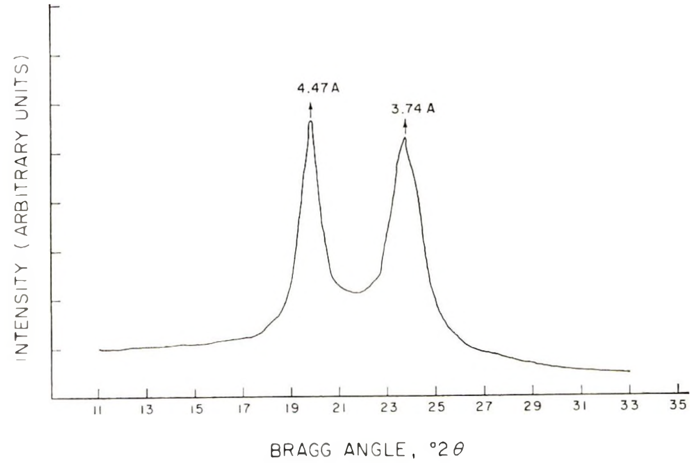

Fig. 1. X-Ray diffraction powder pattern of nylon 6.

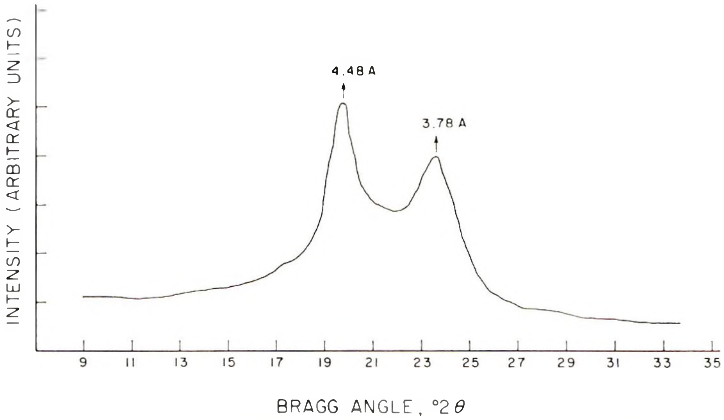

Fig. 2. X-Ray diffraction powder pattern of 90:10 CL–AMCC.

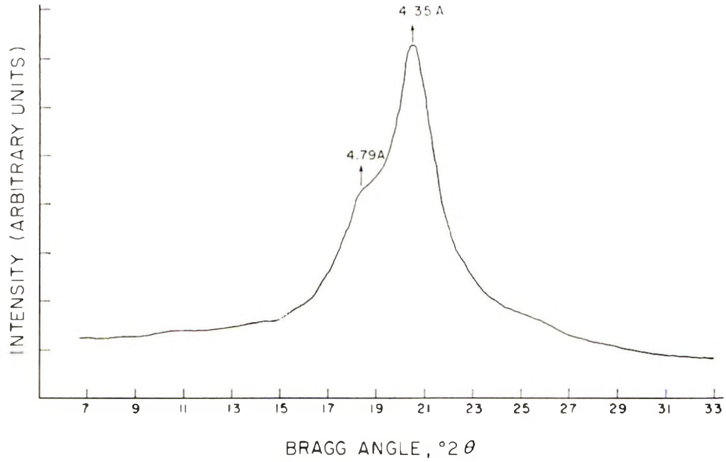

Fig. 3. X-Ray diffraction powder pattern of 70:30 CL–AMCC.

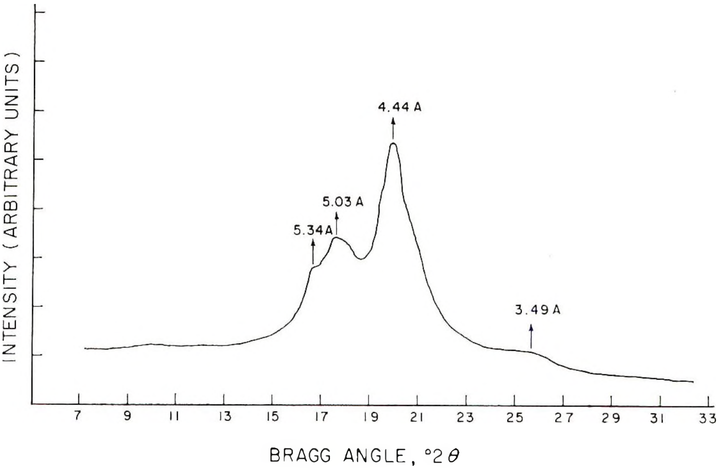

Fig. 4. X-Ray diffraction powder pattern of 50:50 CL–*trans*-AMCC.

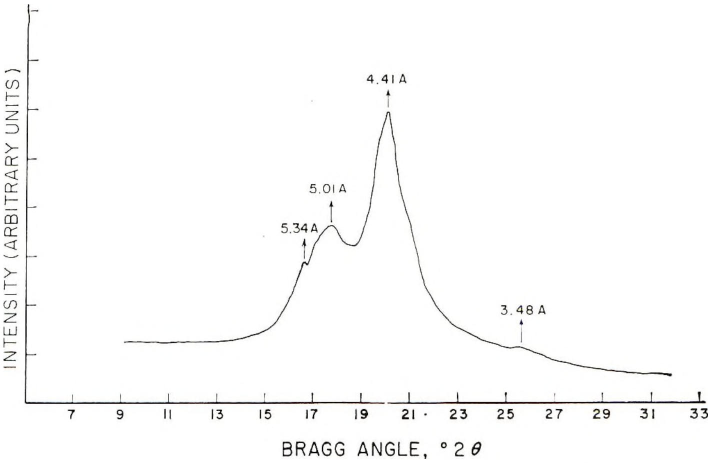

Fig. 5. X-Ray diffraction powder pattern of 50:50 CL–*cis*-AMCC.

made from high-*trans* AMCC and the corresponding copolyamide made from high-*cis* AMCC (Figs. 4 and 5). This could only occur if the two polymer structures resulting from either high-*cis* or high-*trans* monomer were identical. (2) The crystal structures of the 90:10 CL–AMCC copolyamide and nylon 6 were essentially the same (see Figs. 1 and 2). (3) When 30 mole-% or more of AMCC residues is present in the CL–AMCC copolyamide, a new crystal structure results. This is somewhat at variance with the findings of Levine and Temin[3] who reported that up to 40 mole-% AMCC residues in CL–AMCC had no effect on the crystallinity of nylon 6 (see Fig. 3). (4) At 50 mole-% or more of AMCC residues there was further development of this new structure which now closely resembled the structure of the homopolymer of AMCC (see Figs. 4–6).

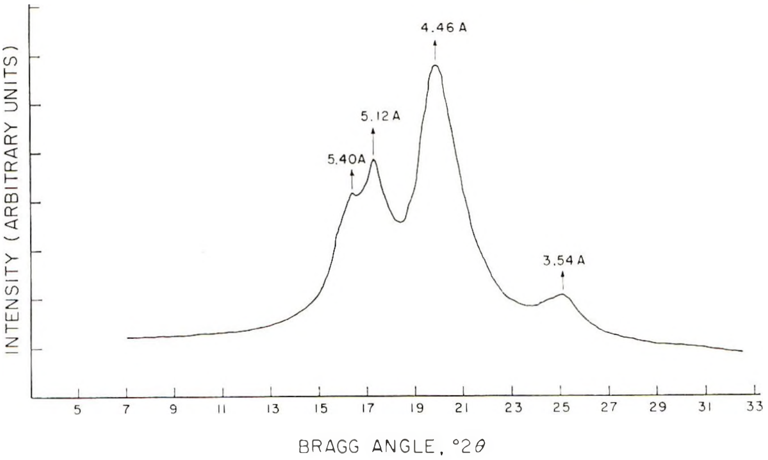

Fig. 6. X-Ray diffraction pattern powder of AMCC homopolymer.

Our diffraction data show that "isomorphous" replacement in the CL–AMCC copolyamide system is simply a cocrystallization phenomenon. Up to about 20 mole-% AMCC, these residues dissolve in the nylon 6 lattice, effecting a decrease in crystallinity without altering the crystal structure of the host. When a critical concentration of about 30 mole-% of AMCC residues is reached, the α-nylon-6 lattice is destroyed and a new transition structure formed. At greater than 50 mole-% AMCC the crystallinity has increased, and the resulting structure is very similar to the homopolymer of AMCC. In the case of true isomorphic replacement there should be little or no change in the lattice constants of the host with copolymer composition. One unique crystal structure should prevail.

Homopolymers of AMCC

Two homopolymers of AMCC from 50:50 and 40:60 *cis–trans* mixtures were prepared by solid-state polymerization at 250°C for 20 hr. The effects of geometric configuration were very similar to those observed in the CL–AMCC copolyamides. Solid-state polymerization of the 60% *trans* AMCC sample at 250°C was noticeably faster than the 50:50 sample. The high-*trans* polymer has about a 50% higher reduced viscosity (Table IV), even though both polymerizations were allowed to proceed for the same length of time. Both polymers had the same T_g, T_m, and a similar T_c. The similarities in properties probably resulted from similar configurations in

TABLE IV

AMCC configuration					
cis, %	*trans*, %	η_{sp}/c	T_g, °C	T_m, °C	T_c, °C
50	50	0.24	193	~410	250
40	60	0.49	192	~410	240

the main chain. The homopolymer from a 50:50 mixture of *cis* and *trans* AMCC was hydrolyzed and gave a mixture of AMCC derivatives, 28% of which were in the *cis* configuration and 66% in the *trans* configuration. The other 6% was a single, unidentified component. This confirms the existence of *cis*→*trans* isomerization of AMCC during homopolymerization.

We wish to acknowledge the contributions of Dr. John Sibilia and Mr. John Frank who did the gas chromatographic analyses of the amino acids and copolyamide hydrolyzates; Mrs. M. H. Riggi for the x-ray diffraction powder diagrams, and Mrs. E. Turi and Mr. Will Wenner for obtaining the DTA and TGA data on the copolyamides.

References

1. S. C. Temin and M. Levine, U. S. Pat. 2,910,457 (1959).
2. M. N. Bogdanov, G. I. Kudryavtsev, F. M. Mandrosova, I. A. Spirina, and D. E. Ostromogol'skii, *Vysokomol. Soedin.*, **3**, 1326 (1961).
3. M. Levine and S. C. Temin, *J. Polym. Sci.*, **49**, 241 (1961).
4. E. W. Pietrusza, G. A. Nesty, and R. Pinter, U. S. Pat. 3,037,002 (1962).
5. T. E. Tranter, *J. Polym. Sci. A*, **2**, 4289 (1964).
6. G. Allegra and I. W. Bassi, *Fortschr. Hochpolym. Forsch.*, **6** (1969).
7. R. S. Muromova and I. N. Afanas'eva, *Vysokomol. Soedin.*, **5**, 1461 (1963).
8. T. M. Frunze, V. V. Korshak, and V. F. Petrova, *Vysokomol. Soedin.*, **1**, 349 (1959); *Chem. Abstr.*, **55**, 11924 (1961).
9. D. Heiheus, *J. Polym. Sci.*, **22**, 65 (1956).

Received May 13, 1970
Revised June 11, 1970

JOURNAL OF POLYMER SCIENCE: PART A-1 VOL. 8, 3543-3555 (1970)

Copolymerization of 2-Sulfoethyl Methacrylate

DONALD A. KANGAS and RONALD R. PELLETIER, *Edgar C. Britton Research Laboratory, The Dow Chemical Company, Midland, Michigan 48640*

Synopsis

Copolymers of 2-sulfoethyl methacrylate, (SEM) were prepared with ethyl methacrylate, ethyl acrylate, vinylidene chloride, and styrene in 1,2-dimethoxyethane solution with N,N'-azobisisobutyronitrile as initiator. The monomer reactivity ratios with SEM(M_1) were: vinylidene chloride, $r_1 = 3.6 \pm 0.5$, $r_2 = 0.22 \pm 0.03$; ethyl acrylate, $r_1 = 3.2 \pm 0.6$, $r_2 = 0.30 \pm 0.05$; ethyl methacrylate, $r_1 = 2.0 \pm 0.4$, $r_2 = 1.0 \pm 0.1$; styrene, $r_1 = 0.6 \pm 0.2$, $r_2 = 0.37 \pm 0.03$. The values of the copolymerization parameters calculated from the monomer reactivity ratios were $e = +0.6$ and $Q = 1.4$. Comparison of the monomer reactivities indicates that SEM is similar to ethyl methacrylate with regard to copolymerization reactivity in 1,2-dimethoxyethane solution. The sodium salt of 2-sulfoethyl methacrylate, $SEM^{\ominus}Na^{\oplus}$, was copolymerized with 2-hydroxyethyl methacrylate (M_2) in water solution. Reactivity ratios of $r_1 = 0.7 \pm 0.1$ and $r_2 = 1.6 \pm 0.1$ were obtained, indicating a lower reactivity of $SEM^{\ominus}Na^{\oplus}$ in water as compared to SEM in 1,2-dimethoxyethane. This decreased reactivity was attributed to greater ionic repulsion between reacting species in the aqueous medium.

INTRODUCTION

2-Sulfoethyl methacrylate (SEM) is soluble in many organic solvents such as benzene, ethylene dichloride and dimethoxyethane. Therefore, it is possible to form copolymers of SEM with monomers such as styrene, acrylate esters, and vinyl chloride by free-radical polymerization in a homogeneous solution of an organic solvent. The choice of organic solvent for copolymerization in a homogeneous medium is limited, since the copolymer may be insoluble although both monomers are soluble. Furthermore, alcohols cannot be used because an interchange reaction occurs with monomeric esters which is catalyzed by the strong sulfonic acid, SEM. Copolymers prepared in organic solvents may be neutralized to form water-soluble salts. SEM is also soluble in water; however, it undergoes an acid-catalyzed hydrolysis. Aqueous solutions of SEM salts are essentially stable to hydrolysis at pH 5 and slowly hydrolyze at pH's between 3 and 8. Copolymers of SEM salts can be produced with water-soluble monomers such as acrylamide and 2-hydroxyethyl methacrylate.

Since SEM is an ionizable monomer, its copolymerization may be affected by ionic repulsion between growing polymer radical and monomer. For example, the termination reaction in the homopolymerization of $SEM^{\ominus}$ $Na^{\oplus}$ is apparently hindered by electrostatic repulsion between the reacting ions resulting in an increased ratio of rate constants for homopolymerization of SEM$^{\ominus}$Na$^{\oplus}$ in solutions of low ionic strength.[1] Because electrostatic repulsion is dependent on the dielectric constant of the medium, monomer reactivity ratios may be dependent on the solvent used for copolymerization. Since SEM is a strong acid, its polymerization could not be expected to be a function of pH as is the case with methacrylic acid. The observed decrease in the polymerization rate of methacrylic acid has been attributed to repulsion between the methacrylate ion and the growing polymer radical ion and the polymerization has been described as a copolymerization between the ionized and unionized methacrylic acid.[2]

Monomer reactivity ratios were determined for copolymerizations of SEM with vinylidene chloride, ethyl acrylate, ethyl methacrylate, and styrene in 1,2-dimethoxyethane solution with *N*,*N*′-azobisisobutyronitrile as initiator and for copolymerization of SEM$^{\ominus}$Na$^{\oplus}$ with 2-hydroxyethyl methacrylate in water with *N*,*N*′-azobisisobutyramidine · HCl as initiator.

EXPERIMENTAL

Materials

The SEM used had an assay of 97% and contained 1.7% methacrylic acid as impurity and 0.2% of the monomethyl ether of hydroquinone as polymerization inhibitor.

A stock solution of SEM in 1,2-dimethoxyethane was prepared by dissolving 14 grams of SEM in 100 ml of 1,2-dimethoxyethane. An insoluble fraction of the SEM was removed by filtering the solution through a fluted filter. An undialyzable residue of 0.4% remains in SEM monomer after filtration. This impurity, which cannot be removed from the copolymer samples, apparently contains about 90% poly-SEM, as calculated from the sulfur content. Ethylenic unsaturation was determined by the bromate–bromide method.

An aqueous solution of SEM$^{\ominus}$Na$^{\oplus}$ was prepared by simultaneous addition of 195 g of SEM and 200 ml of 5*N* NaOH solution to 150 ml of water with stirring. The SEM was added slightly faster than the NaOH to control the pH below 5, and an ice–salt bath was used to control the temperature below 10°C. Ethylenic unsaturation was determined by the bromate-bromide method.

The ethyl acrylate, as received from Dow Badische, contained 1000 ppm of the monomethyl ether of hydroquinone. It was distilled at approximately 30 mm pressure through a 1-ft Vigreaux column to reduce the inhibitor concentration and then stored at -10°C until it was used.

The ethyl methacrylate was used as received from Rohm & Haas with 100 ppm of hydroquinone.

The vinylidene chloride was purified by washing it with about eight volumes of 5% $NaHSO_3$ solution, filtering, rinsing with H_2O, and again filtering. Monomethyl ether of hydroquinone, 200 ppm, was then added to prevent polymerization. The water content was checked by Karl

Fischer reagent and found to be only 30 ppm. The infrared and NMR spectra did not show any significant quantity of impurities.

Styrene was freed of inhibitor by distillation.

The 2-hydroxyethyl methacrylate, inhibited with the monomethyl ether of hydroquinone, was used as received from Rohm & Haas.

N,N'-Azobisisobutyronitrile was used as received from Matheson, Coleman and Bell. *N,N'*-Azobisisobutyramidine·HCl was used as received from du Pont.

The 1,2-dimethoxyethane, obtained from Matheson, Coleman and Bell, was flash distilled at atmospheric pressure before use to destroy peroxides and remove water which distilled out as the azeotrope.

Other materials were used as obtained from laboratory stock.

Preparation of Copolymers

All copolymerizations of SEM run in 1,2-dimethoxyethane solvent were at $1.0M$ total monomer concentration. The copolymers were prepared by the following procedure. The comonomer and SEM stock solution were mixed in a citrate bottle. The concentration of comonomer was calculated from its weight and the concentration of SEM was based on unsaturation which included methacrylic acid as SEM. 1,2-Dimethoxyethane was added to 200 ml total volume and 0.2 g of *N,N'*-azobisisobutyronitrile was added. The bottle was purged with N_2 to remove air, sealed, and rotated end-over-end in a water bath at 50 or 60°C. After 1–4 hr, the time being estimated to give from 5 to 10% conversion, the sample was removed from the bath, cooled, and about 2% $NaNO_2$ inhibitor added along with four volumes of water. The sample was then neutralized with $5N$ NaOH solution. The volatile comonomer and 1,2-dimethoxyethane solvent were removed by steam distillation at 10–20 mm pressure to control the temperature at less than 20°C. $SEM^{\ominus}Na^{\oplus}$ monomer and $NaNO_2$ were removed by dialysis through regenerated cellulose membrane against a continuous flow of deionized water for 2 days. The copolymer sample was obtained upon evaporation of the dialyzed solution. A residue of 0.23% of initial monomers remained after a mixture of 40/60 mole ratio SEM–ethyl methacrylate was run through the above work-up procedure. This amount of residue would be expected from the SEM, so it can be concluded that no polymerization occurred during the work-up procedure and monomers are completely removed by the process.

Copolymers of $SEM^{\ominus}Na^{\oplus}$ with 2-hydroxyethyl methacrylate were prepared in water by using $0.5M$ monomer concentrations and 0.05 g of *N,N'*-azobisisobutyroamidine·HCl initiator/100 ml of solution. The copolymerization procedure was otherwise the same as for the SEM copolymers. The work-up procedure was also the same except that neutralization and steam distillation were unnecessary. The copolymers were isolated simply by dialyzing the solutions and then evaporating off the water.

The copolymer samples were dried in a 60°C vacuum oven for 24–48 hr. The per cent conversion was calculated from the weight of copolymer ob-

TABLE I
SEM–Vinylidene Chloride Copolymer Compositions

Sample	Mole fraction SEM in monomers (f_1)	Conversion, %	Sulfur, %	Chloride, %	$SEM^{\ominus}Na^{\oplus}$, wt-%	VCl_2, wt-%	Total, wt-%	Mole fraction SEM in copolymer (F_1)
A-1	0.10	2.3	7.24	33.43	51.57	48.06	99.63	0.325
A-2	0.20	7.7	9.41	22.54	67.01	32.40	99.41	0.481
A-3	0.30	3.8	11.08	14.50	78.86	20.84	99.70	0.623
A-4	0.40	7.4	11.94	9.80	84.98	14.09	99.07	0.730
A-5	0.50	4.1	12.62	6.72	89.79	9.63	99.42	0.807
A-6	0.50	6.5	12.58	7.54	89.50	10.85	100.35	0.787
A-7	0.60	7.3	13.02	5.21	92.70	7.49	100.19	0.847
A-8	0.70	6.9	13.39	3.22	95.30	4.62	99.92	0.903
A-9	0.90	9.0	13.77	1.02	97.97	1.47	99.44	0.968
A-10	1.00	29.3	14.05	0.15	100.	0	100.	1.00
A-12	0	—	<0.4	69.56	0	100.	100.	0

tained and the starting monomer weight. The copolymers were analyzed for percent sulfur by the Schöniger method. Sulfur analyses had a standard deviation of ±0.06%. Homopolymers of SEM, $SEM^{\ominus}Na^{\oplus}$, and vinylidene chloride, prepared in the same manner as the copolymers, were also analyzed for sulfur. The homopolymer and copolymers of vinylidene chloride were analyzed for chloride. The results of these analyses were used to calculate the mole fractions of $SEM^{\ominus}Na^{\oplus}$ in the copolymers. The per cent sulfur in the homopolymer was used in the calculations rather than the theoretical sulfur content because copolymers were prepared from impure SEM and they may contain other impurities such as moisture and catalyst residues. Values of F_1, mole fraction of SEM in copolymer, calculated from the analytical results of duplicate copolymer samples, had a standard deviation of ±1.0% of F_1. The undialyzable residue from SEM contributes about 3% to the weight of low-conversion copolymer samples. Although the method of calculation corrects F_1 values for the residue, the estimated maximum uncertainty of calculated F_1 values would be ±3% of F_1.

RESULTS AND DISCUSSION

In the SEM–vinylidene chloride copolymerization series, the weight per cent of vinylidene chloride in the copolymers were calculated by using the per cent chloride in vinylidene chloride as determined by analysis in the same way as the weight per cent of $SEM^{\ominus}Na^{\oplus}$ were determined. Good total analyses were obtained with this method as shown in Table I, which lists the starting mole fraction of SEM, the weight per cent conversion, the per cent sulfur and per cent chloride results, the weight per cent $SEM^{\ominus}Na^{\oplus}$ and vinylidene chloride, the total weight per cent accounted for and the mole fraction of SEM in the copolymer.

The results of SEM and styrene copolymerizations are listed in Table II.

TABLE II
SEM–Styrene Copolymer Compositions

Sample	Mole fraction SEM in monomer (f_1)	Conversion, %	Sulfur, %	Mole fraction SEM in copolymer (F_1)
B-1	0.10	5.1	4.72	0.195
B-2	0.20	5.5	7.02	0.323
B-3	0.30	5.4	8.32	0.409
B-4	0.40	5.9	9.26	0.480
B-5	0.50	6.0	9.96	0.537
B-6	0.60	5.7	10.56	0.590
B-7	0.70	10.8	11.48	0.679
B-8	0.80	8.5	12.10	0.745
B-9	0.90	12.9	12.87	0.835
B-10	0.50	7.0	9.96	0.537

The composition of SEM–styrene copolymer, obtained by sulfur analysis, was verified by NMR analysis. A NMR spectrum was obtained on a D_2O solution of a copolymer sample prepared from an equimolar mixture of SEM and styrene (sample B-10 in Table II). The mole fraction of SEM obtained was 0.53 by comparison of aliphatic and aromatic hydrogens. This result compares favorably with the 0.537 calculated from the sulfur analyses.

TABLE III
SEM–Ethyl Acrylate Copolymer Compositions

Sample	Mole fraction SEM in monomer (f_1)	Conversion, %	Sulfur, %	Mole fraction SEM in copolymer (F_1)
C-1	0.10	11.2	6.14	0.263
C-2	0.30	14.0	10.72	0.596
C-3	0.50	15.4	12.40	0.772
C-4	0.70	11.1	13.38	0.897
C-5	0.90	12.3	13.84	0.962
C-6	0.10	13.5	6.14	0.263
C-7	0.50	3.0	12.50	0.785

TABLE IV
SEM–Ethyl Methacrylate Copolymer Compositions

Sample	Mole fraction SEM in monomer (f_1)	Conversion, %	Sulfur, %	Mole fraction SEM in copolymer (F_1)
D-1	0.10	2.9	3.30	0.113
D-2	0.20	5.6	5.15	0.241
D-3	0.30	11.3	7.22	0.370
D-4	0.40	10.2	8.89	0.493
D-5	0.50	10.3	10.28	0.612
D-6	0.60	10.7	11.40	0.722
D-7	0.80	15.7	12.78	0.878
D-8	0.50	18.2	10.16	0.601

TABLE V
SEM$^{\ominus}$Na$^{\oplus}$–2-Hydroxyethyl Methacrylate Copolymer Compositions

Sample	Mole fraction SEM in monomer (f_1)	Conversion, wt-%	Sulfur, %	Mole fraction SEM in copolymer (F_1)
E-1	0.10	47	1.40	0.062
E-2	0.30	12	4.12	0.197
E-3	0.50	32	7.12	0.378
E-4	0.70	18	10.11	0.601
E-5	0.90	11	12.80	0.853
E-6	0.50	12	7.09	0.376
E-7	0.50	25	7.33	0.392
E-8	1·00	20	14.11	1.00

Tables III and IV list the starting mole fractions of SEM monomer, the conversion, the sulfur contents and the mole fractions of SEM in the copolymers with ethyl acrylate and ethyl methacrylate. Table V lists the same data for the $SEM^{\ominus}Na^{\oplus}$-hydroxyethyl methacrylate copolymerizations in water solution.

Copolymerization in 1,2-Dimethoxyethane

The monomer reactivity ratios were calculated from the data listed in Tables I–V by the method described by Fineman and Ross.[3] The errors in the calculated values of r_1 and r_2 were estimated from the maximum and minimum values of the slope and intercept resulting from the expected errors in the analysis. The monomer reactivity ratios and the estimated errors are listed in Table VI.

TABLE VI
Monomer Reactivity Ratios of SEM (M_1)

M_2	r_1	r_2
Vinylidene chloride	3.6 ± 0.5	0.22 ± 0.03
Ethyl acrylate	3.2 ± 0.6	0.30 ± 0.05
Ethyl methacrylate	2.0 ± 0.4	1.0 ± 0.1
Styrene	0.6 ± 0.2	0.37 ± 0.03

The monomer reactivity ratios listed above are in good agreement with the experimentally determined compositions as shown in Figures 1–4 in which the mole fraction of SEM in the increment of copolymer formed is plotted as a function of the mole fraction of SEM in the monomer mixture. The points represent the experimentally determined compositions and the line was calculated from the r_1 and r_2 values listed in Table VI.

It was surprising that styrene could be copolymerized with SEM in 1,2-dimethoxyethane solution. When the strong sulfonic acid, SEM, is added directly to styrene, an explosive cationic polymerization of styrene occurs. However, in 1,2-dimethoxyethane solution, there was no evidence of homopolymerization or copolymerization in the absence of a free-radical initiator. It is assumed that 1,2-dimethoxyethane is sufficiently basic to prevent the formation of the initiating cation of styrene so that ionic polymerization does not occur.

The reactivities of SEM and ethyl methacrylate are nearly the same in 1,2-dimethoxyethane solution. The monomer reactivity ratio r_2 is 1, and the copolymer composition curve (Fig. 3) indicates that the copolymer formed has nearly the same composition as the monomer mixture. However, r_1 is equal to 2, indicating that SEM is slightly more reactive than ethyl methacrylate and so the copolymer formed is slightly richer in SEM than is the monomer mixture.

The reactivity of two monomers such as SEM and ethyl methacrylate can be compared on the basis of reactivity with a third radical in the follow-

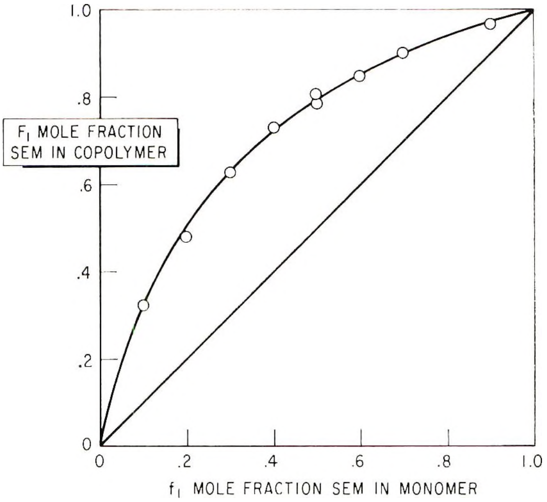

Fig. 1. SEM–vinylidene chloride copolymer composition curve.

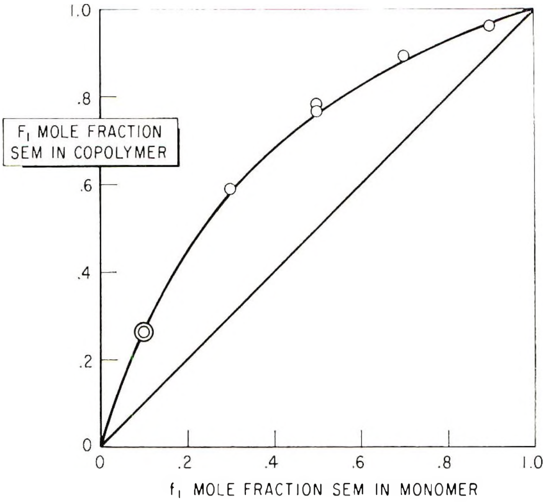

Fig. 2. SEM–ethyl acrylate copolymer composition curve.

ing way. Consider the copolymerization of two pairs of monomers in which a monomer, M_1, is common to both. Propagation reactions involving M_1 type radical and the rate constants are:

$$\sim M_1\cdot + M_1 \xrightarrow{k_{11}} \sim M_1\cdot \tag{1}$$

$$\sim M_1\cdot + M_2 \xrightarrow{k_{12}} \sim M_2\cdot \tag{2}$$

$$\sim M_1\cdot + M_3 \xrightarrow{k_{13}} \sim M_3\cdot \tag{3}$$

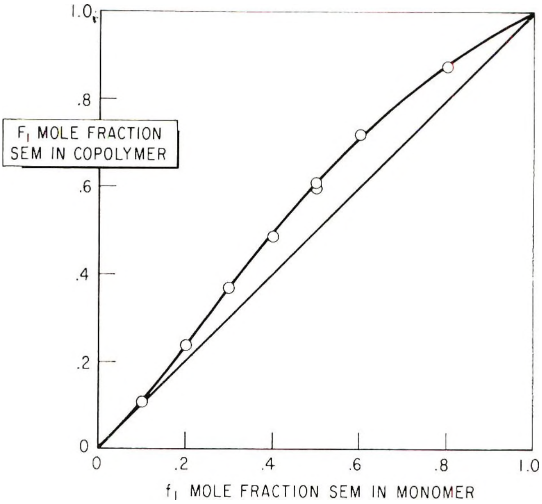

Fig. 3. SEM–ethyl methacrylate copolymer composition curve.

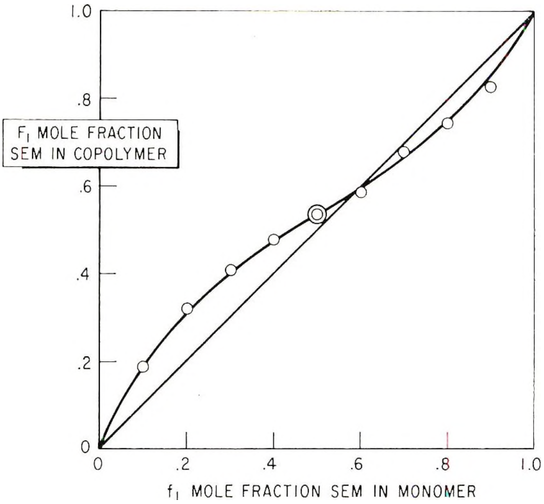

Fig. 4. SEM–styrene copolymer composition curve.

The monomer reactivity ratios are:

$$r = k_{11}/k_{12} \tag{4}$$

$$r' = k_{11}/k_{13} \tag{5}$$

Since k_{11}, the propagation rate constant for the common monomer, appears in both eqs. (4) and (5) the relationship (6) can be written:

$$k_{12} = (r'/r)k_{13} \tag{6}$$

Values of r, r' and the ratio r'/r are listed in Table VII for SEM (M_2) and ethyl methacrylate (M_3) with common radicals.

The reaction rate constant for the addition of SEM to a free radical is on the average 1.5 times greater than the rate constant for addition of ethyl methacrylate to a growing radical. While this cannot be considered a large difference in reaction rate constant it shows a slightly greater reactivity of SEM compared to ethyl methacrylate.

The slight difference in reactivity between SEM and ethyl methacrylate could result from an inductive effect of the sulfonic acid substituent of SEM. Since the sulfonic acid group is remote from the olefinic unsaturation, the change in reactivity is not great. However, the fact that the reactivity of SEM is greater than that of ethyl methacrylate is evidence of the absence of electrostatic repulsion between the polymeric radical and the monomer arising from ionization of the sulfonic acid in 1,2-dimethoxyethane since this should cause a decrease in reactivity.

TABLE VII

Reactivity of SEM and Ethyl Methacrylate

Radical, M_1	r, SEM (M_2)	r', ethyl methacrylate (M_3)	r'/r
Vinylidene chloride	0.22	0.35[a]	1.6
Ethyl acrylate	0.30	0.30[b]	1.0
Ethyl methacrylate	1.0	1	1.0
SEM	1	2.0	2.0
Styrene	0.37	0.66[a]	1.8

[a] Data of Young.[4]

[b] Data of Paxton.[5]

The copolymerization parameters[6] Q and e were calculated for SEM from its monomer reactivity ratios with vinylidene chloride, ethyl acrylate, and styrene and the published[4] values of Q and e for these comonomers. Since the product of the monomer reactivity ratios, r_1r_2, for SEM and ethyl methacrylate copolymerization was greater than 1, it cannot be used in the calculation. The average values calculated for SEM were $Q = 1.4$ and $e = 0.6$.

Copolymerization in Water

The sodium salt of sulfoethyl methacrylate, $SEM^{\ominus}Na^{\oplus}$ (M_1), was copolymerized with 2-hydroxyethyl methacrylate in water to compare its copolymerization behavior with that of SEM in 1,2-dimethoxyethane. The monomer reactivity ratios were $r_1 = 0.7 \pm 0.1$ and $r_2 = 1.6 \pm 0.1$. The copolymer composition curve and experimental points are shown in Figure 5. The copolymer contains less $SEM^{\ominus}Na^{\oplus}$ than the monomer mixture, indicating that $SEM^{\ominus}Na^{\oplus}$ is less reactive than 2-hydroxyethyl methacrylate.

Unfortunately, 2-hydroxyethyl methacrylate undergoes a rapid acid-catalyzed exchange reaction with SEM in 1,2-dimethoxyethane, so that a direct comparison of SEM reactivity in 1,2-dimethoxyethane to SEM$^{\ominus}$Na$^{\oplus}$ reactivity in water could not be made.

The effect of solvent and ionic strength on the rate constant of a reaction between ionic species can be described by the following simplified equation

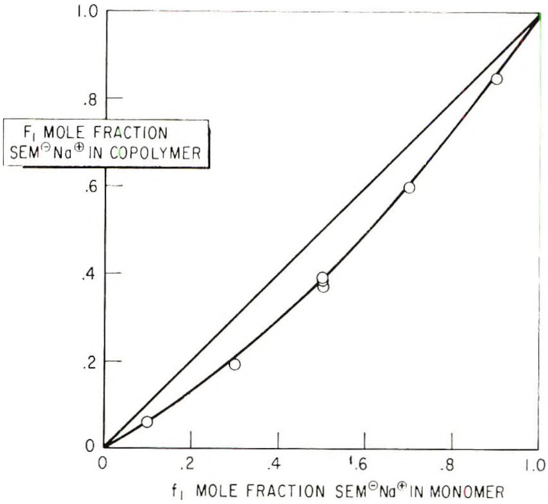

Fig. 5. SEM$^{\ominus}$Na$^{\oplus}$–hydroxyethyl methacrylate copolymer composition curve.

which is derived from the Debye-Hückel theory for dilute electrolyte solutions:[7]

$$\ln k = \ln k_0 + 2Z_aZ_b\alpha\mu^{1/2} \tag{7}$$

where k and k_0 are reaction rate constants at ionic strength μ and zero, respectively; Z_a and Z_b are the valences of the reacting ions, and α is a constant for a given solvent and temperature.

The reaction rate constants used in the monomer reactivity ratios are only those for the propagation reactions:

$$\sim P_1\cdot^{\ominus} \pm M_1^{\ominus} \xrightarrow{k_{11}} \sim P_1\cdot^{\ominus} \tag{8}$$

$$\sim P_1\cdot^{\ominus} + M_2 \xrightarrow{k_{12}} \sim P_2\cdot^{\ominus} \tag{9}$$

$$\sim P_2\cdot^{\ominus} + M_2 \xrightarrow{k_{22}} \sim P_2\cdot^{\ominus} \tag{10}$$

$$\sim P_2\cdot^{\ominus} + M_1^{\ominus} \xrightarrow{k_{21}} \sim P_1\cdot^{\ominus} \tag{11}$$

where $M_1^{\ominus}$ is SEM, M_2 is nonionic comonomer, $\sim P_1\cdot^{\ominus}$ and $\sim P_2\cdot^{\ominus}$ are growing polymer radical with end from monomer 1 or 2, k_{11}, k_{12}, k_{22}, k_{21} are the propagation reaction rate constants.

The effect of solvent and ionic strength on the propagation reactions involving the ionic comonomer can be written from eqs. (7), (8), and (11) as follows:

$$\ln k_{11} = \ln k_{11_0} + 2Z_{\mathrm{p}}\alpha\mu^{1/2} \tag{12}$$

$$\ln k_{21} = \ln k_{21_0} + 2Z_{\mathrm{p}}\alpha\mu^{1/2} \tag{13}$$

where Z_p is the valence of the growing polymer radical.

Since M_2 has a valence of zero no effect of solvent or ionic strength on k_{12} or k_{22} would be predicted from eq. (7). The equations describing the effect of solvent and ionic strength on the monomer reactivity ratios are:

$$r_1 = k_{11_0}/k_{12}\ \exp\{2Z_{\mathrm{p}}\alpha\mu^{1/2}\} \tag{14}$$

$$r_2 = k_{22}/k_{21_0}\ \exp\{-2Z_{\mathrm{p}}\alpha\mu^{1/2}\} \tag{15}$$

$$r_1r_2 = (k_{11_0}/k_{12})\ (k_{22}/k_{21_0}) \tag{16}$$

The product of the monomer reactivity ratios for copolymerization of SEM with ethyl methacrylate in 1,2-dimethoxyethane is 2.0 and for copolymerization of SEM with 2-hydroxyethyl methacrylate in water the product is 1.1. The small difference in these numbers can be attributed to the fact that the propagation rate constant, k_{22}, for ethyl methacyrlate is about two times the propagation rate constant for 2-hydroxyethyl methacrylate.[8] After taking account of the difference between ethyl methacrylate and 2-hydroxyethyl methacrylate the product of the monomer reactivity ratios for copolymerization of SEM in water and in 1,2-dimethoxyethane are essentially the same 1.0 and 1.1, in agreement with eq. (16).

The cross-propagation constant calculated from the ratio of r_2 values for the reaction of SEM monomer with a growing polymer radical with a nonionic end in 1,2-dimethoxyethane is three times that in water, after taking account of the difference in reactivity of ethyl methacrylate and 2-hydroxyethyl methacrylate. The propagation constant calculated from the ratio of r_1 values for the reaction of SEM monomer in 1,2-dimethoxyethane with a growing polymer radical having an SEM and is seven times that in water. The increase in reactivity of SEM in 1,2-dimethoxyethane compared to water is much less than might be expected from the change in dielectric constant of the solvents. It would be expected, however, that the difference might be much greater if the comparison was made to aqueous polymerizations of low ionic strength. The fact that the SEM propagation constant is increased about twice as much as the cross-propagation constant in 1,2-dimethoxyethane can be attributed to a greater repulsion in water between SEM monomer and an SEM radical end than between SEM monomer and a nonionic monomer end which has the ionic group remote from the reacting radical.

References

1. D.A. Kangas, *J. Polym. Sci. A-1*, **8,** 1813 (1970).
2. S. H. Pinner, *J. Polym. Sci.*, **9,** 282 (1952).
3. M. Fineman and S. D. Ross, *J. Polym. Sci.*, **5,** 259 (1950).
4. L. J. Young, *J. Polym. Sci.* **54,** 411 (1961).
5. T. R. Paxton, *J. Polym. Sci., B*, **1,** 73 (1963).
6. T. Alfrey, J. J. Bohrer, and H. Mark, *Copolymerization*, Interscience, New York, 1952, p. 47.
7. A. A. Frost and R. G. Pearson, *Kinetics and Mechanism*, Wiley, New York, 1953, p. 138.
8. K. G. McCurdy and K. J. Laidler, *Can. J. Chem.*, **42,** 825 (1964).

Received June 8, 1970

JOURNAL OF POLYMER SCIENCE: PART A-1 VOL. 8, 3557-3561 (1970)

Polymerization Studies on Allylic Compounds. V. 2-Chloropropenes

SAMUEL F. REED, JR., *Rohm and Haas Company*
Redstone Research Laboratories, Huntsville, Alabama 35807

Synopsis

The free-radical polymerization of three 2-chloro-3-substituted propenes have been investigated. Compounds studied were 2,3-dichloropropane, 2-chloro-3-hydroxypropene, and 2-chloro-3-acetoxypropene. These compounds were found to homopolymerize with difficulty to give low molecular weight polymers. Their effect upon the polymerization of methyl methacrylate and styrene was investigated by rate and viscosity measurements. Copolymerization occurred with a retarding action attributed to significant chain transfer processes and differences in monomer reactivities.

INTRODUCTION

The polymerization study of 2,3-disubstituted propenes[1] has been continued by use of 2-chloro-3-substituted propenes of structure I, where Y was chloro, hydroxy, and acetoxy. The purpose of this paper is to describe the polymerization behavior of these compounds and their effect on the copolymerization of methyl methacrylate (MMA) and styrene. Compounds of type I examined were 2,3-dichloropropene (DCP), 2-chloro-3-hydroxypropene (CHP), and 2-chloro-3-acetoxypropene (CAP). Polymerization rate measurements were made by a dilatometric technique,[2] and the polymers were characterized by solution viscosity properties and elemental analysis.

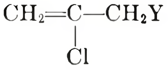

$$CH_2{=}\underset{\displaystyle Cl}{\underset{|}{C}}{-}CH_2Y$$

I

EXPERIMENTAL

Materials

The monomers DCP and CHP were purchased from a commercial source and fractionally distilled prior to use in the polymerization reactions. Acetylation of CHP gave CAP in 81% yield. All monomers were at least 99.5% pure as determined from VPC analysis.

All solvents were reagent grade, distilled.

Azobisisobutyronitrile (AIBN) was recrystallized from methanol, mp 102–103°C with decomposition.

Techniques

Dilatometric polymerization rate determinations have been described elsewhere.[2]

Solution viscosities were determined in toluene at 30°C using Cannon dilution viscometers.

Polymerization Reactions

All polymerization and copolymerization reactions were carried out in toluene at 60°C ± 0.05°. Reactions were carried to approximately 10% completion.

RESULTS

Homopolymerization of DCP, CHP, and CAP was attempted with the use of AIBN (0.0375 mole/l.) in toluene at 60°C. Measured rates were 2.2×10^{-4}, 0.8×10^{-4}, and 2.1×10^{-4} %/min at monomer concentrations of 4.5 (DCP), 5.4 (CHP), and 3.7 mole/l. (CAP), respectively. In no instance could a solid polymer be isolated, and only extremely low molecular weight liquid products were obtained. No attempt was made to purify and characterize these materials. This polymerization behavior is typical of allylic compounds.[3]

The effect of the monomers (I) on the polymerization of MMA and styrene were investigated. Copolymerization rates were measured over the first 8–12% conversion by means of a dilatometric technique. Copolymers were characterized by intrinsic viscosity and elemental analyses. Molar ratios of MMA and styrene to the comonomers I were varied from approximately 25:1 to 2:1. Results are represented in Tables I and II. The R_{p0} values refer to the MMA or styrene polymerization rate in the absence of a comonomer (I) with conditions approximating those for copolymerization. Similarly, the $[\eta]_0$ values are the intrinsic viscosity values for the MMA and styrene homopolymers.

The MMA copolymerization data indicated several interesting points. At the lowest concentrations of comonomers I, the greatest molar ratio of MMA:I, the comonomers I displayed very limited retardation of the polymerization rate as evidenced by the R_p/R_{p0} values near 1.0 or greater. Upon increasing the concentration of I an almost uniform decrease in the rate was observed. DCP showed the greatest rate retardation as would be expected while CAP displayed very little effect.

A sharp decrease in the $[\eta]$ of the copolymers was observed with increasing comonomer I concentrations. Even at the lowest concentration of DCP or CHP the $[\eta]$ was severely reduced. As expected, DCP exhibited the greatest effect in reducing the $[\eta]$ of the copolymers.

TABLE I
Experimental Data for Copolymerization

No.	[MMA], mole/l.	[Styrene], mole/l.	Comonomer	[Comonomer], mole/l.	Mole ratio comonomers	$R_p \times 10^3$, %/min	R_p/R_{p0}	$[\eta]$	$[\eta]/[\eta]_0$
1	5.000	—	None	—	—	2.5	1.00	1.580	1.000
2	4.465	—	DCP	0.275	16.24	2.5	1.00	0.270	0.174
3	3.975	—		0.825	4.82	1.9	0.76	0.132	0.083
4	3.525	—		1.375	2.56	1.6	0.64	0.084	0.053
5	4.465	—	CHP	0.315	14.17	3.0	1.20	0.742	0.469
6	3.975	—		0.950	4.18	2.1	0.84	0.690	0.437
7	3.525	—		1.625	2.17	1.9	0.76	0.500	0.317
8	4.75	—	CAP	0.185	25.00	2.4	0.96	1.360	0.861
9	4.25	—		0.555	7.55	2.5	1.00	1.200	0.759
10	3.75	—		0.925	4.05	2.4	0.96	0.930	0.589
11	—	4.84	None	—	—	0.7	1.00	0.260	1.000
12	—	4.132	DCP	0.275	15.03	1.1	1.57	0.186	0.715
13	—	3.700		0.825	4.48	0.6	0.85	0.148	0.569
14	—	3.275		1.375	2.38	0.5	0.71	0.078	0.300
15	—	4.132	CHP	0.315	13.12	0.9	1.28	0.306	1.176
16	—	3.700		0.950	3.89	0.7	1.00	0.258	0.992
17	—	3.273		1.625	2.02	0.6	0.85	0.156	0.600
18	—	4.56	CAP	0.185	24.40	0.85	1.21	0.358	1.376
19	—	4.09		0.555	7.45	0.9	1.28	0.250	0.961
20	—	3.60		0.925	3.90	0.8	1.14	0.180	0.692

TABLE II
Elemental Analysis of Copolymers

No.[a]	Calculated C, %	Calculated H, %	Calculated Cl, %	Found C, %	Found H, %	Found Cl, %
2	58.24	7.72	4.09	59.5	8.27	0.85
3	54.84	7.18	11.97	59.3	8.11	2.34
4	51.66	6.67	19.35	57.7	7.92	4.14
5	58.71	7.84	2.35	59.7	8.03	0.44
6	56.18	7.53	6.95	58.6	7.97	3.37
7	53.71	7.23	11.46	56.6	7.67	5.04
8	59.22	7.86	1.35	60.2	8.00	0.42
9	57.68	7.58	3.99	59.8	7.78	1.48
10	56.22	7.33	6.57	59.3	7.64	1.51
12	88.34	7.42	4.24	89.6	8.05	1.76
13	80.79	6.91	12.31	86.9	7.67	3.70
14	73.77	6.43	19.80	86.1	7.65	7.68
15	88.92	7.55	2.44	92.2	7.97	0.03
16	82.38	7.27	7.13	88.5	7.69	0.58
17	75.99	6.99	11.72	86.9	7.68	1.17
18	89.87	7.56	1.33	88.7	7.59	0.34
19	85.23	7.32	3.90	87.0	7.39	0.82
20	80.43	7.07	6.57	87.2	7.67	1.13

[a] Numbers correspond to numbers in Table I.

Styrene copolymerizations showed a similar behavior. The copolymerization rates were not affected at the lower comonomer I concentrations, even with DCP; however, slight decreases in rate were observed at the higher concentrations. In all instances, the $[\eta]$ values for the styrene copolymers were less affected than the MMA copolymers.

Chlorine analyses (Table II) of the copolymers showed that they contained comonomers I in a ratio lower than present in the initial comonomer charge. DCP entered the MMA copolymer to the extent of 20% of the initial charge ratio of comonomers and the styrene copolymers to the extent of 30–40%.

The MMA copolymers containing CHP possessed a composition containing 20–48% of the CHP present in the initial charge; however, CHP displayed a reluctance to enter into copolymerization with styrene since the styrene copolymers contained CHP in a ratio well below that present in the comonomer charge (<10%). CAP entered all the copolymers reluctantly also to give a product with a composition decidedly less rich in CAP than found in the comonomer charge.

The observed action of the comonomers I on the polymerization of MMA and styrene results from several factors. It is apparent from the decreasingly lower values of the $[\eta]$ with increased concentrations of comonomers I that chain transfer to monomer assumes significant importance in these reactions. This degradative chain transfer is the major reason for the low molecular weight products obtained in the polymerization of allyl monomers.[3,4] DCP exhibited a greater propensity towards chain transfer than did CHP or CAP. This difference between the effect of DCP and CHP or CAP on the polymerization was also apparent from the differences in their degree of rate retardation.

The major factor contributing to the limited incorporation of the comonomers I into the copolymers arises from the difference in reactivity between the comonomer systems. Both MMA and styrene are reactive monomers in polymerization reactions. In contrast the allylic compounds I are relatively unreactive in polymerization reactions. Comonomer combinations involving a reactive monomer (MMA and styrene) with an unreactive comonomer are known[5] to undergo copolymerization with difficulty, and usually only limited quantities of the unreactive monomer becomes incorporated into the copolymer, i.e., the styrene–vinyl acetate system. This characteristic behavior arises in the free-radical-initiated copolymerizations because each monomer of the pair must compete for the same radicals, and the greater reactivity of the most active monomer becomes very evident.

This study of the 2-chloro-3-substituted propenes (I) has indicated that these type monomers display polymerization characteristics similar to allyl and methallyl compounds in general. It is indicated that degradative chain transfer is occurring to significant extents with 2,3-dichloropropene but to much lesser extents with 2-chloro-3-hydroxypropene or 2-chloro-3-acetoxypropene. It is emphasized that the most important factor controlling their limited copolymerization with MMA and styrene is attributed to gross differences in monomer reactivity.

This work was performed under the sponsorship of the U. S. Army Missile Command, Redstone Arsenal, Alabama, under Contract DAAH01-67-C-0655.

References

1. M. G. Baldwin and S. F. Reed, Jr., *J. Polym. Sci. A-1*, **6**, 2627 (1968).
2. M. G. Baldwin and S. F. Reed, Jr., *J. Polym. Sci. A*, **1**, 1919 (1963).
3. P. D. Bartlett and R. Altschul, *J. Amer. Chem. Soc.*, **67**, 812, 816 (1945).
4. R. L. Harville and S. F. Reed, Jr., *J. Polym. Sci. A-1*, **8**, 2535 (1970).
5. F. R. Mayo, C. Walling, F. M. Lewis, and W. F. Hulse, *J. Amer. Chem. Soc.*, **70**, 1523 (1948).

Received June 30, 1970

JOURNAL OF POLYMER SCIENCE: PART A-1 VOL. 8, 3563–3575 (1970)

Dependence of the Catalytic Activity of Organoaluminum Compounds and Some of Their Complexes on Their Composition

R. MATEVA, CH. KONSTANTINOV, and V. KABAIVANOV,
Technology of Plastics Department, Higher Institute of Chemical Technology, Sofia 56, Bulgaria

Synopsis

The influence of the acidity of organoaluminum compounds and their complexes on the catalytic activity in polymerization of trioxane has been studied. It is found that the catalytic activity of organoaluminum compounds of the type $R_n\mathrm{ALX}_{3-n}$ depends on n as well as the nature of R or X. Catalytic activity of the complexes also depends on the type of cocatalyst used. The change of electroconductivity in the course of formation of some initiator complexes has been studied and an attempt has been made to determine the relation between conductivity and polymerization activity.

Introduction

Organoaluminum compounds of the type R_nAlX_{3-n}, where R represents an alkyl group and X is a halogen atom, can be cationic catalysts[1] and one should expect them to facilitate polymerization of trioxane (TO). The ability of some of these compounds to cause polymerization of TO was proved during the purification process.[2,3]

Results and Discussion

It was of great interest to study the activity of different types of organoaluminum compounds ($R_3Al_2X_3$, R_2AlX, and R_3Al) as well as to determine the influence of the substituents X and R. A special study of these catalysts was carried out under the same conditions. The results are given in Figure 1. Results from experiments with $TiCl_4$ and $BF_3\cdot O(C_2H_5)_2$ are given for comparison. Data for $(C_2H_5)_2AlCl$, $(C_2H_5)_3Al$, and $(i\text{-}C_4H_9)_3Al$ are missing in Figure 1 because polymers were obtained in too small amounts to be included. It was clear from these studies that the activity of the initiators employed decreases in the following order:[4]

$$BF_3\cdot O(C_2H_5)_2 > TiCl_4 > R_3Al_2X_3 > R_3Al$$

The experimental results (Figs. 1 and 2) indicate that bromine derivatives

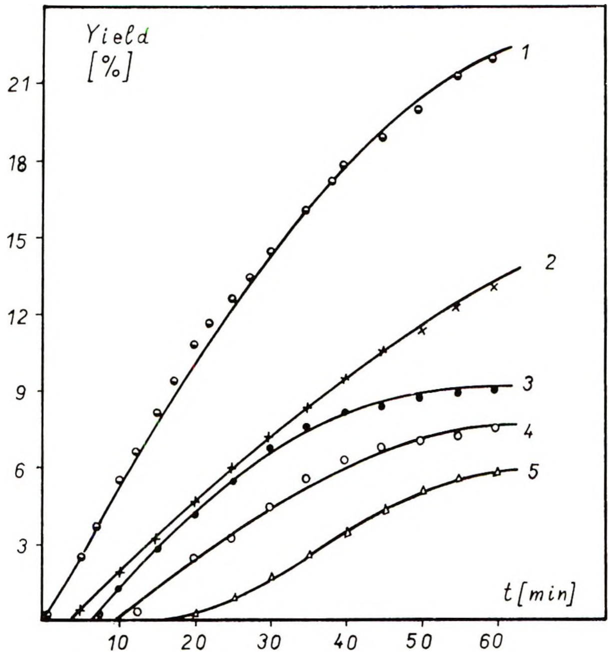

Fig. 1. Dependence of yield on time for polymerization of TO at 65°C, $[H_2O] = 20.9 \times 10^{-3}$ mole/mol TO and with various initiators: (*1*) $BF_3 \cdot O(C_2H_5)_2$, 4×10^{-3} mole/mole TO; (*2*) $TiCl_4$, 8×10^{-3} mole/mole TO; (*3*) $(C_2H_5)_3Al_2Br_3$, 8×10^{-3} mole/-mole TO; (*4*) $(C_2H_5)_3Al_2Br_3$, 8×10^{-3} mole/mole TO; (*5*) $(C_2H_5)_2AlBr$, 8×10^{3} mole/-mole TO.

are more active than the corresponding chlorine compounds and as initiators the halogen derivatives can be arranged as follows:

$$(C_2H_5)_3Al_2Br_3 > (C_2H_5)_3Al_2Cl_3 > (C_2H_5)_2AlBr > (C_2H_5)_2AlCl > (C_2H_5)_3Al$$

According to acidity, the organoaluminum catalysts are arranged in the following order:[5]

$$(C_2H_5)_3Al_2Br_3 > (C_2H_5)_2AlBr > (C_2H_5)_2AlCl > (C_2H_5)_3Al$$

The catalytic activity of the organoaluminium compounds there decreases with decreasing acidity. According to the existing data,[6] the acidity of the catalysts of the type R_nAlX_{3-n} is determined with regard to the Hammett indicators. Imai et al.[6] point out that $(C_2H_5)_2AlCl$ and $(C_2H_5)AlCl_2$ are acid to all Hammett indicators, while $(C_2H_5)_3Al$ and $(i\text{-}C_4H_9)_3Al$ are acid towards the first four of the same indicators but are basic towards anthraquinone.

If the chlorine derivatives of the organoaluminum compounds are arranged in an order dependent on the electronic density of the central atom, calculated according to Pauling's equation:[7]

$$\delta = I - \exp\{-(I/4)(X_a - X_b)^2\}$$

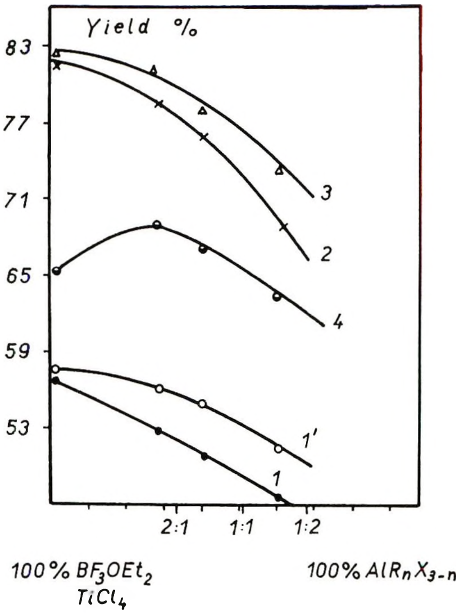

Fig. 2. Dependence of the yield on the molar ratio between the cocatalyst pairs $BF_3 \cdot O(C_2H_5)_2$ + R_nAlX_{3-n} at $[C_0] = 4 \times 10^{-3}$ mole/mole TO and $TiCl_4$ + R_nAlX_{3-n} at $[C_0] = 8 \times 10^{-3}$ mole/mole TO at 75°C at various polymerization times: (*1*) $BF_3 \cdot O(C_2H_5)_2$ + $(C_2H_5)_3Al_2Br_3$, 4 hr; (*1'*) $BF_3 \cdot O(C_2H_5)_2$ + $(C_2H_5)_3Al_2Br_3$, 8 hr; (*2*) $BF_3 \cdot O(C_2H_5)_2$ + $(C_2H_5)_2AlBr$, 4 hr; (*3*) $BF_3 \cdot O(C_2H_5)_2$ + $(C_2H_5)_2AlBr$, 8 hr; (*4*) $TiCl_4$ + $(C_2H_5)_2AlBr$, 8 hr.

where δ represents the electronic density of the central atom and X_a and X_b are the electronegativity of corresponding atoms, the following order will be obtained:

$$\rightarrow \overset{+0.624}{RAlCl_2} > \overset{+0.560}{R_3Al_2Cl_3} > \overset{+0.506}{R_2AlCl} > \overset{+0.388}{R_3Al}$$

If we arrange some of the more commonly employed catalysts in a similar way, we obtain the following dependence:

$$\overset{+0.870}{BF_3.O(C_2H_5)_2} > \overset{+0.660}{TiCl_4} > \overset{+0.560}{(C_2H_5)_3Al_2Cl_3} > \overset{0.506}{(C_2H_5)_2AlCl} > \overset{0.388}{(C_2H_5)_3Al}$$

The catalysts above are arranged in the same descending order according to their catalytic activity when trioxane (TO) is polymerized. As TO is a compound with electron-donor properties, we must expect a transient complex with the rate of decomposition defining the rate of polymerization:

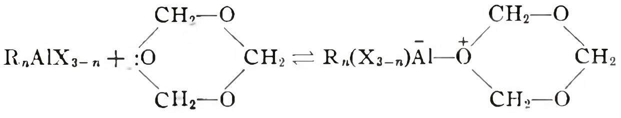

(I)

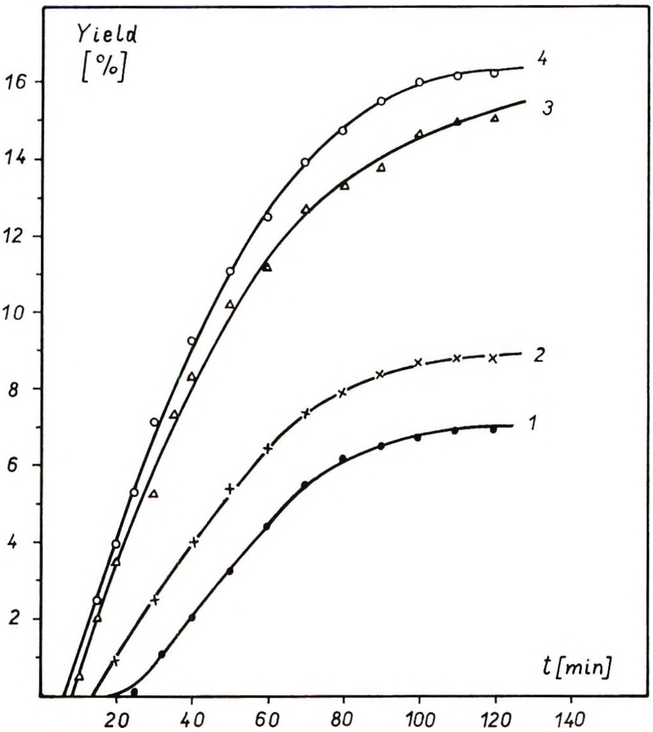

Fig. 3. Dependence of the yield on the polymerization time at 65°C, $[C_0] = 8 \times 10^{-3}$ mole/mole TO, $[H_2O] = 20.9$ mole/mole TO with various catalysts: (*1*) $(C_2H_5)_3Al_2Cl_3$; (*2*) $(C_2H_5)_3Al_2Br_3$; (*3*) $TiCl_4 + (C_2H_5)_3Al_2Cl_3$, 2:1; (*4*) $TiCl_4 + (C_2H_5)_3Al_2Br_3$, 2:1.

The presence of the complex (I) was proved by its isolation at −30°C when TO was mixed with the corresponding R_nAlX_{3-n} in equimolar quantities in petrol.[4]

It was clear from this study that organoaluminum compounds did not give results (at the reaction conditions stated in Fig. 1) which could find a practical application, especially because of the small yields. For this reason a new approach was tried to increase the catalytic activity of these compounds. One of the most promising ways was to select suitable cocatalysts which form active complexes with the organoaluminum compounds. The most frequent cocatalysts were $TiCl_4$, $SnCl_4$, and some other halides of metals of variable valence. It was natural to study the activity of these types of catalytic complexes, as in the most cases the complexes are much more active than the individual compounds.

The first complexes studied were of the type, organoaluminum compound–titanium tetrachloride. The formation of such complexes has been the object of previous studies[8–10] and will not be discussed here. With polymerization in the presence of this type of complex the yield of the polymer is considerably greater than that when only organoaluminum catalysts were used (Figs. 2 and 3). Analogous results are obtained with

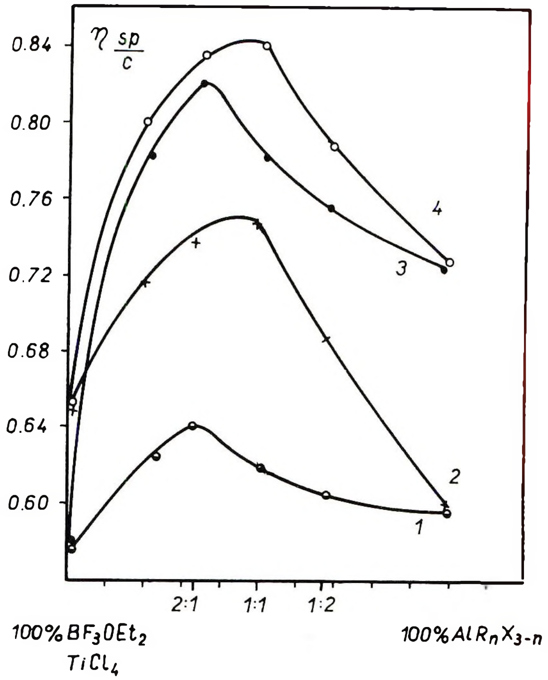

Fig. 4. Dependence of η_{sp}/c of polymer solutions on the molar ratio between cocatalyst pairs $BF_3 \cdot O(C_2H_5)_2$ + R_nAlX_{3-n} at $[C_0] = 4 \times 10^{-3}$ mole/mole TO and $TiCl_4$ + R_n-AlX_{3-n} at $[C_0] = 8 \times 10^{-3}$ mole/mole TO for polymers obtained with various complexes: (*3*) $BF_3 \cdot O(C_2H_5)_2$ + $(C_2H_5)_3Al_2Br_3$; (*4*) $BF_3 \cdot O(C_2H_5)_2$ + $(C_2H_5)_2AlBr$; (*1*) $TiCl_4$ + $(C_2H_5)_3Al_2Br_3$; (*2*) $TiCl_4$ + $(C_2H_5)_2AlBr$. The viscosities were measured at 65°C in *p*-chlorophenol.

regard to molecular weight and the reduced viscosity of the obtained polymers (Fig. 4). At the same time, the results indicate a maximum with respect to reduced viscosity of the polymer solutions (Fig. 4, curves *3*, *4*) is reached at a 2:1 molar ratio of $TiCl_4$ to ethylaluminum halides. The better results obtained with an excess of $TiCl_4$ can be explained on the basis of the results obtained from the study of ethylene polymerization with Ziegler catalysts.[1] It was proved that with increasing molar ratio of $(C_2H_5)_3Al$ to metal halide, the propagation rate and molecular weight of the obtained polymers decreased. It is quite probable that the same processes take place in the polymerization of TO.

From the knowledge that $TiCl_4$ as well as the organoaluminum compounds form complexes with TO, we should logically expect the order of addition to the TO to be of great importance. The components of the catalytic complex can be mixed in advance, after which TO is added; alternatively, portions $TiCl_4$ and then organoaluminum compound, or first organoaluminum compound and then $TiCl_4$ may be added to TO. The study showed that the best results are obtained when the complex components are mixed previously.[4]

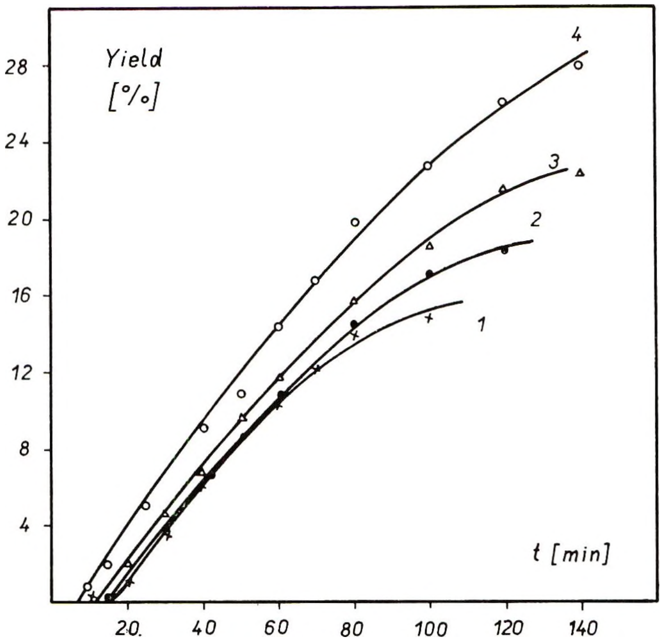

Fig. 5. Dependence of yield on polymerization time at 65°C, $[C_0] = 8 \times 10^{-3}$ mole/mole TO for various complex pairs: (*1*) $TiCl_4 + (C_2H_5)_2AlCl$ (2:1); (*2*) $TiCl_4 + (C_2H_5)_2AlBr$, 2:1; (*3*) $TiCl_4 + (i\text{-}C_4H_9)_3Al$, 2:1; (*4*) $TiCl_4 + (C_2H_5)_3Al$, 2:1.

In this paper we shall not discuss the kinetic studies and the obtained results,[4] but compare only the activities of the catalytic complexes. Taking into account the experimental results (Figs. 3, 5, 6) we may arrange the complexes according to their activity:

$$[TiCl_4 + (C_2H_5)_3Al] > [TiCl_4 + (i\text{-}C_4H_9)_3Al] > [TiCl_4 + (C_2H_5)_2AlX] > [TiCl_4 + (C_2H_5)_3Al_2X_3]$$

$$[TiCl_4 + (C_2H_5)_2AlCl] > [TiCl_4 + (C_2H_5)_2AlBr]$$

$$[TiCl_4 + (C_2H_5)_3AlCl_3] > [TiCl_4 + (C_2H_5)_3Al_2Br_3]$$

The greater activity of the complexes of the type $[TiCl_4 + R_nAlCl_{3-n}]$ compared to that of their bromine analogs can be explained on the basis of the lower electron density of the central atom in the anion which leads to the slower breaking of the growing chain.

Another type of complex studied was the series $BF_3 + R_3Al$. With increasing quantities of BF_3 in the catalytic complex, the rate of polymerization increases abruptly (Fig. 7). Polymers derived from boron trifluoride and organoaluminum compound a ratio of 1:1 (Figs. 4 and 8) have the highest molecular weight and reduced viscosity. The type of the organoaluminum compound is of great importance for the activity of the complex (Figs. 2 and 6):

$$[BF_3 + R_3Al] > [BF_3 + (i - C_4H_9)_3Al] > [BF_3 + R_2AlX] > [BF_3 + R_3Al_2X_3]$$

$$[BF_3 + R_3Al] > [TiCl_4 + R_3Al]$$

Unfortunately we were not able to calculate the charge density of the central atom for the given complexes because the structure of the hydrocarbon radical is not considered when calculating the polarity of the Al–C bond.

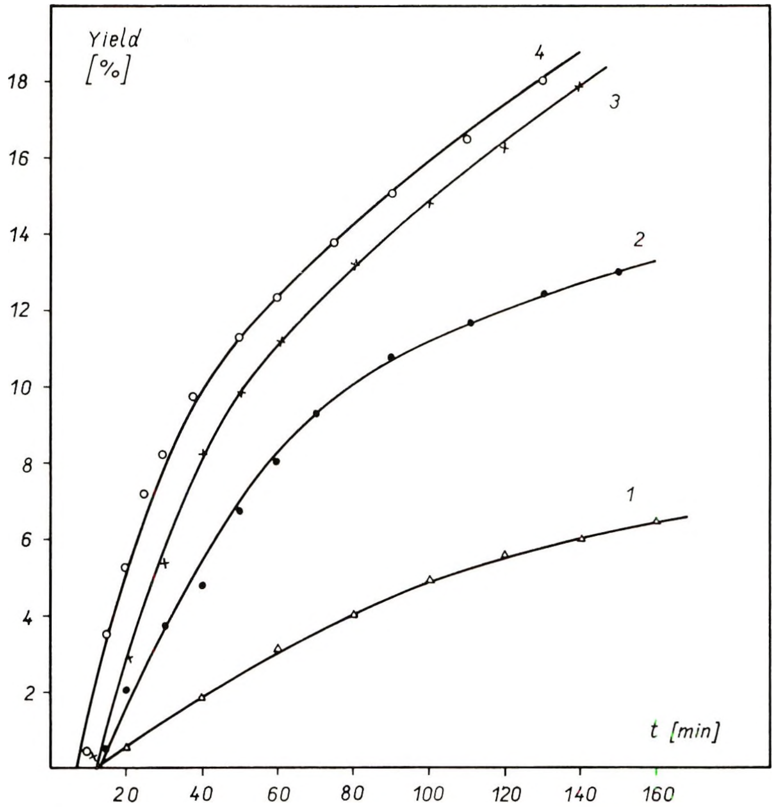

Fig. 6. Dependence of the yield on the polymerization time at 65°C, $[H_2O] = 20.8 \times 10^{-3}$ mole/mole TO, $[C_0] = 8 \times 10^{-3}$ mole/mole TO for various complex pairs: (*1*) $TiCl_4 + (i\text{-}C_4H_9)_3Al$, 1:1; (*2*) $TiCl_4 + (C_2H_5)_3Al$, 1:1; (*3*) $TiCl_4 + (i\text{-}C_4H_9)_3Al$, 2:1; (4) $TiCl_4 + (C_2H_5)_3Al$, 2:1.

On comparing the catalytic activity of the complexes based on BF_3 and $TiCl_4$, one can see the greater activity of the complexes of the type, $BF_3 + R_3Al$ (Figs. 2 and 9). The higher activity of these complexes could be explained on the basis of the considerable density of the cation. As the
+0,629
counterions of the first complex RBF_3 compared to the second complex $RTiCl_4$ is an acid, that one will have a weaker influence on the breaking of

the chain. This is why the probability for the monomer molecules to polymerize to a higher extent is greater.

Therefore, if the character of the monomer is known, a comparatively smaller number of initiators may be selected and studied on the basis of the obtained dependence. This will save much time when a suitable initi-

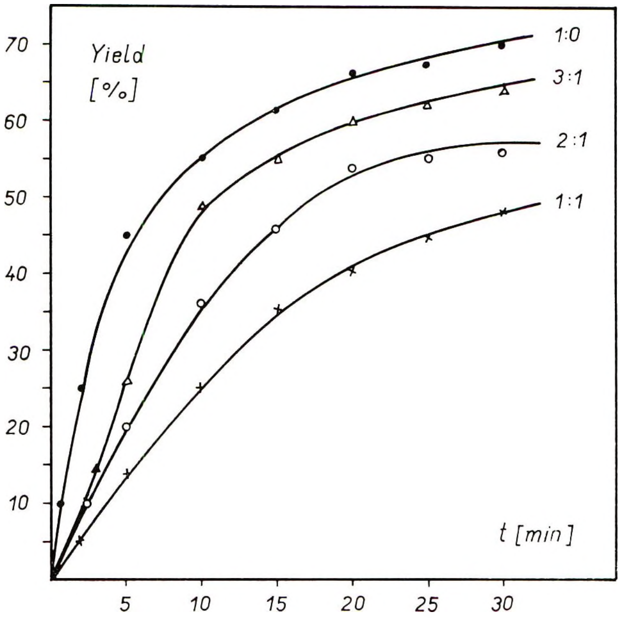

Fig. 7. Dependence of the yield on the polymerization time of TO for the complex $BF_3 \cdot O(C_2H_5)_2 + (C_2H_5)_3Al$ at 65°C, $[C_0] = 2 \times 10^{-3}$ mole/mole TO, $[H_2O] = 1.16 \times 10^{-3}$ mole/mole TO, and the indicated molar ratios between the parts of the complexes.

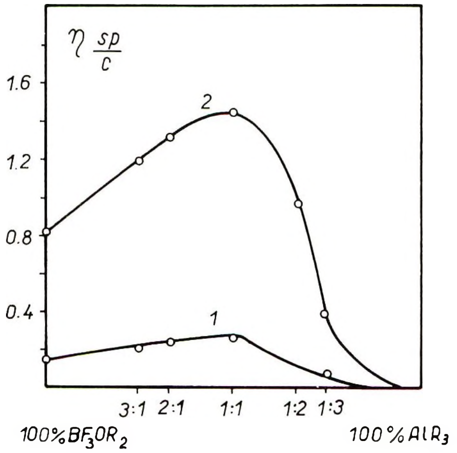

Fig. 8. Dependence of η_{sp}/c of the polymer solutions on the molar ratio between the cocatalysts $BF_3 \cdot O(C_2H_5)_2$ and $(C_2H_5)_3Al$, with polymerization at 65°C, $[C_0] = 2 \times 10^{-3}$ mole/mole TO at various $[H_2O]$: (*1*) 1.16 mole/mole TO; (*2*) 0.28 mole/mole TO.

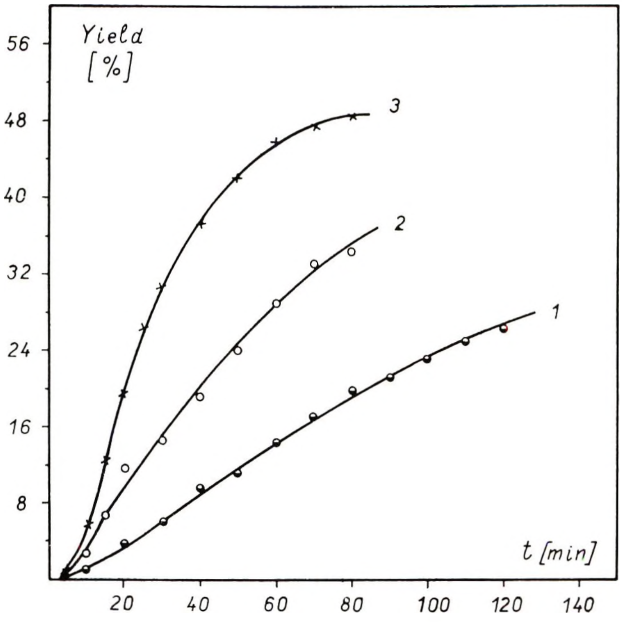

Fig. 9. Dependence of the yield on the polymerization time at 65°C for various complexes and concentrations: (*1*) $TiCl_4 + (C_2H_5)_3Al$, 8×10^{-3} mole/mole TO, 2:1; (*2*) $BF_3 \cdot O(C_2H_5)_2 + (i\text{-}C_4H_9)_3Al$, 4×10^{-3} mole/mole TO, 2:1; (*3*) $BF_3 \cdot O(C_2H_5)_2 + (C_2H_5)_3Al$, 4×10^{-3} mole/mole TO, 2:1.

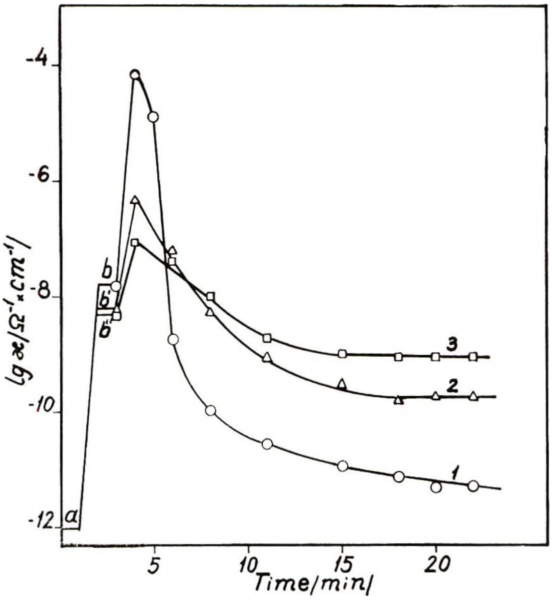

Fig. 10. Electric conductivity of the complexes between BF_3 and (*1*) $(C_2H_5)_3Al$, (*2*) $(C_2H_5)_2AlCl$, and (*3*) $(C_2H_5)AlCl_2$. Temperature, 40°C; component concentration 22.9 $\times 10^{-4}$ mole/mole, in toluene.

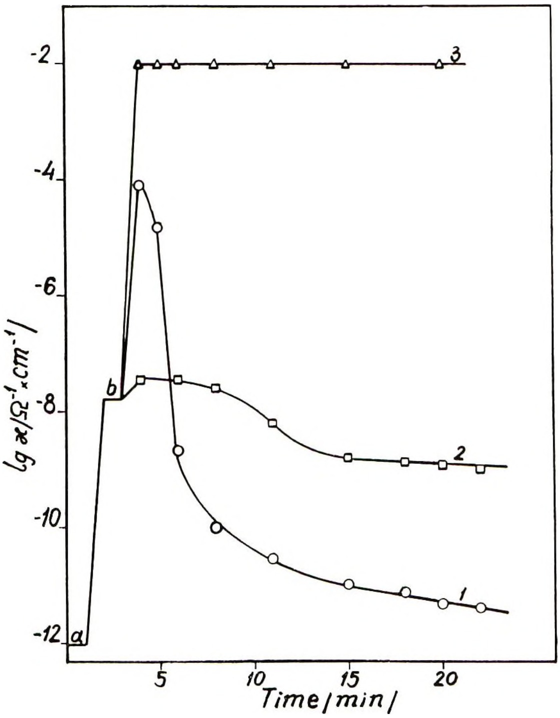

Fig. 11. Electric conductivity at 40°C of the complexes between $(C_2H_5)_3Al$ and (*1*) BF_3, (*2*) $TiCl_4$, and (*3*) $SnCl_4$. Concentration of the components 22.9×10^{-4} mole/mole, in toluene.

ator is selected in each case of polymerization. As the theoretical calculation of the central charge according to the Pauling equation is considerably time-consuming and all the necessary data for such calculations are not always available, our aim was to find a more rapid, more objective, and experimentally easier method for the estimation of the catalytic activity of the different initiators. For this reason we decided to measure electroconductivity of catalytic complexes in the process of their formation and to determine the correlation, if any, between conductivity and polymerization activity of these complexes. A special cell provided with Pt electrodes,[12] which was connected to a megohm-meter, constructed according to a scheme suggested by Švestka and Matyska[13] was used for this purpose.

Measurements of conductivity changes accompanying the formation of different types of catalytic complexes are presented in Figures 10–12. The linear section *a* in these figures shows the conductivity of the medium in equimolar ratio (carefully purified toluene). At the end of the linear section *a* the organoaluminum compound is injected. The conductivity increases abruptly, its final value depending on the number of halogen atoms (Fig. 10) and on the kind of alkyl groups in the organoaluminum com-

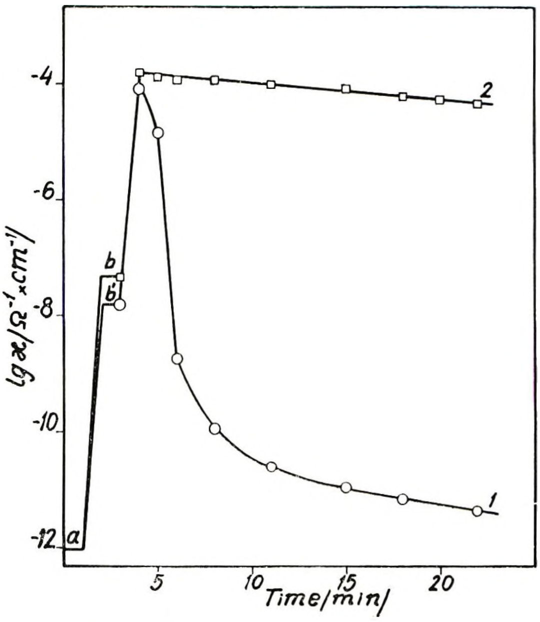

Fig. 12. Electric conductivity at 40°C of the complexes between BF_3 and (*1*) $(C_2H_5)_3$-Al, and (*2*) $(i\text{-}C_4H_9)_3Al$. Concentration of the components 22.9 × 10^{-4} mole/mole in toluene.

pounds (Fig. 12). The chlorine derivatives of $(C_2H_5)_3Al$ can be arranged according to their conductivity:

$$(C_2H_5)_3Al > (C_2H_5)_2AlCl > (C_2H_5)AlCl_2$$

When the conductivity becomes constant (at the end of section *b*), $BF_3 \cdot O(C_2H_5)_2$ is injected. As a result of the addition of the second component the conductivity again increases abruptly at first and then, due to the fact that an insoluble complex is produced, it drops abruptly and approaches the conductivity of the solvent (toluene) (Figs. 10 and 12). If the complexes from Figure 8 are arranged in order of decreasing conductivity, a series is obtained which is identical to the series of the same complexes with regard to their polymerization activity towards TO.

The data in Figure 12 of highest conductivity show a deviation from the corresponding data regarding polymerization activity, however, it is probable that the rate of complex formation is important. From the same figures we can draw a conclusion about this rate on the basis of the slope of the curves after the maximum (Figs. 10–12). If it is assumed that the slope is decisive for the activity of the complexes, then the results from the study on the complex conductivity are completely identical with experimental orders of the same complexes with respect to polymerization activity towards TO.

In Figure 11 the most interesting and difficult to discuss is the complex between $(C_2H_5)_3Al$ and $SnCl_4$. Its conductivity remains constant after reaching a maximum. This is probably due to the solubility of the complex or to the excessively slow rate of its formation. The same complex did not cause polymerization of TO.

There is good correlation according to the data in Figures 10–12 only between the final complex electroconductivity (15 min after the complex components have been mixed) and polymerization activity towards TO. The poorer the final conductivity of the complex, the higher the polymerization activity towards TO.

This study is very interesting and promising but it is still difficult to draw conclusions. We consider that further study will provide the necessary experimental data and will allow us to draw corresponding conclusions as well as to explain some anomalies.

Experimental

TO was purified as described in the previous papers.[7,8] The presence of moisture was checked by coulometric titration with Fisher reagent by the method of Slovàk and Přybyl.[14]

The polymerization of TO was studied dilatometrically under a nitrogen atmosphere. Liquid paraffin, well purified and dried, was employed with the dilatometers as reference. The reduced viscosity of polymer solutions was determined at 90°C in *p*-chlorophenol or a 3:1 mixture of tetrachlorethane and phenol.[15]

Toluene used as a medium for the conductivity measurement of the catalytic complexes was purified from unsaturated compounds and thiophene and was subsequently rectified with potassium–sodium alloy in the presence of anthracene.

Boron trifluoride etherate, a product of The British Drug Houses (England), was distilled *in vacuo* at 123–133°C immediately before use.

Most of organoaluminum compounds were products of Fluka (Switzerland) and were used without additional purifications.

Titanium tetrachloride, from Schuchard (Germany) and stannic tetrachloride, from E. Merck AG (Germany) were distilled before use.

References

1. Belg. Pat. 60, 9208 (Apr. 16, 1962); *Chem. Abstr.*, **58**, 2516 (1963).

2. V. Kabaivanov, R. Mateva, and M. Natov, Avt. sv., Pat. No 11367 cl. 220-7/01 (23/8/65).

3. V. Kabaivanov, R. Mateva, and N. Vanev, *C. R. Acad. Bulg. Sci.*, **22**, 1417 (1969).

4. R. Mateva, dissertation, Higher Institute of Chemical Technology, Sofia, Bulgaria, 1967.

5. U. A. Sangalov, K. S. Mineker, and G. A. Rasuvaev, *Vysokomol. Soedin.*, **7**, 1323 (1967).

6. H. Imai, T. Saegusa, and J. Furukawa, *Makromol. Chem.*, **81**, 92 (1965).

7. J. Furukawa, *Khim. Tekhnol. Polimerov*, **1963**, No. 5, 83.

8. V. Kabaivanov, R. Mateva, and M. Natov, *C. R. Acad. Bulg. Sci.*, **18**, 821 (1969).

9. V. Kabaivanov, R. Mateva, and M. Natov, *Makromol. Chem.*, **99**, 226 (1966).

10. V. Kabaivanov, R. Mateva, and M. Natov, *Makromol. Chem.*, **103,** 183 (1967).
11. E. A. Fushman, V. I. Tsvetkova, and N. M. Chirkov, *Izv. Akzd. Nauk SSSR*, **1965,** 2075.
12. G. A. Chuhadyan, et al., *Armianski Khim. Zh.*, **19,** 840 (1966).
13. M. Švestka and B. Matyska, *Chem. Listy*, **61,** 245 (1967).
14. M. Přybyl and Z. Slovàk, *Mikrochim. Acta*, **1964,** 1097.
15. M. Majer, *Makromol. Chem.* **86,** 253 (1965).

Received February 17, 1970
Revised May 8, 1970

JOURNAL OF POLYMER SCIENCE: PART A-1 VOL. 8, 3577-3589 (1970)

Gel Permeation Chromatography and Cellulose. II. Application of Universal Calibration*

L. SEGAL, J. D. TIMPA, and J. I. WADSWORTH, *Southern Regional Research Laboratory, Southern Utilization Research and Development Division, Agricultural Research Service, U. S. Department of Agriculture, New Orleans, Louisiana 70119*

Synopsis

In previously reported work concerning the chain-length distributions obtained by gel permeation chromatography (GPC) in celluloses, degrees of polymerization (DP) of unusually high magnitude were reported. Later work in GPC has shown that the concept of relating extended nolecular chain length of different polymers to elution volume for obtaining molecular weight is not theoretically sound. Correlation of molecular hydrodynamic volume (indicated by the product of intrinsic viscosity and molecular weight) with elution volume has been found to place polymers of vastly different natures on a single curve, such is now designated universal calibration. Application of universal calibration to the determination of DP distributions in celluloses required a different method of converting counts to DP. This new procedure is described in detail. Weight-average DP's given by the procedure for samples of cellulose I, II, III, and IV were 5190, 4520, 4795, and 3390, respectively. These are decreases of 74–75% from the results obtained by the extended-chain procedure. The results compare favorably with the viscosity-DP's of the samples. Number-average DP's were 1580, 1040, 1140, and 490 for the four samples, respectively, these being decreases of 87–93% from the values formerly reported. The polymolecularity ratios for the samples are now unusually large, being 3.4, 4.7, 4.2, and 7.1, respectively.

Introduction

The application of gel permeation chromatography (GPC) to the characterization of celluloses has already been described in earlier publications.[1,2] In these reports, the elution volumes of the sample fractions expressed in counts were converted to degree of polymerization (DP) by means of extended chain-length calibration. Shortly after these reports were published, a new conversion procedure appeared in the literature. Based on coil size of the solute molecule, this procedure formed the basis for a universal calibration technique for all polymers. Benoit and co-workers[3–5] established a relationship that is valid for any polymer molecule, regardless of its chemical nature and morphological structure. Benoit tested nine polymers of vastly different sorts and markedly different structures and found that a

---

* Presented at the 158th National Meeting, American Chemical Society, New York, New York, September 7–12, 1969.

plot of the logarithm of $[\eta]M$ versus elution volume gave a single curve for all polymers (the product $[\eta]M$ is designated coil size; $[\eta]$ is intrinsic viscosity, and M is molecular weight). This was confirmed by others.[6,7] A significant and important addition to these findings is the work of Grubisic and co-workers,[8] who found that the relationship holds also for a rigid, rodlike molecule as well as for a flexible, coiled one.

In the earlier procedure, DP was arrived at through a series of calculations and the use of the calibration curve relating counts to extended length of the molecule expressed in Angstrom units. Measurements of the height of the chromatogram at each count were then used in conjunction with data from the calibration curve to obtain the DP's for the cellulose fractions (DP_i) and the weight- and number-average DP's ($\overline{DP}_w$, $\overline{DP}_n$). An example of these calculations is given by Harmon.[9] The DP's of 16,000–22,000 which were obtained by the extended chain-length calibration for the cellulose trinitrate samples were very much higher than the values (3000–5000) obtained with a conventional method. However, the high values seemed to be supported by some reports in the literature giving similar high values for various celluloses where conventional methods were employed.

The initial procedure for handling GPC data has become suspect from two important standpoints. One criticism is directed at the use of the characterized polystyrenes as standards for other polymers; the other criticism is directed at the use of extended molecular chain-length as the calibration parameter. The postulate relating elution volume to extended chain length does not, however, require that chains be extended in solution, only that the polymers being compared be similar in chain stiffness—which, of course, is not the case here for polystyrene and cellulose nitrate.

Nakajima[10] was one of the first to point out the desirability of using for GPC standards fractionated material of the same polymer as that being studied. Unfortunately, for cellulose work, standards consisting of narrow-distribution, well-characterized cellulose trinitrates were not and are not readily available.

The postulate of extended molecular chains in solution is contrary to what is known, i.e., (1) that the polymer molecule in solution is coiled, and (2) that the effective size of a polymer coil in dilute solution is dependent on the nature of the polymer and the solute–solvent interactions.[11] Attempts have been made by some workers[12,13] to relate elution volumes to hydrodynamic radii and other parameters, but these were not entirely successful in solving the problem because of the approaches used.

Benoit's approach is a breakthrough for GPC studies of cellulose. The need for narrow-distribution, well-characterized cellulose standards for calibration is eliminated; the readily available polystyrene standards can be used. That the cellulose trinitrate chain becomes rigid and extended at a DP of about 300 is no longer a problem—"the calibration is independent of the shape of the molecules and is valid for elongated particles as well."[5] This paper describes the manner in which Benoit's calibration technique was applied in an investigation of the chain-length distributions in various celluloses and presents the results which were obtained.

Experimental

The GPC instrumentation and experimental procedure were the same as those used earlier[1] with three modifications: First, an analog-to-digital converter was incorporated into the system to provide a punched-tape readout of GPC data. The punched tape was used for direct processing of data by computer; this involved all of the calculations for obtaining $\overline{\text{DP}}_w$, $\overline{\text{DP}}_n$, polymolecularity ratios ($\overline{\text{DP}}_w/\overline{\text{DP}}_n$), and plots of the normalized, differential molecular-weight distribution curves. Second, instead of measuring the height of the curve above the baseline at the count as shown in *A* of Figure 1, the area under the curve from count to count, centered about the half-count, as shown in *B* of Figure 1, was measured; these area measurements were performed by computer using the punched-tape data. The significance of the change to area measurement will be explained later. Third, the sample injection time, i.e., the period of time that the sample loop is held in the solvent stream, was changed from 120 sec (approx. 0.4 count) to approximately 10 min (2 counts). Calculations based on the assumption of laminar, incompressible, steady-state flow of a Newtonian fluid, neglecting end effects, indicated that about 0.5 ml of solution could still be held in the sample loop after 120 sec. This would amount to 25% of the dissolved polymer; measurements of the areas under the chromatograms obtained by using 120-sec and 10-min (approximate) injection times verified this percentage. Because the procedure for obtaining concentration of polymer in the eluted solutions requires complete transfer of dissolved sample to the solvent stream, the shorter injection time was abandoned. An injection time longer than 2 counts or 10 min was considered unnecessary.

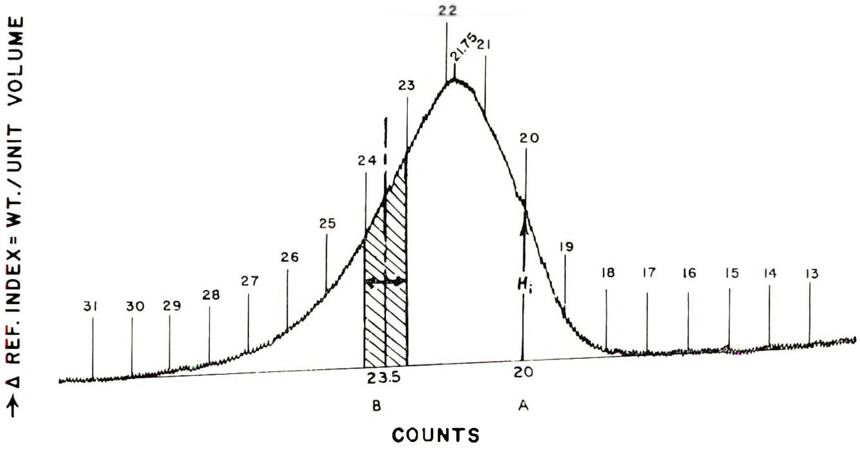

Fig. 1. Measurements made on chromatogram: (*A*) height of curve at the count, for the usual procedure of calculating DP's; (*B*) area under the curve centered on the half-count for the present method of calculating DP's.

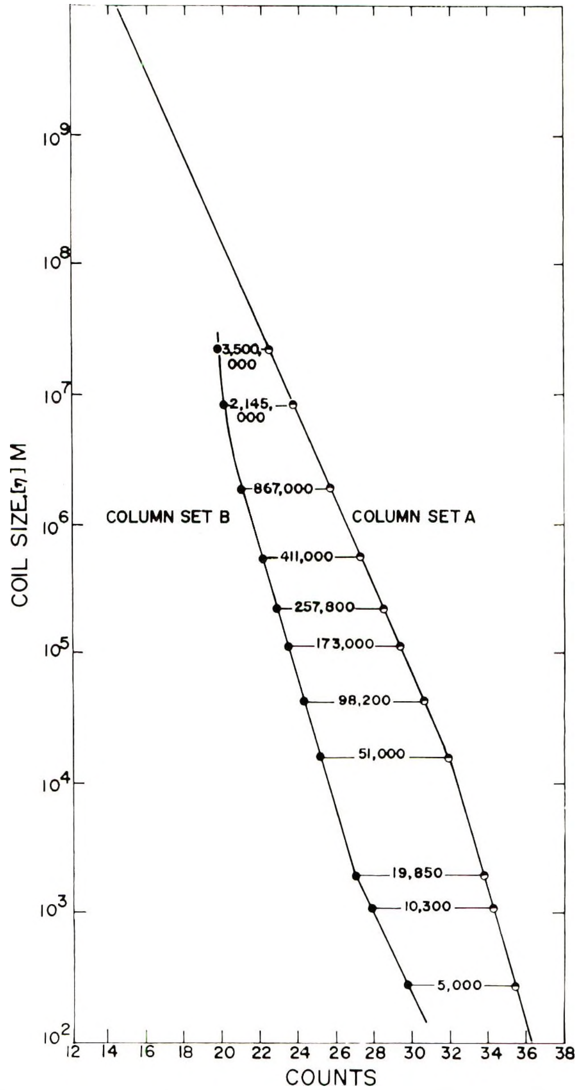

Fig. 2. Calibration curves for column sets used in the gel permeation chromatograph: (set A) four columns of 10^7, 1.5×10^6, 10^5, and 3×10^4 Å permeability limits; (set B) four columns of 1.5×10^5, 10^4, 10^3, and 5×10^2 Å permeability limits. Numbers identifying the standards are weight-average molecular weights.

The intrinsic viscosities of the polystyrene standards in tetrahydrofuran (THF) were obtained at 25°C by means of calibrated Cannon-Ubbelohde dilution viscometers and successive dilution; no shear dependence was noted. Because of the high vapor pressure of THF, the solutions were forced into the bulbs by means of cylinder nitrogen and a system of valves designed to reduce and control the nitrogen pressure. The usual method of drawing in solution by means of vacuum caused considerable changes in solution concentration because of evaporation of the solvent.

The products (coil size) of the intrinsic viscosities and the weight-average molecular weights of the polystyrene standards were plotted versus half-counts on semilog graph paper to give the calibration curves shown in Figure 2. The weight-average molecular weights furnished with the standards and the intrinsic viscosities obtained experimentally were inserted into the Mark-Houwink equation to obtain the constants K and a for the purpose of checking the precision and accuracy of the experimental procedure. As the values obtained, $K = 1.36 \times 10^{-2}$ and $a = 0.71$, are in good agreement with those of Benoit,[4] $K = 1.41 \times 10^{-2}$ and $a = 0.70$, and with the values $K = 1.28 \times 10^{-2}$ and $a = 0.72$ calculated from the viscometric data of Schulz and Baumann,[14] confidence could be placed in the coil size data used in the calibration curve. It is noteworthy that the experimental constants determined here are in excellent agreement with the averages of the literature values, $K = 1.34 \times 10^{-2}$ and $a = 0.71$.

The celluloses were the four polymorphic forms, celluloses I, II, III, and IV, which were the subjects of an earlier report.[1] Details of the preparation of these materials are given in that report. Because of the high DP's of these samples, only the A set of GPC columns was used in the present study.

Average degrees of polymerization of the four celluloses were determined viscometrically ($\overline{\mathrm{DP}}_v$) in cadmium ethylenediamine hydroxide (cadoxen) solutions. The cadoxen was prepared by Henley's[15] procedure. The viscosities were measured at 25°C in calibrated Cannon-Ubbelohde four-bulb dilution shear-gradient viscometers at four concentrations. The reduced viscosities, η_{sp}/c, taken at $\bar{G} = 500 \text{ sec}^{-1}$, were extrapolated to zero concentration for obtaining intrinsic viscosity, $[\eta]$. The DP's calculated according to Brown and Wikstrom's[16] relationship were as follows: cellulose I, 4990; cellulose II, 3760; cellulose III, 3780; and cellulose IV, 2330. Because of interskein variations these values are somewhat different from those given earlier.[1]

The four celluloses were nitrated according to the procedure used by Newman and co-workers.[17] The alcohol-wet nitrates, however, were kept in alcohol in screw-cap bottles stored in the refrigerator until needed. Nitrogen contents determined by the semimicro Kjeldahl method of Timell and Purves[18] varied from 13.55 to 13.85%; variation in the degree of substitution within this range has been shown to have negligible effect on GPC data.[2] Aliquant portions of the nitrated celluloses were dried as needed in a vacuum oven (15 mm Hg) for 1 hr at 50–55°C, and 0.0250-g quantities for preparing $^1/_8$% solutions in THF (24.0 ml) were weighed out in a stainless-steel weighing boat. The fiber mats, while still in the boat, were teased apart with dissecting needles in order to put the sample into the optimal form for pinch-wise addition to the solvent.

Dry nitrated cellulose becomes charged quite easily with static electricity, and this interferes very greatly with quantitative transfer of the sample. However, this problem was solved by slowly passing a high-frequency coil of the Tesla type (as used for detecting leaks in vacuum systems) close to the weighing boat. The static-free sample was added to the solvent pinch-wise by means of tweezers with stirring (magnetic stirring bar; 4-oz, brown-glass, screw-cap bottle). The stirring bar was then lifted out, rinsed with a measured volume of THF, 1.0 ml, after which dissolution was completed by placing the capped bottle in a shaking apparatus for 1 hr. All liquid measurements were made with previously dried hypodermic syringes of appropriate volumes.

The intrinsic viscosities of the eluted fractions of the nitrated celluloses were measured by means of special Cannon-Ubbelohde semimicro shear-gradient viscometers. These viscometers have three measuring bulbs and need only 4 ml of solution; they were required because of the limited amount of eluate (5 ml). It was established very quickly that the usual procedure of diluting the initial solution in order to obtain the necessary number of concentrations for extrapolation to zero concentration could not be used with the eluates because of their low concentrations. The intrinsic viscosities were, therefore, calculated by means of the Schulz-Blaschke equation.[19] The Schulz-Blaschke constant for the cellulose trinitrate–tetrahydrofuran system had to be determined because it is not to be found in the literature. From the viscosity data obtained from 10 samples of nitrated cellulose, ranging from 7.3 to 47.6 dl/g, an average value of 0.35 was established for this constant. As the relative viscosities at zero shear gradient are used in the calculations, the intrinsic viscosities obtained by means of the Schulz-Blaschke equation are also at zero shear gradient.

For calculating intrinsic viscosity, one must have the concentration of the solution. The eluates, however, are too dilute to permit accurate, reproducible weighings of the residues left by evaporation to dryness of measured volumes of the solutions. Other means for determining concentration directly could not be used for the same reason. This problem was resolved by using the half-count area measurements mentioned earlier. With the area under the chromatogram directly proportional to the weight percent of dissolved polymer[20] and the amount of sample injected into the sample loop held constant (2.08 mg) in all runs, the concentration of sample in each eluate was calculated by computer from the punched-tape data.

Because of the low eluate concentrations, it was found that reliable measurement of the intrinsic viscosities of the fractionated solutions could be made on only those four eluates which lay about the peak of the chromatogram. A plot of the logarithm of the intrinsic viscosities of the four eluates versus the logarithm of their respective half-counts produced a straight line, and from this the intrinsic viscosities of the more dilute eluates could be estimated by extrapolation. Calculation of intrinsic viscosities from the measured flow-times, calculation of the least-squares regression of the viscosities versus half-counts, and extrapolation to obtain the viscosities of the more dilute eluates were carried out by computer.

Calculation of the average degrees of polymerization for the nitrated celluloses was carried out by means of the scheme[21] exemplified in the equations and arbitrary fraction number, weight, and DP data shown in Table I.

TABLE I
Calculation of Weight- and Number-Average Degrees of Polymerization from Fractionation Data[a,b]

Fraction	Weight W in polymer, g	DP	W/DP	$W \times$ DP
1	10	500	0.0200	5,000
2	20	1,000	0.0200	20,000
3	25	2,000	0.0125	50,000
4	25	2,500	0.0100	62,500
5	10	3,000	0.0033	30,000
6	10	4,000	0.0025	40,000
	100		0.0683	207,500

[a] The data in columns 1, 2, and 3 are strictly arbitrary.

[b] $$\overline{\mathrm{DP}}_w = \frac{\Sigma(W \times \mathrm{DP})}{\Sigma W} = \frac{207,500}{100} = 2075$$

$$\overline{\mathrm{DP}}_n = \frac{\Sigma W}{\Sigma(W/\mathrm{DP})} = \frac{100}{0.0683} = 1464$$

$$\overline{\mathrm{DP}}_w/\overline{\mathrm{DP}}_n = 1.42$$

The required weight and DP data of columns 2 and 3 are obtained from the chromatogram. The weight of polymer (in grams) in the eluate comes directly from the area measurement about the half-count as described earlier. The DP is calculated from the coil size in the following manner. The calibration chart is entered at the pertinent half-count, and the corresponding coil size is read off on the ordinate. The intrinsic viscosity of the eluate at the pertinent half-count, measured separately, is then divided into the coil size to give the molecular weight for the fraction. Degree of polymerization is then the quotient of molecular weight divided by the proper monomer unit weight of the nitrated anhydroglucose unit (Table II).

TABLE II
Nitrogen Content and Related Parameters of the Nitrated Anhydroglucose Unit

Nitrogen, %	Monomer unit weight	Degree of substitution
13.50	286.4	2.76
13.60	288.0	2.80
13.70	289.6	2.83
13.80	291.3	2.87
13.90	293.0	2.91
14.14[a]	297.1	3.00

[a] Completely substituted ester.

All of the calculations required were done by computer. Programs are available on request for the calculonatis mentioned in the preceding text.

Results and Discussion

The previous calibration procedure employing extended molecular chainlength is superficially simple, in that the only data involved are the calibration curve, the linear measurements taken from the chromatogram, and the *Q* factor (molecular weight per unit Angstrom length) which usually can be calculated from appropriate data in the literature. The present procedure is more complex: but it is based on more acceptable concepts and gives more acceptable results. Automation of data acquisition through the analog-to-digital converter as well as speedy data handling and processing by computer of the greater number of computations that are now involved balance out the added time introduced by the viscosity measurement.

Results obtained by the new procedure are illustrated in Figures 3 and 4, where data for several portions of the cellulose II sample are compiled. Each linear plot of intrinsic viscosity versus count in Figure 3 has its corresponding normalized chromatogram in Figure 4. In the present experi-

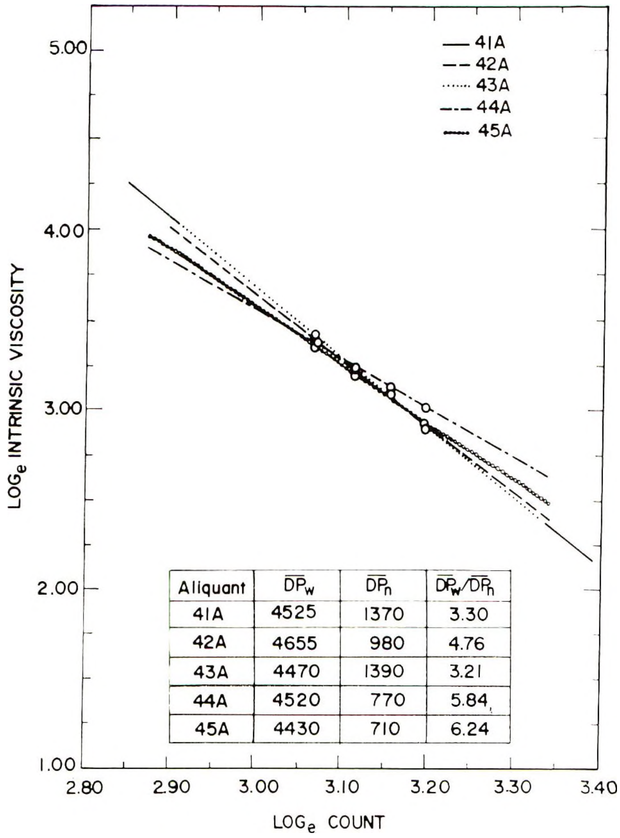

Aliquant	$\overline{DP}_w$	$\overline{DP}_n$	$\overline{DP}_w/\overline{DP}_n$
41A	4525	1370	3.30
42A	4655	980	4.76
43A	4470	1390	3.21
44A	4520	770	5.84
45A	4430	710	6.24

Fig. 3. Relationship between intrinsic viscosity and count for portions of the nitrated cellulose II sample: (——) Portion 41A, (- - -) Portion 42A, (· · ·) Portion 43A, (- · -) Portion 44A, (oooo) Portion 45A.

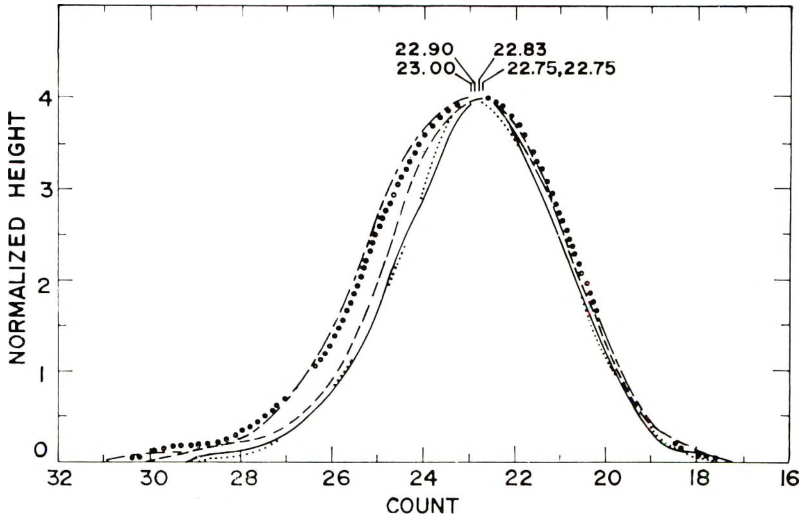

Fig. 4. Normalized chromatograms for portions of the cellulose II sample: (——) Portion 41A, (- -) Portion 42A, (. . .) Portion 43A, (– • –) Portion 44A, (oooo) Portion 45A. Heights at the peaks of the chromatograms set arbitrarily to 4.

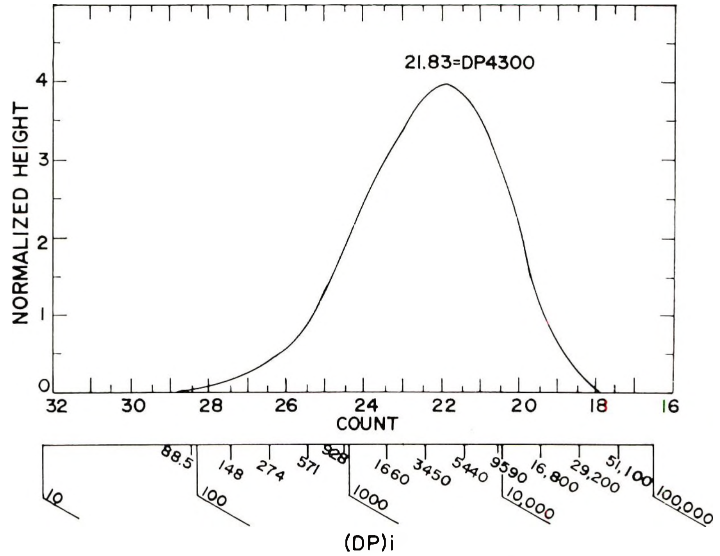

Fig. 5. Normalized chromatogram for a portion of the cellulose I sample. Scale for DP added to show the range of the molecular chain-length in the sample.

ments, four to six aliquants were taken from each sample, and the results averaged. The normalized chromatogram is useful "as is" for comparative purposes, but for computations of DP, data from the actual chromatogram must be used.

The slopes of the plots of viscosity versus count (Fig. 3) are related to the DP range of the chromatograms. Thus in Figure 4 the chromatogram for aliquant 44A is furthest to the left, in the direction of lower DP, and the viscosity-count plot has the lowest slope. The chromatogram for aliquant 41A is furthest to the right, towards higher DP, and the viscosity-count plot has the steepest slope. The slopes of the plots and the chromatograms for the rest of the aliquants, except one, lie between in the order indicated, that is, slope increasing as the position of the chromatogram moves toward higher DP. This relationship between the position of the chromatogram and the slope of the viscosity–count plot closely reflects the parameter being measured at each count. Because of the shifts in chain-length distribution resulting from as yet undetermined factors, changes occur in viscosity of the particular fraction concerned, caused by differences in the DP of that fraction.

Conversion of counts to DP in the chromatogram is not so straightforward as before; there are still two parameters, now coil size and count, but only count is single-ended. Coil size is a product, $[\eta]M$, and therefore intrinsic viscosity at the count must be measured before molecular weight, and hence DP can be established. A fixed DP scale cannot be simply substituted once for count and used thereafter for all samples. The DP's arrived at in the present calculations are tabulated in the computer print-out so that it is a simple matter to substitute these values for the appropriate half counts (Fig. 5).

From the data in Table III it is obvious that the present results are markedly different from those obtained by the extended-chain calibration. The $\overline{\mathrm{DP}}_w$'s given in Table III are now in the order of magnitude of those usually reported for celluloses. It is noteworthy that $\overline{\mathrm{DP}}_w$'s by coil size are 74–75% less than those calculated by extended chain-length calibration. Meyerhoff's[22] data obtained from fractionated trinitrate samples led to an earlier postulate[1] that if his correlations were correct, then the GPC trinitrate DP's based on polystyrene standards and extended chain lengths (Table III) should be reduced by some 65%. This earlier postulate is in reasonably good agreement with the present findings.

It is well-known that the $\overline{\mathrm{DP}}_w$ of a polymer is somewhat greater than its $\overline{\mathrm{DP}}_v$, and in the present instance, the $\overline{\mathrm{DP}}_w$ obtained from the GPC data (nitrated sample dissolved in THF, calibration by coil size) is greater than the $\overline{\mathrm{DP}}_v$ obtained for the original untreated cotton dissolved in cadoxen. This latter situation is consistent with the findings of others[23,24] that viscosity measurements of cellulose trinitrates in organic solvents often give higher DP values than do those of the initial cellulose in the alkaline cellulose solvents. Agster[23] attributes the observed difference to certain ester-type bonds in cellulose which are alkali-sensitive, while Ellefsen[24] considers it due to some deviations in structure (e.g., carbonyl groups) which lead to degradative effects during the viscosity measurement. The possible effects of the highly alkaline solvent, cadoxen, on cellulose during viscosity measurements has already been discussed.[25] Creation of alkali-sensitive linkages or structural deviations seems to be suggested in the present data. Thus, there is a 3.9% difference between $\overline{\mathrm{DP}}_w$ and $\overline{\mathrm{DP}}_v$ for the cellulose I

TABLE III
Comparison of Results Obtained According to Calibration Procedure Employed

Nitrated sample	Average Degree of Polymerization					Ratio $\overline{DP}_w/\overline{DP}_n$	
	Viscosity-average DP using cadoxen	Weight-average DP		Number-average DP			
		Using coil size	Using extended chain-length[a]	Using coil size	Using extended chain-length[a]	Using coil size	Using extended chain-length[a]
Cellulose I	4990	5190	20,940	1580	12,570	3.35	1.67
Cellulose II	3760	4520	18,200	1040	9,050	4.67	2.01
Cellulose III	3780	4795	18,930	1140	9,780	4.21	1.94
Cellulose IV	2330	3390	13,180	490	6,680	7.07	1.97

[a] Data of Segal.[1]

sample, and the difference increases for the celluloses II, III, and IV, amounting to 16.8, 21.1, and 31.2%, respectively. The order of increase in the differences is in accord with the direction suggested by the conditions for preparation of these celluloses. Thus, all of three of the latter samples were exposed to alkaline reagents which could cause actual or potential degradation, but in addition an elevated temperature (150°C) was included in the case of the cellulose IV. Actual degradation is, of course, indicated by the decrease in the DP's themselves.

Also in Table III, one can see that very marked differentiation of the cellulose samples in terms of their polymolecularities, given by the ratio $\overline{\mathrm{DP}}_w/\overline{\mathrm{DP}}_n$, is apparent in the present data, much more so than in the earlier data. The most degraded sample, cellulose IV, did not, according to the previous data, differ in polymolecularity from the less-degraded cellulose II and III samples, yet this could have been expected because of the treatments employed. Such a difference is clearly denoted by the present data. The present values for the polymolecularities are considerably greater than the previous ones and may be greater than the actual case. This would be in accord with recent findings with polypropylene and polystyrene. Alliet[26] and Crouzet and co-workers[27] reported that GPC results consistently indicated larger distribution ratios or greater polymolecularity than the conventional methods, while Boni and Sliemers[28] found that $\overline{M}_n$ by GPC was lower than that determined by osmometry.

In the present data, wide variations have been noted in $\overline{\mathrm{DP}}_n$ when the related $\overline{\mathrm{DP}}_w$'s are in good agreement. An example of this is to be seen in the data tabulated in the body of Figure 3. The variation may be an effect of the long injection time being used, apparently from an exaggerated tailing of the sample plug as it passes through the system. The long injection time may also be the cause of an effect to be noted in the compiled chromatograms of Figure 4. Between lowest count and peak position (high-DP sector) the legs of the curves are almost coincident, but the legs of the curves between peak position and highest count (low-DP sector) are separated.

A potential error that could be of serious magnitude is that attributable to zone broadening or peak spreading arising from axial dispersion in the columns. Corrections for this effect were not applied to the present chromatograms because they were not considered necessary in view of the broad distributions of the samples. Tung[29,30] has indicated that a correction for peak spreading is negligible for a broad-distribution polymer. Pierce and Armonas[31] also have shown this to be true. Huang and Jenkins[32] applied zone-broadening corrections to chromatograms obtained from cellulose samples, and their results confirm the earlier conclusions of Tung. In the present work, zone-broadening corrections led to anomalous results.

References

1. L. Segal, *J. Polym. Sci. B*, **4**, 1011 (1966); in *Analytical Gel Permeation Chromatography* (*J. Polym. Sci. C*, **21**), J. F. Johnson and R. S. Porter, Eds., Interscience, New York, 1968, p. 267.

2. L. Segal, J. D. Timpa, and J. I. Wadsworth, *J. Polym. Sci. A-1*, **8**, 25 (1970).

3. H. Benoit, Z. Grubisic, P. Rempp, D. Decker, and J.-G. Ziliox, paper presented at the Third International Symposium on GPC, Geneva, Switzerland, May 19–20, 1966.

4. H. Benoit, Z. Grubisic, P. Rempp, D. Decker, and J.-G. Ziliox, *J. Chim. Phys.*, **63**, 1507 (1966).

5. Z. Grubisic, P. Rempp, and H. Benoit, *J. Polym. Sci. B*, **5**, 753 (1967).

6. L. Wild and R. Guliana, *J. Polym. Sci. A-2*, **5**, 1087 (1967).

7. M. J. R. Cantow, R. S. Porter, and J. F. Johnson, *J. Polym. Sci. A-1*, **5**, 987 (1967).

8. Z. Grubisic, L. Reibel, and G. Spach, *C. R. Acad. Sci.* (Paris), **C246**, 1690 (1967).

9. D. J. Harmon, in *International Symposium on Polymer Characterization* (*J. Polym. Sci. C*. **8**), K. A. Boni and F. A. Sliemers, Eds., Interscience, New York, 1965, p. 243.

10. N. Nakajima, *J. Polym. Sci. A-2*, **5**, 101 (1966).

11. P. J. Flory, *Principles of Polymer Chemistry*, Cornell Univ. Press, Ithaca, N. Y., 1953, pp. 399–426.

12. G. Meyerhoff, *Makromol. Chem.*, **89**, 282 (1965).

13. H. Coll and L. R. Prusinowski, *J. Polym. Sci. B*, **5**, 1153 (1967).

14. G. V. Schulz and H. Baumann, *Makromol. Chem.*, **114**, 122 (1968).

15. D. Henley, *Svensk Papperstidn.*, **63**, 143 (1960).

16. W. Brown and R. Wikstrom, *Europ. Polym. J.*, **1**, 1 (1965).

17. S. Newman, L. Loeb, and C. M. Conrad, *J. Polym. Sci.*, **10**, 463 (1953).

18. T. Timell and C. B. Purves, *Svensk Papperstidn.*, **54**, 303 (1951).

19. G. V. Schulz and F. Blaschke, *J. Prakt. Chem.*, **158**, 130 (1941).

20. J. E. Hazell, L. A. Prince, and H. E. Stapelfeldt, in *Analytical Gel Permeation Chromatography* (*J. Polym. Sci. C*, **21**), J. F. Johnson and R. S. Porter, Eds., Interscience, New York, 1968, p. 43.

21. C. B. Purves, in *Cellulose and Cellulose Derivatives*, 2nd ed., E. Ott and H. M. Spurlin, Eds., Interscience, New York, 1954, p. 81.

22. G. Meyerhoff and S. Jovanovic, *J. Polym. Sci. B*, **5**, 495 (1967).

23. A. Agster, *Deut. Textiltech.*, **18**, 363 (1968).

24. Ø. Ellefsen, in *Fourth Cellulose Conference* (*J. Polym. Sci. C*, **2**), R. H. Marchessault, Ed., Interscience, New York, 1963, p. 321.

25. L. Segal and J. D. Timpa, *Svensk Papperstidn.*, **72**, 6561 (1969).

26. D. F. Alliet, in *International Symposium on Polymer Characterization* (*Appl. Polym. Symp.*, **8**), K. A. Boni and F. A. Sliemers, Eds., Interscience, New York, 1969, p. 39.

27. P. Crouzet, F. Fine, and P. Mangin, *J. Appl. Polym. Sci.*, **13**, 205 (1969).

28. K. A. Boni and F. A. Sliemers, in *International Symposium on Polymer Characterization* (*Appl. Polym. Symp.* **8**), K. A. Boni and F. A. Sliemers, Eds., Interscience, New York, 1969, p. 65.

29. L. H. Tung, *Characterization of Macromolecular Structure*, Publ. 1573, National Academy of Sciences, Washington, D. C., 1968, p. 268.

30. L. H. Tung, personal communications. See also K. H. Altgelt and J. C. Moore, in *Polymer Fractionation*, M. J. R. Cantor, Ed., Academic Press, New York, 1967, p. 173.

31. P. E. Pierce and J. E. Armonas, in *Analytical Gel Permeation Chromatography* (*J. Polym. Sci. C*, **21**), J. F. Johnson and R. S. Porter, Eds., Interscience, New York, 1968, p. 23.

32. R. Y. M. Huang and R. G. Jenkins, *Tappi*, **52**, 1505 (1969).

Received November 3, 1969

Studies in Ring-Opening Polymerization.
I. 5,5-Diethyl-1,3,2-dioxathiolan-4-one-2-oxide

G. P. BLACKBOURN and B. J. TIGHE, *Department of Chemistry, The University of Aston, Birmingham 4, England*

Synopsis

The polymerization of 5,5-diethyl-1,3,2-dioxathiolan-4-one-2-oxide has been examined in various solvents at 60–100°C. Kinetic studies have shown that steric hindrance by the C_5 ethyl substituents prevents the occurrence of a bimolecular propagation reaction involving direct attack by a terminal hydroxyl group on the ring. In dry, nonhydroxylic solvents, the first-order rate-determining step in the sequence of reactions leading to polymer formation is a primary ring scission reaction in which a reactive intermediate is formed and sulfur dioxide eliminated. This intermediate, which is formally depicted as an α-lactone, then takes part in a very rapid chain-propagation process, the individual steps of which govern the molecular weight distribution of the polymer. The values of the activation energy (25–30 kcal/mole) and frequency factor (10^{11}–10^{13} $\sec^{-1}$) for this polymerization reaction are, therefore, those associated with monomer decomposition and not the chain growth process. The molecular weight of the resultant polymer, poly-(3-pentylidene carboxylate) is controlled by adventitious traces of water which produce one carboxyl and one hydroxyl group per chain. Polymers having $\bar{M}_n \sim 20{,}000$ are readily obtained; these are materials of moderately high melting point ($T_m \simeq 200°C$) which crystallize from the melt into a banded spherulitic structure.

INTRODUCTION

1,3,2-Dioxathiolan-4-one-2-oxides (I) are more commonly known as α-hydroxycarboxylic acid anhydrosulfites, the parent α-hydroxy acid being used as a prefix to identify individual members (e.g. glycollic, lactic, and α-hydroxyisobutyric acid anhydrosulfites, I; $R^1 = R^2 = $ —H; $R^1 = $ —CH_3, $R^2 = $ —H; $R^1 = R^2 = $ —CH_3, respectively). Their conversion to poly-α-esters (II) has been known for some time and we have previously discussed polymerization mechanisms[1–3] for these simpler members of the series. Trivial names are also used for the derived polymers (e.g., polyglycollic acid or polyglycollide), but for higher homologs the trivial and derived nomenclature becomes confusing and the systematic nomenclature is to be preferred. Hence 5,5-diethyl-1,3,2-dioxathiolan-4-one-2-oxide

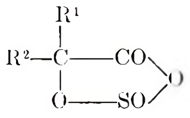

I

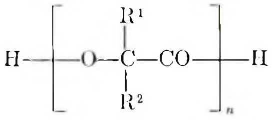

$$\mathrm{H}-\left[\mathrm{O}-\underset{\mathrm{R}^2}{\overset{\mathrm{R}^1}{\mathrm{C}}}-\mathrm{CO}\right]_n-\mathrm{H}$$

II

(DEAS, I; $R^1 = R^2 = —C_2H_5$) polymerizes to give poly (3-pentylidene carboxylate), II; $R^1 = R^2 = —C_2H_5$.

Aliphatic polyesters do not in general lend themselves to useful application because of low softening points and poor resistance to hydrolysis. Poly-α-esters, however, often have melting points above 200°C, and because of the short repeat unit, substituents are able to shield the ester function and thus hinder chain scission reactions. Hence the nonsubstituted polymer (polyglycollide or polymethylene carboxylate II; $R^1 = R^2 = —H$) is hydrolyzed in boiling water, while high molecular weight dimethyl-substituted polymer (polyisopropylidene carboxylate, II; $R^1 = R^2 = —CH_3$) is stable to boiling alcoholic alkali ($3N$) for over 5 hr.

Poly-α-esters have been described as potentially useful in the fields of films, fibers, coatings, and surgical inserts, but methods for their preparation are not numerous and often result in poor yields of polymer and/or low molecular weights. Methods such as self-condensation of acids or metal salts involve polymerization in the melt at temperatures in the region of 200°C and are accompanied by degradation reactions and discoloration. The apparently attractive polymerization of the appropriate glycollide by suitable catalysts, at lower temperatures, is limited to simple derivatives, monosubstituted at the 1 and 4 positions,[5] although copolymers derived from a monosubstituted, and a symmetrical disubstituted, glycollide may be prepared, providing that at least 50 mole-% of the former is present.[6] Alternative routes via decomposition of the appropriate tert-butyl perester[7] or by oxygenation of the appropriate ketene[8] are limited by the feasibility of preparing the required intermediates.

Kinetic studies of the decomposition and polymerization of anhydrosulfites have led to the elucidation of the contributory mechanisms, and enabled an assessment to be made of the role which impurities play during these processes. If impurities are removed or their formation prevented, then the controlled thermal extrusion of sulfur dioxide from anhydrosulfites in solution represents the best general method for the preparation of poly-α-esters, particularly as the polymerization proceeds at convenient rates at temperatures below 100°C. Although the analogous 1,3-dioxolan-2,4-diones (III) possess similar structural features, the greater thermal stability of this ring system[9] prevents the occurrence of an effective chain propagation reaction.

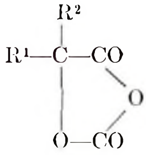

III

In earlier papers we have discussed various aspects of the decomposition of 5,5-dimethyl,[1] 5-methyl,[2] 5,5-bis(chloromethyl)-,[10] 5-phenyl-, 5,5-diphenyl,[11] and nonsubstituted[3] 1,3,2-dioxathiolan-4-one-2-oxides. We now describe the decomposition of the 5,5-diethyl derivative and the characteristics of the polymer thereby formed. Previous attempts[12] to polymerize this compound produced only low molecular weight material. The conditions used were identical to those under which the 5,5-dimethyl derivative (α-hydroxyisobutyric acid anhydrosulfite HBAS[1]) decomposed to yield polymer having a molecular weight in excess of 100,000. The inference drawn from these results was that the structural features of the former were in some way responsible for its inferior polymerizability. In this paper we compare the polymerization mechanism for the two compounds and assess the factors governing the degree of polymerization of the final polymer.

EXPERIMENTAL

α-Hydroxy-α-ethylbutyric acid was obtained from diethyl ketone by the conventional cyanohydrin route.

5,5-Diethyl-1,3,2-dioxathiolan-4-one-2-oxide was prepared by the direct action of thionyl chloride on α-hydroxy-α-ethylbutyric acid and by using conditions described in previous papers.[1,13] The crude anhydrosulfite was purified by distillation, treatment with silver oxide, and prepolymerization,[3,13] purity being assessed by chloride ion titration and instrumental analysis.

Rate measurements were carried out with constant volume gas evolution apparatus designed for use at high temperature, and similar to that used for previous studies.[1,2]

Solvents were purified by the recommended methods of Weissberger[14] or Vogel.[15] With the exception of dioctyl phthalate, all were refluxed over a suitable drying agent, fractionally distilled, and the middle fraction collected over fresh desiccant. The solvents were again distilled just prior to use and the middle fraction only was used. Dioctyl phthalate was shaken with calcium chloride for two days, the suspension allowed to settle, and the required quantities removed by hypodermic syringe.

Infrared and mass spectra were recorded by using Perkin-Elmer 237 and A.E.I. MS9 instruments, respectively.

Differential thermal analysis (DTA) traces were obtained by using the Du Pont 900 thermal analyzer in conjunction with a differential scanning calorimeter (DSC) cell.

Molecular weights were measured by carboxylic acid endgroup determinations by using a hot micro-titration technique. Accurately weighed polymer (0.04–0.05 g) was stirred on 5.0 ml of pure benzyl alcohol for 3 minutes at 160°C. The solution was then poured onto 10.0 ml of distilled chloroform and the original vessel washed with a further 5.0 ml of benzyl alcohol, which was then transferred to the polymer solution. Three drops of 0.1% Phenol Red in ethanol were added and the whole stirred. Standardized benzyl alcoholic caustic soda was added from a microliter syringe until the endpoint was reached. A blank run on solvents alone (10.0 ml benzyl alcohol + 10.0 ml chloroform) gave a background titer which was subtracted from the subsequent values obtained when carboxylic endgroups were determined. The solvents were not considered of sufficient purity until the blank titration was below 10 μl of 0.1N alcoholic sodium hydroxide.

Rates of spherulite growth were followed by optical microscopy and a depolarized light intensity technique as used by Barrall and Johnson,[16] employing the Du Pont 900 console as recorder and temperature programmer.

RESULTS

In order to obtain high molecular weight polymer and reproducible kinetic results the DEAS was required in a high degree of purity. Other workers[4,12,17] rely upon prepolymerization followed by fractional distillation as means of purification, but we did not find these methods alone to be satisfactory,[13] particularly for the removal of chloride containing impurities. Use of the silver oxide purification technique, however, enabled the chlorine content to be reduced to a concentration level of 2.8×10^{-3} moles per mole of DEAS before the final prepolymerization step.

Thermal Polymerization

The rate of appearance of polymer and disappearance of monomer were followed by gravimetry and gas evolution techniques, respectively. The evolution of sulfur dioxide as a function of time was found, in dry nonhydroxylic solvents, to correspond directly to polymer formation. This type of behavior, in which the ring-opening decomposition to the monomer represents the rate-determining step in the sequence of reactions leading to polymer formation, was also observed with the 5,5-dimethyl-substituted monomer.[1]

DEAS decomposition was measured in a range of solvents between 50 and 100°C. Monomer decomposition was shown to be a first-order process by computing the gas evolution data graphically in the form log $[(p_\infty - p)/p_\infty]$ versus time, where p is the pressure of sulfur dioxide. Typi-

TABLE I

First-Order Rate Constants (k_1) and Half Lives ($t_{1/2}$) for the Decomposition of DEAS in Various Solvents at [DEAS] = 0.5 mole/l.

Solvent	Dielectric constant ($\epsilon_{90°}$)	Temperature, °C	$10^5 \times k_1$, sec^{-1}	$t_{1/2}$, min
Dimethyl sulfoxide	~36	89.3	138	8.4
Glycerol	~32	89.1	130	8.9
Nitrobenzene	~25	90.0	20.1	57.5
p-Nitrotoluene	~17	88.1	10.5	110
Chlorobenzene	~4.5	88.1	6.3	183
Dioctyl phthalate	~3.5	91.0	7.3	145

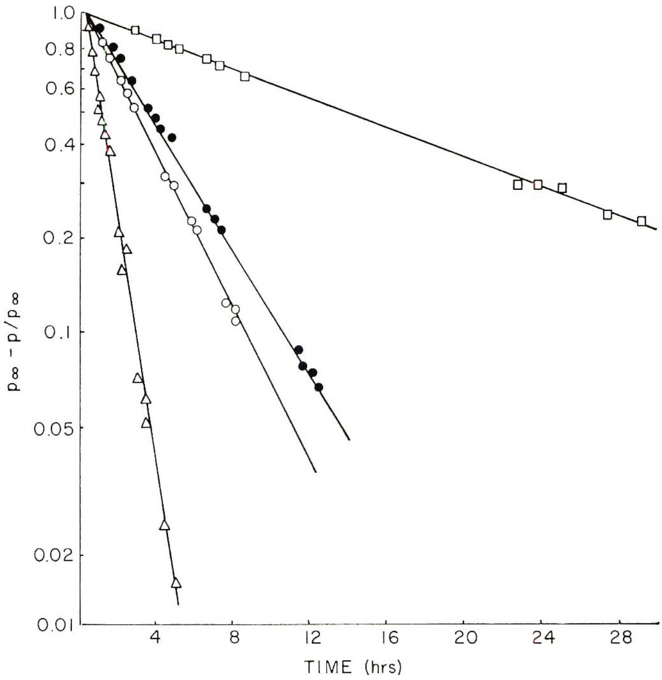

Fig. 1. First-order decomposition of DEAS in various solvents at 90°C: (△) nitrobenzene; (○) dioctyl phthalate; (●) chlorobenzene; (□) decalin. $[\mathrm{DEAS}]_0 = 0.56$ mole/l. Gas evolution data expressed in terms of sulfur dioxide pressure (p) as a function of time.

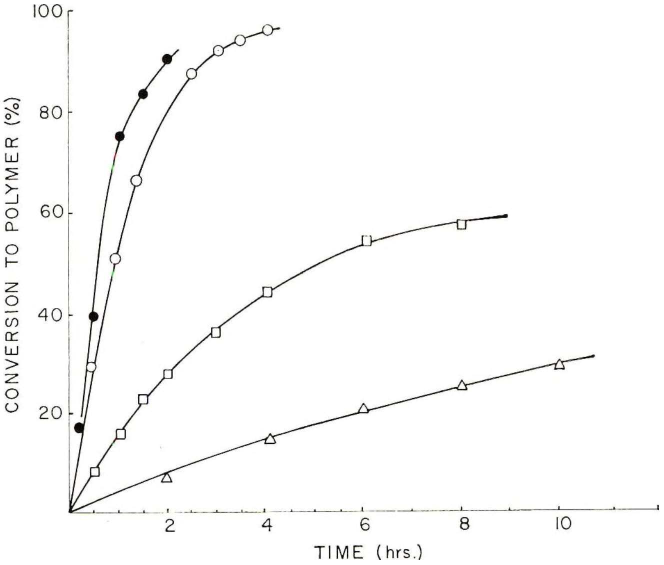

Fig. 2. Polymerization of DEAS in nitrobenzene at various temperatures: (●) 94°C; (○) 89°C; (□) 74°C; (△) 66°C. $[\mathrm{DEAS}]_0 = 0.5$ mole/l.

cal examples are shown in Figure 1. The overall process can therefore be expressed by the equation:

$$d[\mathrm{P}]/dt = -d[\mathrm{DEAS}]/dt = d[\mathrm{SO_2}]/dt = k_1[\mathrm{DEAS}] \qquad (1)$$

where [P] is the concentration of polymer. Changes in initial concentration, and variation of sulfur dioxide pressure were investigated and did not significantly alter the measured values of k_1.

Table I presents the rate constants observed for the decomposition of DEAS in a series of solvents at temperatures in the region of 90°C. It will be evident that in solvents of increasing dielectric constant there is a trend to faster reaction; attempts to find a quantitative relationship between a function of rate and dielectric were not altogether successful. The figures in Table I demonstrate that DEAS is more sensitive than the 5,5-dimethyl derivative[1] (HBAS) to this change in solvent property.

Plots of conversion to polymer versus time for DEAS in nitrobenzene at various temperatures are given in Figure 2 and typical rate constants and kinetic parameters shown in Table II. The values obtained for activation energy E, pre-exponential factor A, and entropy of activation $\Delta S\ddagger$ were derived from Arrhenius plots and are of the order expected for a genuine unimolecular process.

TABLE II

First-Order Rate Constants k_1, Half Lives $t_{1/2}$, Energies of Activation E, Entropies of Activation $\Delta S\ddagger$ and Frequency Factors A for the Polymerization of DEAS in Nitrobenzene at $[\mathrm{DEAS}]_0 = 0.5$ mole/l.

Temp, °C	$10^6 \times k_1$, sec^{-1}	$t_{1/2}$, min	E, kcal/mole	A, sec^{-1}	$\Delta S\ddagger$, cal/deg-mole
63	0.65	1777	28.7	4.02×10^{13}	+1.3
82	5.67	203.7			
90	20.1	57.5			
96	37.0	31.2			

Transient formation of an α-lactone intermediate has been proposed during the thermal decomposition of HBAS; further evidence for these species is found in the mass spectra of anhydrosulfites. As the sample attains high temperature in the instrument no parent peak is observed for DEAS, but the cracking pattern involved mass numbers of 114(M-64),

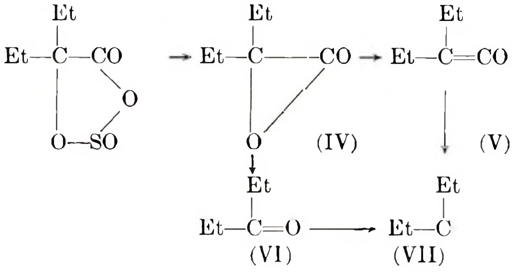

98(M-80), 86(M-92) and 70(M-108) which on consulting the whole spectrum can be assigned to the fragments (IV), (V), (VI), and (VII), respectively, of which signals for (IV) and (VI) are particularly strong.

Ketone formation was observed to a minor degree when flash distillation was employed during the purification of DEAS (under these conditions the crude monomer was subjected to temperatures in excess of 130°C); in other systems, e.g., 5,5-bis(chloromethyl),[10] ketone formation is a major competitive reaction.

Initiated Polymerization

In certain cases[2,3] simple anhydrosulfites undergo a bimolecular ring-opening reaction, in the presence of alcohols leading to regeneration of a hydroxyl group. The regenerated hydroxyl group can then take part in a bimolecular chain propagation reaction analogous to that observed to occur[18] with *N*-carboxy-α-amino acid anhydrides. The steric hindrance of the two C_5 methyl substituents in 5,5-dimethyl-1,3,2-dioxathiolan-4-oen-2-oxide effectively prevents such a reaction, however. In order to determine the sensitivity of DEAS to hydroxyl group attack rates of decomposition in nitrobenzene solution ($[M]_0 = 0.5$ mole/l.) containing various quantities of added benzyl alcohol ($[OH]_0 = 0.1$–0.5 mole/l.) were added. The rate of DEAS decomposition was found to be independent of initial hydroxyl group concentration, i.e.,

$$-d[\mathrm{DEAS}]/dt = k'[\mathrm{DEAS}]^1[\mathrm{OH}]^0 \tag{2}$$

Finally the decomposition of DEAS was examined in pure dry benzyl alcohol ($[OH] \sim 8$ mole/l.) at various temperatures. The values of the rate constants and derived kinetic parameters which are shown in Table III, demonstrate that the decomposition of DEAS takes place less rapidly in benzyl alcohol than in nitrobenzene. The reaction product obtained in benzyl alcohol was not poly(3-pentylidene carboxylate) but benzyl α-ethyl-α-hydroxybutyrate.

TABLE III

First-Order Rate Constants k', Energies of Activation E, and Frequency Factors A for the Decomposition of DEAS in Benzyl Alcohol at $[\mathrm{DEAS}]_0 = 0.5$ mole/l.

Temp, °C	$10^6 \times k'$, sec^{-1}	E, kcal/mole	A, sec^{-1}
79	5.6	25.1	1.9×10^{10}
90	13.9		
99	42.4		
109	80		
121	244.0		

More active nucleophiles were examined as potential initiators. Primary and secondary amines reacted very rapidly with an equimolar amount of DEAS to yield the appropriate amide. When less than stoichiometric amounts of amine were used, a rapid reaction with an approximately equimolar amount of DEAS again occurred, but the rate of the subsequent first-order decomposition of DEAS was practically identical to that in the absence of amine. Similarly when less than stoichiometric amounts of amide were used, no evidence of initiated polymerization was observed. Dimethyl sulfoxide, when used as a reaction medium, has been observed (Table II) to produce rapid decomposition of DEAS. When used in less than stoichiometric amounts, however, no evidence of initiating activity was observed. Table IV presents typical results obtained at 60°C.

TABLE IV
Effect of Additives (X) on the First-Order Rate Constant k_1 for the Decomposition of DEAS in Nitrobenzene at 60°C

Additive	$[X]_0$, mole/l.	$[DEAS]_0$, mole/l.	$10^6 \times k_1$, sec^{-1}
None	—	0.5	4.3(5)
Dimethylformamide	0.01	0.5	4.3(5)
Dimethylformamide	0.05	0.5	4.5(4)
Dimethylsulfoxide	0.01	0.5	4.4(0)
Dimethylsulfoxide	0.05	0.5	4.5(0)

Structure and Properties of the Polymer

Examination[1,2] of the polymers produced by the thermal decomposition of DEAS showed that they were linear poly-α-esters, having the structure (VIII).

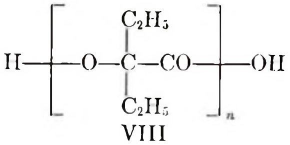

$$H-\left[O-\overset{C_2H_5}{\underset{C_2H_5}{\overset{|}{\underset{|}{C}}}}-CO\right]_n-OH$$

VIII

The value of n is governed, primarily, by the purity of the system. Thus although alcohols, for example, do not react directly with DEAS, their presence lowers the molecular weight attainable and at the equimolar concentration level prevents polymer formation altogether. For any nucleophile (N) containing a labile hydrogen atom (e.g., benzyl alcohol, benzylamine, water) the degree of polymerization n at complete conversion is given by the expression:

$$n = [DEAS]_0/[N]_0 \tag{3}$$

In the absence of added nucleophiles, adventitious traces of water control the molecular weight, and under these conditions each chain is terminated by one hydroxyl and one carboxyl group.

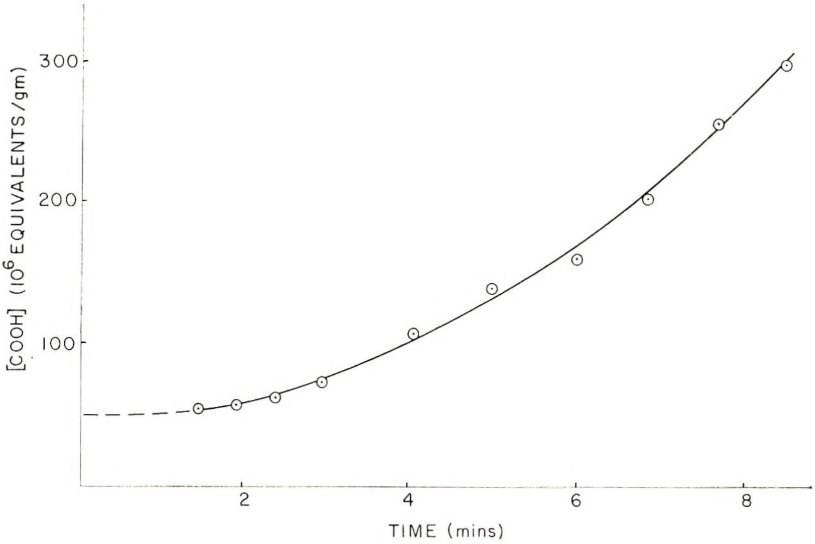

Fig. 3. Effect of dissolution time (benzyl alcohol, 150°C) on the carboxyl endgroup concentration of poly(3-pentylidene carboxylate).

For polymers having $n = 10$–50, quantitative infrared spectroscopy with normal precautions[19] provides a fairly ready and convenient means of assessing molecular weight. A calibration graph based on the relative intensity of hydroxyl ($\sim$3470 cm^{-1}) and ester carbonyl ($\sim$1760 cm^{-1}) frequencies correlated well with molecular weights assessed by other methods. Vapor-pressure osmometry, which had proved valuable for simpler members of the series,[1,2] was of limited use due to the general insolubility of polymers of structure VIII in organic solvents. The polymers were soluble in substituted phenols, but these solvents are not ideally suited to vapor-pressure measurements. Solution viscometry was useful for comparative work only.

The most successful method for obtaining reliable molecular weight data was found to be carboxyl endgroup titration, using a modification of Pohl's method.[20] Sources of error in the method were carefully investigated. Titrimetric precision was checked and found to be of the order of ±5%, absorption of atmospheric carbon dioxide which would have drastic effects on alkaline titers of this order was efficiently prevented by the blanket of chloroform vapor above the polymer solution. Degradation (in the hot benzyl alcohol necessary to achieve complete solution) was measured by endgroup carboxyl concentration and found to increase with time of dissolution as shown in Figure 3. Although reducing the temperature reduced degradation rate, the time for complete solution is much longer and no improvement in total degradation was found. At 160°C the minimum time for complete solution is approximately 2 min, whereas at temperatures below 100°C the solubility is incomplete even after 15 min. In practice a dissolution temperature of 160°C was used and a graphical cor-

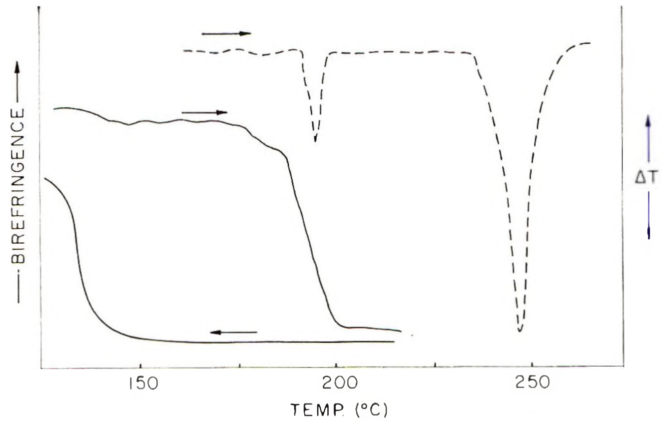

Fig. 4. Plots of (— —) DTA and (——) DLI traces obtained for poly(3-pentylidene carboxylate) in air at a constant heating and cooling rate of 10°C/min.

rection applied to the result. Polymers having a true number-average molecular weight in the region of 20,000 corresponding to $n \sim 200$, were readily obtained by thermal polymerization of DEAS. These were hydroxyl/carboxyl-terminated. In order to obtain higher molecular weight polymer more stringent precautions to exclude traces of moisture were necessary.

The polymer was found to crystallize when cooled from the melt at a suitable rate. Depolarized light intensity (DLI) and optical microscopy were used for observing spherulite growth. Figure 4 (full line) shows a typical trace of intensity of polarized light versus time. Large banded spherulites were obtained under these conditions. It is of interest that there is a relatively large difference between the crystalline melting point (200°C) and onset of crystallization temperature (ca. 140°C), which implies that crystallization occurs with some difficulty. During repeated melting and cooling the melting point was observed to rise by up to 10°C, this being associated with removal of imperfections in the crystalline regions. A DTA trace (Fig. 4) on unannealed polymer shows a slightly lower melting point (195°C) for this reason. Decomposition, under the conditions shown, sets in at around 250°C.

DISCUSSION

Ring-opening polymerization reactions in which the propagation step consists of a bimolecular reaction between a terminal nucleophile and an active site in the ring are well known. Typical of this type of chain growth process is the amine-initiated polymerization of *N*-carboxy-α-amino acid anhydrides.[18] In this reaction a terminal (primary or secondary) amino group attacks an active carbonyl site. The resultant ring opening and concurrent expulsion of carbon dioxide leads to chain extension (by one repeat unit) and regeneration of the terminal amino group [Eq. (4)].

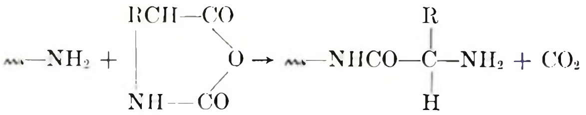

(4)

An analogous polymerization mechanism has been shown to occur with those members of the 1,3,2-dioxathiolan-4-one-2-oxide series which contain at least one C_5 hydrogen atom. In this case the propagating species is a terminal hydroxyl group, attack takes place at the C_4 carbonyl group, sulfur dioxide is expelled, and the polymer has a repeating ester rather than amide group. Both processes are characterized by second-order kinetic behavior, low (6–12 kcal/mole) activation energies, very low frequency factors (10^2–10^5 l./mole-sec), and pronounced sensitivity to reaction medium polarity.

The kinetic features associated with DEAS polymerization are quite different from these and strongly resemble the observed behavior of HBAS.[1] The reaction shows first-order dependence on monomer concentration, zero-order dependence on hydroxyl group concentration, and yet the degree of polymerization is controlled by initial concentration of hydroxyl groups. Furthermore in the presence of moisture the chains are carboxyl/hydroxyl-terminated, and when monomer decomposition takes place in the presence of a molar excess of hydroxyl groups, the product is apparently formed by direct combination of the ring and attacking species. The values of the activation energy (25–30 kcal/mole) and frequency factor (10^{12}–10^{13} sec^{-1}) associated with monomer decomposition, both in nonhydroxylic solvents to form polymer and in alcohols to form esters, are typical of reactions in which thermal cleavage of a weak covalent bond is the rate determining step.

The sensitivity of the various members of the dioxathiolan-4-one-2-oxide series to bimolecular hydroxyl group attack is conveniently assessed[21] by the ratio k_b/k_n, where k_b and k_n represent the first-order rate constants obtained in benzyl alcohol and nitrobenzene respectively. Since the hydroxyl group concentration in benzyl alcohol is of the order of 8 mole/l., direct attack by this species is readily detected. Thus for 1,3,2-dioxathiolan-4-one-2-oxide itself, the value of the ratio k_b/k_n at 90°C is in excess of 500. The 5,5-dimethyl derivative (HBAS) has a value of 0.9 at the same temperature, whereas that for DEAS is 0.07. In the case of HBAS and DEAS the steric hindrance of C_5 substituents effectively prevents hydroxyl group attack. The fact that DEAS has a much lower k_b/k_n ratio than HBAS may imply that the steric hindrance in the latter case was not as total as had been supposed. Alternatively it may be due to the greater sensitivity to dielectric constant of DEAS. In neither case, however, can hydroxyl attack form the basis of an effective bimolecular chain propagation reaction, since for this to occur a k_b/k_n ratio, above 100, and preferably around 500, is needed.[21]

The fact that primary and secondary amines can attack DEAS directly is entirely consistent with the observed interrelation of steric and electronic effects in this series.[21] The more powerful amine nucleophile overcomes the steric hindrance of the C_5 ethyl substituents, but the hydroxyl-terminated product is unable to do this, thus no direct bimolecular chain propagation reaction is observed. Similarly tertiary amides are not able to act as chain propagating species, since in substoichiometric amounts they do not sensibly alter the rate of monomer decomposition. Solvents of high polarity, or basicity, which do not contain a labile hydrogen atom, can markedly affect the rate of monomer decomposition, however, when used as reaction media. Other workers claim to have observed catalyzed polymerization of HBAS with such materials but were unable to obtain high molecular weight polymer.[17] We find that the increased difficulty of purification outweighs the possible advantage of faster reaction rates and have commented elsewhere on the abnormal reactivity of aprotic bases.[3]

The apparent inconsistencies in the behavior of DEAS can be explained by a modification of the mechanism proposed for HBAS polymerization.

Adventitious traces of moisture will react with an equimolar quantity of DEAS to regenerate α-hydroxy-α-ethylbutyric acid [Eq. (5)]. This is an extremely rapid reaction, even at room temperature.

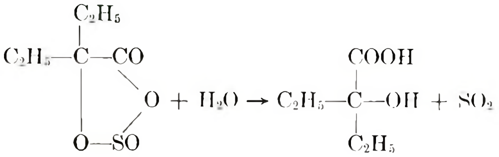

(5)

The rate-determining step is the decomposition of DEAS to form a polymerizable intermediate with concurrent expulsion of sulfur dioxide [Eq. (6)]. The intermediate which fulfils this requirement is considered, formally to be an α-lactone (IX).

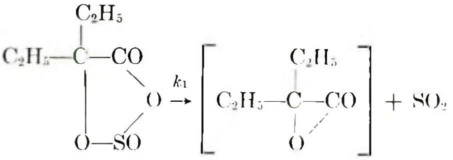

IX

(6)

A rapid chain growth process then takes place, as shown in eq. (7).

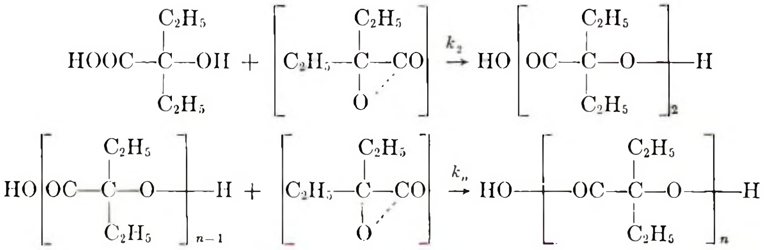

(7)

Since we have proposed that IX is a very reactive species which can react rapidly with hydroxyl groups, $k_2, k_3, \ldots, k_n$ are very much larger than k_1, and reaction (6) is rate-determining. We may therefore write:

$$k_1[\text{DEAS}] = k_2[\text{IX}][\text{X}_1] + k_n[\text{IX}]\left(\sum_{2} [\text{X}_{n-1}]\right) \tag{8}$$

where, for example, X_n would represent structure VIII and X represents the parent acid. Thus sulfur dioxide evolution and polymer formation may be equated in the following way:

$$d[\text{SO}_2]/dt = -d[\text{DEAS}]/dt = k[\text{DEAS}] = d[\text{P}]/dt \tag{9}$$

which is identical with eq. (1).

Radiotracers studies enabled values of k_3/k_2 to be obtained for the polymerization of HBAS in different solvents. It was demonstrated that this ratio remained sensibly constant during the polymerization and that its magnitude determines the molecular weight distribution in this type of polymerization process. Although the value of k_3 was somewhat greater than that of k_2 added quantities of parent α-hydroxy acid were always incorporated into the polymer before monomer decomposition was complete. Equation (3) demonstrates that this is also the case in DEAS polymerization.

α-Lactone intermediates have been proposed in other systems,[7] and supporting mass spectral evidence for the formation of fragments having appropriate mass numbers has been obtained in the thermal decomposition of several 1,3,2-dioxathiolan-4-one-2-oxides.[11,13] The precise nature of the intermediate formed in the decomposition of HBAS has been considered in some detail.[1] Although the preferred form is considered to be an α-lactone, it may possess some radical or ionic character as indicated in eq. (10).

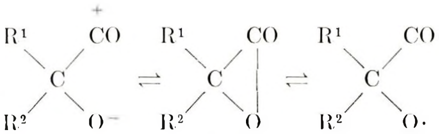

XI

(10)

The rate of decomposition of DEAS is considerably more sensitive than that of HBAS, to the polarity of the reaction medium. On the other hand, HBAS, when freshly distilled, shows an intense violet coloration which slowly disappears, together with other evidence[1] of radical character, which is not apparent in the case of DEAS. It is likely, therefore, that the DEAS intermediate is more polar than that formed from HBAS.

The fact DEAS polymerization in polar nonhydroxylic solvents occurs more rapidly than that of HBAS is attributable to increased ring strain due to C_5 substituent size. Thus the first-order rate constants for thermal polymerization of symmetrically substituted 1,3,2-dioxathiolan-4-one-2-oxides at 90°C in nitrobenzene are: 5,5-diethyl, $k_1 = 2 \times 10^{-4}$ sec^{-1}; and

5,5-dimethyl, $k_1 = 6 \times 10^{-5}$ sec $^{-1}$; the unsubstituted ring is appreciably more stable ($k_1 = 5 \times 10^{-6}$ sec^{-1}). To alleviate steric repulsion between the C_5 substituents this bond angle is widened, which thus imposes compressive strain on the ring. The effect becomes more apparent as substituent size is increased, being most marked in 5,5-diphenyl-1,3,2-dioxathiolan-4-one-2-oxide[11] ($k_1 = 3 \times 10^{-3}$ sec^{-1}, 90°C, nitrobenzene).

Structural features which favor polymer crystallinity include chain polarity, linearity, molecular symmetry, and regularity. Simple poly-α-esters, e.g., polyglycollide, polylactide, and poly(isopropylidene carboxylate), are crystalline because such requirements are satisfied but primarily because of the high interchain cohesion consequent upon the highly polar nature of the backbone. As the size of substituent groups is increased in a given class of polymer, however, interchain cohesion is reduced, and chain packing becomes more difficult. Thus, if substituent groups larger than methyl are introduced, the optimum interchain distance of ~5 Å cannot be readily attained, and the crystallization process is impeded.

In the light of this it is perhaps surprising that the polymer obtained from DEAS, poly-(3-pentylidine carboxylate), is crystalline. The rate of crystallization is monitored by DLI measurements andis, however, very slow, this being a consequence of chain-packing difficulties. A measure of the ease of incorporation of chain segments into crystalline regions is provided by the difference between the melting point (T_m) and the temperature of first appearance of spherulites (T_c). A comparison of values obtained for various polyesters under identical conditions is shown in Table VI.

TABLE VI
DLI Measurement of the Onset of Polyester Crystallization at a Constant Cooling Rate of 10°C/min

Polymer	($T_m - T_c$), °C
Poly(hexamethylene adipate)	8
Poly(ethylene terephthalate)	~20
Poly(tetramethylene terephthalate)	~20
Poly(3-pentylidene carboxylate)	~58

The formation of large banded spherulites, as obtained from poly(3-pentylidene carboxylate) is not a common phenomenon, although this type of crystallization has been observed with other polymer systems including polyethylene, polyoxymethylene, and poly(ethylene terephthalate). No uniformly acceptable explanation of this behavior has been proposed although some suggestions have been made as to its origin.[22] At present we can only speculate on the conformation of the polymer chains. Although polylactic acid chains are helical[23] and ability to form helical chains has been suggested as one requirement for banded spherulite formation, polyglycollic acid has been shown to exist in the planar extended zigzag form. It seems most probable, however that poly(3-pentylidene carboxylate) crystallizes in a helical conformation, since in this manner the ethyl substituents can be most readily accommodated.

References

1. D. G. H. Ballard and B. J. Tighe, *J. Chem. Soc. B*, **1967,** 702.
2. D. G. H. Ballard and B. J. Tighe, *J. Chem. Soc. B*, **1967,** 976.
3. M. D. Thomas and B. J. Tighe, *J. Chem. Soc. B*, **1970,** 1039.
4. T. Alderson, U.S. Pat. 2,811,511 (1957).
5. H. K. Hall, M. K. Brandt, and R. M. Mason, *J. Amer. Chem. Soc.*, **80,** 6409 (1958).
6. C. E. Lowe, U.S. Patent, 2,688,162 (1954).
7. P. D. Bartlett and L. B. Gortler, *J. Amer. Chem. Soc.*, **85,** 1874 (1963).
8. H. Staudinger, K. Dyckerhoff, H. W. Klever, and L. Ruzicka, *Ber.*, **58,** 1079 (1925).
9. B. J. Tighe, *Chem. Ind.* (London), **1969,** 1837.
10. A. J. Crowe and B. J. Tighe, *Chem. Ind.* (London), **1969,** 170.
11. B. W. Evans, D. J. Fenn and B. J. Tighe, *J. Chem. Soc. B*, **1970,** 1049
12. J. B. Rose and C. K. Warren, *J. Chem. Soc.*, **1965,** 791.
13. G. P. Blackbourn and B. J. Tighe, *J. Chem. Soc.*, in press.
14. A. Weissberger, Ed. *Technique of Organic Chemistry*, Vol. VII, 2nd ed., Interscience, New York, 1955.
15. A. I. Vogel, *Practical Organic Chemistry*, Longmans, London, 1964.
16. E. M. Barrall, J. E. Johnson, and R. S. Porter, in *International Symposium on Polymer Characterization* (*Appl. Polym. Symp.*, 8), K. A. Boni and F. A. Sliemers, Eds., Interscience, New York, 1969, p. 191.
17. S. Inoue, K. Tsubaki, and T. Isurata, *Makromol. Chem.*, **125,** 170 (1969).
18. M. Szwarc, *Fortsch. Hochpolym. Forsch.*, **4,** 1 (1965).
19. G. M. Kline, Ed., *Analytical Chemistry of Polymers*, Vol. II, Interscience, New York, 1962, Chap. VII.
20. H. Pohl, *Anal. Chem.*, **26,** 1614 (1954).
21. D. J. Fenn, M. D. Thomas, and B. J. Tighe, *J. Chem. Soc. B*, **1970,** 1044.
22. A. Keller, in *Growth and Perfection of Crystal*, Ed. Doremus, Roberts, and Tunstall, Eds., Wiley, New York, 1958, p. 509.
23. P. De Santes and A. J. Kovacs, *Biopolymers*, **6,** 299 (1968).

Received April 20, 1970

JOURNAL OF POLYMER SCIENCE: PART A-1 VOL. 8, 3607-3649 (1970)

Emulsion Polymerization of Vinyl Acetate. II

M. LITT, *Division of Macromolecular Science, Case Western Reserve University, Cleveland, Ohio 44106, and* R. PATSIGA* and V. STANNETT,† *State University of New York, College of Forestry, Syracuse, New York*

Synopsis

The emulsion polymerization of vinyl acetate was investigated at low ionic strengths and has quite unusual kinetics. The rate of polymerization is dependent on the initiator concentration to the first power and independent of soap concentration. In seeded polymerizations, the rate of polymerization depends on initiator to the 0.8 power, particle concentration to the 0.2 power, and monomer volume to 0.35 power. In all cases the rate of polymerization is almost independent of monomer concentration in the particles until 85–90% conversion. These results were rationalized by the following mechanism: (a) polymerization initiates in the aqueous phase because of the solubility of the monomer and is stabilized there by adsorption of ionic soap on the growing polymer molecule; (b) the growing polymer is swept up by a particle at a degree of polymerization (under our conditions) of about 50–200. Growth continues in the particle. This sweep-up is activation-controlled as both particle and polymer are charged. (c) Chain transfer to the acetyl group of monomer gives a new small radical which cyclizes to the water-soluble butyrolactonyl radical, and reinitiates polymerization in the aqueous phase; (d) the main termination step is reaction of an uncharged butyrolactonyl radical with a growing aqueous polymer radical. A secondary reaction at low ionic strength is sweep-up of an aqueous radical by a particle containing a radical. At high ionic strength, this is the major termination step. The unusual kinetic steps are justified by data from the literature. They are combined with the usual mechanisms operating for vinyl acetate polymerization and kinetic equations are derived and integrated. The integral equations were compared with the experimental data and shown to match it almost completely over the whole range of experimental variables.

INTRODUCTION

In the previous paper,[1] a study of emulsion polymerization of vinyl acetate, initiated by potassium persulfate and with the use of a poly(vinyl acetate) seed latex, was reported. It was found that the dependence of the rate of polymerization on the number of particles, initiator concentration and emulsifier was quite different from that anticipated from the classical Smith-Ewart theory.[2] It was postulated that much of the polymerization took place in the aqueous phase, and a picture of the mechanism of

---

* Present address: Indiana University of Pennsylvania, Indiana, Pennsylvania.

† Present address: North Carolina State University, Box 5035, Raleigh, North Carolina 27607.

vinyl acetate emulsion polymerization initiated by potassium persulfate was presented. In the present paper additional experimental data are presented both with direct and with seeded polymerizing systems. The mechanism of the polymerization presented in the first paper has been modified and extended. The complex formal kinetics have been worked out in detail and a number of alternative steps eliminated. The final scheme selected is shown to be in reasonable agreement with the experimental results.

EXPERIMENTAL

Materials

Vinyl acetate and styrene were obtained from the Eastman Kodak Company and purified by distillation through a 2-ft glass column filled with pyrex helices. The monomer was stored over anhydrous sodium sulfate at 5°C and filtered before use to remove suspended salt. The emulsifier used was a purified grade of sodium lauryl sulfate (Sipon WD) obtained from the American Alcolac Corporation and used directly. The initiator, potassium persulfate, was Fisher-certified reagent grade and was used directly from the bottle.

Polymerization Procedure

The polymerizations were conducted in a dilatometer modified from that designed by Corrin.[3] The apparatus, which gave very reproducible results, is illustrated in Figure 1. The total contraction of the latex, as the monomer polymerized, was measured on scale F. This was accomplished by using nitrogen pressure to control the level of latex in the flask. Nitrogen was directed into inlet A until the pressure forced the latex level to a convenient reference point on scale D. At the same time latex was forced up side arm E where the level of latex was again measured on F. If polymerization took place in the time interval between readings, there would be a noticeable drop of the latex level in the side arm E. With this apparatus, accurate conversions could be determined as often as once every minute. The total volume contraction was about 8–10 cc. Since this was greater than the side arm volume, different reference points were used on scale D as polymerization progressed. These were calibrated against the side-arm scale.

When measurements were not being made, the direction of nitrogen flow was reversed. Nitrogen entered at B (with C and G closed), went down side arm E and bubbled through the latex to be exhausted at A after passing through the condenser. The bubbling action of the nitrogen enabled good mixing to occur in the neck D.

All polymerizations were conducted at 60 ± 0.03°C (water bath) under an atmosphere of nitrogen. The nitrogen was freed of any traces of oxygen by passing it through Fieser's oxygen absorption solution. Before immersion into the bath the reactants in the vessel were flushed for 30–60 min at room temperature with nitrogen. The polymerizing apparatus was attached to a rack in such a way that it could be raised or lowered into the bath as a complete unit. Stirring speeds were kept as constant as possible during each run, in the range of 150–200 rpm.

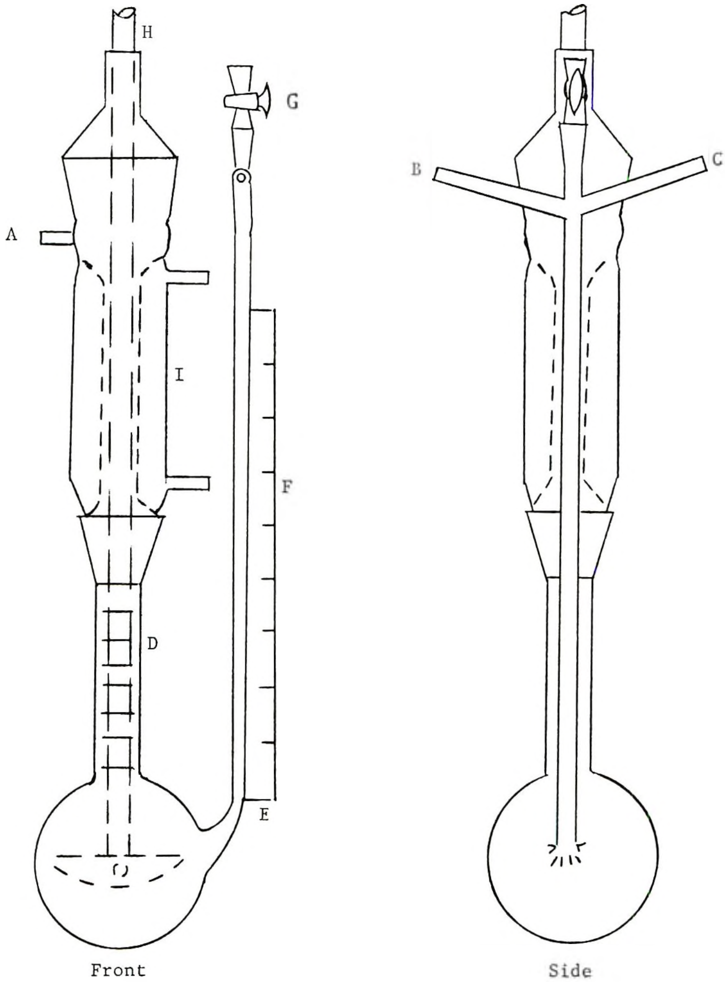

Fig. 1. Dilatometer: (A) nitrogen inlet or exhaust; (B) nitrogen inlet; (C) nitrogen exhaust; (D) reference scale; (E) side arm; (F) scale; (G) stopcock; (H) truebore stirrer; (I) condenser. Capacity: 215 ml.

Most of the polymerizing systems were based on a recipe that gave a latex with 25 wt-% of polymer. The typical recipe used was: H_2O, 180.0 g; vinyl acetate, 60.0 g; sodium lauryl sulfate (SLS), 1.2 g; potassium persulfate, 0.04 g. Polymerization rates are therefore expressed as moles/180 ml H_2O-min. For kinetic purposes, we have sometimes converted to moles per liter second. Concentrations of ingredients used are given in terms of moles per liter of aqueous phase.

Seeded polymerizations were conducted by the same technique and apparatus described above. The general method was to prepare a latex which was used as seed. This latex could be used directly or diluted to any solids content. A desired amount of seed was placed in the reaction vessel with additional monomer, adjusted to 25% solids, along with water, initiator, and emulsifier. Polymerizations were then performed in the normal manner.

Particle size measurements were made by light scattering or by electron microscopy as described previously.[1]

EXPERIMENTAL RESULTS

Studies of the polymerization of vinyl acetate were made either on the standard system of water, emulsifier, monomer, and initiator or on the

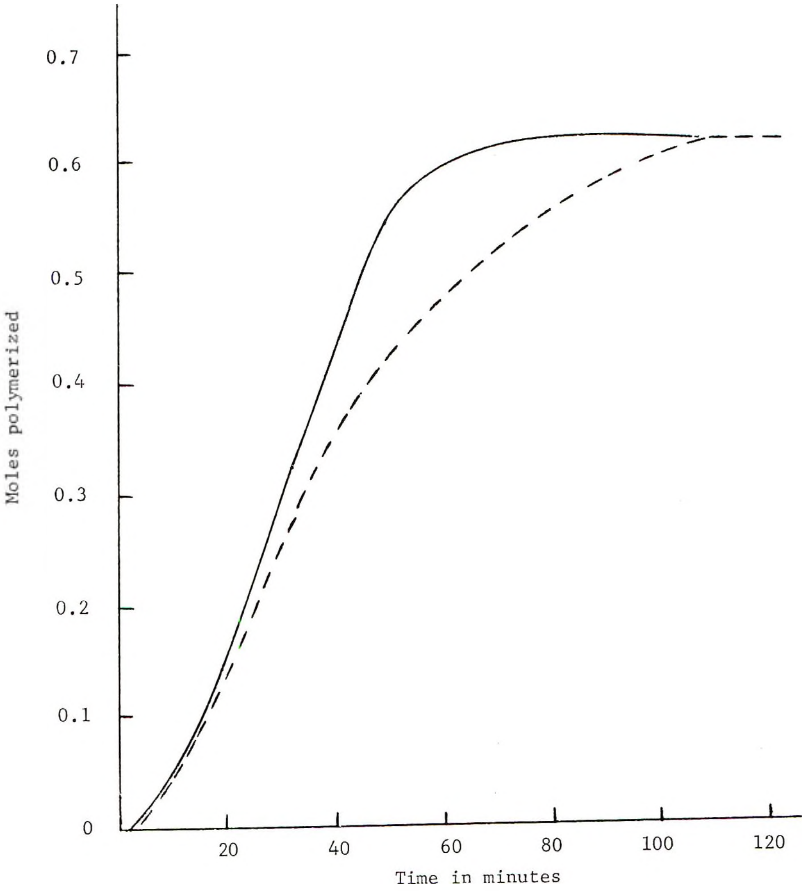

Fig. 2. Polymerization curves of vinyl acetate and styrene at 60°C: (—) vinyl acetate; (- -) styrene.

seed polymerizing system. The results of the polymerizations will be divided into these two approaches.

The Standard System

The general appearance of a vinyl acetate emulsion polymerization curve is shown in Figure 2. Most curves were approximately linear between 15 and 85% conversion. The duration of the induction period was between 5 and 10 min and varied with persulfate concentration as well as the length of nitrogen purge before each run. This indicated that traces of oxygen could inhibit the polymerization until flushed from the system or consumed by free radical reactions. Styrene had an induction period of about 2 min when polymerized with a similar recipe and exhibited a linear curve for only a small portion of the total reaction in agreement with that found by other investigators when the particle concentrations were in the range

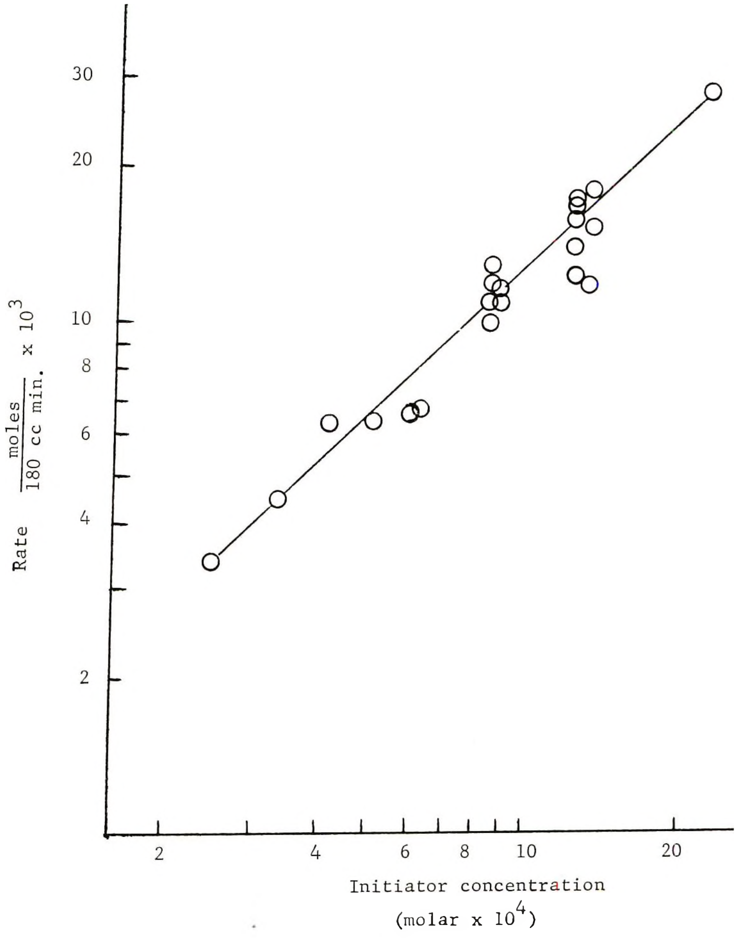

Fig. 3. Log–log plot of rate vs. initiator concentration. The line drawn has a slope equal to unity.

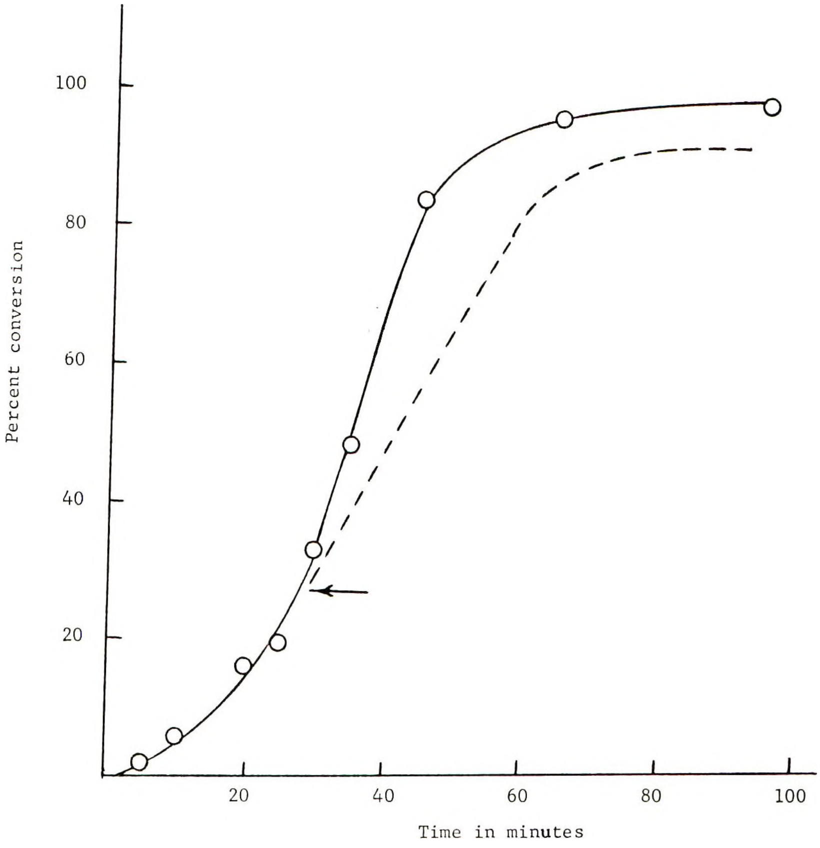

Fig. 4. Effect of injection of initiator (arrow) during polymerization. The dotted line represents the polymerization when no persulfate is injected.

of 10^{12} to 10^{15}/cc.[4-6] A gradual decrease in rate was observed after 50% conversion; a typical curve is included in Figure 2. The induction periods have been removed from the graph, and concentration adjusted to equal moles of each monomer. This figure is illustrative of the differences in mode of polymerization of the two monomers in the range of particle sizes with which we are concerned.

Initiator Dependence. The effect of initiator on the rate of polymerization was determined in a large number of experiments over a wide range of potassium persulfate concentrations. Rates could be conveniently measured in the range 2×10^{-4} to 2×10^{-3} mole/l. (aqueous phase) of persulfate. A plot of log rate versus log initiator concentration is shown in Figure 3. There is considerable scatter of points; however, a slope of unity is strongly indicated. This is a great deal higher than the dependency of 0.4 predicted in the original work on styrene polymerization.[2] Moreover, experiments similar to those conducted by Morton et al.,[4] in which an additional amount of initiator was injected during the reaction,

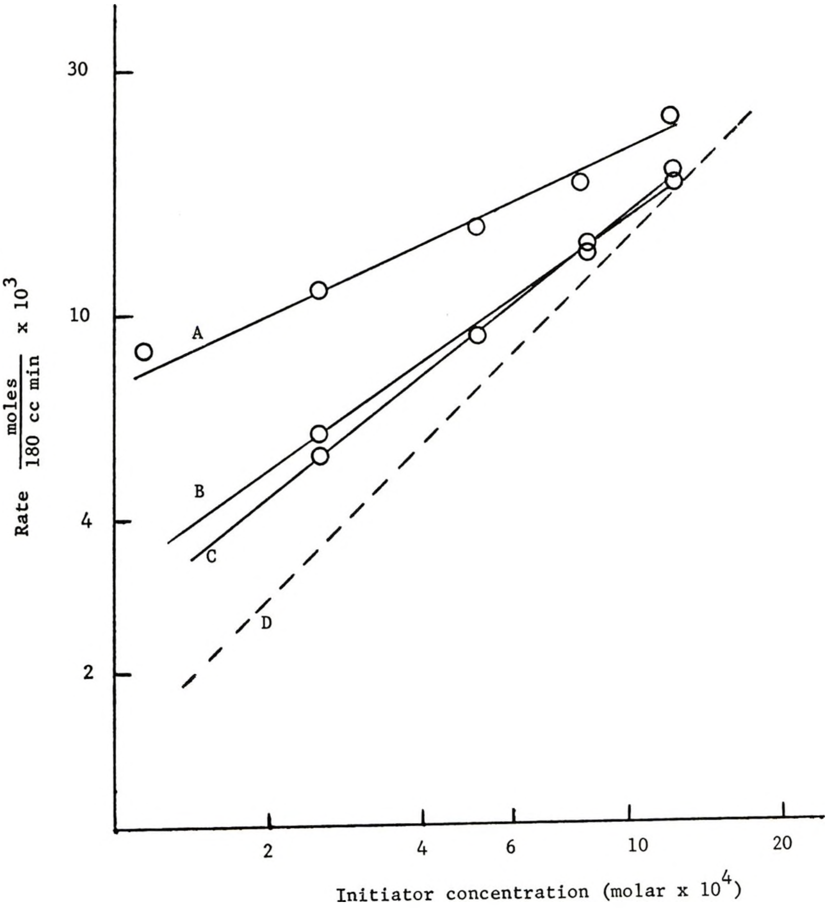

Fig. 5. Log-log plot of rate versus initiator concentration in the presence of salts: (*A*) 0.05 *M* phosphate buffer; (*B*) 0.05 *M* potassium sulfate; (*C*) with potassium sulfate added to give constant salt concentration of $12.0 \times 10^{-4}M$; (*D*) without additives (see also Fig. 3).

also show a considerable difference in behavior from the styrene system. Particle sizes were comparable to those in our work.

The injection of initiator must occur at a time during the polymerization when the number of latex particles is constant. That is, no free emulsifier in the form of micelles should be present at the time of injection.

The introduction of persulfate into a polymerizing latex of vinyl acetate resulted in an increase in rate which was directly proportional to the amount of initiator added (Fig. 4). The recipe used was the normal one composed of 180 g water, 60 g vinyl acetate, and 1.2 g SLS. The initial amount of persulfate was 0.05 g (1.0×10^{-3} mole) and the rate before injection was estimated as 0.0113 mole/180 ml-min. (This is the average rate found for 1×10^{-3} mole persulfate in this system.), but when an additional 0.5 g of persulfate was added (as an aqueous solution) the rate increased to 0.0290 mole/180 ml-min. Morton and co-workers[4] found no change in the rate of emulsion polymerization of styrene when more initiator was added.

Salt Dependence. When salt (K_2SO_4, 0.05M), or salt in the form of phosphate buffer (KH_2SO_4/K_2HSO_4), total 0.05M, pH = 7.0 was present, the dependence of rate on initiator was decreased although the rate, at a given initiator concentration, increased. Phosphate buffer increased the rate to a greater extent than did potassium sulfate at the same concentration. The exponential dependence on initiator in the presence of 0.05M buffer was 0.46, while in 0.05M potassium sulfate the dependence was 0.72 (Fig. 5).

When the total salt concentration was adjusted to $12.0 \times 10^{-4}M$ by adding K_2SO_4 to initiator to keep constant ionic strength, the initiator dependency decreased from unity to 0.77, but it was greater than with 0.05M salt. The decrease does indicate, however, that there is a small amount of influence by the initiator acting as a salt.

The particle size of the latices prepared with added salts was difficult to determine because of their instability at high salt concentration. However, a comparison of experiments with zero and 0.05M K_2SO_4 ($[I] = 1.2 \times 10^{-3}$ mole 1. H_2O) showed that the particle diameter doubled at the high salt concentration.

Effect of Possible Decomposition Products. The high order dependence of the rate on the persulfate concentration was puzzling, and it was thought that the decrease in pH during polymerization may have been the reason. In these polymerizations, the pH was initially 5 to 6, but dropped gradually to 3.7 at the end of a polymerization (about 2 hr). The decrease in pH was probably due to accumulation of acidic persulfate decomposition products and/or monomer hydrolysis liberating acetic acid. Experiments were therefore conducted with the deliberate addition of acetic and sulfuric acids to decrease the initial pH to 4.5 and 2.9, respectively; no change in rate could be observed. In a similar set of experiments, acetaldehyde, known to be a product of the acid hydrolysis of vinyl acetate, was deliberately added at the beginning of the polymerization. Again no effect on the rate was found up to a concentration of $8 \times 10^{-3}M$ of acetaldehyde.

Analyses were made for residual persulfate after each run was completed. While induced decomposition had occurred, the remaining persulfate was 70–90% of the initial charge, even though all emulsions were kept at 60°C for $^1/_2$ hr to several hours after completion of a run to insure complete polymerization. We feel, therefore, that while some error is introduced by use of initial persulfate concentrations to characterize the whole run, the error probably averages less than 10% overall, and is less than 20% in the worst case.

Dependence of Particle Formation on Initiator. Polymerizations were run at various initiator ($K_2S_2O_8$) concentrations, and the resultant average particle size of the latices was determined by light scattering. There was a direct relationship between initiator concentration and the final number of particles in the latices. The number of particles per milli-

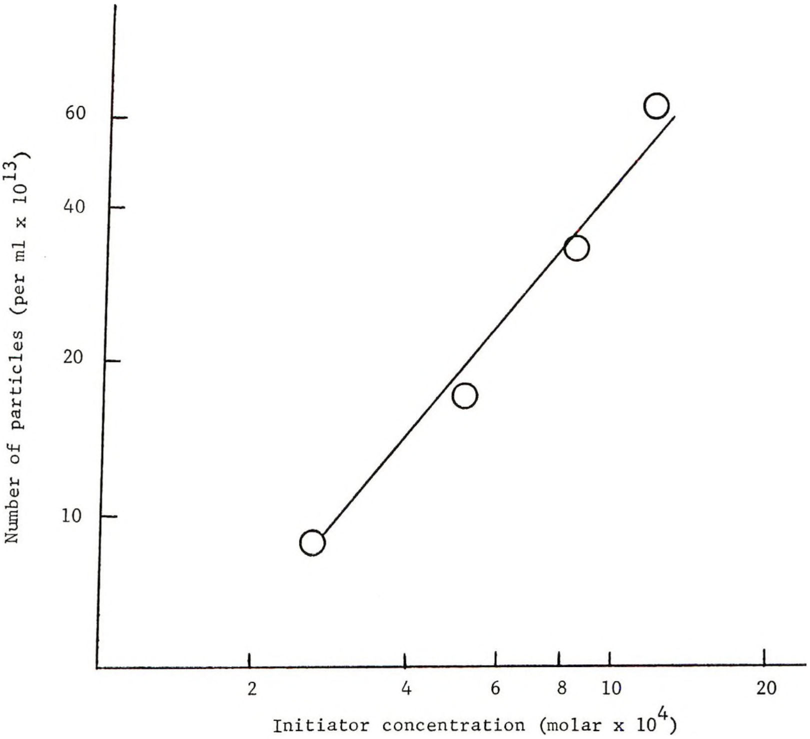

Fig. 6. Effect of initiator concentration on number of particles, log–log plot. Slope = 1.20.

liter of latex was calculated by dividing the average volume of a particle into the total volume of polymer per milliliter of latex

Figure 6 shows the number of polymer particles formed per milliliter at various concentrations of initiator. The number of particles increased with initiator, but at a considerably greater dependence than would be predicted by the Smith-Ewart theory.[2] The log–log plot shown is curved, but has an average slope of 1.2 in this initiator range. The number of particles is known to an accuracy of only ±20%. (From run to run the particle concentrations can vary by this much.) With this range of variation, a straight line is a reasonable approximation. More accurate work over a larger initiator concentration range would be needed to define the exact dependence.

Determination of Particle Size. In general, standard light-scattering techniques were used to measure particle weight average volumes. These have been described earlier.[1] Initial attempts to use the electron microscope to measure the average diameter of unshadowed particles failed as all particles with diameters less than 0.05μ were invisible. One emulsion sample, run 165, was hardened by post-polymerization of styrene, shadowed with germanium to keep the particle temperature low, and photographed by electron microscope. The technique is described, and agreement was found between a weight-average particle weight measured by this method and light-scattering values.[7] For run 165, the number average concentration of particles was 1.7 × 10^{16}/ml. We feel that this technique can count all the particles and have used this determination to correlate the data.

A weight average volume, obtained by light scattering measurements, overestimates the larger particles and therefore underestimates the total number of particles. For surface area calculations, the use of particle concentrations determined from weight-average volumes is even more inappropriate, as the total surface area is very strongly dependent on the number of smaller particles. Thus the value for particle concentration that should be used is at least double that derived from the light-scattering determinations and probably should be larger yet. (We will show that due to the low dependence of rate on particle concentration, the exact value of particle concentration used does not affect the derivation of the rate equations, though it will change the calculated rate constants somewhat.)

Rate and Emulsifier Concentration. The dependence of the rate of polymerization on emulsifier did not follow the Smith-Ewart prediction of 3/5 power but agreed with the results of Motoyama.[8]

No effect on rate was found over a fourfold change in sodium lauryl sulfate concentration. However, the rate was considerably reduced when no emulsifier was present. The results are presented in Table I.

Effect of Monomer–Water Ratio. Varying the monomer–water ratio changes the total volume of polymer possessed by the particles during polymerization. No significant change in rate was observed, however, for a

TABLE I

Effect of Emulsifier on Rate[a]

SLS, g/180 ml H_2O	Rate, mole/180 ml-min
2.4	0.0103
1.2	0.0100
0.6	0.0105
0	0.0036

[a] Persulfate concentration = 8.25 × $10^{-4}M$.

TABLE II

Effect of Monomer–Water Ratio on Rate[a]

Monomer water ratio	Rate, mole/180 ml-min
0.22	0.011
0.33	0.012
0.44	0.010

[a] Persulfate concentration = 8.25 × $10^{-4}M$.

twofold variance in the monomer–water ratio, as shown in Table II. These were very early experiments, however, and were not repeated.

Seed Polymerizations

Two types of seed latex were used in this study. One was composed of very small particles estimated by light scattering to average 0.032 μ in diameter. This work was reported earlier.[4]

The seed reported in this work had larger particles which were measured both by light scattering and electron microscopy. The results of the particle size determinations of this seed are summarized in Table III.

TABLE III
Particle Size

Method	Average diameter, μ
Light scattering	
436 mμ	0.0811
546 mμ	0.0765
Electron microscopy	
Unshadowed	0.0885

Using an average light scattering diameter of 0.079 μ gives a particle concentration in the seed of 1.4×10^{15}/ml H_2O. A calculated value, based on run 165 and the finding that the number of particles is proportional to [I],[1,2] is 1.08×10^{16} particles/ml H_2O. This latter value agrees with results of Elgood, et al.[9] when they used an anionic surfactant. A partial explanation of this difference is in the different methods of measurement. Light scattering measures a weight-average volume which is much larger than the number-average volume. In counting of shadowed particles, the number of particles, N_i, in each diameter interval, d_i, was counted, and an average volume $\bar{V}_n$ calculated as

$$\bar{V}_n = (\pi/6)\ \Sigma\ N_i d_i^3 / \Sigma\ N_i$$

A variation by a factor of two can be expected between the two measurements, and four is far from impossible. Since we were interested in the number of particles we used a value relating to that measurement. The large value for the unshadowed electron microscope diameter is probably due to the lack of visibility of all particles under 0.05 μ diameter.

An extensive study was performed with this seed which involved variation of rate with particle concentration, initiator concentration, emulsifier concentration, and polymer volume. The relative particle size of representative latices was measured by light scattering, and the amount of initiator decomposed was determined. While we will use the value of 1.08×10^{16} particles/ml H_2O for the seed, we will show later that the exact number of particles is unimportant in the kinetic analyses.

TABLE IV
Effect of Emulsifier on Seed Polymerizations[a]

Expt. no.	SLS, g/180 ml H_2O	Rate, mol/180 ml-min	Final number of particles/ml $\times 10^{-14}$[b]
106	0.24[c]	0.00968	3.2
107	0.26	0.00830	
108	0.34	0.00865	
109	0.77	0.00878	2.3
110	2.38	0.00872	2.6
111	3.98	0.00785	

[a] Recipe: 168 g H_2O, 11.2 g of polymer as latex particles; initiator concentration of $8.25 \times 10^{-4}M$, vinyl acetate monomer (44.8 g) to adjust to 25% solids. Rates adjusted to those for 180 ml H_2O.

[b] From light-scattering measurements; initial concentration = 2.8×10^{14}/ml.

[c] No soap added; soap from seed only.

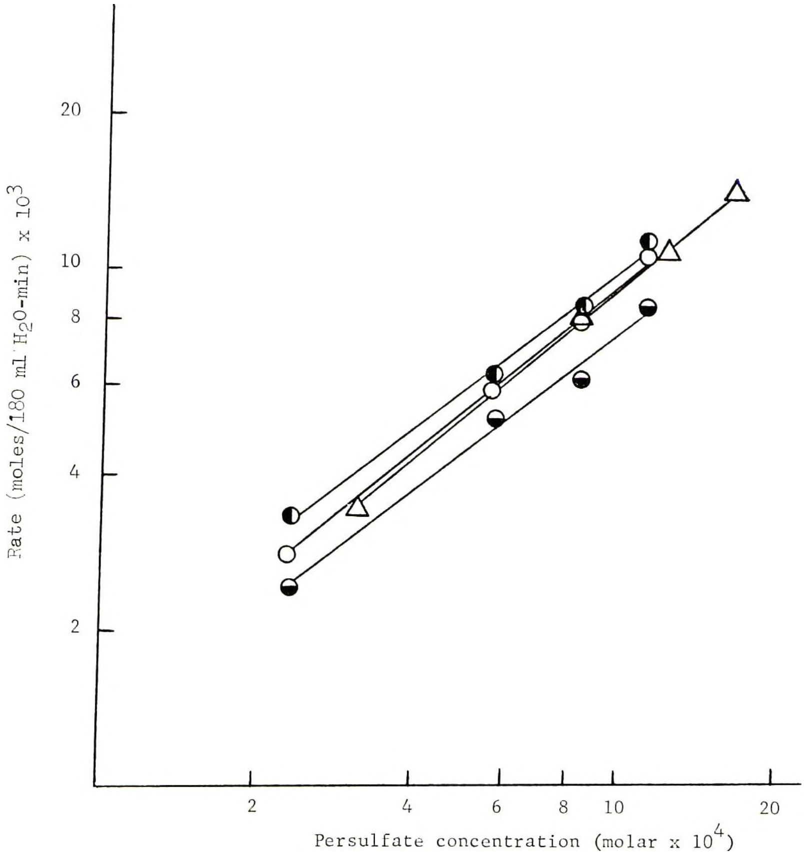

Fig. 7. Rate of polymerization vs. initiator concentration in seeded polymerization at various seed dilutions, log–log plot: (△) 0.50 dilution; (◐) 0.20 dilution; (○) 0.10 dilution; (◒) 0.050 dilution. Average slope $\simeq$ 0.80.

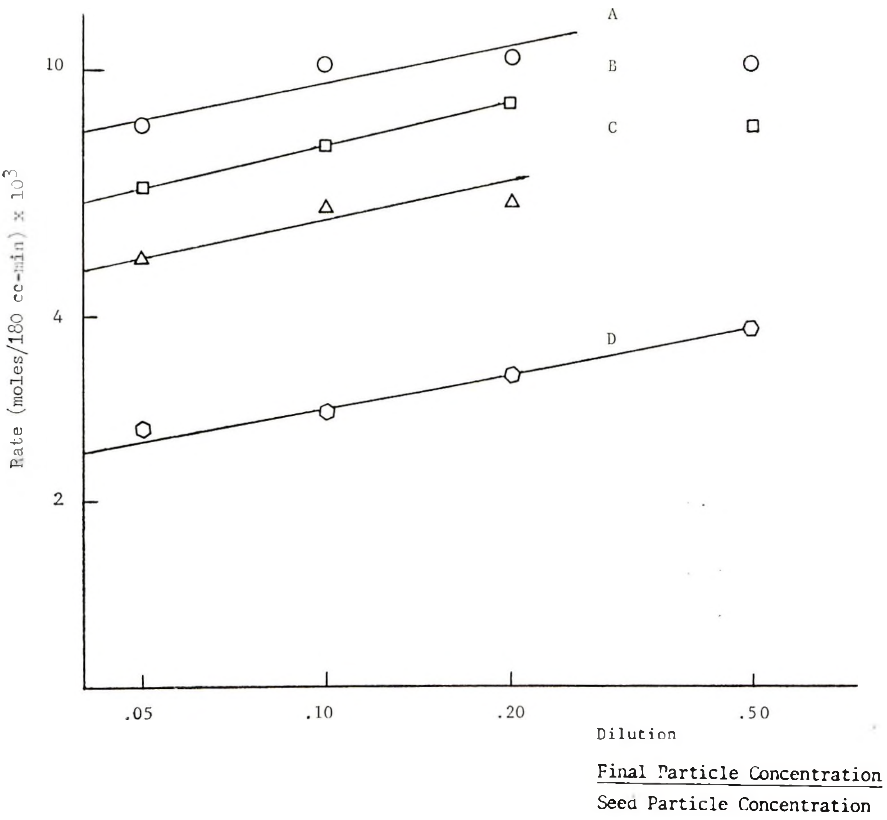

Fig. 8. Dependence of polymerization rate on initial particle concentration of seed, log–log plot at various initiator concentrations: [I] = (*A*) 11.0 × 10^{-4} *M*; (*B*) 8.3 × 10^{-4} *M*; (*C*) 5.6 × 10^{-4} *M*; (*D*) 2.3 × 10^{-4} *M*. Lines drawn at slopes of 0.2; ± 0.02.

Variation of Rate with Emulsifier. The insensitivity of the rates of polymerization toward emulsifier by the standard recipe was confirmed in a similar study on the seed. The original seed was diluted to one-fifth its original concentration and to it was added vinyl acetate monomer to adjust to a total solids of 25%, to which were added calculated amounts of sodium lauryl sulfate. The amount of initiator present in the seed was determined by analysis and then more was added to give the desired final concentration in these experiments of 8.25 × 10^{-4}*M*. The results of the study are given in Table IV. It is apparent that there is only a minor effect due to emulsifier. In fact, the greatest rate was found when no extra emulsifier was added (run 106). The seed emulsion was diluted by five for these experiments. Initial particle concentration was therefore 2.8 × 10^{14}/ml H_2O (light scattering). The particle concentrations for three runs were measured (light scattering) after polymerization and are given in Table IV.

The lack of any significant differences in the particle numbers indicates that even at high emulsifier concentration there is no tendency for new particle formation. If new particles would have been formed, this would

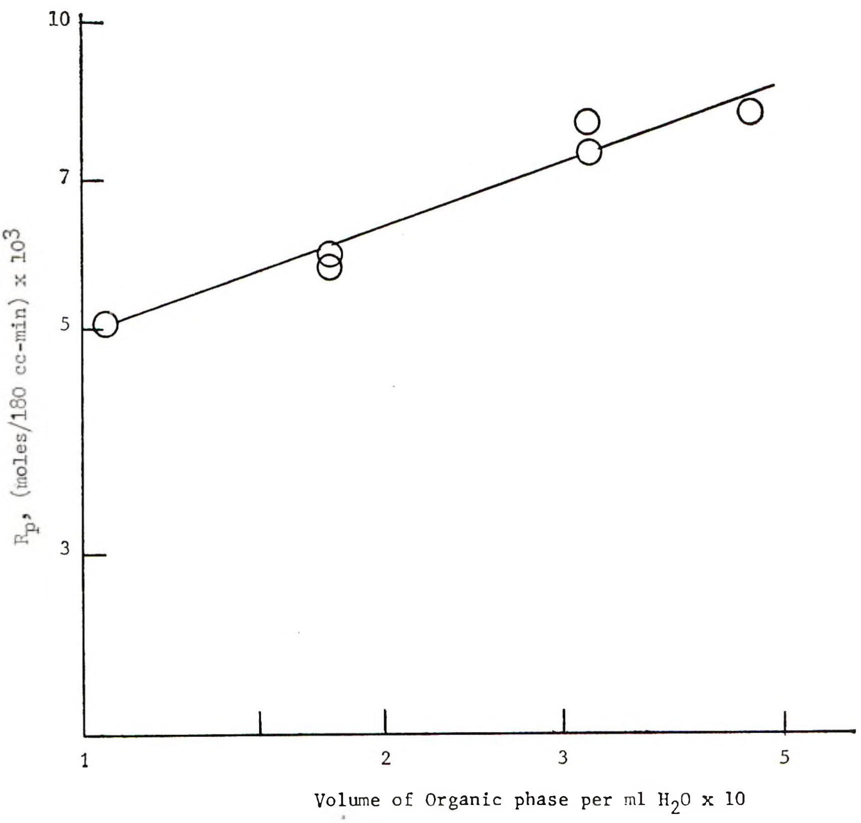

Fig. 9. Dependence of polymerization rate on the volume of the organic phase with $[N_p]$ constant, log–log plot. Slope = 0.35.

be evident in the particle size and the ratio of particles before and after polymerization. A similar study by Vanderhoff and co-workers[10] on styrene emulsion polymerization demonstrated that at high soap concentration new particles were formed. These new particles could be seen in photographs of the magnified latices. Electron-photomicrographs of latex particles in the present work did not reveal any small second-generation particles.

Variation of Rate with Initiator and Particles. The method of study was to polymerize at a given seed dilution while varying the initiator concentration. The initial particle concentration in the seed was calculated as 1.08 $\times 10^{16}$ particles/ml. This was diluted with water to give portions containing $^1/_2$, $^1/_5$, $^1/_{10}$, and $^1/_{20}$ of the concentration in the above seed. These diluted seed latices were then used in the subsequent seed polymerizations. Enough monomer to give 25% solids was added with a small amount of SLS, usually 0.19–0.31%. The emulsifier was added to keep the seed particles from coagulating as they grew and increased their surface area during polymerization. Two important relationships were obtained from this series of polymerizations: the dependence of rate on initiator and on particle concentration. Log–log plots of the initiator and particle dependence are given in Figures 7 and 8.

The average dependence of rate on initiator is about 0.80 and on particles, 0.20. The value for initiator is less than that which was observed for the standard recipe unseeded. The dependence on particles, about 0.20, was also found when seed with small particles was used.[1]

Dependence of Rate on Polymer Volume. This was essentially a repetition of the experiments performed on standard recipe. However, the results with the seed polymerization method were quite different.

Various amounts of monomer were combined with the seed at $^1/_{10}$ dilution. SLS (0.3 g) and persulfate to adjust to $8.25 \times 10^{-4}M$ were added in the recipe. The ratio of volumes of the organic phase to aqueous phase $V_{\text{org}}/V_{\text{aq}}$ was calculated by dividing the total volume of the polymer/monomer phase at the middle of the polymerization by the total volume of water. The correlation between rate and $V_{\text{org}}/V_{\text{aq}}$ is shown in Figure 9. The rate is given in the usual terms of moles/180 ml H_2O-min. It can be seen that rate is proportional to the particle volume to about the 0.35 power.

ANALYSIS OF THE DATA

Before considering a kinetic scheme in detail we can postulate various steps and try to estimate which can be important and which unimportant. This can be estimated from the rates of unimolecular decomposition of catalyst, and the concentration of particles in the polymerizing system.

Two extreme cases of polymerization may be defined; these are polymerization wholly in the aqueous phase and polymerization completely within the particles. Polymerization wholly in the aqueous phase is clearly impossible. The rate of polymerization is affected by the concentration of particles and the relative volume of the organic phase. Also, if the polymerization was in the aqueous phase, the rate should be proportional to the monomer concentration in the aqueous phase. While our first paper[1] suggested that it remained relatively constant even after disappearance of the separate monomer phase, further study showed that the rate was still almost zero order even when the aqueous monomer concentration had decreased by more than 50%. The possibility of polymerization completely in the particles may also be eliminated by a simple consideration of the kinetic results. Smith and Ewart have shown[2] that when there are 0.5 or less radicals per particle and all polymerization is in the particles, the rate of polymerization is first-order in monomer. This is exemplified by the polymerization of styrene (Fig. 2). Vinyl acetate is quite different with the rate of polymerization remaining almost constant to 85% conversion long after the separate monomer phase has disappeared. Therefore, we will consider the complex case where there is polymerization and termination in both phases and try to assess the importance of each.

Calculation of Radical Lifetimes

We shall use the data of experiment 165 (Table V) for the calculations, since the particle size was measured accurately in this case by using the styrene-hardening technique plus shadowing.[7] When considering other experiments, where only the weight average volume W of the particles was measured by light scattering techniques, one must assume particle size distributions similar to those of experiment 165 for seeded and normal polymerizations and hope that the light-scattering measurements would be proportional to the shadowing measurements.

TABLE V
Data for Experiment 165

[I], mole/l.	12×10^{-4}
V_{org}/V_{aq}	0.320
$\bar{V}_p$, cm^3	1.95×10^{-17}
R_p, mole/l. H$_2$O-sec	1.81×10^{-3}

The number of radicals present at any one time can be calculated easily for the case when most of the polymerization is in the organic phase. The monomer concentration in the particles is calculated to be about 6.3M up to 40–50% conversion, as there is a separate monomer phase up to 50% conversion. The number of radicals present can be calculated from the polymerization rate. Rate constants for polymerization and chain transfer are chosen from recent literature.[11a] The best value of k_p is calculated by Ulbricht to be between 9.5×10^3 and 19×10^3 l./mole-sec at 60°C.[11a] The exact values are not important; a change by a factor of 4 would not alter the argument significantly. We will therefore take $k_p \simeq 1.4 \times 10^4$ l./mole-sec, the mean value of Ulbricht.[11a]

$$R_p = k_p\,(\mathrm{R\cdot})(\mathrm{M}_p) = 1.81 \times 10^{-3} = 1.4 \times 10^4 \times 6.3(\mathrm{R\cdot})$$

$$(\mathrm{R\cdot}) = 2.1 \times 10^{-8} \text{ mol./l. H}_2\text{O}$$

where R_p is the rate of polymerization, [R·] is the radical concentration (phase unspecified), and [M$_p$] is the molar concentration of monomer in particles. (An equal number of radicals could be present in the aqueous phase without changing R_p significantly, as [M$_{aq}$], the concentration of monomer in the aqueous phase, is only 0.32 mole/l. when saturated.) The lifetime τ_p of a radical in the particles is calculated by dividing the average number of radicals by the rate of radical production. (For this case, $2k_1[\mathrm{I}] = 2 \times 10^{-8}$ mole/l.-sec as $k_1 = 8.3 \times 10^{-6}$ sec^{-1}.[12])

$$\tau_p = 2.1 \times 10^{-8}/2 \times 10^{-8} = 1.05 \text{ sec}$$

The number of monomer units polymerized per radical is therefore:

$$k_p[\mathrm{M}_p]\tau_p = (1.4 \times 10^4)(6.3)(1.05) = 9.0 \times 10^4$$

The number of chain transfers to monomer per radical, which will be a crucial factor in deciding on a kinetic scheme, is calculated below. The chain transfer constant of vinyl acetate radical to monomer C_t was found to be between 2.0 and 2.8 $\times 10^{-4}$ by recent workers.[11b] We have picked 2.5 $\times 10^{-4}$ as an average. The rate constant for chain transfer is then $k_{ct} = C_t k_p$ and is 3.5 l./mole-sec, and the number of chain transfers per radical is then:

$$k_{ct}[M_p]\tau_p = (3.5)(6.3)(1.05) = 23$$

Even if much of the polymerization is in the aqueous phase, the last figure remains the same.

If all polymerization is in the organic phase, the number of particles containing radicals is the same as the number of radicals present. This is

$$2.1 \times 10^{-8} \text{ mole/l. } H_2O \times 6.02 \times 10^{23} = 1.26 \times 10^{16} \text{ particles/l. } H_2O$$

The total number of particles in this volume at an organic phase volume of 320 cm^3 is $320/1.95 \times 10^{-17} = 1.64 \times 10^{19}$ particles/l. H_2O.

Since maximally 1.26×10^{16} particles are occupied, about one particle in 1300 contains radicals at any one time. [For the concentration of particles measured by light scattering, one particle in 180 contains a radical.] If some polymerization occurs in the aqueous phase, the proportion of particles containing radicals is even lower. This means that the standard Smith-Ewart picture[2] (case 2), where 50% of the particles contain radicals at any time, does not apply.

Case 1 of the Smith-Ewart theory,[2] where chain transfer and free diffusion is postulated, can be considered since only a small fraction of particles need be occupied. However, in the kinetic equations derived by Smith and Ewart, the polymerization rate has a one-half-order dependence on initiator and a first-order dependence on monomer. We find first-order dependence on catalyst and an almost zero-order dependence on monomer. These are major deviations; there are other minor ones. Therefore, the polymerization does not follow the postulated case 1 kinetics. This does not mean that the Smith-Ewart model is inapplicable; it is just that, with vinyl acetate, a water-soluble monomer, other factors must be considered as well as those in the original model.

Presentation of the Kinetic Picture

The model of polymerization given here is basically the same as that presented in the first paper of this series.[1] The initial stage, where particles are being generated, can not be understood on the basis of the data we have gathered. We therefore start where the number of particles is stabilized—at about 10–20% conversion in unseeded polymerizations. Unimolecular decomposition of persulfate generates two radical ions which react with vinyl acetate in the aqueous phase. Efficiency is considered as 100% for convenience. A lower efficiency will increase radical lifetimes. The polymer molecule, $P\cdot_{aq}$, then grows in the aqueous phase. adsorbing soap molecules as it grows; $[P\cdot_{aq}]$ denotes the molar concentration of these growing polymer molecules in the aqueous phase. It becomes thus a polyelectrolyte and can not be swept up easily by a particle which is also electrically charged. After numerous collisions with many particles, it is absorbed and continues its growth within the particle. Even if absorption occurs at a $\overline{DP}$ of 100, only 2.5% of the polymerization would be in the aqueous phase. (This implies that polymer absorption by an emulsion particle is not diffusion controlled. If it were, radicals would have only one or two units polymerized before they were swept up. We have reported previously[1] that substantial amounts of polymer are found in the aqueous phase in some cases.) Chain transfer to monomer can occur in either phase. The chain transferred monomer radical ($M\cdot$) re-initiates polymerization by cyclizing. (The carboxymethylene radical attacks the vinyl group to form a butyrolactone radical.) This is almost completely excluded from the organic phase; it is much more soluble in water than in a vinyl acetate–poly(vinyl acetate) solution, and therefore the new polymer molecule ($B\cdot$) starts growing in the aqueous phase. While $B\cdot$ is still uncharged, it can react with other aqueous radicals and thus possibly terminate. As it grows, it will adsorb soap and become a polyelectrolyte. Thus the sequence starts again.

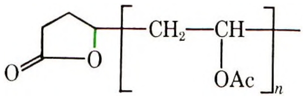

$0 < n < 10$

B·

Persulfate can be attacked by any radical in the aqueous phase. However, only attack by $M\cdot$ or $B\cdot$ may affect the rate of polymerization.

Termination steps can not be deduced *a priori*. Seven are possible: *(1)* sweep-up of an aqueous radical, $P\cdot_{aq}$, by a particle containing a radical; *(2)* reaction of $B\cdot$ with $P\cdot_{aq}$, *(3)* reaction of two aqueous radicals; *(4)* reaction of a chain-transferred radical $M\cdot$ with an aqueous radical; *(5)* reaction of $M\cdot$ with a radical in a particle; *(6)* reaction of $B\cdot$ with a radical in a particle; *(7)* reaction of $B\cdot$ with itself. These are discussed in the next section.

The polymerization model is almost static while a separate monomer phase remains, except that the particles are increasing in size. After about 40–50% conversion, monomer concentration in the particles, $[M_p]$, starts decreasing but the rate of polymerization remains constant to 85% conversion. It seems likely that the model remains fairly faithful up to this conversion. Above that the first termination step (Smith-Ewart type) may become dominant. We will attempt to show that the picture as presented, postulating the major termination reactions to be steps (1) and (2) above is an adequate description of vinyl acetate emulsion polymerization. After the mathematical consequences of the model have been developed, we will give a more refined picture of the polymerization.

Justification for Postulated Kinetic Steps

The model outlined in the last section can be written as a sequence of elementary reactions. All are fairly well defined and are normal reactions of vinyl acetate and initiator. The kinetics are modified only because we are operating in a two-phase system containing an ionic soap. The postulated termination steps seem reasonable also, but all can not occur at significant rates. The next task is then to analyze the various steps in the light of the data and known rate constants of vinyl acetate polymerization in order to decide which are important.

$$I \rightarrow 2\cdot\mathrm{SO_4^-} \tag{1a}$$

$$\cdot\mathrm{SO_4^-} + M_{\mathrm{aq}} \rightarrow \mathrm{P}\cdot_{\mathrm{aq}} \tag{1b}$$

$$\mathrm{P}\cdot_{\mathrm{aq}} + \mathrm{M}_{\mathrm{aq}} \rightarrow \mathrm{P}\cdot_{\mathrm{aq}} \tag{2}$$

$$\mathrm{P}\cdot_{\mathrm{aq}} + \mathrm{M}_{\mathrm{aq}} \rightarrow \mathrm{PH} + \mathrm{M}\cdot \tag{3}$$

$$\mathrm{P}\cdot_{\mathrm{aq}} + \mathrm{Particle} \rightarrow \mathrm{P_p}\cdot \tag{4}$$

$$\mathrm{P_p}\cdot + \mathrm{M_p} \rightarrow \mathrm{P}\cdot_{\mathrm{p}} \tag{5}$$

$$\mathrm{P}\cdot_{\mathrm{p}} + \mathrm{M_p} \rightarrow \mathrm{PH} + \mathrm{M}\cdot \tag{6}$$

$$\mathrm{M}\cdot \rightarrow \mathrm{B}\cdot\ \text{(cyclization)} \tag{7}$$

$$\mathrm{B}\cdot + \mathrm{M}_{\mathrm{aq}} \xrightarrow{\text{soap}} \mathrm{P}\cdot_{\mathrm{aq}} \tag{8}$$

$$\mathrm{M}\cdot + \mathrm{I} \rightarrow \mathrm{MSO_4^-} + \cdot\mathrm{SO_4^-} \tag{9a}$$

$$\mathrm{B}\cdot + \mathrm{I} \rightarrow \mathrm{BSO_4^-} + \cdot\mathrm{SO_4^-} \tag{9b}$$

$$\mathrm{P}\cdot_{\mathrm{aq}} + \mathrm{P}\cdot_{\mathrm{p}} \rightarrow \text{Termination} \tag{10a}$$

$$\mathrm{P}\cdot_{\mathrm{aq}} + \mathrm{B}\cdot \rightarrow \text{Termination} \tag{10b}$$

$$\mathrm{P}\cdot_{\mathrm{aq}} + \mathrm{P}\cdot_{\mathrm{aq}} \rightarrow \text{Termination} \tag{10c}$$

$$\mathrm{P}\cdot_{\mathrm{aq}} + \mathrm{M}\cdot \rightarrow \text{Termination} \tag{10d}$$

$$\mathrm{P}\cdot_{\mathrm{p}} + \mathrm{M}\cdot \rightarrow \text{Termination} \tag{10e}$$

$$\mathrm{P}\cdot_{\mathrm{p}} + \mathrm{B}\cdot \rightarrow \text{Termination} \tag{10f}$$

$$\mathrm{B}\cdot + \mathrm{B}\cdot \rightarrow \text{Termination} \tag{10g}$$

The following analyzes the kinetic steps where this is needed and provide some justification from the literature for the more unusual postulates.

The reaction of the sulfate radical ion $\cdot\mathrm{SO_4^-}$ with monomer [eq. (1)] is assumed to be quantitative. Catalyst efficiency is low even so, due to a large amount of induced decomposition. A portion of this could be due to steps (9a) and (9b). If addition of $\cdot\mathrm{SO_4^-}$ to monomer is less than 100%, the arguments presented below become even stronger.

Equation (2) is the propagation step, $k_2 = k_5 = 1.4 \times 10^4$ l./mole-sec.[11a] The rate constant for propagation is considered to be identical in water and vinyl acetate; it is known that radical rate constants are essentially unaffected by the medium. We will therefore use k_5 as the rate constant for polymerization in both media.

For step (3), $k_3 = k_6 \simeq 3.5$ l/mole-sec.[11b] The rate constant for chain transfer to monomer is again considered to be the same in both media. We will therefore use k_6 as the symbol for the chain transfer constant in both media.

In step (4), a growing radical in the aqueous phase is assumed to be stabilized by adsorbed soap. This has not been demonstrated explictly to our knowledge, for example, by polymerizing a saturated solution ($0.3M$) of vinyl acetate in water, in the presence of sufficient soap to stabilize all the molecules formed. This should be about $0.05M$ of sodium lauryl sulfate, just about the critical micelle concentration (CMC). Our previous work[1] showed that a large amount of polymer can be stabilized in the aqueous phase even when particles are formed. It has also been shown that poly(vinyl acetate) dissolved in soap solution remains as a polyelectrolyte in the aqueous phase even when the soap is diluted to below the CMC.[13–15]

The stabilizing effect on anionic surfactants on the particle size at very low monomer concentration was shown by Napper and Alexander,[16,17] where a concentration of sodium cetyl sulfate of 8.7×10^{-5}M (about one fifth of the C.M.C.) decreased particle volumes about fiftyfold over none or a non-ionic surfactant. Priest[18] has reported similar effects.

Eventually the growing radical is swept up by a particle after many collisions. The sweeping up is not a simple case of diffusion; if it were, the radical would be absorbed before it could grow at all and we would be dealing with the normal Smith-Ewart case 1.[2] Therefore, collision theory is applicable where the sum of the cross-sectional areas of the colliding particles (in this case a polymer molecule and a large particle) must be considered. The rate in such a case should be proportional to the product of the concentration of aqueous radicals, the concentration of particles, and the collision volume of the two. The last term may be written as

$$\text{Collision volume} \propto 4\pi(R + r)^2\bar{\delta}r$$

where R and r are the radii of the particle and aqueous radical, respectively, and $\bar{\delta}r$ is the shell thickness around the particle where reaction can take place.[19] If, as in this case, the particle is much larger than the aqueous radical, $r \ll R$, the collision volume simplifies to $K4\pi R^2\bar{\delta}r$. If all constants are subsumed under one rate constant k_4, and particle radius R is changed to particle diameter d, the rate of sweep-up would then be $k_4[\mathrm{P}\cdot_{\mathrm{aq}}]d^2\,[\mathrm{N_p}]$ (where $[\mathrm{N_p}]$ is the molal concentration of particles), which we will use in the subsequent discussion.

The rate constant for step (4) should be affected by salt concentration. An increase in the salt concentration will decrease the thickness of the electrical double layer and allow polymer chains to be swept up more easily. Thus, k_4 should increase as salt concentration increases.

If some fraction f of the particles contains radicals, the rate of step (4) is then $k_4d^2N_\mathrm{p}(1\text{-}f)[\mathrm{P}\cdot_{\mathrm{aq}}]$. Step (10a) would then have a rate of $k_4d^2N_\mathrm{p}f(\mathrm{P}\cdot_{\mathrm{aq}})$. We have shown that in a typical polymerization f is about 1/1,300.

Step (7) is postulated to be cycloaddition which regenerates a radical of about the same reactivity and electronegativity as the vinyl acetate radical:

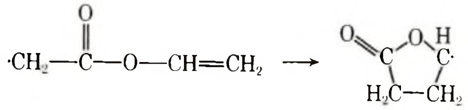

This reaction is the expected one. In order to start a new chain, the carboxymethylene radical must add to a vinyl group. The only question one can ask is then: does the radical add to a vinyl group on a different molecule or to the adjacent vinyl group? Since a five membered ring will be formed, cycloaddition to form a butyrolactonyl radical should be favored greatly over intermolecular addition. In free radical polymerization of nonconjugated dienes, cyclization to form five- or six-membered rings is much faster than intermolecular attack.[20]

The rate constant of step (7) can be estimated to about a factor of 10 from the literature as shown in Table VI and the following discussion.

By eliminating the electron-donating methyl group and also its steric hindrance, acrylate radicals become about ten times as reactive as the corresponding methacrylate radicals towards vinyl acetate. Since on going to the carboxymethylene radical, a further electron-donating group with high steric hindrance is removed, we would expect k_{12} to be at least ten times higher than that of the acrylate radical in adding to a vinyl acetate molecule. In addition, when the vinyl group is on the same molecule, entropy considerations increase the rate of reaction still further. From experimental data, Butler[20] shows that cyclopolymerization of nonconjugated dienes to six-membered rings must occur about 20 to 50 times as rapidly as addition to another molecule at 5–10M monomer concentration. The rate

TABLE VI

Calculation of Rate Constant of Reaction of Various Radicals with Vinyl Acetate[a]

Radical	k_{11}, l./mole-sec	$r_1 = k_{11}/k_{12}$	k_{12}, l./mole-sec
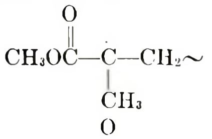 $CH_3OC(=O)-\dot{C}(CH_3)-CH_2\sim$	400–600[b]	20–22[c]	~20–30
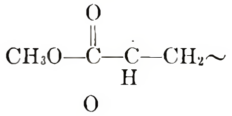 $CH_3O-C(=O)-\dot{C}H-CH_2\sim$	1000–2000[d]	9 ± 2.5[e]	~100–200
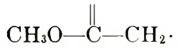 $CH_3O-C(=O)-CH_2\cdot$			>1,300–2000 (estimate)

[a] k_{11} and k_{12} are the rate constants for attack of a radical on its own monomer, k_{11}, and on a different monomer, k_{12}.

[b] Literature value.[11c]

[c] Literature data.[11d]

[d] Literature data.[11e]

[e] Literature data.[11f]

constant for cyclopolymerization to a six-membered ring therefore is about one hundred times greater than the rate constant for normal polymerization.

While data on free-radical cyclopolymerization to form five-membered rings are almost nonexistent, there are data on nucleophilic cylization of compounds to form five- and six-membered rings. In a case quoted by Hine,[21] cyclization of $NH_2(CH_2)_nBr$ has a rate constant of 0.5 sec^{-1} when $n = 4$, and only 0.008 sec^{-1} when $n = 5$, with formation of five- and six membered rings, respectively. This is a factor of about 60 in favor of the five membered ring. Hine also states that two factors control the cyclization rate. Below the five-atom ring, ring strain is important. From the five-atom ring up, where ring strain is negligible, entropy factors control the rate. Thus, a five-membered ring will form faster than a six-membered ring in most cases, since the reacting groups tend to be closer. The factor seems to be about 50 to 100.

Other data confirm the estimate in a general manner, though with nucleophilic reactions in solvating media, the picture tends to be confused. In the cyclization of phenyl chloroalkyl sulfides to the corresponding sulfonium ions, the rate of closure to a five-membered ring was 76 times as fast as that to form a six-membered ring.[22]

The hydrolysis of chlorohydrins in water showed that the five-membered ring formed about 25 times as rapidly as the six-membered ring.[23]

The hydrolysis of phenyl hydrogen succinate is 140 times faster than the hydrolysis of phenyl hydrogen glutarate[24] at pH 7.0 and 25.3°C.

While other data could be added to the list, these are the best as the others involve either very good leaving groups, which tend to diminish the role of the attacking group, or the reacting groups are already part of a ring, and the steric factors are not comparable. Of the cases presented, the last comes the closest to the vinyl acetate case, in that cyclization can occur without immediate elimination of the leaving group, and the geometries are reasonably close.

When the data of Butler[20] are combined with those reported above,[21–24] we reach the conclusion that cyclization to form a five membered ring should be about 10^3 to 10^4 faster than attack of a $\cdot CH_2COOR$ group on another vinyl group. Since the rate constant for this reaction is at least 2×10^3/sec. (eliminating the monomer concentration by assuming 1 M), the rate constant for cyclization must be about 10^6–10^7/sec. This estimate is very important as it gives us a criterion to judge between the different termination steps.

Butyrolactone is very water-soluble, and the partition coefficient favors water rather than vinyl acetate. (We have partitioned butyrolactone between vinyl acetate and water in our laboratory. At a 0.25 weight fraction of vinyl acetate, $^5/_6$ of butyrolactone was found to be in the aqueous phase. Since the particles contain 50% polymer or more, the partition coefficient should be even more in favor of the water than with pure vinyl acetate.) In such a case, polymerization initiated by a butyrolactonyl radical would start in the water phase. The polymer, stabilized by the lactone end, would have difficulty diffusing into the particles, and would rapidly add soap as it grows.

If the cycloaddition step occurred while M· was in the organic phase, one might expect that polymerization should start there. However, at normal rates of diffusion, a small molecule such as butyrolactone can diffuse out of a particle long before it has time to react. This is easily demonstrated. The particles have average diameters of about 0.1 μ (10^{-5}cm) or less. A radical formed in such a particle would have to diffuse an average of 0.05 μ to escape. If its diffusion constant is about 10^{-5} cm^2/sec, a normal one for small molecules, the time it takes to diffuse out can be estimated to be about 10^{-6} sec. At a monomer concentration in the particles of 6 molar, a radical would react in about 0.3×10^{-4} sec. Thus, almost all radicals will escape before reaction.

While the butyrolactonyl radical is in the aqueous phase [eq (8)] it can do two things. It may add monomer or react with growing polymer molecules in the aqueous phase, $P\cdot_{aq}$ [step (10b)]. Even though it adds several monomer units, it will still be able to react with $P\cdot_{aq}$ until it picks up a soap molecule and becomes charged. (The soap concentration is considered the equilibrium concentration obtained in the presence of partly covered particles. It should depend only slightly on the fractional surface area of the particles covered).

There will be an average size for B· when it picks up soap, probably when it has added between five and ten monomer units. We take five units as the minimum number necessary to adsorb one molecule of sodium lauryl sulfate because we consider the adsorption due to hydrophobic bonding. Therefore the polymer molecule needs to be about as long as the soap molecule for the two to interact. Since soap is obviously picked up soon after this point, polymer molecules in dilute aqueous soap solution are stable,[1,13-15] we have taken the value of $5 < \overline{DP} < 10$ for the length at which the first soap molecule is adsorbed. The rate of transformation of B· into $P\cdot_{aq}$ is then the rate at which the butyrolactonyl radical adds five to ten monomers in the aqueous phase before picking up soap. This means that $k_8 = k_2/n$ where $5 < n < 10$ and is therefore about $2 \times 10^{+3}$ l./mole-sec.

We can now calculate the approximate rate at which B· will terminate with $P\cdot_{aq}$. The lifetime of B· before transformation to $P\cdot_{aq}$ is the reciprocal of k_8 $[M_{aq}]$ and will be about 10^{-3} to 2×10^{-3} sec. Since k_{10b} will be about $5 \times 10^{+8}$ l./mole-sec, the normal bulk termination rate constant for vinyl acetate radicals, with a concentration ($P\cdot_{aq}$), for example, of $\sim 10^{-7}$ mole/l., the highest concentration possible, average lifetime before termination of B· would be 2×10^{-2} sec. At the very worst, therefore, the B· radicals would go through ten to twenty cycles before terminating. Since we found above that each radical undergoes about 25 chain transfers before termination, the above calculations make steps (8) and (10b) quite reasonable kinetically. Of course, there is a severalfold uncertainty factor in all these estimates.

A second induced decomposition step, in addition to eqs. (9), is $P\cdot_{aq}$ + I → $P\text{-}SO_4^-$ + $\cdot SO_4^-$. This was omitted because it does not affect the rate of disappearance of monomer, the function we are most interested in. No accurate measurements were made on properties which would have been affected by this step. The question still remains—while much induced decomposition can occur by steps (9a) and (9b), is this reaction rapid enough to remove a kinetically significant percentage of B· or M·? We believe it is not. The value for k_{9b} is estimated to be about 10^2 l./mole-sec.[11g] Rate constant k_{9a} will be lower. Since the concentration of initiator is $\sim 10^{-3}\,M$ or less, the minimum lifetime of B· or M· would have to be greater than 10 sec if all disappeared by chain transfer. Twenty-five cycles of M· to B· or B· to $P\cdot_{aq}$ would take a maximum of about 0.05 sec. Thus, chain transfer to I converts less than 1% of the radicals at most and is not kinetically significant. These steps will therefore be omitted from the subsequent kinetic development.

Step (10a) is not the termination step postulated by Smith and Ewart,[2] though related to it. In their case, sweep-up of the growing radical is diffusion-controlled, while in our case it is not. Although we have shown that standard Smith-Ewart kinetics cannot apply, this step must be considered, as significant fraction of radicals may terminate in this way.

Step (10b) is probably the major termination step; the calculations show that this is a reasonable postulate. It will be shown that none of the other termination steps fit as well.

The termination step (10c) is unlikely. The strongest argument against it is that solutions of poly(vinyl acetate) in water stabilized by soap are quite stable even when the soap is below the critical micelle concentration.[15–18] In fact, we found it impossible to precipitate all the polymer from the aqueous phase in one case, even when using 10% $MgSO_4$ solution as a coagulant.[1]

Since step (10c) requires the collision of two polymeric radicals in the aqueous phase to produce termination, it implies that the molecules are unstable as polyelectrolytes and react with each other in a matter of seconds. We think that a collision extensive enough to allow the reaction of the buried radical ends would entangle the molecules sufficiently so that they would not easily separate again. After several such collisions between molecules, which could be dead, a particle would be formed. Since these solutions are quite stable, step (10c) cannot be very important.

We can calculate whether reaction (10d) should occur. If M· has the same partition coefficient as vinyl acetate, it would spend about one sixth of its time in the aqueous phase at the organic/aqueous ratio used. The concentration of $P\cdot_{aq}$ may be as much as 10^{-7} mole/l. (25% polymerization in the aqueous phase.) Since the cross-termination rate will be at least five to ten times the solution termination rate constant for vinyl acetate radicals (the cross-termination rate constant would therefore be $k_{10d} \simeq 5 \times 10^{+9}$ l./mole-sec) the average lifetime for M· before termination would be 2×10^{-3} sec or more.

We calculated previously that each radical undergoes about 25 chain transfers before termination. Above we calculated an average lifetime of M· before cyclopolymerization of 10^{-6}–10^{-7} sec. Since step (7) must occur about 25 times for each termination, the average lifetime for M· before termination must be about 2.5×10^{-5} sec if step (10d) is significant. Comparing the lifetime of M· calculated from steps (7) and (10d), we find that even under these conditions (25% polymerization in aqueous phase) a maximum of 1% of the termination could be by step (10d). Thus, this step could be important only if the cross-termination rate constant is one hundred times or more that of the homotermination constant and at least 25% of the polymerization is in the aqueous phase. Thus this termination step will be omitted since M· probably cyclizes much faster than it can react with $P\cdot_{aq}$.

Step (10e) can be eliminated by the same sort of reasoning. For it to be important, it must occur about 0.04 times as often as step (7) or the rate per M· must be about 4×10^4 sec^{-1} or greater. This means a lifetime before termination of 2.5×10^{-5} sec.

We showed that a small molecule can diffuse into and out of a particle in about 10^{-6} sec. If we assume free diffusion, since only 25% of the volume is organic, a radical will diffuse into a new particle every 4×10^{-6} sec. Thus it can diffuse into only about six particles before termination, if step (10e) is to be important. Since only one particle in 1300 contains a radical, it is easily seen that this termination step is not important. (Even if one particle in 180 contains a radical, this step is not significant.) Thus, the only kinetically significant reaction M· undergoes is cyclopolymerization.

Step (10f) cannot be easily eliminated by *a priori* argument. However, since B· has a highly polar butyrolactonyl end which is highly water-solvated, sweeping up of this radical by a particle should be activation-controlled rather than diffusion controlled. If that is the case, it can be lumped together with step (10a), as both will have similar rate constants and dependencies. We shall consider B· then to act exactly like $P\cdot_{aq}$ in a sweep-up. However, it is much smaller and present in lower concentration than $P\cdot_{aq}$. Thus step (10f) will probably not be important compared to step (10a).

A hypothetical concentration of B· can be calculated easily for any case, since the rates of polymerization were measured. It should equal the rate of its formation divided by the rate of its disappearance: $[B\cdot] \simeq k_6 f[N_p][M_p]/k_8[M_{aq}]$. This should be about 1.0×10^{-8} mole/l. for run 165, one of the fast polymerizations. Other runs should have lower concentrations.

The average lifetime of B· in run 165 if it disappeared by step (10g) alone, $k \simeq 5 \times 10^8$ l./mole-sec, would be then about 0.2 sec. Since it transforms into $P\cdot_{aq}$ in about 10^{-3}–2×10^{-3} sec, step (10g) can only be a minor termination step in the cases we are considering though it may become important for runs with very high polymerization rates. It will not be discussed further.

Evaluation of Kinetic Equation and Correspondence of Theory with Data

In the previous section, we presented a model for the emulsion polymerization of vinyl acetate and examined each step critically. Justification for the inclusion or rejection of each step was presented. From all the steps considered, it was found that steps (9a) and (9b) were kinetically insignificant, as were all the termination steps except steps (10a) and (10b). Kinetic equations based on this model are developed in Appendix I. The final rate equation, ignoring polymerization in the aqueous phase, is given below.

$$R_p = -dM/dt = (k_5/k_6)(k_1k_6[\mathrm{I}][\mathrm{N_p}][\mathrm{M_p}])^{1/2}(1 + (k_{10b}k_6[\mathrm{M_p}]/k_4k_8\mathrm{d}^2[\mathrm{M_{aq}}]))^{-1/2} \quad (11)$$

All terms in eq. (11) are known (rate constants), or are experimentally available, except for the combination of rate constants in the last term, k_{10b}/k_4k_8. Thus, at constant ionic strength, there is only one parameter to be determined. This can be found by using the data from run 165. We should then be able to tell whether we must consider aqueous polymerization.

We shall use the data given in Table V for run 165 and the rate constants discussed above. Since $[\mathrm{N_p}]$ is 2.4×10^{-5} molal, d^2 is easily calculated and equals 1.2×10^{-3} μ^2/particle. $(\mathrm{M_{aq}})$ was found to be 0.32 mole/l. at 60°C,[25] while $(\mathrm{M_p})$ is about 6.3 mole/l. when excess monomer is present. On substituting these values and known rate constants into eq. (11), we find that $k_{10b}/k_4k_8 = 4.25 \times 10^{-4}$ mole-sec-μ^2/l. (If the lower value of $[\mathrm{N_p}]$ is used, $[\mathrm{N_p}] = 3.1 \times 10^{-6}$ molal, k_{10b}/k_4k_8 is calculated to be 1.3×10^{-4} mole-sec-μ^2/l. which does not affect the arguments.)

We know approximate values for k_8 and $k_{10.2}$ (these were discussed above), and we can therefore solve approximately for the value of k_4 in run 165. From this, we can estimate the fraction of aqueous polymerization. The value of k_4 is then 5.5×10^8 with an uncertainty factor of at least 300%. The lifetime of $\mathrm{P\cdot_{aq}}$ is then calculated from $1/\tau = k_4d^2[\mathrm{N_p}]$; $\tau = 0.06$ sec. In this time, $\mathrm{P\cdot_{aq}}$ will polymerize about 260 monomer units and thus will account for about 6% of the total polymerization. Of course, within the estimate of error it means that aqueous polymerization may be between 2 and 15% for run 165. (If the lower value for $[\mathrm{N_p}]$ is used, aqueous polymerization may be between 1.5 and 12% of the total.)

Two facts emerge from this analysis. First, aqueous polymerization may be important in cases where there are very few particles (seeded polymerizations) and therefore the whole equation must be considered in correlating experimental and theoretical dependencies of R_p. Secondly, and very important, the model is internally consistent. Using the best literature values for rate constants, we find that there is aqueous polymerization which gives fairly large molecules before sweep-up. It is such that the fastest polymerizations will still conform to the model and the slowest will still have most of the polymerization in the organic phase.

Two factors not in the kinetic equations must be considered before the equations can be tested. First, the dependence of $[\mathrm{N_p}]$ on $[\mathrm{I}]$ was measured, and we found that $[\mathrm{N_p}] \propto [\mathrm{I}]^{1.2}$. At present this is not explainable. Secondly, there is a strong dependence of rate on the ionic strength μ of the water phase. This is reasonable; k_4 should depend on the ionic strength as two electrically charged species must interact, and thus R_p depends on the ionic strength. The best empirical approach is to multiply k_4 by a factor dependent upon ionic strength. The dependency is picked to reproduce the best tested relationship, $R_p \propto [\mathrm{I}]^{1.0}$, where the ionic strength is due to the initiator added, $K_2S_2O_8$. A good fit is found when the dependence is to the 0.60 power:

$$k_4 = k_4' (\mu)^{0.60} \simeq 1.60 \times 10^{10} \mu^{0.60} \simeq 5.5 \times 10^8 \text{ (Run 165)}$$

$$2 \times 10^8 < k_4 < 17 \times 10^8$$

or

$$k_{10b}/k_4k_8 \simeq 1.46 \times 10^{-5} \mu^{-0.60} = 4.25 \times 10^{-4} \text{ (Run 165)}$$

We can now proceed to compare theory with experiment, having solved for our two adjustable parameters. (In the following treatment, we will ignore polymerization in the aqueous phase. We get a slightly better fit and much greater mathematical simplicity if aqueous polymerization is neglected. If it is 2% for run 165 it is not more than 10% for any run in the range investigated. The lower value of 2% for run 165 is probably therefore the better one, as aqueous polymerization can be neglected.) Five dependencies were investigated quantitatively and several others qualitatively. Therefore, the fit should be a good test of the model. In addition, the course of the polymerization under various conditions will be looked at. The equation should also reproduce the kinetic curves.

Equation (11) can be written for polymerization at 60°C by putting in the estimated values for the rate constants, and including the dependence on ionic strength. This is given as eq. (12)

$$R_p = 21.2([\mathrm{I}][\mathrm{M_p}][\mathrm{N_p}])^{1/2}/(1 + 5.1 \times 10^{-5}{-}\mu^{0.60}[\mathrm{M_p}]/d^2[\mathrm{M_{aq}}])^{1/2} \quad (12)$$

The comparison of experimental with calculated dependencies is shown in Table VII.

It can be seen that the fit between all calculated and quantitative experimental results is within the limit of error for the values found. From Figure 3, one can see that reproducibility of a run is about ±5% with an occasional deviation of as much as 20%. Thus over a tenfold range in variable concentration, e.g., $[\mathrm{I}]$ or $[\mathrm{N_p}]$, error in dependence of rate of polymerization on that variable could be as high as ±0.1 in the exponent if only one set of experiments were run. As more are run, we can be more confident of the dependency found. At this stage we see again that the

TABLE VII
Comparison of Experimental and Predicted R_p from Equation (2) as a Function of Polymerization Variables

	Theoretical	Experimental
Unseeded polymerizations		
Constant ionic strength, $[N_p] \propto [I]^{1.2}$	$R_p \propto [I]^{0.70}$	$R_p \propto [I]^{0.77}$
No added salt, $[N_p] \propto [I]^{1.2}$	$R_p \propto [I]^{1.00}$[a]	$R_p \propto [I]^{1.00}$
Seeded polymerizations		
$[N_p]$ constant, [I] varied (all dilutions)	$R_p \propto [I]^{0.75-0.80}$[b]	$R_p \propto [I]^{0.80}$
[I] constant, $[N_p]$ varied	$R_p \propto [N_p]^{0.19-0.22}$[c]	$R_p \propto [N_p]^{0.18-0.23}$
$[N_p]$ constant at 1/10 dilution, [I] constant	$R_p \propto (V_{org}/V_{aq})^{0.30}$	$R_p \propto (V_{org}/V_{aq})^{0.35}$

[a] This value is predetermined. See previous discussion.

[b] The calculated dependence varies from 0.75 to 1/20 dilution of seed to 0.80 at 1/2 dilution of seed.

[c] The calculated dependence varies from 0.19 at $[I] = 11 \times 10^{-4}$ mole/l. to 0.21 at $[I] = 2 \times 10^{-4}$ mole/l.

exact value of $[N_p]$ used is not very important. A change by a factor of five would not affect significantly the dependencies observed, though it changes k_{10b}/k_4k_8.

In addition to the quantitative relationships, eq. (12) also agrees with, or at least does not contradict the more qualitative observations. These in general were earlier observations and less accurate. The following observations were made.

In unseeded polymerizations, there is no observed dependence on emulsifier concentration (Table I). We do not know the dependence of $[N_p]$ on soap, so our rate equation is not applicable. If it follows the Smith-Ewart dependence, R_p would be proportional to $[\text{soap}]^{0.12}$. The maximum rate change is 18%, which is just detectable.

In unseeded polymerizations, there was no dependence on the monomer/water ratio (Table II). The maximum expected change in rate is only 15% over the range studied. As these were early results with an error of 10–20% per run, the lack of dependence is understandable. However, if Smith-Ewart case 1 kinetics were followed,[2] R_p should be proportional to V_{org}/V_{total}. This large change should be easily observable, thus demonstrating again that vinyl acetate polymerization does not follow Smith-Ewart kinetics.

In seeded polymerizations, addition of soap seems to lower R_p slightly (Table IV). More soap in the aqueous phase should stabilize $P\cdot_{aq}$ and thus lower k_4. This should lower R_p. Since most of the added soap is adsorbed on the particles, the change in k_4 should depend on soap to a low power only.

Addition of new initiator during a run increases R_p (Fig. 4). At constant $[N]_p$, $R_p \propto [I]^{0.8}$; this was shown quantitatively earlier. This run demonstrates the same effect qualitatively in a single run. We think that the more than doubling of the measured R_p with the doubling of [I] is probably due both to experimental artifact (it was an early run) and to the difficulty of measuring rates accurately under such circumstances.

Addition of excess electrolyte lowers dependence of R_p on [I] to the 0.72 power with 0.5M K_2SO_4 added, and to the 0.47 power with 0.05 K_2HPO_4/KH_2PO_4 buffer (Fig. 5). Increasing ionic strength has two related effects: it destabilizes particles ($[N_p]$ decreasing) and increases k_4. Both increase the term, $k_4k_8d^2[M_{aq}]$, of eq. (11) to the point where it may simplify to eq. (13):

$$R_p = (k_5/k_6)(k_1k_6[I][M_p][N_p])^{1/2} \tag{13}$$

The minimum dependence of R_p on [I] is obviously $R_p \propto [I]^{0.5}$ when $[N_p]$ is determined only by ionic strength and soap concentration. This is found with the phosphate buffer.[26] With added K_2SO_4, the dependence on R_p on [I] is to the 0.7 power. Here $[N_p]$ may still depend somewhat on [I] as sulfate ion does not shield as powerfully as phosphate ion.

Particle size was measured in only one case (run 151). A recipe was used identical to that of run 165, except that it was 0.05 mole/l. in K_2SO_4. Particle diameter was measured (light scattering) as 0.144 μ, compared to 0.07 μ for run 165.

If we use the postulated $[N_p]$ for run 165 of 24 × 10^{-6} molal, $[N_p]$ for run 151 is 2.8 × 10^{-6} molal. Substituting this into eq. (13) we can estimate R_p for this run as 3.1 × 10^{-3} mole/l.-sec. The experimental value was 1.6 × 10^{-3} mole/l.-sec., about one half that calculated. However, we can also use the measured light scattering volume as a basis of calculation of $[N_p]$, though this is a weight-average volume. Using this lower value of $[N_p]$, we find from eq. (13) that $R_p = 1.1 \times 10^{-3}$ mole/l.-sec. Thus, the two values for $[N_p]$ give calculated polymerization rates which bracket the experimental value.

The discussion above shows that eq. (13), which has no arbitrary parameters, can predict reaction rates. It also predicts the shape of the polymerization curves of those runs with added electrolyte. These differ from normal vinyl acetate polymerization curves, in that the portion of the curve above 50% conversion is curved rather than linear. However, the curvature is one-half order in $[M_p]$ as predicted by eq. (13) rather than first order as the Smith-Ewart theory gives. This will be discussed fully in the next section.

In summary, where exact data have been obtained we find good agreement between our theory and experiment. In scouting experiments and early work, the results fall within the limits of the theory, but in general there is too much scatter or not enough data to draw conclusions. However, there is no fit at any point with Smith-Ewart equations. When excess electrolyte is added, we find that a modified kinetic equation can still predict the observed rates of polymerization.

Prediction of Polymerization Curves

We have shown in the previous section that the kinetic equation developed has the same dependencies of R_p under various experimental conditions as the experimental data. In addition to this, if the equation is meaningful, it should predict the course of polymerization under any given set of experimental conditions. We shall discuss that portion of the theory in this section.

The course of any polymerization we shall discuss can be conveniently divided into three parts. The first, formation of particles, terminates somewhere between 5 and 20% conversion and is beyond the scope of this paper. Our theory should hold from that point to about 95% conversion where the basic assumptions start to break down. For seeded polymerizations, the theoretical curve should be followed as soon as the induction period is completed.

The rest of the polymerization where $[N_p]$ is constant includes the last two parts of the three.

In the second part of the polymerization, $[N_p]$ is constant and a separate monomer phase is present. During this time, there is approximate equilibrium for $[M_{aq}]$ and $[M_p]$ as they are replenished by fresh monomer. As polymerization proceeds, the only gross variable is particle size; both the particle volume and surface area increase. $[M_p]$ is considered ~6.3 mole/l. in this phase as a separate monomer layer was observed up to about 50% conversion. (A careful study under equilibrium conditions gave a monomer concentration of 7.6 mole/l. in polymer particles.[27] This may show that we do not reach complete equilibrium during polymerization, or that we have that much experimental variation in our observations. Happily, it does not affect the kinetics appreciably as long as we remain consistent.)

The integrated equation for this part is derived in Appendix II and is given below.

$$\left\{\left(\frac{[M_0] - [M]}{b[M_0]}\right)^{2/3} + K_2\right\}^{3/2} - K_2^{3/2} = \frac{K_1}{b[M_0]}t \tag{14}$$

where $[M_0]$, $[M]$ denote the moles of monomer in the whole system per liter of H_2O at the beginning of polymerization and during polymerization, respectively, and b is the fractional conversion at which monomer phase disappears.

K_1 and K_2 are combinations of constant terms defined in Appendix II. (K_2 includes $k_{10b}k_6/k_4k_8$. The value calculated earlier is from the maximum R_p possible in a polymerization, rather than the average from 20 to 80% conversion. This term has to be changed from 5.1×10^{-5} to $4.6 \pm .3 \times 10^{-5}$ to get fit over the integration.)

In the third part of the polymerization, the separate monomer phase has been used up. From this time on, the particle volumes are essentially constant as is their surface area. $[M_p]$ starts decreasing, as does $[M_{aq}]$. This portion of the kinetic curve has been integrated in Appendix II also and is given in eq. (15)

$$(1 + K_2)^{3/2} - \{1 + K_2([\mathrm{M_p}]/6.3)^{1/2}\}^{3/2} = {}^3/_4(K_1K_2/6.3a)(t - t_i) \quad (15)$$

where t_i is the time at which the separate monomer phase disappears.

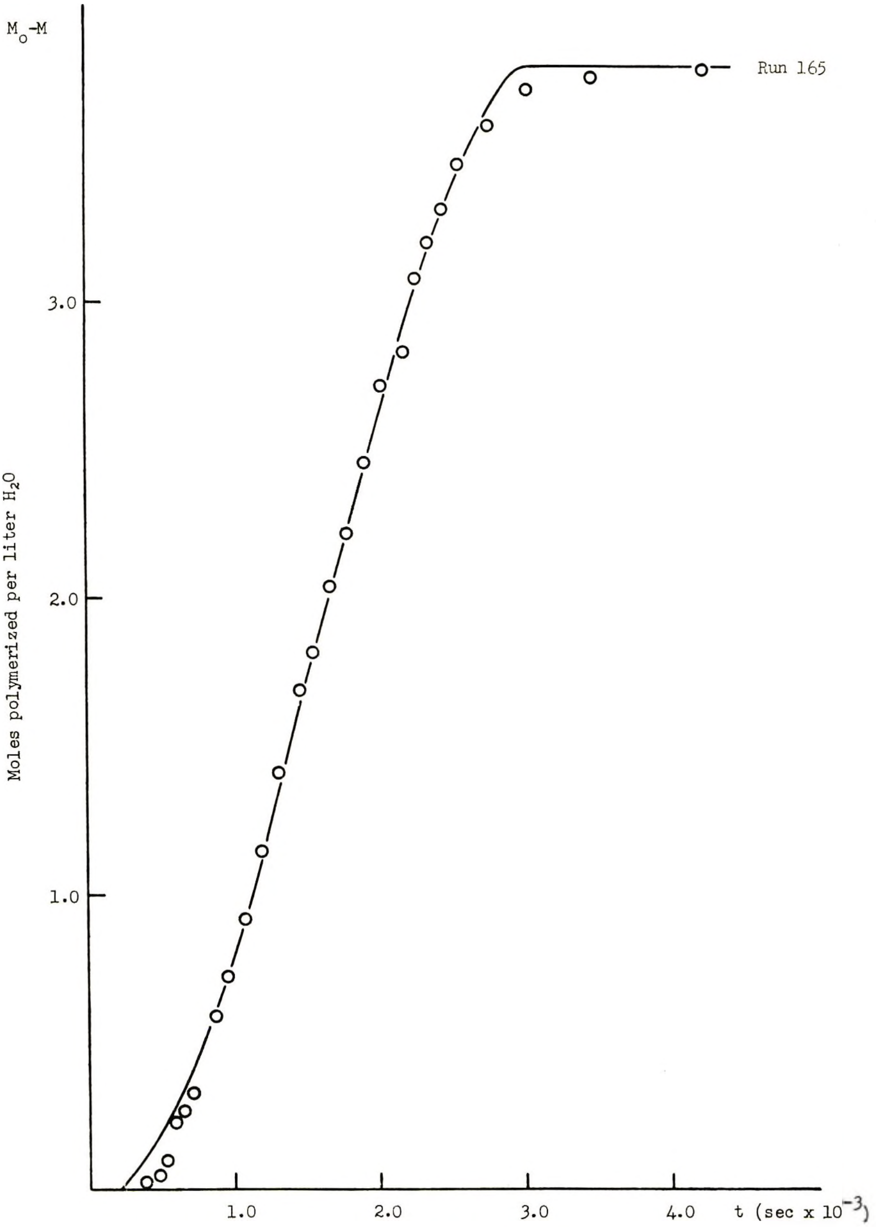

Fig. 10. Comparison of experimental data and theoretical curve for run 165. (O) observed; (—) calculated.

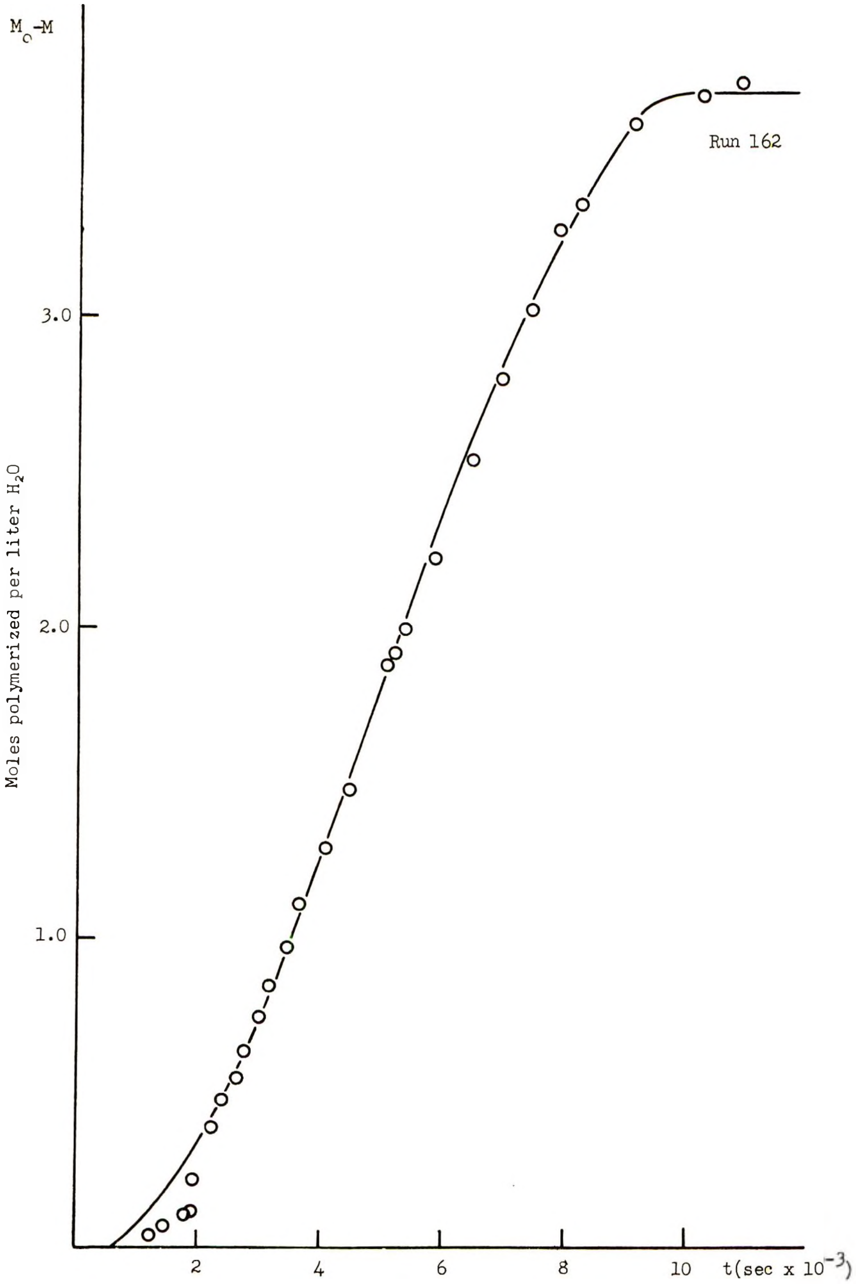

Fig. 11. Comparison of experimental data and theoretical curve for run 162: (○) observed; (—) calculated.

Equations (14) and (15) should define the course of polymerization at relatively low ionic strength. We have therefore picked four polymerizations: two unseeded and two seeded, all of which were runs done after per-

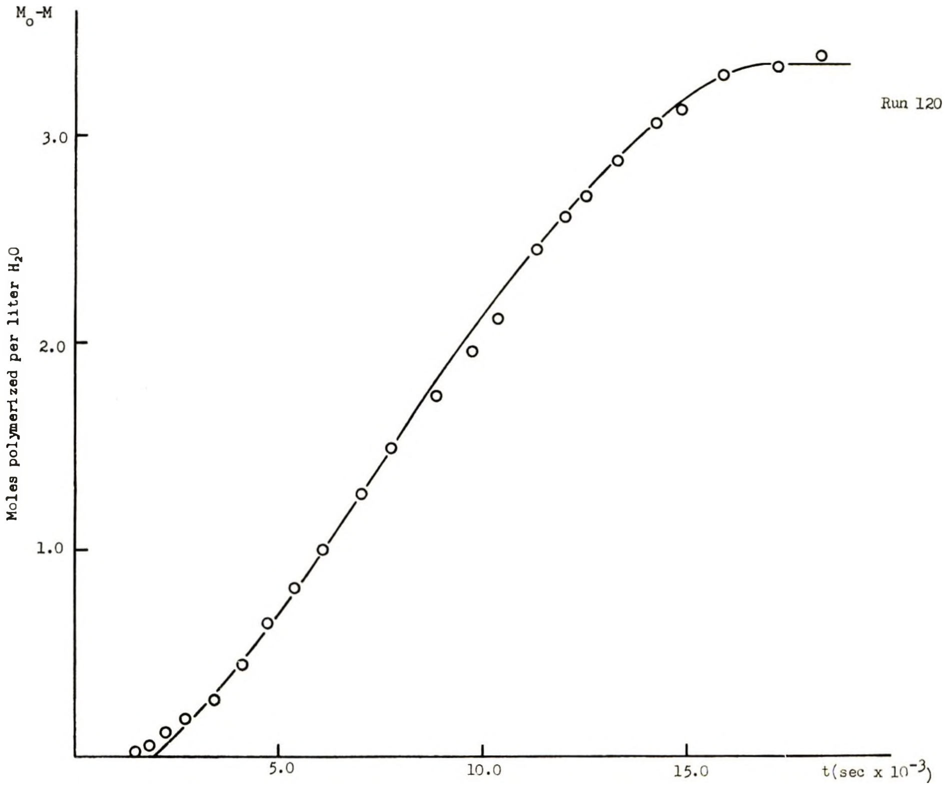

Fig. 12. Comparison of experimental data and theoretical curve for run 120: (O) observed; (—) calculated.

TABLE VIII

Data for Calculation of Equations (14) and (15)

Run	$[I] \times 10^4$	$[N_p] \times 10^6$	$d_0^2 \times 10^3$, μ^2	$a = V_{org}/V_{aq}$	Ionic strength, $\mu \times 10^3$
165	12.0	24.	1.22	0.320	3.6
162[a]	2.5	3.65	4.3	0.320	3.6
120[b]	2.3	1.54	7.6	0.320	0.7
132[b]	8.25	1.54	3.6	0.106	2.5

[a] N_p calculated from $[N_p] \propto [I]^{1.2}$ with run 165 as standard.

[b] Seed polymerizations, 1/10 dilution. $[N_p]$ for seed calculated as in note a. Measured $[N_p]$ for seed shows same ratio to $[N_p]$ for run 165 by use of light-scattering values.

fection of the experimental technique and which cover the range of variables investigated. The information for these runs is given in Table VIII.

The comparisons of the theoretical curves for these runs with the experimental points are given in Figures 10–13. Run 165 was calculated by using $k_{10b}k_6/k_4k_8 = 4.4 \times 10^{-5}\, y^{-0.60}$, while the other three runs were calculated by using a value of $k_{10b}k_6/k_4k_8 = 4.9 \times 10^{-5}\, y^{-0.60}$. The second value diminishes the slope of the theoretical curve by 5% over that using the

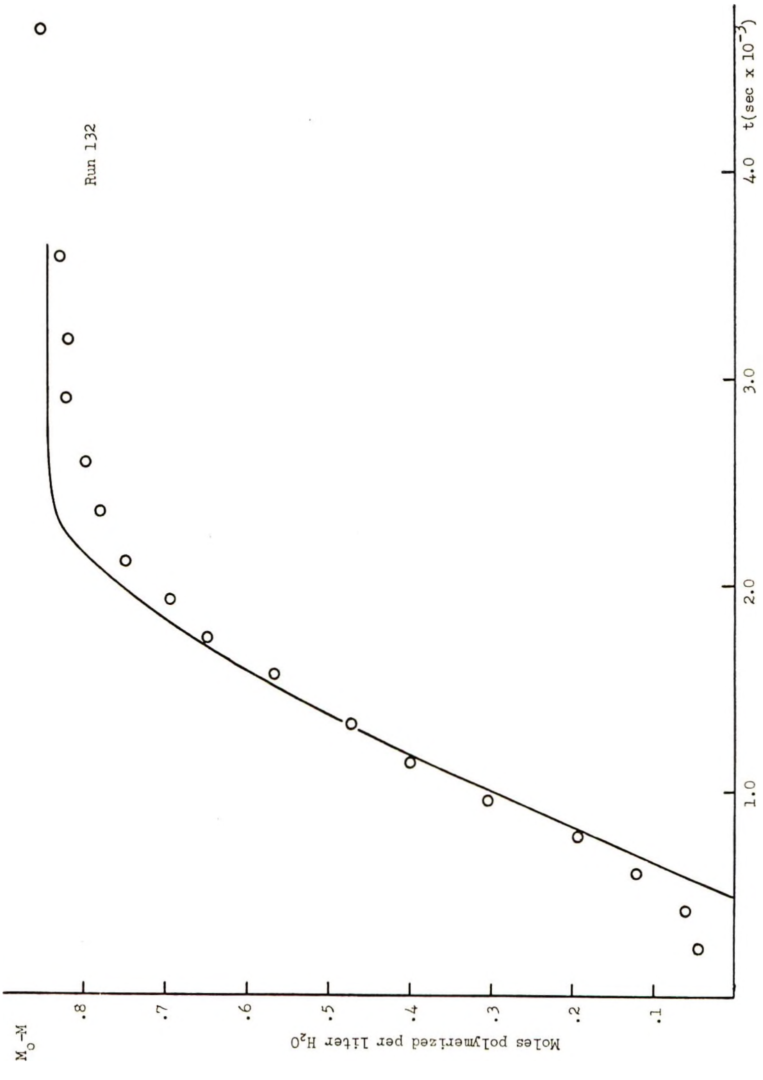

Fig. 13. Comparison of experimental data and theoretical curve for run 132: (O) observed; (—) calculated.

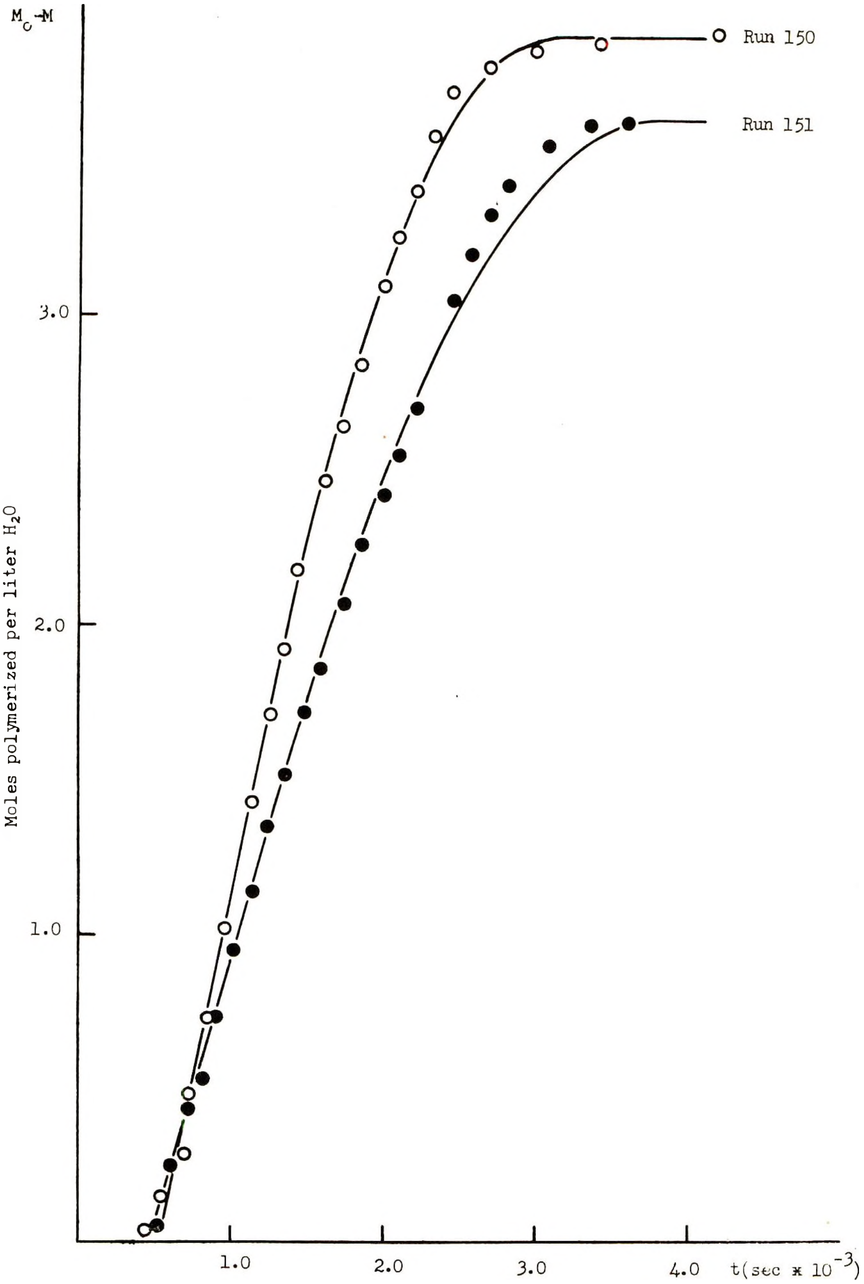

Fig. 14. Comparison of experimental data with eqs. (16) and (17) for runs 150 and 151: (○) observed for run 150, recipe normal, [I] = 1.2 × $10^{-3}M$; $0.05M$ K_2HPO_4/KH_2PO_4; K_1 = 2.35 × 10^{-3} mole/l.-sec; (●) observed for run 151, recipe normal, [I] = 1.2 × $10^{-3}M$, $0.05M$ K_2SO_4, K_1 = 1.72 × 10^{-3} mole/l.-sec; (—)calculated.

first value of the rate constants. This is within the experimental variation of runs done at different times using supposedly identical recipes. We deliberately do this in order to show how good the fit can be between the theoretical curves and the experimental results. It is the sort of fit which confirms that eqs. (12), (14) and (15) are a good description of vinyl acetate emulsion polymerization. In run 132 (Fig. 13) at one third the organic volume usually used, the calculated rate is too high by 20% though the shape of the polymerization curve is correct. Such a difference is at the outside limit of the experimental variation. As the run was also at the outside limit of the experimental variations, high dilution of seeds and very low V_{org}, deviations might be expected. Without repetitions of the run, we can not tell whether the discrepancy is experimental or due to the choice of improper parameters. In addition, with the addition of only a small amount of monomer the rates tend to be lower than expected (see Fig. 8 for the results at a relative seed concentration of 0.50).

In unseeded polymerizations, inspection of Figures 10 and 11 shows that the equations hold between about 10–15% to 95% conversion. Above 95% conversion, R_p seems to be slightly slower than that calculated. This may be due to the high viscosity of the system at such high conversions. Since we used the two termination steps which we felt were important, Equation (15) should hold, theoretically, as long as the rate constants remain constant.

As mentioned in the last section, addition of salts should raise k_4 and thereby change eq. (12) into eq. (13). Since $[N_p]$ is not known in those cases, the best that can be done is to curve fit the integrated eq. (13) to the data.

The kinetic curve in this case falls into two parts. In the first, where a separate monomer phase is present, the rate should be constant as soon as $[N_p]$ is constant. This seems to happen very early in the polymerization. The polymerization in this phase can be expressed by eq. (16):

$$[M_0] - [M] = K_1 t \tag{16}$$

In the last phase, monomer concentration in the particles is decreasing. Integration of eq. (13) then gives eq. (17),

$$1 - ([M_p]/[M_{p0}])^{1/2} = (K_1/2[M_{p0}]a)(t - t_i) \tag{17}$$

where t_i is the time at which the separate monomer phase disappears.

K_1, obtained from the linear portion of the polymerization curve, can be used in eq. (17) to calculate the whole dependence of conversion versus time. This was done for two runs which were identical in recipe, except that one contained 0.05 mole/l. K_2SO_4 (run 151) and the other 0.05 mole/l. KH_2PO_4–K_2HPO_4 buffer (run 150). The comparison of experimental points with theoretical curves is shown in Figure 14.

It can be seen that the predictions follow run 150 with phosphate buffer exactly, but run 151 with K_2SO_4 polymerizes slightly faster than the predictions. This probably means that the sweep-up step still has slight effect here, lowering the monomer dependence of R_p from one-half towards one quarter power. All the other runs with added salts show essentially identical curves, though of course K_1 depends on initiator concentration and $[N_p]$.

The foregoing analysis suggests a convenient method to obtain very rapid rates in vinyl acetate polymerization. The polymerization should be started with no buffer present and the use of anionic surfactant. After $[N_p]$ has stabilized, phosphate buffer containing extra soap is added. Depending on the initiator concentration, the rate should increase by a factor of two to five over the rate in the absence of salt. Of course this can only happen if $[N_p]$ does not decrease, which is why extra soap is needed.

Comparison with Literature

There are three reports on emulsion polymerization of vinyl acetate which are close enough in experimental methods to this investigation for a comparison to be made[26,28,29] The latest and most comprehensive is that of Gershberg.[26] His only major experimental difference was that some phosphate buffer was present.[30] He finds $R_p \propto [I]^{0.6}$, which indicates a reaction that has rapid sweep-up by particles, though less than we found using $0.05M$ phosphate buffer. His measured dependencies were of R_p on soap and V_{org}/V_{aq}. Using eq. (13), we predict no dependence on V_{org}/V_{aq}, which is what Gershberg finds. At high ionic strength, the function of soap should be to stabilize the particles and thus $[N_p]$ should depend on soap concentration. Gershberg does find a 0.25 power dependence of $[N_p]$ on soap.

Vinyl propionate, which should follow similar kinetics to vinyl acetate, is anomalous; Gershberg reports that R_p remains linear to high conversions, as with vinyl acetate. However, the rate is independent of the particle concentration and the total organic volume as well. Thus, from his data, it does not follow our equations nor those of Smith-Ewart, case 1. For this monomer, $[N_p] \propto [\text{soap}]^{1.9}$; this also does not agree with results for vinyl acetate.

The other two reports[28,29] used nonionic emulsifiers, which distinguishes these data from ours, since aqueous polymer radicals are not sufficiently stabilized by the sulfate or butyrolactone endgroup to exist for long. Nevertheless, since the dependence on $[M_p]$ is less than first order, we shall consider them.

In the work of French,[28] only one persulfate concentration was used, and no correlation can be made. French found $[N_p] \propto [\text{soap}]^3$. R_p varied randomly with emulsifier concentration and also $[N_p]$ for the four runs given. It usually accelerated slightly after 30% conversion. We can draw no conclusions from this work except to hypothesize that for nonionic surfactants $[N_p] \propto [\text{soap}]^3$.

In the work of O'Donnell et al.,[29] no particle measurements were made, but dependence of R_p on emulsifier [partly hydrolyzed poly(vinyl acetate)], and persulfate concentration was measured. Results showed were

$R_p \propto (\text{soap})^{0.9\pm.1}$ (recalculated from the data given), and $R_p \propto [\mathrm{I}]^{0.7}$. If we postulate that $[\mathrm{N_p}] \propto (\text{soap})^3$, as found by French,[28] and if eq. (13) of our work is followed, we would expect to get R_p dependent on soap to the 1.5 power. If $[\mathrm{N_p}] \propto [\mathrm{I}]^{0.4}$ as calculated for the Smith-Ewart theory of particle formation, then R_p should be proportional to $[\mathrm{I}]^{0.7}$ as found.

The comparison with literature is obviously very tentative, as no investigators used exactly the same experimental conditions we did, nor did any except Gershberg measure enough of the variables to make a comparison really meaningful. In his case, a general area of agreement is found, though experimental conditions are not completely comparable.

SUMMARY AND CONCLUSIONS

We have considered in this paper the effect on the rate of vinyl acetate emulsion polymerization of soap (sodium lauryl sulfate), concentration of particles, initiator concentration, total organic volume and ionic strength. We have presented a polymerization mechanism, derived its mathematical consequences and have shown that it fits our data reasonably in every respect.

The scheme presented differs from the standard thinking on emulsion polymerization in two important aspects.

(1) Initiation starts in the aqueous phase, and chain growth proceeds there up to DP $\cong$ 50–300. We postulate that this happens because ionic soap is adsorbed on the aqueous polymer, transforming it into a water-soluble polyelectrolyte. Sweep-up therefore is not diffusion-controlled when an ionic soap is used (and may not be so even when a nonionic surfactant is used, since solvating water molecules must be desorbed).

(2) Because there is a significant concentration of radicals in the aqueous phase and we have chain transfer to monomer to give small, water-soluble radicals, two termination steps are postulated. Neither of these correspond to the Smith-Ewart termination. The standard step, sweep-up of a radical into an active particle, is now of minor importance if the ionic strength is low, and not diffusion-controlled. It is proportional to the surface area of the particle. The second and major step, termination of a growing butyrolactonyl radical $\mathrm{B}\cdot$ with a stabilized aqueous polymer radical is reasonable from the analysis. It has not been postulated before. The combination of these with the standard steps of vinyl acetate polymerization leads directly to the final kinetic equations.

The model presented initially can now be confirmed. Polymerization is initiated in the aqueous phase. As the polymer grows it picks up soap and becomes a polyelectrolyte. (Even before this, it contains highly water-soluble groups.) After many collisions, the polymer with an average DP between 50 and 300 is swept up by a particle. This implies a non-diffusion-controlled process with an activation energy necessary for breaking through the ionic double layers of the polymer and the particle. Growth of the now nonsolvated radical continues in the particle until chain transfer to monomer occurs. The monomer radical cyclizes to a butyrolactonyl radical which partitions into the aqueous phase and usually reinitiates chain growth there. This completes the cycle. The major termination occurs when the neutral butyrolactonyl radical with perhaps several vinyl acetate residues added, (B·), reacts with a growing aqueous radical ($P\cdot_{aq}$). A secondary termination step, which probably become the major one when salts are present, is sweep-up of a growing radical into a particle containing a radical.

It now is clear why vinyl acetate polymerization has an almost zero-order dependence on $[M_p]$, even after the monomer phase has been used up. While polymerization proceeds mainly in the particles, termination occurs mainly in the aqueous phase. Since $[M_{aq}] \propto [M_p]^{1/2}$, conditions in the aqueous phase change very slowly and sweep-up rates are almost constant. Meanwhile, as $[M_p]$ decreases, the rate of chain transfer to monomer decreases also. Thus, radicals stay in particles longer and their concentration, $f[N_p]$, increases almost inversely to $[M_p]$ as that decreases. The rate of polymerization then remains almost constant. At about 90% conversion, $[M_{aq}]$ starts decreasing rapidly, radical termination is favored, and R_p decreases.

APPENDIX I

Solution of Complete Kinetic Equations by Using Steps (10a) and (10b)

The elementary reactions considered in this derivation are listed in eqs. (1)–(10).

$$I \longrightarrow 2P\cdot_{aq} \tag{1}$$

$$P\cdot_{aq} + M_{aq} \xrightarrow{k_2 = k_5} P\cdot_{aq} \tag{2}$$

$$P\cdot_{aq} + M_{aq} \xrightarrow{k_3 = k_6} PH_{aq} + M\cdot \tag{3}$$

$$P\cdot_{aq} + P \longrightarrow P\cdot_{p} \tag{4}$$

$$P\cdot_{p} + M_{p} \longrightarrow P\cdot_{p} \tag{5}$$

$$P\cdot_{p} + M_{p} \longrightarrow P + M\cdot \tag{6}$$

$$M\cdot \longrightarrow B\cdot \tag{7}$$

$$B\cdot + M_{aq} \xrightarrow{\text{soap}} P\cdot_{aq} \tag{8}$$

$$P\cdot_{aq} + P\cdot_{p} \longrightarrow \text{Termination} \tag{10a}$$

$$P\cdot_{aq} + B\cdot \longrightarrow \text{Termination} \tag{10b}$$

By using the steady state assumption, the following eqs. (A-1)–(A-4) can be written.

$$d(\mathrm{P}\cdot_{\mathrm{aq}})/dt = 2k_1[\mathrm{I}] - k_6[\mathrm{M}_{\mathrm{aq}}][\mathrm{P}\cdot_{\mathrm{aq}}] - k_4 d^2[\mathrm{N}_{\mathrm{p}}](1 - f)[\mathrm{P}\cdot_{\mathrm{aq}}] + k_8[\mathrm{M}_{\mathrm{aq}}](\mathrm{B}\cdot) - k_4 d^2[\mathrm{N}_{\mathrm{p}}]f[\mathrm{P}\cdot_{\mathrm{aq}}] - k_{10\mathrm{b}}[\mathrm{B}\cdot][\mathrm{P}\cdot_{\mathrm{aq}}] = 0 \quad \text{(A-1)}$$

$$df[\mathrm{N}_{\mathrm{p}}]/dt = k_4 d^2[\mathrm{N}_{\mathrm{p}}](1 - 2f)[\mathrm{P}\cdot_{\mathrm{aq}}] - k_6[\mathrm{M}_{\mathrm{p}}]f[\mathrm{N}_{\mathrm{p}}] = 0 \quad \text{(A-2)}$$

$$d[\mathrm{M}\cdot]/dt = k_6[\mathrm{M}_{\mathrm{p}}]f[\mathrm{N}_{\mathrm{p}}] + k_6[\mathrm{M}_{\mathrm{aq}}][\mathrm{P}\cdot_{\mathrm{aq}}] - k_7[\mathrm{M}\cdot] = 0 \quad \text{(A-3)}$$

$$d[B\cdot]/dt = k_7[\mathrm{M}\cdot] - k_8[\mathrm{M}_{\mathrm{aq}}][\mathrm{B}\cdot] - k_{10\mathrm{b}}[\mathrm{B}\cdot][\mathrm{P}\cdot_{\mathrm{aq}}] = 0 \quad \text{(A-4)}$$

From eq. (A-2) we can solve for $[\mathrm{P}\cdot_{\mathrm{aq}}]$, obtaining eq. (A-5):

$$[\mathrm{P}\cdot_{\mathrm{aq}}] = \frac{k_6[\mathrm{M}_{\mathrm{p}}]f}{k_4 d^2(1 - 2f)} \quad \text{(A-5)}$$

We can substitute eqs. (A-3) and (A-5) into eq. (A-4) and omit $k_{10\mathrm{b}}$ $[\mathrm{B}\cdot][\mathrm{P}\cdot_{\mathrm{aq}}]$ as it is only about 4% of the other terms. Solving for $[\mathrm{B}\cdot]$, we obtain eq. (A-6):

$$[\mathrm{B}\cdot] = \frac{k_6[\mathrm{M}_{\mathrm{p}}]f[\mathrm{N}_{\mathrm{p}}]}{k_8[\mathrm{M}_{\mathrm{aq}}]}\left\{1 + \frac{k_6[\mathrm{M}_{\mathrm{aq}}]}{k_4 d^2[\mathrm{N}_{\mathrm{p}}](1 - 2f)}\right\} \quad \text{(A-6)}$$

As usual, the initiation rate equals the termination rate [eq. (A-7)]:

$$k_1[\mathrm{I}] = k_4 d^2[\mathrm{N}_{\mathrm{p}}]f[\mathrm{P}\cdot_{\mathrm{aq}}] + k_{10\mathrm{b}}[\mathrm{B}\cdot][\mathrm{P}\cdot_{\mathrm{aq}}] \quad \text{(A-7)}$$

Substituting eqs. (A-5) and (A-6) in eq. (A-7) and collecting terms in $f[\mathrm{N}_{\mathrm{p}}]$, we obtain eq. (A-8):

$$\frac{[\mathrm{N}_{\mathrm{p}}]^2 f^2}{1 - 2f} = (k_6[\mathrm{M}_{\mathrm{p}}])^{-2}(k_1 k_6[\mathrm{I}][\mathrm{M}_{\mathrm{p}}][\mathrm{N}_{\mathrm{p}}]) \times \left\{1 + \frac{k_{10\mathrm{b}}k_6[\mathrm{M}_{\mathrm{p}}]}{k_4 k_8 d^2[\mathrm{M}_{\mathrm{aq}}]}\left(1 + \frac{k_6[\mathrm{M}_{\mathrm{aq}}]}{k_4 d^2[\mathrm{N}_{\mathrm{p}}](1 - 2f)}\right)\right\}^{-1} \quad \text{(A-8)}$$

Since f is about 1/1300 for run 165, up to 50% conversion $1 - 2f = 0.998$. Thus, during most of the run $(1 - 2f)$ will be about equal to 1.00. This is true for all the unseeded runs, as $R_p \propto [\mathrm{I}]^{1.0}$ while $[\mathrm{N}_{\mathrm{p}}] \propto [\mathrm{I}]^{1.2}$. In the seeded runs, f can be as much as five to twenty times higher (~0.004 to 0.010), at the highest dilutions. Even so, within our kinetic error, $(1 - 2f) \simeq 1.0$. Towards the end of the reaction, f will increase and will be inversely proportional to $[\mathrm{M}_{\mathrm{p}}]$ [from eq. (A-8)]. Therefore, in the worst case f will be about 0.07 at 90% conversion. Omission of $1 - 2f$ in the term, $f^2/(1 - 2f)$, will then change the value of f by about 7%. Thus we can say that in all the cases we are considering where 1% or less of the particles are occupied by radicals during most of the polymerization, it is legitimate to omit $1 - 2f$ completely. Solving now for (A-8) we obtain eq. (A-9):

$$[\mathrm{N}_{\mathrm{p}}]f = (k_6[\mathrm{M}_{\mathrm{p}}])^{-1}(k_1 k_6[\mathrm{I}][\mathrm{M}_{\mathrm{p}}][\mathrm{N}_{\mathrm{p}}])^{1/2} \times \left\{1 + \frac{k_{10\mathrm{b}}k_6(\mathrm{M}_{\mathrm{p}})}{k_4 k_8 d^2[\mathrm{M}_{\mathrm{aq}}]}\left(1 + \frac{k_6[\mathrm{M}_{\mathrm{aq}}]}{k_4 d^2[\mathrm{N}_{\mathrm{p}}]}\right)\right\}^{-1/2} \quad \text{(A-9)}$$

The rate of polymerization is:

$$R_p = k_5(\mathrm{M}_{aq})(\mathrm{P}\cdot_{aq}) + k_5(\mathrm{M}_p)f(\mathrm{N}_p)$$

On substituting eqs. (A-5) and (A-9) in this we obtain eq. (A-10):

$$R_p = \frac{-dM}{dt} = \frac{k_5}{k_6}\frac{(k_1k_6[\mathrm{I}][\mathrm{M}_p][\mathrm{N}_p])^{1/2}\left(1 + \dfrac{k_6[\mathrm{M}_{aq}]}{k_4d^2[\mathrm{N}_p]}\right)}{\left\{1 + \dfrac{k_{10b}k_6[\mathrm{M}_p]}{k_4k_8d^2[\mathrm{M}_{aq}]}\left(1 + \dfrac{k_6[\mathrm{M}_{aq}]}{k_4d^2[\mathrm{N}_p]}\right)\right\}^{1/2}} \qquad \text{(A-10)}$$

If polymerization in the aqueous phase is considered kinetically insignificant, terms involving $k_6[\mathrm{M}_{aq}]$ drop out and we obtain eq. (A-11):

$$R_p = -dM/dt = \frac{k_5}{k_6}(k_1k_6[\mathrm{I}][\mathrm{M}_p][\mathrm{N}_p])^{1/2}\left(1 + \frac{k_{10b}k_6[\mathrm{M}_p]}{k_4k_8d^2[\mathrm{M}_{aq}]}\right)^{-1/2} \qquad \text{(A-11)}$$

APPENDIX II

Integration of Equation (A-11)

Polymerization in the Presence of Separate Monomer Phase. The polymerization was be divided into two sections as discussed in the text. In the first part, when no new particles are being formed and a separate monomer phase is present, $[\mathrm{M}_p]$ and $[\mathrm{M}_{aq}]$ remain constant. $[\mathrm{I}]$ and $[\mathrm{N}_p]$ are always considered constant during one polymerization. The kinetic equation we are considering is

$$\frac{-dM}{dt} = \frac{k_5}{k_6}(k_1k_6[\mathrm{I}][\mathrm{M}_p][\mathrm{N}_p])^{1/2}\left(1 + \frac{k_{10b}k_6[\mathrm{M}_p]}{k_4k_8d^2[\mathrm{M}_{aq}]}\right)^{-1/2} \qquad \text{(A-11)}$$

In the first part of the polymerization, everything is constant but d; as each particle grows, eq. (A-11) can be written as (A-12)

$$\frac{-dM}{dt} = K_1[1 + K_2(d_0/d)^2]^{-1/2} \qquad \text{(A-12)}$$

where

$$K_1 = (k_5/k_6)(k_1k_6[\mathrm{I}][\mathrm{M}_{p0}][\mathrm{N}_p])^{1/2}$$

and

$$K_2 = k_{10b}k_6[\mathrm{M}_{p0}]/k_4k_8d_0^2[\mathrm{M}_{aq0}]$$

$[\mathrm{M}]$ and d can be cast as functions of one variable by making the following substitution:

$$y^3 = (d/d_0)^3 = ([\mathrm{M}_0] - [M])/b[\mathrm{M}_0] \qquad \text{(A-13)}$$

Solving for dy/dt and substituting this and eq. (A-13) into eq. (A-12), we obtain eq. (A-14):

$$y^2(1 + K_2y^{-2})^{1/2}dy = (K_1/3[\mathrm{M}_0]b)dt \qquad \text{(A-14)}$$

This is easily integrated. The final equation after integrating from $y = 0$ to $y = 1$ and replacing y by a function of $[\mathrm{M}]$ is eq. (A-15):

$$\{[([\mathrm{M}_0] - [\mathrm{M}])/[\mathrm{M}_0]b]^{2/3} + K_2\}^{3/2} - K_2^{3/2} = (K_1/[\mathrm{M}_0]b)t \qquad \text{(A-15)}$$

Polymerization after Separate Monomer Phase Is Consumed. During the second part of the polymerization, monomer concentration in the organic phase, $[\mathrm{M}_\mathrm{p}]$, is decreasing, as is also $[\mathrm{M}_\mathrm{aq}]$. Here d remains approximately constant at d_0. (d does decrease slightly as monomer is converted into polymer, but this is neglected for simplicity since it is a second-order effect.) Over most of the polymerization range $[\mathrm{M}_\mathrm{aq}]$ was found[31,32] to be proportional to $[\mathrm{M}_\mathrm{p}]^{1/2}$. We have also checked this relationship and it is approximately valid when $[\mathrm{M}_\mathrm{p}] > 1.0M$, about 92% conversion. Below this, it approaches the expected linear relationship. This will be the subject of a separate communication. With the postulate, (A-16),

$$[\mathrm{M}_\mathrm{aq}] = [\mathrm{M}_\mathrm{aq0}]\left(\frac{[\mathrm{M}_\mathrm{p}]}{[\mathrm{M}_\mathrm{p0}]}\right)^{1/2} \qquad \text{(A-16)}$$

eq. (A-11) can be put in integrable form for this part of the polymerization:

$$-dM/dt = K_1([\mathrm{M}_\mathrm{p}]/[\mathrm{M}_\mathrm{p0}])^{1/2}\{1 + K_2([\mathrm{M}_\mathrm{p}]/[\mathrm{M}_\mathrm{p0}])^{1/2}\}^{-1/2} \qquad \text{(A-17)}$$

This can be integrated when one realizes that $[\mathrm{M}] = a[\mathrm{M}_\mathrm{p}]$ once the separate monomer phase has disappeared, and substituting $y = [\mathrm{M}_\mathrm{p}]/[\mathrm{M}_\mathrm{p0}]$. Integrating between the limits of $y = 1.0$ to $[\mathrm{M}_\mathrm{p}]/[\mathrm{M}_\mathrm{p0}]$ and t_i to t, we obtain eq. (A-18)

$$(1 + K_2)^{3/2} - \{1 + K_2([\mathrm{M}_\mathrm{p}]/[\mathrm{M}_\mathrm{p0}])^{1/2}\}^{3/2} = {}^3/_4(K_1K_2/a[\mathrm{M}_\mathrm{p0}])(t - t_i) \qquad \text{(A-18)}$$

We thank National Starch and Resin Corporation for support to one of us (R. P.) while the experimental work was performed. M. L. thanks the other authors for their patience and encouragement while the theory was being worked out. We wish to thank Dr. L. Utracki for his criticism of the manuscript.

The present paper is abstracted from the thesis of R. Patsiga, State University of New York, College of Forestry, Syracuse, New York.

References

1. R. Patsiga, M. Litt, and V. T. Stannett, *J. Phys. Chem.*, **64**, 801 (1960).
2. W. V. Smith and R. W. Ewart, *J. Chem. Phys.*, **16**, 592 (1948).
3. M. L. Corrin, *J. Polym. Sci.*, **2**, 257 (1947).
4. M. Morton, P. P. Salatiello, and H. Landfield, *J. Polym. Sci.*, **8**, 111 (1952).
5. W. V. Smith, *J. Amer. Chem. Soc.*, **70**, 3695 (1948).
6. E. Bartholomé, H. Gerrens, R. Herbeck, and R. M. Weitz, *Z. Eleсktrochem.*, **61**, 522 (1957).
7. E. Vanzo, R. H. Marchessault, and V. T. Stannett, *J. Colloid Sci.*, **19**, 578 (1964).
8. T. Motoyama, *Kogyo Kagaku Zasshi*, **61**, 348 (1958).
9. B. C. Elgood, E. V. Gulbekian, and D. Kinsler, *J. Polym. Sci. B*, **2**, 257 (1964).
10. J. W. Vanderhoff, J. F. Vitkushe, E. B. Bradford, and T. Alfrey, Jr., *J. Polym. Sci.*, **20**, 255 (1956).

11. J. Brandrup and E. H. Immergut, eds., *Polymer Handbook*, Interscience, New York, 1966, (a) p. II-63; (b) p. II-81; (c) pp. II-59, 60; (d) p. II-212; (e) p. II-58; (f) p. II-201; (g) p. II-90.

12. I. M. Kolthoff and I. K. Miller, *J. Amer. Chem. Soc.*, **73**, 3055 (1951).

13. N. Sata and S. Saito, *Kolloid-Z.*, **128**, 154 (1952).

14. W. Prins and J. J. Hermans, *Proc. Koninkl. Ned. Akad. Wetenschap.*, **359**, 298 (1956).

15. T. Isemura and A. Imanishi, *J. Polym. Sci.*, **33**, 337 (1958).

16. D. H. Napper and A. E. Alexander, *J. Polym. Sci.*, **61**, 127 (1962).

17. A. E. Alexander and D. H. Napper, *Chem. Ind.* (London), **67**, 1936 (1967).

18. W. J. Priest, *J. Phys. Chem.*, **56**, 1077 (1952).

19. A. M. North, *The Collision Theory of Chemical Reactions*, Wiley, New York, 1964, p. 38.

20. G. B. Butler and M. A. Raymond, *J. Polym. Sci. A*, **3**, 3413 (1965).

21. J. Hine, *Physical Organic Chemistry*, McGraw-Hill, New York, 1962, p. 181.

22. G. M. Bennett, F. Heathcoat, and A. N. Mosses, *J. Chem. Soc.*, **1929**, 2567.

23. B. Capon, *Quart. Rev.*, **18**, 56 (1964).

24. B. Capon, *Quart. Rev.*, **18**, 77 (1964).

25. R. Patsiga, thesis, State University of New York, 1962.

26. D. Gershberg, paper presented at Joint Meeting of AIChE and IChE (England), London, England, June 18, 1965.

27. E. Vanzo, R. H. Marchessault, and V. T. Stannett, *J. Colloid Sci.*, **20**, 62 (1965).

28. D. M. French, *J. Polym. Sci.*, **32**, 395 (1958).

29. J. T. O'Donnell, R. B. Mesrobian, and A. E. Woodward, *J. Polym. Sci.*, **28**, 171 (1958).

30. D. Gershberg, private communication.

31. A. S. Dunn and P. A. Taylor, *Makromol. Chem.*, **83**, 207 (1965).

32. D. H. Napper and A. G. Parts, *J. Polym. Sci.*, **61**, 113 (1962).

Received February 20, 1970
Revised May 22, 1970

JOURNAL OF POLYMER SCIENCE: PART A-1 VOL. 8 (1970)

NOTES

A Determination of the Molecular Weight of Nylon 6

The number-average molecular weight of nylon 6 (Perlon staple fiber) has been determined by the methylation method described in an earlier note[1] on nylon 66, the assumption again being that fibers methylated with ethereal diazomethane would contain one methyl ester end group per chain molecule if the end groups were fully accessile to the reagent.

Before methylation, the fiber was extracted with hot methanol and with 60% formic acid to remove caprolactam and oligomers. The figures given in Table I show that the formic acid treatment, which dissolved 5.4% of the fiber, made little difference to the results. Methylation was initially very rapid and the methoxyl content reached 0.175% in 2 hr compared with 0.191% after 24 hr. There was very little increase after the second methylation (91 hr) and the highest figure obtained corresponds to a molecular weight of about 14,000. Previous results based on viscosity measurements or titration of end-groups indicate that polycaprolactam suitable for fiber production has a molecular weight ranging from 14,000–20,000 (Ref. 2).

TABLE I
Methylation of Nylon 6 with Diazomethane

Pre-treatment of nylon 6	No. of methylations	Total time (hr)	Methoxyl content (parts per 100,000)					
								Mean
Extracted with methanol	0	—	5	2	5	6	0	4
	1	24	219	199	200	201	192	202
	2	89	227	227	235	213	223	225
Extracted with (*1*) methanol and (*2*) 60% formic acid	0	—	4	3	12	0	11	6
	1	24	191	196	199	179	188	191
	2	91	216	223	223	226	211	220
	3	163	231	228	226	231	220	227

Materials

Perlon fiber (3 den; 1½ in. staple) was extracted with methanol in a hot Soxhlet extractor for 8 hr and was air dried. Part of it, to be used directly for methylation, was steeped in 10% acetic acid for 30 min, washed free from acid by repeated changes of distilled water, dried *in vacuo* over phosphorus pentoxide and exposed to moist air. The remainder was steeped in 60% w/w formic acid (50 cc per g) for 75 min at 25°C, rinsed three times with 60% and once with 30% acid, washed with distilled water until free from acid, and dried as above.

Alcohol-free ethereal diazomethane was prepared by De Boer's second method[3] and its concentration determined.[1] Before use it was diluted to 0.25*M*, mixed with water (10 g/l. of ethereal solution), shaken at intervals during ½–1 hr, and separated from surplus water.

Methylation Procedure

Perlon fiber was suspended in moist 0.25M ethereal diazomethane (50 cc/g) and stored in a refrigerator at about 6–7°C for the required time. It was collected, washed with ether, air dried, soaked in 10% acetic acid and washed and dried as already described. The washing procedure frees the fibers from adsorbed ether which otherwise interferes with the Ziesel determinations. Perlon soaked in moist ether and washed in this way had the same apparent methoxyl content (0.006%) as the untreated Perlon; determination of the methoxyl content of one of the methylated products by a procedure involving gas-liquid chromatography indicated the presence of methoxyl in about the expected amount, but no ethoxyl. Increases in weight on methylation were less than 1%.

Determination of Methoxyl Content

The modified Zeisel procedure was as indicated in the earlier note,[1] but all results were corrected by subtracting the mean titer of six blank determinations.

The author wishes to thank Mrs. I. Williams for help with the analytical work.

References

1. F. S. H. Head, *J. Polym. Sci. A-1*, **7**, 2456 (1969).
2. H. F. Mark, S. M. Atlas, and E. Cernia, *Man-made Fibers*, Vol. 2, Interscience, New York, 1968.
3. J. DeBoer, *Rec. Trav. Chim.*, **73**, 229 (1954).

FRANK S. H. HEAD

Cotton Silk and Man-made Fibres Research Association
Shirley Institute
Manchester, England

Received March 4, 1970

Living Anionic Polymerizations of o- *and* p-*Methylstyrenes in 2-Methyltetrahydrofuran*

It is well known that, in living anionic polymerizations of styrene in ethereal solvents, the active ends can be ion pairs, free ions,[1,2] and triple ions.[3-5] When only the two types of the active ends, ion pairs and free ions, are responsible for the propagation and when the concentration of the free ions is much less than that of the ion pairs, the apparent propagation rate constant k_p is given[1,2] by

$$k_p = k_p' + k_p''K^{1/2}/[\mathrm{LE}]^{1/2} \qquad (1)$$

where k_p' and k_p'' are the rate constants of ion pairs and free ions, respectively, K is the dissociation constant of ion pairs, and [LE] is the concentration of living ends. It has been found that k_p' and K for the anionic polymerizations of styrene are highly dependent on gegenions as well as on solvents.[3-12] Furthermore, a comparison of anionic polymerizations in tetrahydrofuran of *p*-methoxystyrene with that of styrene has revealed that the k_p' and K values of living poly-*p*-methoxystyrene are much smaller than those of living polystyrene when Na$^+$ ion is used as a gegenion.[13] On the other hand, the values for Cs salts of these two living polymers are about the same.[13] Most recently, we have studied systematically the effects of the alkali metal cations on the propagation kinetics of styrene in 2-methyltetrahydrofuran (MTHF) and found that the k_p' and K in this solvent are not sensitive toward the gegenions.[14] Therefore, this solvent seemed suitable for comparative study of anionic reactivities of various monomers. Thus, in the present paper, we report anionic polymerizations of sodium salts of poly-*o*-methylstyrene and poly-*p*-methylstyrene in MTHF and describe the influence of methyl group on the kinetic and dissociation behavior in comparison with the results of styrene.

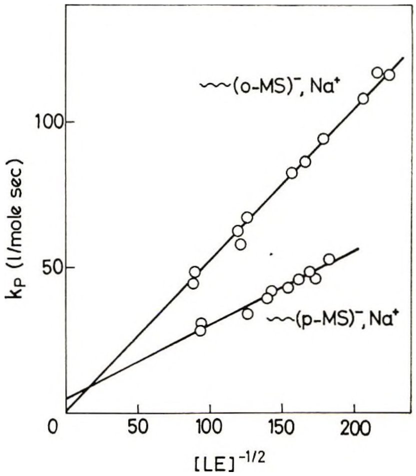

Fig. 1. Linear dependence of k_p of *o*- and *p*-methylstyrylsodium on [LE]$^{-1/2}$ in MTHF at 25°C.

The propagation rate constant was determined spectrophotometrically. Though living polymers in MTHF were not so stable as in THF, kinetic and conductivity studies are possible if MTHF is most elaborately purified. Equation (1) also applies to the polymerizations of *o*- and *p*-methylstyrenes in MTHF, as is shown in Figure 1. Apparently, the slope $k_p''K^{1/2}$ of *o*-methylstyrene is larger than that of *p*-methylstyrene.

The intercepts and slopes obtained from Figure 1, together with those of styrene, are given in Table I. The k_p' can also be determined in the presence of $NaBPh_4$. Recently, the validity of this method was questioned by Schulz et al.[15] They found that in the presence of the added salt, the ultraviolet absorption measurement gives higher values of the living end concentration and lower values of the k_p' than in the absence of the salt. Thus, we determined the k_p' by the extrapolation procedure. Since the slope is not so steep in the present case, the k_p' values we obtained seem reliable. The dissociation constant K obtained from conductivity values is listed in the fourth column of Table I. Furthermore, from the K value and the slope of k_p versus $[\mathrm{LE}]^{-1/2}$ plot, the free-ion rate constant k_p'' was obtained and is given in the last column of Table I. We note that *o*-methylstyrene has the smallest k_p' and k_p'', and its K value is largest. Therefore, the steep slope of *o*-methylstyrene in Figure 1 is attributed to the large dissociation constant.

TABLE I
Kinetic Results of Living Anionic Polymerizations of *o*- and *p*-Methylstyrenes in MTHF at 25°C[a]

Monomer	k_p', l./mole-sec	$k_p''K^{1/2}$, $\mathrm{l.}^{1/2}/\mathrm{mole}^{1/2}$-sec	$K \times 10^{10}$ mole/l.	$k_p'' \times 10^{-4}$ l./mole-sec
o-Methylstyrene	1	0.51	2.7	3.0
p-Methylstyrene	5	0.25	0.5_0	3.7
Styrene[b]	23	1.1_5	2.4	7.4

[a] Gegenion: Na^+.
[b] From Hirohara et al.[14]

Consequently, the difference between the k_p', k_p'', and K values of *p*-methylstyrene and those of styrene is attributed to the difference of the reactivities of monomers due to an electron-repelling effect of the methyl group. On the other hand, the behavior of *o*-methylstyrene cannot be accounted for in a similar manner. The methyl group in the *ortho* position prevents the gegenions and the monomers from approaching the negatively charged growing center. Accordingly, the K value is large, and the k_p' and k_p'' values are small compared with the respective values of styrene. In short, the steric hindrance of the substituent group has an influence on the kinetic and dissociation behavior of living anionic polymers. A detailed study is in progress and will be published in due course.

References

1. D. N. Bhattacharyya, C. L. Lee, J. Smid, and M. Szwarc, *Polymer*, **5**, 54 (1964).
2. H. Hostalka, R. V. Figini, and G. V. Schulz, *Makromol. Chem.*, **71**, 198 (1964).
3. D. N. Bhattacharyya, C. L. Lee, J. Smid, and M. Szwarc, *J. Phys. Chem.*, **69**, 612 (1965).
4. D. N. Bhattacharyya, J. Smid, and M. Szwarc, *J. Am. Chem. Soc.*, **86**, 5024 (1964).
5. N. Ise, H. Hirohara, T. Makino, K. Takaya, and M. Nakayama, *J. Phys. Chem.*, **74**, 606 (1970).
6. D. N. Bhattacharyya, J. Smid, and M. Szwarc, *J. Phys. Chem.*, **69**, 624 (1965).
7. T. Shimomura, J. Smid, and M. Szwarc, *J. Amer. Chem. Soc.*, **89**, 796 (1967).
8. F. S. Dainton, G. C. East, G. A. Harpell, N. R. Hurworth, K. J. Ivin, R. T. LaFlair, R. H. Pallen, and K. M. Hui, *Makromol. Chem.*, **89**, 257 (1965).
9. F. S. Dainton, K. J. Ivin, and R. T. LaFlair, *Europ. Polym. J.*, **5**, 379 (1969).

10. H. Hirohara, M. Nakayama, K. Takaya, and N. Ise, *Trans. Faraday Soc.*, **66,** 1165 (1970).
11. J. E. L. Roovers and S. Bywater, *Trans. Faraday Soc.*, **62,** 701 (1966).
12. J. E. L. Roovers and S. Bywater, *Canad. J. Chem.*, **46,** 2711 (1968).
13. K. Takaya, H. Hirohara, M. Nakayama, and N. Ise, *Trans. Faraday Soc.*, in press.
14. H. Hirohara, K. Takaya, M. Nakayama, and N. Ise, *Trans. Faraday Soc.*, in press.
15. B. J. Schmitt and G. V. Schulz, *Makromol. Chem.*, **121,** 184 (1969).

Masatoshi Nakayama
Hideo Hirohara
Katsuhiko Takaya
Norio Ise

Department of Polymer Chemistry
Kyoto University
Kyoto, Japan

Received April 28, 1970

Overall Activation Energies for Addition Polymerization by Differential Thermal Analysis

Reed et al.[1] have presented methods for using differential thermal analysis (DTA) to determine chemical reaction kinetic parameters. These authors extend the theory of Borchardt and Daniels[2] and point out the shortcomings of the Kissinger[3] method. Recently, Piloyan et al.[4] have described a much simpler means for determining the activation energy E_p. This method requires only a single DTA curve obtained at some arbitrary reasonably normal rate of heating (10–40°C/min). Their analysis predicts that

$$\ln \Delta T = C - (E_a/RT) \tag{1}$$

where C is a constant and ΔT is the extent of departure of the DTA curve from the baseline at T. E_a is obtained from the slope of a ($\ln \Delta T$) vs. ($1/T$) plot. Results are presented by Piloyan et al.[4] for a number of endothermic dehydration and dissociation reactions which show excellent agreement between E_a values obtained by their DTA method and literature values.

DTA has also been used for determining activation energies of very exothermic reactions, i.e., the decomposition of explosives.[5] Using differential scanning calorimetry (DSC), Rogers and Morris[6] obtained erroneously high activation energies for the decomposition of explosives, (RDX, Tetryl, HMX and $KMnO_4$) when measurements were made on the pure solids but true values when the measurements were made in solution. The reasons for this are obvious. The heat output from the decomposition of the solid explosive can exceed the rate at which heat is supplied by the instrument and therefore the former contributes to the rate of departure of the curve from the baseline. Since most high explosives follow first-order decomposition kinetics which are sometimes complicated by autocatalysis,[7] solution of the explosive in a suitable solvent controllably reduces the rate and probably also reduces the extent of autocatalytic decomposition.

A recent paper describes the use of sealed vials for DTA measurements at high temperatures and pressures.[8] To illustrate the technique these authors chose to study an exothermic radical chain reaction, i.e., the determination of the overall E_a for styrene homopolymerization. They obtained very similar values (21.3–24.0 kcal/mole) for the thermal bulk polymerization, the thermal solution polymerization in toluene, and the benzoyl peroxide initiated bulk polymerization. The method they used was that of Piloyan et al.[4] and their values are those normally found for the thermal and catalyzed polymerization of styrene.[9] A possibly unintentional implication of this work is that DTA is a suitable means of obtaining overall activation energies for vinyl polymerizations. This, we feel, is misleading.

Using the Model 900 duPont Differential Thermal Analyzer, we attempted to obtain overall activation energies of polymerization for various monomers under different conditions of concentrations and heating rate. Sample sizes ranged from 7–15 mgs and they were contained in small sealed aluminum caps. Values of E_a were calculated by the method of Piloyan et al.[4] Data are presented in Table I.

Again, the value found for styrene is normal whereas the other values are erroneously high. For many catalyzed vinyl polymerizations, the rate of polymerization R_p is given by:

$$R_p = k_p(fk_d[I]/k_t)^{1/2}[M] \tag{2}$$

where k_p, k_d, and k_t are rate constants for propagation, initiator decomposition and termination, respectively: $[I]$ and $[M]$ are initiator and monomer concentrations; and f is a measure of initiator efficiency. The overall activation energy is then

$$E_a = {}^1/_2E_d + E_p - {}^1/_2E_t \tag{3}$$

TABLE I
Overall E_a for Vinyl Polymerizations by DTA

Monomer	Concentration	Heating rate (°C/min)	F_a, kcal/mole Obs.	Lit.
Acrylylglycinamide	20% in DMF	20	47.8 ± 10.5	
	0.1% benzoyl peroxide			
	20% in DMF	20	47.3 ± 8.7	
	0.2% AIBN[a]	10	31.8 ± 3.4	
	20% in DMSO	20	57.3 ± 12.5	
	0.2% AIBN			
	20% in H_2O	20	44.8 ± 10.5	15.8[10]
	0.5% $K_2S_2O_8$			
	Bulk (solid)	20	Very high	
Methacrylylglycinamide	20% in DMF	20	33.9 ± 3.1	
	0.1% benzoyl peroxide			
	20% in DMSO	20	18.5 ± 1.7	
	0.2% AIBN			
Acrylonitrile	Bulk			
	0.1% benzoyl peroxide	1	70.8 ± 14.5	
		2.5	66.0 ± 12.2	
		5	78 ± 7.6	
		10	64.8 ± 5.9	
	8.5% in DMF	10	33.9 ± 2.6	17.0
	0.034% AIBN	10	31.5 ± 6.2 to	21.4[11]
Vinyl acetate	Bulk	10	130.2 ± 10.0	
	0.1% benzoyl peroxide	10	252.6 ± 34.7	
		10	190.0 ± 35.5	19.7[9]
	5% in toluene			
	0.017% AIBN	10	(No exotherm)	
Styrene	Bulk			
	0.1% benzoyl peroxide	10	23.0 ± 1.5	
		10	21.9 ± 1.4	22.0[9]
		10	23.5 ± 1.2	

[a] AIBN is azobisobutyronitrile.

Since E_d for many initiators (benzoyl peroxide, AIBN, $K_2S_2O_8$, etc.) is 30 ±1 kcal/mole, and $(E_p - {}^1/_2E_t)$ can range from slightly negative values[10] up to about 7 kcal, values for E_a for initiated vinyl polymerizations will normally fall in the 15–22 kcal/mole range. E_a for acrylonitrile (Table I) was calculated from E_p and E_t data[11] by eq. (3).

Vinyl polymerizations are radical chain reactions and they maintain this kinetic character regardless of dilution or other variations in reaction conditions. If under the conditions selected, R_p is too fast, or the heat of polymerization, ΔH_p is at the high end of the ΔH_p range, or both simultaneously exist, erroneous values of E_a will be observed as determined by DTA. Styrene fortuitously has only a moderate[12] ΔH_p of −16 kcal/mole and a relatively low $(k_p/k_t)^{1/2}$ ratio[11] and therefore DTA yields a reasonable value for E_a under almost all conditions. For many other monomers, the use of DTA for the measurement of E_a is worthless as can be seen from the data of Table I. Considerable dilution of acrylylglycinamide and acrylonitrile still results in values of E_a which are much too high. Vinylacetate with a high value[12] for ΔH_p of −21.2 kcal/mole and a high $(k_p/k_t)^{1/2}$ ratio[11] yields an extremely high value for E_a. When the necessary drastic dilutions were made in both monomer and catalyst, the polymerization failed to occur. Only methacrylylglycinamide gave one value (18.5 kcal) which falls within the normal range of E_a values. This is probably the result of an abnormally low ΔH_p of only -6 kcal/mole for this very sterically hindered 1,1 disubstituted ethylene.[13] If by DTA, for example, a value of E_a of 22 kcal/mole is obtained for a vinyl polymerization, conditions would still have to be varied to be sure that the value is the experimentally observable minimum. As shown by some recent publications,[14] DSC allows isothermal measurements of polymerization reaction rates from which E_a can be calculated. The difference results from basic instrument designs. Whereas in DTA there is a built-in constant rate of temperature increase with time, with DSC the heat input is modulated so as to maintain the sample temperature constant. Consequently, for rapid exothermic reactions, DSC should be the method of choice since it is less likely that the reaction exothermicity will contribute to its own rate of reaction.

References

1. R. L. Reed, L. Weber, and B. S. Gottfield, *Ind. and Eng. Chem. Fundamentals*, **4**, 38 (1965).

2. H. G. Borchardt and F. Daniels, *J. Am. Chem. Soc.*, **79**, 41 (1957).

3. H. E. Kissinger, *J. Res. Nat. Bur. Stand.*, **57**, 217 (1956); *Anal. Chem.*, **29**, 1702 (1957).

4. G. O. Piloyan, I. D. Ryabchikov, and O. S. Novikova, *Nature*, **212**, 1229 (1966).

5. G. Krein, *Explosionstoffe*, **13**, 205 (1965).

6. R. N. Rogers and E. D. Morris, Jr., *Anal. Chem.*, **38**, 412 (1966).

7. M. A. Cook, *The Science of High Explosives*, Reinhold, New York, 1958, pp. 133, 176–178.

8. H. W. Hoyer, A. V. Santoro, and E. J. Barrett, *J. Polymer Sci.*, *A-1*, **6**, 1033 (1968).

9. P. J. Flory, *Principles of Polymer Chemistry*, Cornell, New York, 1953, pp. 123–124, 132.

10. H. C. Haas, R. L. MacDonald, and A. N. Schuler, *J. Polymer Sci.*, *A-1*, **8**, 1213 (1970).

11. J. Brandrup and E. H. Immergut, *Polymer Handbook*, Interscience, New York, 1966, p. II-67.

12. H. Sawada, *Macromol. Sci.*, *C-3*, **2**, 313 (1969).

13. H. C. Haas, R. L. MacDonald, and A. N. Schuler, "Synthetic Thermally Reversible Gel Systems. VII," to be submitted to *J. Polymer Sci.*

14. K. Horie, I. Mita, and H. Kambe, *J. Polymer Sci.*, *A-1*, **6**, 2663 (1968); **7**, 2561 (1969).

H. C. Haas
M. J. Manning
S. A. Hollander

Research Laboratories
Polaroid Corporation
Cambridge, Massachusetts 02139

Received May 19, 1970

Synthesis of Polyamide from Bisanhydrides and Diamines

Polyamide is usually prepared by the polycondensation of ω-amino acid or diamine-dicarboxylic acid. The reaction is carried out in the melt by heating the reactants together above the melting point of the final polyamide, and driving the process to completion by removing the last traces of water. Polyamide can be also prepared at a relatively low temperature by the interfacial or low-temperature solution polycondensation which are related with the Schotten-Bauman reaction where acid chloride is used in place of carboxylic acid.

Recently, it was found that the exchange reaction is an effective method for preparing condensation polymers at low temperature. For instance, the exchange reactions (1) and (2) are known[1,2] to be effective to prepare polyamide or polyester at room temperature:

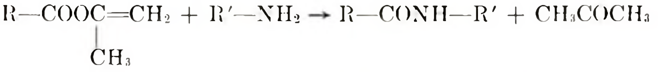

$$R\text{—}COOC(CH_3)\text{=}CH_2 + R'\text{—}NH_2 \rightarrow R\text{—}CONH\text{—}R' + CH_3COCH_3 \qquad (1)$$

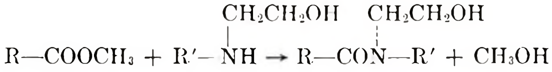

$$R\text{—}COOCH_3 + R'\text{—}NH(CH_2CH_2OH) \rightarrow R\text{—}CON(CH_2CH_2OH)\text{—}R' + CH_3OH \qquad (2)$$

Aromatic polyamides with a high molecular weight were obtained[3] at room temperature by the exchange reaction of imidazolide of carboxylic acid with aromatic diamines, which is caused by the difference in basicity between imidazole and aromatic amine.

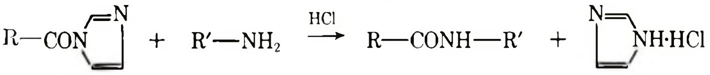

(3)

Polyimide is prepared from bisanhydride and diamine and a soluble polyamide acid is obtained at the first stage on the course of the reaction.

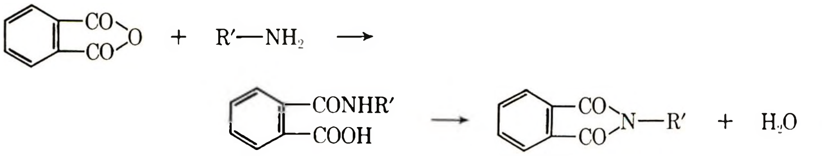

(4)

This reaction is the exchange reaction between anhydride and amine to form amide and acid. Therefore, it is possibly expected to form polyamide from bisanhydride and diamine through the exchange reaction (5).

$$RCO\text{—}O\text{—}CO\text{—}R'\text{—}CO\text{—}O\text{—}COR + NH_2\text{—}R''\text{—}NH_2 \rightarrow \;\; \text{+}CO\text{—}R'\text{—}CONH\text{—}R''\text{—}NH\text{+} + 2RCOOH \qquad (5)$$

It is expected in this reaction that the difference in dissociation constant of carboxylic acids and the acid acceptor may play important roles on the formation of a high molecular weight polyamide, and the reaction conditions were investigated in this paper.

EXPERIMENTAL

Synthesis of Bisanhydrides

Bisanhydrides were synthesized by the reaction of dicarboxylic acid chloride with sodium salt of monocarboxylic acid such as acetic acid or trichloroacetic acid in tetrahydrofuran. After evaporating tetrahydrofuran, the bisanhydrides were purified by reprecipitation from tetrahydrofuran–*n*-hexane or by distillation in a high vacuum. The yields, melting points and elementary analyses of bisanhydrides are as shown in Table I.

TABLE I

RCO—O—CO—R′— CO—O—COR R	 R′	Yield, %	Mp, °C	Elementary analysis Found C, %	 H, %	 Calcd C, %	 H, %
CH_3	$—(CH_2)_8—$	72	117–120	59.5	7.83	58.7	7.75
CCl_3	$—(CH_2)_8—$	46	63–66	35.2	3.71	34.1	3.24
C_6H_5	$—(CH_2)_8—$	68	87–90	69.7	5.83	70.2	6.39
CH_3		65	>220[a]	58.5	4.60	57.6	4.03

[a] Sublimes.

Polycondensation

Interfacial polycondensation was carried out by dissolving diamine and acid acceptor in water and bisanhydride in organic solvent, and by mixing two solutions at 20°C. The polymers were filtered, washed with acetone, and dried. The inherent viscosity of polymers was measured in concentrated sulfuric acid at 30°C.

Solution polycondensation was carried out in *N*-methyl pyrrolidone or cyclohexanone at room temperature by dissolving stoichiometric amount of the two monomers and acid acceptor, and the solution was poured into water. The polymers were filtered and washed with acetone.

RESULTS

Results of the interfacial polycondensation are summarized in Table II, which indicates that triethylamine is an effective acid acceptor although the yield and inherent viscosity of polymers are poor.

Results of the solution polycondensation in *N*-methylpyrrolidone are shown in Table III, where it is seen that among the monomer combinations of bisanhydride of sebacic acid and diamines, trichloroacetic acid is an effective partner to yield polyamide. The kind of diamine was not related to the yield or inherent viscosity of polyamide, while the acid acceptor did have an influence on the polycondensation. No polymer was obtained in cyclohexanone solution. The infrared spectrum of polymers from sebacic acid showed a spectrum characteristic of polyamide as shown in Figure 1.

TABLE II
Interfacial Polycondensation of Hexamethylenediamine with Acid Anhydride[a]

RCO—O—CO— $(CH_2)_8$— CO—O—COR R	Acid acceptor	Solvent	Yield, %	η_{inh}, dl/g[b]
CH_3	NaOH	$CHCl_3/H_2O$	0	–
CH_3	Et_3N	$CHCl_3/H_2O$	46.0	0.05
CH_3	Et_3N	THF/H_2O	40.0	0.05
C_6H_5	NaOH	$CHCl_3/H_2O$	8.4	0.06
C_6H_5	Et_3N	$CHCl_3/H_2O$	21.6	0.06
C_6H_5	Na_2CO_3	$CHCl_3/H_2O$	28.7	0.10
C_6H_5	Imidazole	$CHCl_3/H_2O$	24.8	0.08

[a] Concn, 0.125 mole/l. at 20°C for 2 hr.
[b] In H_2SO_4 at 30°C.

TABLE III

Solution Polycondensation of Diamines with Bisanhydrides[a,b]

Diamine	RCO—O—CO—R′—CO—O—COR R	R′	Concn mole/l.	Acid acceptor	Time, hr	Yield, %	η_{inh}, dl/g[c]
$H_2N(CH_2)_6NH_2$	CH_3	$—(CH_2)_8—$	0.50	Et_3N	2	43.0	0.11
$H_2N(CH_2)_6NH_2$	CH_3	$—(CH_2)_8—$	0.25	Imidazole	18	22.5	0.07
$H_2N(CH_2)_6NH_2$	CCl_3	$—(CH_2)_8—$	0.25	Et_3N	2	42.6	0.23
$H_2N(CH_2)_6NH_2$	CCl_3	$—(CH_2)_8—$	0.25	None	2	35.5	0.15
$H_2N(CH_2)_6NH_2$	C_6H_5	$—(CH_2)_8—$	0.50	Et_3N	2	21.0	0.08
$H_2N(CH_2)_6NH_2$	C_6H_5	$—(CH_2)_8—$	0.25	Imidazole	18	17.0	0.07
$H_2N(CH_2)_6NH_2$	CH_3		0.25	Et_3N	2	0	—
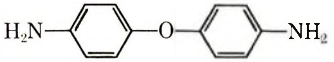	CCl_3	$—(CH_2)_8—$	0.25	Et_3N	2	76.5	0.12
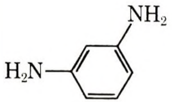	CH_3	$—(CH_2)_8—$	0.25	Et_3N	18	12.3	0.07
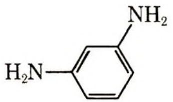	C_6H_5	$—(CH_2)_8—$	0.25	Et_3N	18	36.5	0.06
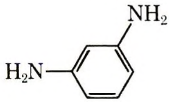	CH_3		0.25	Et_3N	18	0	—
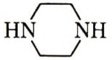	CH_3	$—(CH_2)_8—$	0.25	Et_3N	18	68.0	0.07
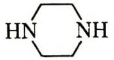	C_6H_5	$—(CH_2)_8—$	0.25	Et_3N	18	35.0	0.06

[a] Solvent: NMP, at room temperature.

[b] The reaction temperature was usually −5 to −10°C upon addition of the acid anhydride.

[c] In H_2SO_4 at 30°C.

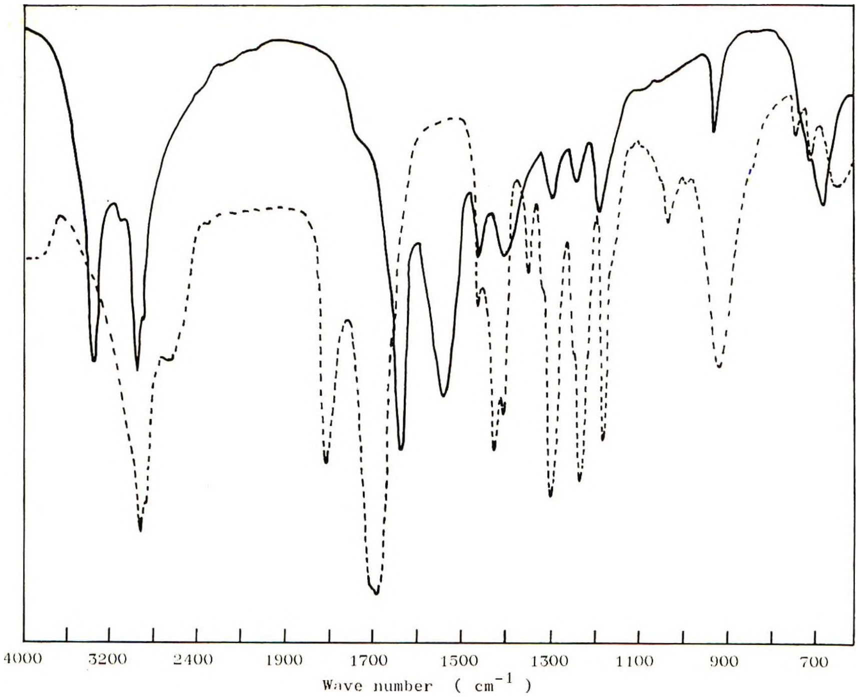

Fig. 1. Infrared spectra of (---) $CH_3CO—O—CO(CH_2)_8CO—O—COCH_3$ and (——) polymer obtained from bisanhydride and hexamethylenediamine.

It was difficult to obtain polyamide with a high molecular weight in a quantitative yield by the exchange reaction of bisanhydrides with diamines. The reason might be attributed to the small difference in the dissociation constants among carboxylic acids and the cross-amidation reaction might take place between dicarboxylic and monocarboxylic acids, which caused low yield and low molecular weight of polyamide in the course of the polycondensation.

References

1. R. W. Stackman and H. W. Steinmann, paper presented at American Chemical Society Meeting, 1968; *Polym. Preprints*, **9,** 628 (1968).
2. N. Ogata and K. Sanui, *J. Polym. Sci. A-1*, **7,** 2847 (1969).
3. K. Kuze, *Kogyo Kagaku Zasshi*, **72,** 1603 (1969).

K. Sanui
N. Ogata

Department of Chemistry
Sophia University
Chiyoda-Ku, Tokyo, Japan

Received May 19, 1970

Polybenzimidazole Containing Adamantane Units

Vogel and Marvel[1] have demonstrated the extreme thermal stability of polybenzimidazoles prepared by condensation of diesters with 3,3′-diaminobenzidine. If the esters were derived from aliphatic acids such as adipic acid, the polymers decomposed at about 470°C. Those polymers which were purely aromatic were stable to 590°C.

We have synthesized diphenyl adamantane-1,3-dicarboxylate (I) and have used this

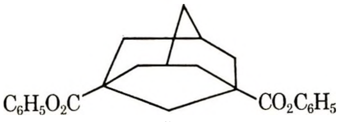

I

novel building block for preparation of a polybenzimidazole by reaction with 3,3′-diaminobenzidine. Our reason for choosing the adamantane skeleton is its outstanding stability resulting from a strain-free geometry.[2]

Figure 1 shows the thermal gravimetric analysis of the new polybenzimidazole (II).

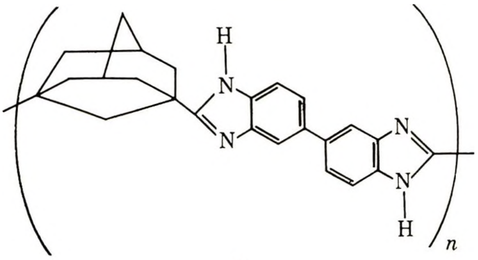

II

As expected, the decomposition temperature of the adamantane-containing polymer (540°C) was higher than that of other polybenzimidazoles with aliphatic linkages. The new polymer, however, was not so stable as the wholly aromatic polybenzimidazoles prepared by Vogel and Marvel.[1]

Experimental

TGA analysis was carried out on a Fisher Model 260-F thermal gravimetric analyzer equipped with a Cahn electrobalance. DTA was carried out with a DuPont 900 differential thermal analyzer.

All melting points are uncorrected.

Diphenyl Adamantane-1,3-dicarboxylate. A solution of 1.8 g (0.0080 mole) of adamantane-1,3-dicarboxylic acid[3] in 150 ml of thionyl chloride was refluxed for 20 hr. The resulting mixture was filtered to remove suspended solid and concentrated under reduced pressure yielding 2.1 g (90%) of crude adamantane-1,3-dicarbonyl chloride, mp 80–83°C ($\nu_{CCl_4}^{max}$ = 1780 cm^{-1}). A sample of 2.0 g (0.0068 mole) of the diacid chloride was ground together with 2.8 g (0.030 mole) of phenol. The liquid mixture was then stirred in a nitrogen atmosphere at room temperature for 1 hr and at 100°C for 0.5 hr. The product was dissolved in 80 ml of methylene chloride and washed twice with 75-ml portions of 3% aqueous sodium hydroxide. The methylene chloride solution was dried over magnesium sulfate and concentrated yielding 1.4 g (55%) of white crystalline diester, mp 121–124°C. Infrared and NMR spectra were consistent with the proposed structure (I). Recrystallization from methylene chloride–hexane gave an analytical sample, mp 125–126°C.

ANAL. Calcd for $C_{24}H_{24}O_4$: C, 76.57%; H, 6.43%. Found: C, 76.87%; H, 6.65%.

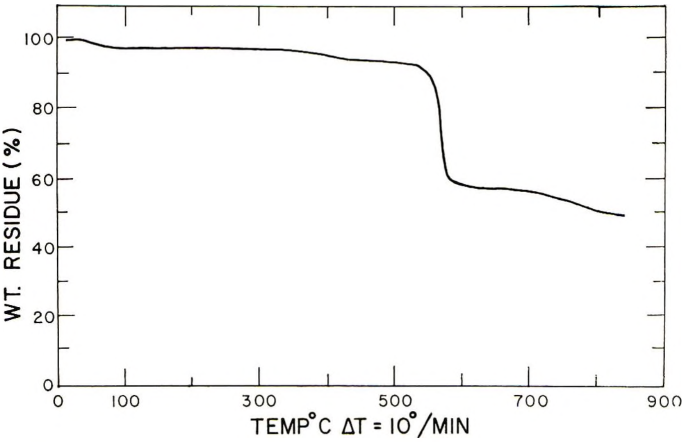

Fig. 1. Thermal gravimetric analysis of the polybenzimidazole II.

Preparation of the Polybenzimidazole. A finely pulverized mixture of 1.07 g (0.0028 mole) of the diester and 0.61 g (0.0028 mole) of 3,3′-diaminobenzidine (recrystallized twice from methanol) was placed in a 50 ml round-bottomed flask and purged for 1 hr with nitrogen. The flask and contents were then heated at 290–310° for 2 hr, forming an amber, glassy foam. This foam was crushed to a pale orange powder and was heated at 290–310°C for 3 hr at 0.20 torr. The yield of polymer was 0.54 g (52%). The inherent viscosity of the polymer was 0.19 (measured as a 0.5% solution in formic acid at 30°C).

Anal. Calcd for $C_{24}H_{22}N_4$: C, 78.69%; H, 6.01%; N, 15.30%. Found: C, 76.39%; H, 6.07%; N, 13.84%.

The polymer was also soluble in dimethyl sulfoxide and hot dimethylformamide but was insoluble in all other common organic solvents. DTA analysis revealed no significant change up to 500°C; TGA showed decomposition at 540°C in a nitrogen atmosphere.

Acknowledgment is made to the National Aeronautics and Space Administration under which support was afforded one of us (A. L. S.) under multidisciplinary research grant NsG-394.

We wish to thank Mr. Ronald D'Amelia (Adelphi) for the thermal gravimetric analysis of the polymer, and Mr. Thomas P. Brady (Dow) for DTA data.

References

1. H. Vogel and C. S. Marvel, *J. Polym. Sci.*, **50**, 511 (1961).
2. R. C. Fort and P. von R. Schleyer, *Chem. Revs.*, **64**, 277 (1964).
3. H. Stetter and C. Wulff, *Chem. Ber.*, **93**, 1366 (1960).

Sung Moon
Arthur L. Schwartz

Department of Chemistry
Adelphi University
Garden City, New York 11530

Jeffrey K. Hecht

Eastern Research Laboratory
The Dow Chemical Company
Wayland, Massachusetts 01778

Received June 17, 1970

Preparation of Polystyrene with Terminal Functional Groups

Introduction

The unusual and useful properties of block copolymers are now widely recognized; one may mention the styrene–butadiene–styrene nonvulcanized elastomer and spandex elastomeric fibers as striking examples of the unique character of block copolymers.

In this paper we report a new approach to the preparation of vinyl polymers with reactive functional groups which may be coupled to form blocks.

Results and Discussion

In order to prepare vinyl polymers or copolymers containing reactive functional groups, styrene was copolymerized with vinylene carbonate,[1] followed by methanolysis of the copolymer(I) to the 1,2-glycol(II) and cleavage with periodate. This polymer has been prepared earlier by Judge and Price[1] and by Hayashi and Smets.[2]

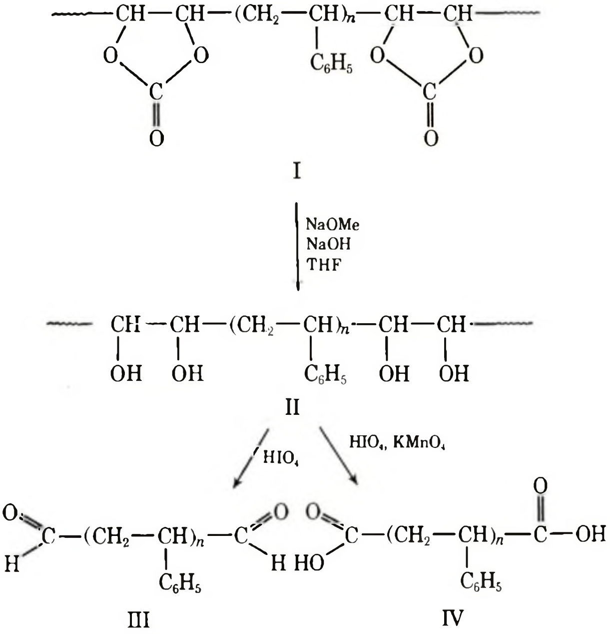

Poly(styrene-*co*-vinylene carbonate), I, was prepared in bulk with the use of azobisisobutyronitrile as initiator. The copolymer composition was determined by elemental analysis and quantitative infrared spectroscopy. Homopolymer mixtures of known composition were used to prepare a calibration curve by utilizing the 1800 cm^{-1} absorption due to carbonyl stretching and phenyl deformation and the 1946 cm^{-1} band due to phenyl deformation only. Results are presented in Table I.

Although copolymer I is not hydrolyzed at any appreciable rate in heterogeneous systems consisting of sodium hydroxide in aqueous dioxane or sodium methoxide at room temperature, methanolysis did occur with sodium methoxide in a tetrahydrofuran-methanol solution to yield the copolymer of styrene and vinylene glycol (II). The contribution to the 1800 cm^{-1} band in the infrared spectrum of II due to the carbonate had largely disappeared.

Copolymer II was then cleaved by periodic acid in THF to yield polystyrene terminated by aldehyde groups (III); alternatively, cleavage by periodic acid and potassium permanganate yielded polystyrene terminated by carboxylic acid endgroups. The fact

TABLE I

Intrinsic Viscosities, Number-Average Molecular Weight, and Composition of Styrene–Vinylene Carbonate Copolymers and Their Products

	Copolymer I				Copolymer II		Copolymer III		Copolymer IV	
			Vinylene carbonate, mole-%							
Run	$[\eta]$	$\bar{M}_n$	By elementary analysis	By IR	$[\eta]$	$\bar{M}_n$	$[\eta]$	$\bar{M}_n$	$[\eta]$	$\bar{M}_n$
A	0.47	64,000	1.5	1.4	0.43	56,400	0.26	27,900		
B	0.92	164,000	2.4	2.8	0.90	159,000	0.20	19,400	0.11	8,300
C	0.47	64,000		4.9			0.13	10,500		

that cleavage occurred is shown very clearly by the drop in intrinsic viscosity and by the appearance of weak carbonyl bands in the infrared.

Number-average molecular weights have been calculated from intrinsic viscosities by using a relationship found by Gregg and Mayo.[3] Although the Gregg-Mayo equation would not be expected to be quantitative in our case, one can get a qualitative idea of the degree of cleavage from Table I.

A simple calculation reveals that the decrease in molecular weight after hydrolysis and cleavage of copolymer I is less than what one would expect on the basis of the vinylene carbonate content. This may be due to incomplete hydrolysis of the carbonate, to incomplete cleavage of the glycol or both. It is not necessary, however, that all vinylene carbonate linkages cleave in order to obtain a polymer terminated with functional groups at each end.

Experimental

Vinylene Carbonate. Chloroethylene carbonate[4] was pyrolyzed according to the procedure of Johnson and Patton.[5] Physical properties and spectra were in accord with the previously reported information. The compound was distilled from sodium borohydride prior to use.

Determination of Copolymer Composition. Films containing homopolymer mixtures of polystyrene and poly(vinylene carbonate) of known content were used to determine the composition of the copolymers of styrene and vinylene carbonate (IA, B, and C). Solutions of 13% polymer concentration in 73% carbon tetrachloride and 14% dimethylformamide were used to deposit films on a metal gauze. Upon drying, infrared spectra were obtained from the films. The area of the absorption at 1946 cm^{-1}, phenyl combination band, was used to standardize the area at 1800 cm^{-1}, which consists of an overlap of phenyl overtone and carbonyl carbonate stretching bands.

Poly(styrene-*co*-Vinylene Carbonate) (IA). A solution of styrene (23.4 g, 0.225 mole), vinylene carbonate (7.21 g, 0.0838 mole), and azobisisobutyronitrile (0.155 g, 0.944 mmole) was degassed by freeze-thawing and heated under a nitrogen atmosphere at 60 ± 2°C for 17.5 hr. The resulting polymer was reprecipitated twice from benzene into methanol (19.2 g, 62.8%) and freeze-dried from benzene.

ANAL. Found: C, 91.65%; H, 7.68%; O (by difference), 0.67%. The infrared (film) spectrum was nearly identical to that of polystyrene except for a larger peak at 1800 cm^{-1} due to overlap of carbonyl carbonate absorption with a polystyrene band.

Poly(styrene-*co*-Vinylene Carbonate) (IB). A solution of styrene (13.0 g, 0.0833 mole), vinylene carbonate (21.5 g, 0.250 mole), and azobisisobutyronitrile (5.47 mg, 0.0333 mmole) was polymerized for 4 days at 60 ± 2°C. After 28 hr, styrene (5.0 g, 0.048 mole) and initiator (0.0031 g, 0.019 mmole) were added. After 2 hr of polymerization, a second liquid phase formed. At the end of the polymerization period, the upper phase was very viscous and tacky, while the lower phase was a fluid material. The lower phase upon pouring into methanol yielded only a small amount of precipitate and was discarded. The upper layer was worked up in the same manner as IA. The yield was 4.7 g (13.6% based on initial feed) of polymer; [η] 0.92, benzene, 25.00 ± 0.05°.

ANAL. Found: C, 91.27%; H, 7.61%; O, 1.12% (by difference).

Poly(styrene-*co*-Vinylene Carbonate) (IC). A solution of styrene (27.5 g, 0.320 mole) vinylene carbonate (8.33 g, 0.0800 mole), azobisisobutyronitrile (3.28 mg, 0.0200 mmole), in 8 ml of benzene was polymerized at 60°C for 22 days; styrene (2.0 g, 19 mmole) was added after 2, 4, 11, 15, and 19 days. Initiator (3.30 mg, 0.0201 mmole), and (1.00 mg, 0.00609 mmole) was added after 4 and 15 days, respectively. An additional 10 ml of benzene was added after four days to redissolve a second phase which appeared after 3 days. The product was worked up as previously described to yield 3.9 g of polymer; [η] 0.47 ± 0.01 (benzene, 25.00 ± 0.05°C).

Poly(styrene-*co*-Vinylene Glycol) (IIA). A solution of 2.0 g (IA) and sodium (1 g, 0.04 mole), 10 ml of methanol, and 100 ml of tetrahydrofuran was stirred for three days. The polymer (1.8 g, 90%, [η] 0.43 ± 0.01) was purified in the same manner as (IA). The infrared spectrum (film) indicated no measurable carbonyl carbonate band.

Poly(styrene-*co*-Vinylene Glycol) (IIB). A solution of 1.0 g of (IB) and 0.2 g of sodium in 3 ml of methanol and 20 ml of THF was stirred for 2 days. After work-up, 1.0 g (100%) of polymer was obtained, [η] 0.90 ± 0.02, benzene, 25.00 ± 0.05.

Poly(styrene-*co*-Vinylene Glycol) (IIC). This material was prepared in an analogous manner to IIB. The infrared (film) was nearly identical to polystyrene except for a slight hydroxyl absorption at 3580 cm^{-1}.

Preparation of Aldehyde-Terminated Polystyrene (IIIA). A slurry of IIA (1.5 g), periodic acid (1.0 g, 4.4 mmole), and 8 ml of THF was stirred for 18 days at room temperature under nitrogen. A solution of periodic acid (0.5 g, 2 mmole) and 4 ml of THF was added after three days. The color of the THF solution changed from colorless to pale red-brown, and increasing amounts of white, insoluble materials (HIO_3 ?) were formed. The precipitate was soluble in water. The solution was filtered and the polymer purified in the usual manner. A total of 1.5 g (100%) of polymer which slowly turns pale pink on standing was obtained: [η] 0.265 ± 0.002, 25.00 ± 0.05°C.

Preparation of Aldehyde-Terminated Polystyrene (IIIB). A solution of IIB (0.9 g), periodic acid (1.0 g, 4.4 mmole), and 20 ml of THF was stirred for 3 days and treated in an analogous manner to IIIA: [η] 0.200 ± 0.005, benzene, 25.00 ± 0.05°C.

Preparation of Aldehyde-Terminated Polystyrene (IIIC). This was prepared in an analogous manner to IIIA from IIC; [η] 0.13 ± 0.02, benzene, 25.00 ± 0.05°C.

Preparation of Carboxyl-Terminated Polystyrene (IVB). A total of 0.3 g of IIB, 0.3 g (1 mmole) of periodic acid, 0.3 g (2 mmole) of potassium permanganate (insoluble in THF), 50 ml of THF, and sufficient water (ca. 0.2 ml) to cause a slight pink-gray coloration was stirred for 25 days. The polymer was precipitated in a 4*N* hydrochloric acid solution, washed twice with a mixture of 30 ml of methanol and 10 ml of concentrated hydrochloric acid, washed with methanol, and vacuum dried. A white polymer, 0.3 g (100%), was obtained; [η] 0.11, benzene, 25.10 ± 0.05°C. The infrared spectrum showed a carbonyl band at 1720 cm^{-1} which was of the same intensity as the 1800 cm^{-1} band.

References

1. J. M. Judge and C. C. Price, *J. Polym. Sci.*, **41**, 435 (1959).
2. K. Hayashi and G. Smets, *ibid.*, **27**, 275 (1958).
3. R. A. Gregg and F. R. Mayo, *J. Amer. Chem. Soc.*, **70**, 2375 (1948).

4. J. R. Schaefgen and N. D. Field, in *Macromolecular Syntheses*, Vol. 2, J. R. Elliot, Ed., Wiley, New York, 1966, pp. 15–20.
5. W. K. Johnson and T. L. Patton, *J. Org. Chem.*, **25**, 1042 (1960).

J. E. Mulvaney
H. G. Gollmar
J. R. Gross

Department of Chemistry
The University of Arizona
Tucson, Arizona 85721

Received June 8, 1970
Revised August 10, 1970

ERRATUM

Stereospecific Polymerization of Methacrylonitrile. VI. Effect of Esters as a Complexing Agent with Diethylmagnesium Catalyst

YASUSHI JOH, SEIKI KURIHARA, TOSHIO SAKURAI, and TATSUNORI TOMITA

[article in *J. Polym. Sci. A-1*, **8**, 2383 (1970)]

In the title, the word **Esters** should read **Ethers.**

AUTHOR INDEX, VOLUME 8

SUBJECT INDEX, VOLUME 8

Journal of Polymer Science

PART A-1: POLYMER CHEMISTRY

Volume 8, 1970

Board of Editors: H. MARK · C. G. OVERBERGER · T. G FOX

Advisory Editors: R. M. FUOSS · J. J. HERMANS · H. W. MELVILLE · G. SMETS

Editor: C. G. OVERBERGER · **Associate Editor:** E. M. PEARCE

Advisory Board:

T. Alfrey, Jr.
Midland, Mich.
W. J. Bailey
Baltimore, Md.
D. S. Ballantine
Washington, D. C.
M. B. Birenbaum
Trenton, N. J.
F. A. Bovey
Murray Hill, N. J.
J. W. Breitenbach
Wien
W. J. Burlant
Dearborn, Mich.
G. B. Butler
Gainesville, Fla.
S. Bywater
Ottawa
T. W. Campbell
Waynesboro, Va.
W. L. Carrick
Bound Brook, N. J.
H. W. Coover, Jr.
Kingsport, Tenn.
F. Danusso
Milano
F. R. Eirich
Brooklyn, N. Y.
E. M. Fettes
Monroeville, Pa.
N. D. Field
Easton, Pa.
F. C. Foster
Rolling Meadows, Ill.
H. N. Friedlander
Durham, N. C.

K. C. Frisch
Wyandotte, Mich.
N. G. Gaylord
New Providence, N. J.
W. E. Gibbs
Dayton, Ohio
A. R. Gilbert
Schenectady, N. Y.
J. E. Guillet
Toronto
H. C. Haas
Cambridge, Mass.
J. P. Kennedy
Linden, N. J.
W. Kern
Mainz
J. Lal
Akron, Ohio
R. W. Lenz
Amherst, Mass.
C. S. Marvel
Tucson, Ariz.
F. R. Mayo
Menlo Park, Calif.
R. B. Mesrobian
Chicago, Ill.
H. Morawetz
Brooklyn, N. Y.
M. Morton
Akron, Ohio
S. Murahashi
Osaka
G. Natta
Milano
K. F. O'Driscoll
Villanova, Pa.

S. Okamura
Kyoto
P. Pino
Pisa
C. C. Price
Philadelphia, Pa.
B. Rånby
Stockholm
J. H. Saunders
New Martensville, West Va.
C. Schuerch
Syracuse, N. Y.
W. H. Sharkey
Wilmington, Del.
W. R. Sorenson
Ponca City, Okla.
V. T. Stannett
Raleigh, N. C.
J. K. Stille
Iowa City, Iowa
M. Szwarc
Syracuse, N. Y.
A. V. Tobolsky
Princeton, N. J.
E. J. Vandenberg
Wilmington, Del.
L. A. Wall
Washington, D. C.
F. X. Werber
Garfield, N. J.
O. Wichterle
Prague
F. H. Winslow
Murray Hill, N. J.
M. Wismer
Springdale, Pa.
E. A. Youngman
Emeryville, Calif.

INTERSCIENCE PUBLISHERS

Copyright © 1970, by John Wiley & Sons, Inc

Statement of ownership, management, and circulation (Act of October 23, 1962: Section 4369, Title 39 United States Code)

1. Date of filing: October 12, 1970
2. Title of Publication: JOURNAL OF POLYMER SCIENCE
3. Frequency of issue: monthly
4. Location of known office of publication: 20th and Northampton Streets, Easton, Pennsylvania 18042
5. Location of headquarters of general business offices of publisher: 605 Third Avenue, New York, New York 10016
6. The names and addresses of publisher, editor, and managing editor:

Publisher: John Wiley & Sons, Inc., 605 Third Avenue, New York, New York 10016

Editor: Herman Mark, Polytechnic Institute of Brooklyn, 333 Jay Street, Brooklyn, New York 11201, C. G. Overberger, Univ. of Michigan, Ann Arbor, Mich., and T. G Fox, Mellon Institute, Pittsburgh, Pennsylvania 15213

Managing Editor: None

7. Owner: John Wiley & Sons, Inc., 605 Third Avenue, New York, New York 10016

The following is a list of stockholders owning or holding 1% or more of John Wiley and Sons, Inc. stock as of August 31, 1970:

Cynthia W. Darby, Box 651, Bridgehampton, New York 11932; John P. Gilbert, Executive of Estate of Julia Wiley Gilbert, c/o Wells Fargo Bank, Trust Division 37165, P. O. Box 3820, San Francisco, California 94120; Edward P. Hamilton, 605 Third Avenue, New York, New York 10016; W. Bradford Wiley & Francis Lobdell, Trustees Elizabeth W. Hamilton Trust, 605 Third Avenue, New York, New York 10016; Edward P. Hamilton, Trustee under will of Elizabeth Wiley Hamilton, c/o Gifford, Woody, Carter & Hayes, 1 Wall Street, New York, New York 10005; I. M. Kolthoff, University of Minnesota, School of Chemistry, Minneapolis, Minnesota; Charlotte Levinger, Executive of Estate of Willy Levinger, 336 Central Park West, New York, New York; Eric S. Proskauer & Charles H. Lieb, Trustees u/a by Jenny R. Proskauer, 220 Central Park South, New York, New York 10019; Francis Lobdell & William J. Seawright, Trustees f/b/o Deborah Elizabeth Wiley, c/o John Wiley & Sons, Inc., 605 Third Avenue, New York, New York; Cynthia W. Darby & Julia Gilbert, Trustees under will of Kate R. Q. Wiley, c/o Gifford, Woody, Carter & Hays, 1 Wall Street, New York, New York; Francis Lobdell & William J. Seawright, Trustees f/b/o Peter Booth Wiley, c/o John Wiley & Sons, Inc., 605 Third Avenue, New York, New York; Francis Lobdell & William J. Seawright, Trustees f/b/o William Bradford Wiley II, c/o John Wiley & Sons, Inc., 605 Third Avenue, New York ,New York; Edward P. Hamilton & Cynthia Wiley Darby, Trustees under will of William O. Wiley, c/o Gifford, Woody, Carter & Hays, 1 Wall Street, New York, New York; Adele E. Windheim, 8 Dundee Road, Larchmont, New York; Cudd & Company, 1 Chase Manhattan Plaza, New York, New York; Dif & Company, P. O. Box 1447, 135 Devonshire Street, Boston, Massachusetts; W. Bradford Wiley & E. P. Hamilton, Trustees for Edward P. Hamilton Foundation, c/o John Wiley & Sons, Inc., 605 Third Avenue, New York, New York; Pitt & Company, P. O. Box 2444, Church Street Station, New York, New York; Reing & Company, P. O. Box 491, Church Street Station, New York, New York; Shaw & Company, P. O. Box 491, Church Street Station, New York, New York 10015; Jog & Company, P. O. Box 1447, Boston, Massachusetts 02104; Sigler & Company, c/o Manufacturers Hanover Trust Company, New York, New York 10015; and Trussal & Company, National Bank of Detroit, c/o Trust Department, Detroit, Michigan

8. Known bondholders, mortagees, and other security holders owning or holding 1 per cent or more of total amount of bonds, mortgages, or other securities: None

9. Paragraphs 7 and 8 include, in cases where the stockholder or security holder appears upon the books of the company as trustee or in any other fiduciary relation, the name of the person or corporation for whom such trustee is acting, also the statements in the two paragraphs show the affiant's full knowledge and belief as to the circumstances and conditions under which stockholders and security holders who do not appear upon the books of the company as trustees, hold stock and securities in a capacity other than that of a bona fide owner. Name and addresses of individuals who are stockholders of a corporation which itself is a stockholder or holder of bonds, mortgages or other securities of the publishing corporation have been included in paragraphs 7 and 8 when the interests of such individuals are equivalent to 1 per cent or more of the total amount of the stock or securities of the publishing corporation.

10.	Extent and nature of circulation	Average no. copies each issue during preceding 12 months	Single issue nearest to filing date
A.	Total no. copies printed (*net press run*)	2900	2900
B.	Paid circulation		
	1. Sales through dealers and carriers, street vendors and counter sales	—	—
	2. Mail subscriptions	2400	2400
C.	Total paid circulation	2400	2400
D.	Free distribution (*including samples*) by mail, carrier or other means	104	104
E.	Total distribution (*Sum of C and D*)	2504	2504
F.	Office use, left-over, unaccounted, spiled after printing	396	396
G.	Total (*Sum of E & F—should equal net press run shown in A*)	2900	2900

(Signature of editor, business manager, or owner)

I certify that the statements made by me above are correct and complete.

James A. McNeish

CONTENTS

Vol. 8, Issue Nos. 1–12

Journal of Polymer Science
Part A-1: Polymer Chemistry

ISSUE NO. 1, JANUARY

Notes

Book Reviews

ISSUE NO. 2, FEBRUARY

ISSUE NO. 3, MARCH

Notes

ISSUE NO. 4, APRIL

Notes

ISSUE NO. 5, MAY

Notes

ISSUE NO. 6, JUNE

Notes

Issue No. 7, July

Note

ISSUE NO. 8, AUGUST

ISSUE NO. 9, SEPTEMBER

Notes

ISSUE NO. 10, OCTOBER

Notes

Erratum

Issue No. 11, November

Notes

Erratum

Issue No. 12, December

Notes

Erratum

Journal of Polymer Science **Part A-1: Polymer Chemistry**

Contents (*continued*)

The *Journal of Polymer Science* publishes results of fundamental research in all areas of high polymer chemistry and physics. The *Journal* is selective in accepting contributions on the basis of merit and originality. It is not intended as a repository for unevaluated data. Preference is given to contributions that offer new or more comprehensive concepts, interpretations, experimental approaches, and results. Part A-1 *Polymer Chemistry* is devoted to studies in general polymer chemistry and physical organic chemistry. Contributions in physics and physical chemistry appear in Part A-2 *Polymer Physics*. Contributions may be submitted as full-length papers or as "Notes." Notes are ordinarily to be considered as complete publications of limited scope.

Three copies of every manuscript are required. They may be submitted directly to the editor: For Part A-1, to C. G. Overberger, Department of Chemistry, University of Michigan, Ann Arbor, Michigan 48104; and for Part A-2, to T. G Fox, Mellon Institute, Pittsburgh, Pennsylvania 15213. Three copies of a short but comprehensive synopsis are required with every paper; no synopsis is needed for notes. Books for review may also be sent to the appropriate editor. Alternatively, manuscripts may be submitted through the Editorial Office, c/o H. Mark, Polytechnic Institute of Brooklyn, 333 Jay Street, Brooklyn, New York 11201. All other correspondence is to be addressed to Periodicals Division, Interscience Publishers, a Division of John Wiley & Sons, Inc., 605 Third Avenue, New York, New York 10016.

Detailed instructions in preparation of manuscripts are given frequently in Parts A-1 and A-2 and may also be obtained from the publisher.

Polymer Chemistry from Wiley-Interscience

THE CHEMISTRY AND USES OF FIRE RETARDANTS

By John W. Lyons, *Monsanto Company*

The chemistry of phosphorus, antimony, boron, chlorine, and bromine is prepared in enough detail to enable the reader to understand the use of compounds of these elements as fire retardants. The applications are discussed in terms of substrates: wood, paper, other cellulosics, paints and mastics, polymers with all-carbon backbones, and polymers with heterogeneous backbones.

The Chemistry and Uses of Fire Retardants reviews current progress in the area of fire retardation and sets the stage for the recent surge of technical activity initiated by the increased efforts of the last decade. The author offers the broadest possible view of the field of natural and synthetic polymers in terms of flammability and its control. More than 2000 references are included, deficiencies in the state of the art are pointed out, and future developments are speculated upon.

1970 462 pages $22.50

THE CHEMISTRY OF ALKENES

Volume 2

Edited by Jacob Zabicky, *Institute for Fibres and Forest Products Research, Jerusalem, and The Weizmann Institute of Science, Rehovoth, Israel*

A volume in the Chemistry of Functional Groups series, edited by Saul Patai

This volume deals with the chemistry of the carbon-carbon double bond, with emphasis on comparative critical discussion of the chemistry of alkenes. The material is presented in three main parts. The first part is concerned with general-theoretical aspects and includes a chapter on nuclear magnetic resonance spectroscopy. The second part deals with chemical behavior and includes chapters on rearrangements, hydrogenation, olefinic ions, complexes with transition metals, and the effects of various types of radiation. The third part treats related compounds in chapters on olefinic polymers and cyclopropanes.

1970 669 pages $31.00

VINYL AND DIENE MONOMERS

Parts 1, 2, and 3

Edited by Edward C. Leonard, *Kraftco Corporation*

Volume 24 of High Polymers, edited by H. Mark, C. S. Marvel, H. W. Melville and P. J. Flory

Vinyl and Diene Monomers offers, in three volumes a comprehensive, systematic, and uniform treatment of vinyl and diene monomers. Part One describes the manufacture, chemical and physical properties, purification and polymerization behavior of some of the commercially important vinyl monomers. Part Two describes the manufacture, chemical and physical properties, and polymerization and polymer characteristics of styrene, ethylene, isobutylene, butadiene, isoprene, and chloroprene. Part Three describes the manufacture, physical and chemical properties, and polymerization and polymer characteristics of vinyl and vinylidene chloride, the fluorocarbon monomers, and certain miscellaneous monomers.

Part 1	1970	477 pages	$19.95
Part 2	1970	704 pages	$37.50
Part 3	1970	432 pages	$24.95

VISCOELASTIC PROPERTIES OF POLYMERS

Second Edition

By John D. Ferry, *University of Wisconsin*

About eighty per cent of the material in the first edition of this well-known and widely used book has been rewritten for the second edition to take into account new developments since the book's first publication in 1961. Two new chapters have been added: on viscoelastic properties of dilute solutions and on the behavior of cross-linked polymers.

The book is concerned with the phenomenological and molecular theory of viscoelastic behavior of macromolecular systems, ranging from dilute solutions of rodlike and coiled polymers to rubbery, glassy and polycrystalline solids. It also describes methods for measuring transient and oscillatory viscoelastic properties, and their dependence on chemical structure, molecular weight, temperature, pressure, and plasticization.

1970 671 pages $29.95

WILEY-INTERSCIENCE
a division of JOHN WILEY & SONS, Inc.
605 Third Avenue, New York, N.Y. 10016
In Canada: 22 Worcester Road, Rexdale, Ontario

2 5 มี.ค. 2514